Ana Teresa Tavares de Lima e Crujeira
Diploma in Chemical Engineering
Instituto Superior Técnico

Identification of atmospheric pollutants control mechanisms during co-combustion of coal and non-toxic wastes

Doctoral dissertation for Ph.D. degree in Sustainable Chemistry

Supervisor	Prof. Isabel Maria Palma Aleixo Cabrita, LNEG, I.P.
Co-Supervisors:	Prof. Ibrahim Kadri Gülyurtlu, LNEG, I.P.
	Prof. Manuel Luís Magalhães Nunes da Ponte, REQUIMTE, FCT/UNL

Jury:

President:	Prof. Maria Adelaide de Almeida Pedro de Jesus, FCT/UNL
Examiners:	Prof. Carlos Alberto Diogo Soares Borrego, Aveiro University
	Prof. Maria Arminda Costa Alves, Engineering Faculty of Oporto University
Members:	Prof. Francisco Manuel da Silva Lemos
	Prof. José Carlos Fernandes Teixeira, Minho University
	Prof. Isabel Maria Palma Aleixo Cabrita, LNEG, I.P.
	Prof. Ibrahim Kadri Gülyurtlu, LNEG, I.P.
	Prof. Manuel Luís Magalhães Nunes da Ponte, REQUIMTE, FCT/UNL

FACULDADE DE CIÊNCIAS E TECNOLOGIA
UNIVERSIDADE NOVA DE LISBOA

Lisbon – Portugal, 23rd July 2013

Title: Identification of atmospheric pollutants control mechanisms during co-combustion of coal and non-toxic wastes
Author: Ana Teresa Tavares de Lima e Crujeira

To the memory of my father, Fernando Amante Crujeira.

To my dear daughter, Ana Leonor Crujeira da Silva Curto.

Acknowledgments

To Prof. Isabel Cabrita, Supervisor of this Thesis, for the constant stimulus and confidence in all these years, for the encouragement to achieve this goal and for helping me to reach it, as well as for the orientation, discussions and exchange of ideas while developing this Dissertation.

To Prof. Ibrahim Gulyurtlu, co-Supervisor of this Thesis, for the orientation and opportunity given to me to achieve my Ph.D. as a result of the COPOWER Project, a 6th Framework Project of the European Commission under his coordination in which I had the privilege of participating, and also by the valuable and rich discussions within the area of fluidised bed technology and pollutants emissions.

To Prof. Nunes da Ponte, coordinator of the 1st Portuguese Doctoral Programme in Sustainable Chemistry, to which this thesis was submitted, and co-Supervisor of this Thesis, for the orientation and the support namely related to the modelling work.

To Prof. Luís Moreira, for the advice and support given with the statistical treatment of the results and Prof. Susana Piçarra Gonçalves for the help with the thermodynamic calculations.

To the COPOWER project colleagues M. Helena Lopes, Pedro Abelha, and David Salema, for the excellent team spirit achieved along the project development and a special thanks to M. Helena Lopes for the constant stimulus and scientific discussion.

Ackowledgements

To INETI (today the National Laboratory of Energy and Geology - LNEG), for the possibility of developing the experimental work and framework, which allowed me to get valuable knowledge in several domains.

To the Head of Department of INETI and Heads of Unit of LNEG and the Director of LEN, in LNEG, for the conditions given for the development and writing of this Thesis.

To Ricardo Rodrigues (IDAD) and to Pedro Antunes (APA), for the helpful discussions and suggestions while implementing and validating PCCD/F sampling methodology.

To all the DEECA/UEZ colleagues and ex-colleagues, for the encouragement and good company in this long way.

To Paulo Torres Martins and Sandra Espadana, for assuring me the conditions that enabled me to achieve this goal.

To my parents, for the extraordinary education provided and to my mother, for her constant support in the raising of my daughter and to be always available for everything. As well as to my sisters Ana Margarida, Ana Rita e Ana Sofia, and my brother-in-law Jorge, and my nieces Caetana and Ana Pilar, for the permanent enthusiasm, joy and for sharing with me this journey through life.

To my mother's mother, Maria Otília, the first woman in the family to achieve a higher education degree, for my not being so present to assist her as much as she would like at her 96 years old; and also to my other "grand-mother" Ti Juca, also with 96 years old, for the constant enthusiasm in witnessing this Thesis conclusion.

To all my Girl Guide friends, both from Portugal and Japan and São Tomé e Princípice, with whom I lived unforgetable adventures that enriched me and upgraded my individual formation.

To Maria Elvira, Dapakara Karunaratne, Tatiana Diall, Paulo Curto, Helder Curto, Custódia Curto, Carlos Franco and Pedro Azevedo, for their friendship.

To ´João Seabra e Barros, for the remarkable teachings on QA/QC and metrology, who took me to IPAC, the Portuguese accreditation body.

Acknowledgments

To IPAC for the opportunity of enlarging my sights by auditing stack-gas emissions Laboratories and also for the comprehension along the last months of this thesis writing.

To Alexandra Passos Silva (IDAD) for the uncountless talks about sampling stack-gas emissions.

To Manuela Jogo, for the helpful discussions on uncertainties.

To all my friends, who supported and encouraged me and understood my absences.

To Sérgio, for his unlimited patience and support while writing this Thesis.

To my daughter Ana Leonor, for the time and attention I took away from her.

Abstract

The use of renewable energy sources (RES) for energy will contribute to meet the targets set up by the commitments of the Portuguese State with the European Union (EU) in energy and climate change combat policies. The reduction of CO_2 emissions is the primary goal when partially replacing coal with RES of biomass origin, but could also lead to the reduction of other pollutant emissions. At the same time, this particular renewable resource (pRES), *i.e.* biomass, could be mixed with coal, reducing the amount of fossil fuel used and due to positive synergies arising from the introduction of different amounts of volatile matter, ash, sulphur, calcium, chlorine, and heavy metals that react, may contribute to lower levels of certain emissions bringing environmental advantages.

The option for the co-combustion of coal with biomass type of fuel using fluidised bed technology presents some advantages related to the control of operation conditions, energetically and also towards lower levels of certain emissions, which could contribute to the fulfilment of the EU objectives in terms of environmental protection and sustainable energy production.

The aim of this work was the identification of the controlling mechanisms for the formation of pollutants and their subsequent destruction, during co-combustion of coal with biomass or non-toxic wastes, in a fluidised bed pilot unit. Different combinations of fuels were burned with the aim of identifying the main parameters that will lead to minimising the level of emissions, including CO_2, through the application of the principles of sustainable chemistry.

Two different bituminous coals were used as the base fossil fuel, a Colombian and a Polish coal. The coals were partly replaced by different pRES (straw and olive cake) and a non-toxic waste (Meat and Bone Meal). Rice husk was also tested as a renewable energy source.

Emissions of particulate matter, CO, SO_2, NO_X, heavy metals (HM), Cl, and dioxins and furans (PCDD/F) were evaluated, comparing the values obtained with different fuels compositions, *i.e.* different contents of volatile matter, ash, Cl, S, Ca, and HM.

Abstract

Special attention was given to emissions of PCCD/F compounds, both in the gas and solid phases. It was also studied the catalytic effect of Cu and the fly ash particle size distribution in these emissions.

It was observed that, in general, the emissions resulting from biomass combustion were lower than those observed for conventional fossil fuels. In addition, most of the combustion of pRES occurred in the gas phase, which is believed to be due to the release of volatiles, which constitute about 70% of the fuel mass.

It was possible to establish a diagram for prediction of SO_2 and HCl emissions simply by the knowledge of Ca, S and Cl fuel content. Separate equations were obtained for two ranges of S-Fuel (%, d.b.) - < 0.15 and > 0.15 – and for two ranges of Cl-fuel (%, d.b.) - < 0.03 and > 0.03.

A statistical analysis by standard multiple linear regressions (MLR) was performed, using the Data Analysis add-in, available in Microsoft Excel, as well as a statistical validation test to ensure the reliability of the model. It was possible to identify a relation between the total PCDD/F formed and the chlorine and sulphur content of the fuels:

$$y_{(D+F)Total} \propto x_{Cl} / x_S^{2.5}$$

When the PCDD/F data was disaggregated by the different streams, *i.e.* 1st Cyclone, 2nd Cyclone and Stack gas, two relations were found:

a) The stack-gas PCDD/F emissions were correlated with the Ca, S and Cl content of the fuel by the following general relation:

$$y_{(D+F)Stack-gas} \propto n_{Ca}/(n_S + n_{Cl})/x_S * x_{Cl}$$

The reproductibility of the results between the two installations were confirmed.

b) The PCDD/F in the 1st and 2nd Cyclones was correlated within each series of tests, by the following relation:

$$y_{(D+F)Cyclones} \propto Cu_{ash} * Cl_{ash}\ \%C_{ash} * T/d50$$

where Cu_{ash} and Cl_{ash} are the Cu and Cl contents in the cyclone ashes, T is the Cyclone temperature and d_{50} is the mean diameter of the fly ash.

It was also possible to find a condition, for which PCDD/F emissions in a fluidized bed combustor are lower than the Emission Limit Value (ELV), when S>0.15% (d.b.) and Cl > 0.03% (d.b.):

$$[nCa/(nS+nCl)]/(\%Cl\text{-}Fuel,db)/(\%S\text{-}Fuel,db) > 4.84$$

Finally, it was also developed a kinetic model, the FB-OWL model, to estimate possible PCDD/F emissions from the co-combustion of renewable fuels mixed with coal in fluidized bed through precursors and *de novo* mechanisms.

Key-words: Co-combustion, Fluidised bed, Emissions, PCDD/F, Non-toxic wastes, Renewable energy sources.

Resumo (Abstract in Portuguese)

A utilização de fontes de energia renovável (FER) contribuirá para atingir os compromissos de Portugal com a União Europeia (UE) em termos de políticas de energia e de alterações climáticas. A substituição de carvão por FER de origem biomássica tem por principal objectivo a redução das emissões de CO_2, podendo também levar à redução de outras emissões poluentes. Simultaneamente, estas fontes de energia de origem renovável em particular (FERp), como a biomassa, pode ser misturada com carvão, reduzindo a quantidade de fonte fóssil e, dadas as sinergias positivas que resultam da introdução de diferentes quantidades de material volátil, cinzas, enxofre, cálcio, cloro e metais pesados, terá vantagens também relativamente às emissões de poluentes.

A opção pela tecnologia de leito fluidizado para a co-combustão de carvão com combustíveis de origem biomássica poderá contribuir para um melhor controlo de operação tanto energeticamente como no que se refere ao controlo de emissões poluentes e, assim, contribuir para o cumprimento dos objectivos da UE em termos de protecção ambiental e produção sustentável de energia.

O objectivo deste trabalho foi a identificação de mecanismos de controlo da formação de poluentes e a sua subsequente destruição durante a co-combustão de carvão com biomassa ou resíduos não-tóxicos, numa unidade piloto de leito fluidizado. Foram testadas diferentes combinações de combustíveis, procurando determinar os parâmetros fundamentais para minimizar o nível de emissões produzidas, incluindo o CO_2, aplicando os princípios da química sustentável.

Dois carvões betuminosos diferentes foram utilizados como combustível de base, um carvão Colombiano e um carvão Polaco.

Resumo (Abstract in Portuguese)

Os carvões foram parcialmente substituídos por diferentes FERp (palha e bagaço de azeitona) e resíduos não-tóxicos (farinha de carne). Foi também testada a casca de arroz, uma fonte de energia de origem renovável.As emissões de partículas, CO, SO_2, NO_X, Metais Pesados (MP), Cl e Dioxinas e Furanos (PCDD/F) foram avaliadas, comparando os valores obtidos para as diferentes composições dos combustíveis, isto é, diferentes teores introduzidos em material volátil, cinzas, Cl, S, Ca, e MP.

Foi dada especial atenção às emissões de PCDD/F, quer na fase sólida quer na fase gasosa; foi também avaliado o possível efeito catalítico do cobre e da distribuição granulométrica das partículas nessas emissões.

Foi possível desenhar um diagrama para prever as emissões de SO_2 e HCl simplesmente através do conhecimento dos teores em Ca, S e Cl no combustível. Foram obtidas diferentes equações para duas gamas de teores em S-Fuel (%, d.b.), <0,15 e >0,15, e duas gamas para Cl-fuel (%, d.b.), < 0,03 e > 0,03.

Realizou-se uma análise estatística por regressão linear múltipla, assim como teste de validação estatística por forma a assegurar a confiança no modelo. Foi possível identificar uma correlação entre a quantidade total de PCDD/F formados e os teores em cloro e enxofre no combustível:

$$y_{(D+F)Total} \propto x_{Cl} / x_S^{2,5}$$

Quando os dados foram desagregados pelos diferentes fluxos, isto é, 1º Ciclone, 2º Ciclone e Emissões Gasosas, encontraram-se duas relações:

a) As emissões de PCDD/F estavam correlacionadas com os teores em Ca, S e Cl do combustível através da seguinte relação geral:

$$y_{(D+F)Efluentes\ Gasosos} \propto n_{Ca}/(n_S + n_{Cl})/x_S * x_{Cl}$$

Foi ainda verificada a reproductibilidade dos resultados obtidos em ambas as instalações.

b) Os teores de PCDD/F nos 1º e 2º Ciclones estavam correlacionados entre si para cada série de testes através da seguinte relação:

$$y_{(D+F)Cyclones} \propto Cu_{ash} * Cl_{ash}\ \%C_{ash} * T/d50$$

onde Cu_{ash} e Cl_{ash} são os teores em Cu e Cl nas cinzas dos ciclones, T é a temperatura do ciclone e d_{50} é o diâmetro médio das cinzas dos ciclones.

Foi ainda apossível identificar umacondição para que as emissões de PCDD/F dum sistema de Leiro fluidizado sejam inferiores ao VLE (Valor Limite de Emissão) quando S>0,15% (d.b.) e Cl > 0,03% (d.b.):

$$[nCa/(nS+nCl)]/(\%Cl\text{-}Fuel,db)/(\%S\text{-}Fuel,db) > 4,84$$

Finalmente, foi também desenvolvido um modelo conético, o modelo FB-OWL, para estimar as possíveis emissões de PCDD/F através dos mecanismos "Precursores" e "*de novo*" resultantes da co-combustão de carvão com combustíveis de origem renovável em leito fluidizado.

Palavras-chave: Co-combustão, Leito Fluidizado, Emissões, PCDD/F, Resíduos não-tóxicos, Fontes de Energia Renováveis.

Table of Contents

List of abbreviations and definitions

a.r.	as received
BA	Bed Ash
BAT	Best Available Technology
BREF	Best available technology REFerence document
CAA	Clean Air Act
CAFE	Clean Air For Europe
CAIR	Clean Air Interstate Rules
CAMR	Clean Air Mercury Rule
CC	Colombian Coal
CFR	40 Code of Federal Regulations
CLTRAP	Convention on Long-Range Transboundary Air Pollution
CSI	Clear Skies Initiative
Cyc 1	Cyclone 1
Cyc 2	Cyclone 2
CO_2-eq	Carbon dioxide equivalent
d	Particle diameter
d10	Particle aerodynamic diameter corresponding to 10% of the mass of a sample of fly ash
d50	Particle aerodynamic diameter corresponding to 50% of the mass of a sample of fly ash
d90	Particle aerodynamic diameter corresponding to 90% of the mass of a sample of fly ash
d_p	Particles mean diameter
d_{SV}	Mean particle diameter corrected for the surface/volume ratio
d.b.	dry basis
EIPCCB	European Integrated Pollution Prevention and Control Bureau
ELV	Emission Limit Value

List of abbreviations and definitions

EMEP	European Monitoring and Evaluation Programme
EPER	European Pollutant Emission Register
ESP	Electrostatic Precipitator
EU	European Union
F	Fisher's value
FBC	Fluidised Bed Combustor
FC	Fixed Carbon
FDG	flue-gas desulphurization
FER	Fontes de Energia Renovavéis (Portuguese)
FF	Fabric Filters
GHG	Green House Gases
HCB	HexaChloroBenzene
HM	Heavy Metals
IED	Industrial Emmisions Directive
IPCC	Intergovernmental Panel on Climate Change
I-TEF	International Toxicity Emission Factor
I-TEQ	International Toxic Equivalent
LCP	Large Combustion Plants
MACT	Maximum Achievable Control Technology
MBM	Meat and Bone Meal
MSW	Municipal Solid Waste
OB	Olive Bagasse
PAC	Polycyclic Aromatic Compounds
PAH	Polycyclic Aromatic Hydrocarbons
PBDD	PolyBrominated Dibenzo-p-Dioxins
PBDF	PolyBrominated DibenzoFurans
PC	Polish Coal
PCB	Polychlorinated Biphenyls
PCBz	Polychlorinated Benzenes
PCPh	Polychlorinated Phenols
PCDD	PolyChlorinated Dibenzo-p-Dioxins
PCDF	PolyChlorinated DibenzoFurans
PIC	Products from Incomplete Combustion
PM	Particulate Matter
Q^2	Cross-validated *leave-one-out* correlation coefficient
r^2	Regression coefficient
R^2	Determination coefficient
RDF	Refuse Derived Fuel

List of abbreviations and definitions

RES	Renewable Energy Source
RH	Rice Husk
s	Standard deviation
SIP	State Implementation Plans
SL	Significance Level
SP	Straw Pellets
TEQ	Toxic Equivalent
toe	tonnes of oil equivalent
U_f	Fluidization velocity
U_{mf}	Minimum fluidization velocity
U_t	Particle terminal velocity
UNECE	United Nations Economic Commission for Europe
UNEP	United Nations Environment Programme
UNFCCC	United Nations Framework Convention on Climate Change
VM	Volatile Matter
VOC	Volatile Organic Compounds
WHO	World Health Organisation
WMO	World Meteorological Organization
WP	Wood Pellets
x_i	molar fraction of the *i* element in terms of the total fuel mol
y_{D+F}	molar fractions of total formed PCDD/F in terms of the total fuel mol

List of Tables

List of Figures

1. Preamble

This thesis focuses on a theoretical kinetic model for the formation and destruction of dioxins and furans in combustion and co-combustion processes with coal and different types of wastes. For this work, experimental results obtained in a European project funded by the 6th EU Framework Programme were used. The project entitled COPOWER - "Synergy Effects of Co-Processing of Biomass with Coal and Non-Toxic Wastes for Heat and Power Generation" was coordinated by the National Institute of Engineering Technology and Innovation (INETI) through the Department of Energy Engineering and Environmental Control, with the collaboration of the Faculty of Sciences and Technology of the University Nova of Lisbon through the Unit of Environmental Biotechnology, among other European participating entities.

Various mixtures of different types of wastes and biomasses were studied, mixed and non-mixed with two types of coal (Colombian and Polish), having determined the levels of emissions of dioxins and furans for mixtures containing MBM and straw as biomassic materials. These mixtures were selected based on Chlorine and Sulphur compositions present in the mixtures, expected to lead to different kinds of synergies related to the presence of those elements that would have an impact on the reactions' mechanisms. The project was proven successful in immediate terms, as it introduced a new perspective in the context of multi-fuel systems which could avoid the dependence on any one fuel for energy production. The studies aimed at improving the knowledge for fuel blending. Combinations of coal, biomass and waste were tried and the results show that multi-fuel use could lead to overcoming many problems like reducing heavy metal vaporisation by the presence of S and Cl. It was also identified beneficial effects of fixing mainly sulphur and chlorine, in the ashes rather than their emissions to the atmosphere. Thus, the combination of high S fuels with high Cl ones could have beneficial effect on suppressing dioxin emissions.

Furthermore, fifteen positive synergies were identified in the co-combustion of fuel blends while only five negative synergies were found. At present, it gives the opportunity to investigate further on the mechanisms of formation and destruction of chemical species like dioxins and furans, essential to identify parameters that can be used to control their emissions.

Not only the data produced during the course of work were used but also results from other combustion tests using rice husk and a different mixture from those used in the COPOWER project studies, with straw and Colombian coal. The sampling of the stack-gas emissions, as well as the implementation and validation of PCDD/F sampling, was done by the author, who contributed to the experimental runs including planning of the experiments. These studies were previously analysed and validated for publication, with a significant contribution by the author to the writing of the papers submitted to international journals and conferences. These publications are listed below:

Paper 1 - Lopes M. Helena, Gulyurtlu I., Abelha P., Teixeira P., Crujeira T., Boavida D., Marques F., Cabrita I., (2006) "Co-combustion for Fossil Fuel Replacement and Better Environment", Proceedings of the 7th European Conference on Industrial Boilers and Furnaces, April, Porto, Portugal, Paper Infub_92; ISBN 972-99309-1-0.

Paper 2 - Gulyurtlu, I., Lopes, H., Crujeira, T., Boavida, D., Abelha, P., (2007a) "COPOWER - Co-Firing of Biomass and other Wastes in Fluidised Bed Systems", Proceedings of the International Conference on Coal Science and Technology, August 28 – 31, Nottingham, United Kingdom.

Paper 3 - Crujeira T., Lopes H., Abelha P., Cabrita I., Gulyurtlu I., (2007) "Minimization of Flue Gas Emissions Produced by Co-combustion with Biomass and Wastes" (paper in Portuguese), Proceedings of the 9th National Environmental Conference, April 18 – 20, Aveiro, Portugal, Ed. Borrego, C. *et al.,* pp. 723-731; ISBN 978-972-789-230-3.

Paper 4 - Gulyurtlu I., Abelha P., Lopes H., Crujeira A., Cabrita I., (2007b) "Considerations on Valorization of Biomass Origin Materials in Co-combustion with Coal in Fluidized Bed", Proceedings of the 3rd International Conference on Clean Coal Technologies for Our Future, May 15 – 17, Sardinia, Italy.

Paper 5 - Gulyurtlu I., Crujeira A. T., Abelha P., Cabrita I., (2007c) "Measurements of dioxin emissions during co-firing in a fluidised bed", Fuel 86, pp. 2090–2100; DOI:10.1016/j.fuel.2007.01.037.

Paper 6 - Crujeira, T., Gulyurtlu, I., Lopes, H., Abelha, P., Cabrita, I., (2008) "Bioenergy originating from biomass combustion in a fluidized bed", Proceedings of the International Conference and Exhibition on Bioenergy - Bioenergy: Challenges and Opportunities, April 6 – 9, Minho University, Guimarães, Portugal.

Paper 7 – Abelha P., Gulyurtlu I., Crujeira T., Cabrita I., (2008) "Co-Combustion of Several Biomass Materials with a Bituminous Coal in a Circulating Fluidised Bed Combustor", Proceedings of 9th International Conference on Circulating Fluidized Beds, May 13–16, Hamburg, Germany.

Paper 8 - Lopes H., Gulyurtlu I., Abelha P., Crujeira T., Salema D., Freire M., Pereira R., Cabrita I., (2009) "Particulate and PCDD/F emissions from coal co-firing with solid biofuels in a bubbling fluidised bed reactor", Fuel 88, pp. 2373-2384; DOI:10.1016/j.fuel.2009.02.024.

Paper 9 - Crujeira T., Moreira L., Cabrita I., Gulyurtlu I., (2013) , "PCDD/F formation in the co-combustion of biomass and coal: the influence of chlorine, copper, calcium and sulphur", Proceedings of the 1st International Congress on Bioenergy, 23-25 May, Portalegre, Portugal, ISBN 978-989-98406-2-1.

2. Introduction

2.1 Energy Outlook

In the last century the use of fossil fuels as energy source, namely oil, coal and natural gas, allowed a significant increase in economic, scientific and technical development. More recently, the sustainability of the energy systems and the environmental concerns due to the fossil fuels combustion emissions are key issues to tackle. In 2011, oil reserves were estimated to last for 54.2 years, natural gas for 63.6 years and coal for 112 years (BP, 2012) considering that consumption would be maintained at 2011's rate.

Coal and peat accounted in 1973's world energy balance with 24.6 %, contribution that increased in 2010 to 27.3% (IEA, 2012). Projections to 2015 depend upon the success of policy implementation towards near-zero emissions and the technical and economic progress on carbon capture, use and sequestration technologies; however, coal is expected to continue having a significant role, especially in the power sector (IEA, 2010).

World Energy Outlook (WEO, 2011) considers three scenarios for the world primary energy demand, depending on assumptions made with regard to policy orientations. The "*New Policies*" Scenario takes into account existing government policies and declared policy intentions; the "*Current Policies*" Scenario is a "*Business-as-usual*" scenario that considers existing government policies and measures enacted or adopted by mid-2011, considering that they remain unchanged; the third Scenario is an Outcome-driven Scenario, which considers a 50% chance of limiting the increase in the average global temperature to 2°C. This last scenario is the most stringent one, which would require a concentration of greenhouse gases in the atmosphere to be limited to about 450 ppm of CO_2-eq (*i.e.* carbon dioxide equivalent) on a long-term basis.

In the *New Policies* Scenario, world primary energy demand is projected to increase at a rate of 1.3% per year, from 12 150 million tonnes of oil equivalent (Mtoe) in 2009 to 16 950 Mtoe in 2035, leading to a 40% overall increase (Figure 2.1). Coal is projected to have a share of 28% in the overall demand by 2035, compared to a 27% contribution in the year 2009.

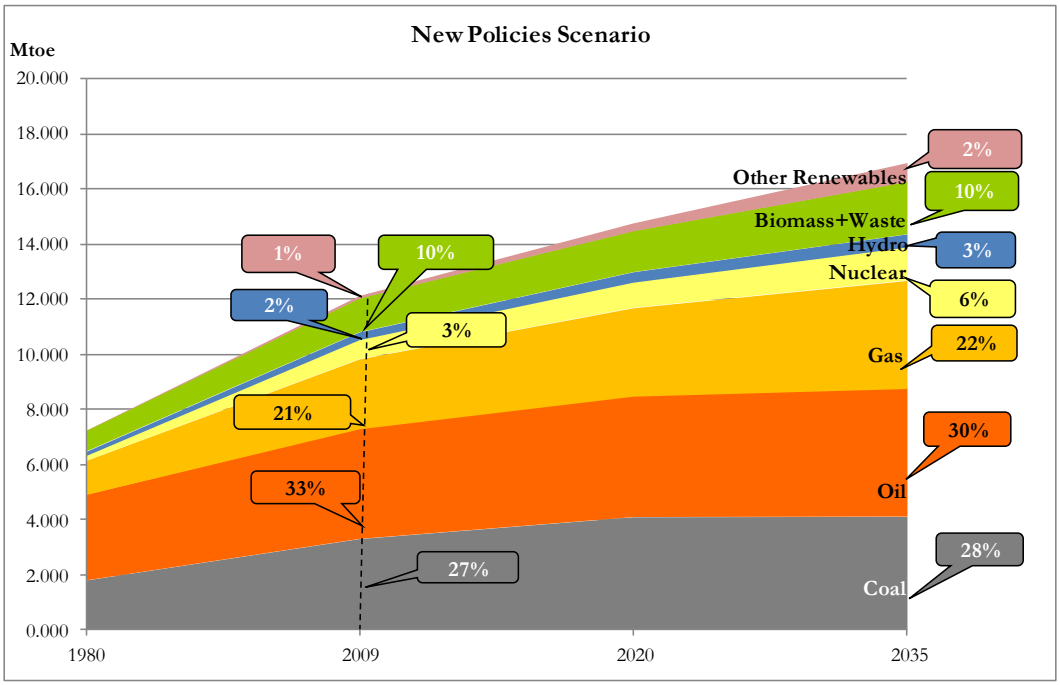

Figure 2.1 - World Primary Energy Demand Growth projected in the IEA "*New Policies*" Scenario (WEO, 2011).

Figure 2.2 shows the global energy demand in the Current Policies Scenario, showing a faster increase in the overall primary energy demand (1.6% per year), reaching 18 300 Mtoe in 2035, 51% higher than demand in 2009.

In the "450 ppm targeted" Scenario, illustrated in Figure 2.3, the global energy demand still increases between 2009 and 2035, reaching 14 850 Mtoe in 2035, which represents a global increase of 23%, *i.e.* 0.8% per year. In 2035, energy demand is 9% lower than in the *Current Policies* Scenario and more than 12% lower than in the *New Policies* Scenario.

The differences accounted in the three scenarios are basically related to the extent to which policies are implemented to improve energy efficiency. In terms of the use of coal, its share increases to 30% in the *Current Policies* Scenario; however, in the more stringent Greenhouse gases' emissions scenario, Figure 7.3 shows a lower share for coal contribution in the overall balance, of 16%.

In all scenarios, fossil fuels (coal, oil and natural gas) remain the dominant sources of energy in 2035, varying each share in the energy mix.

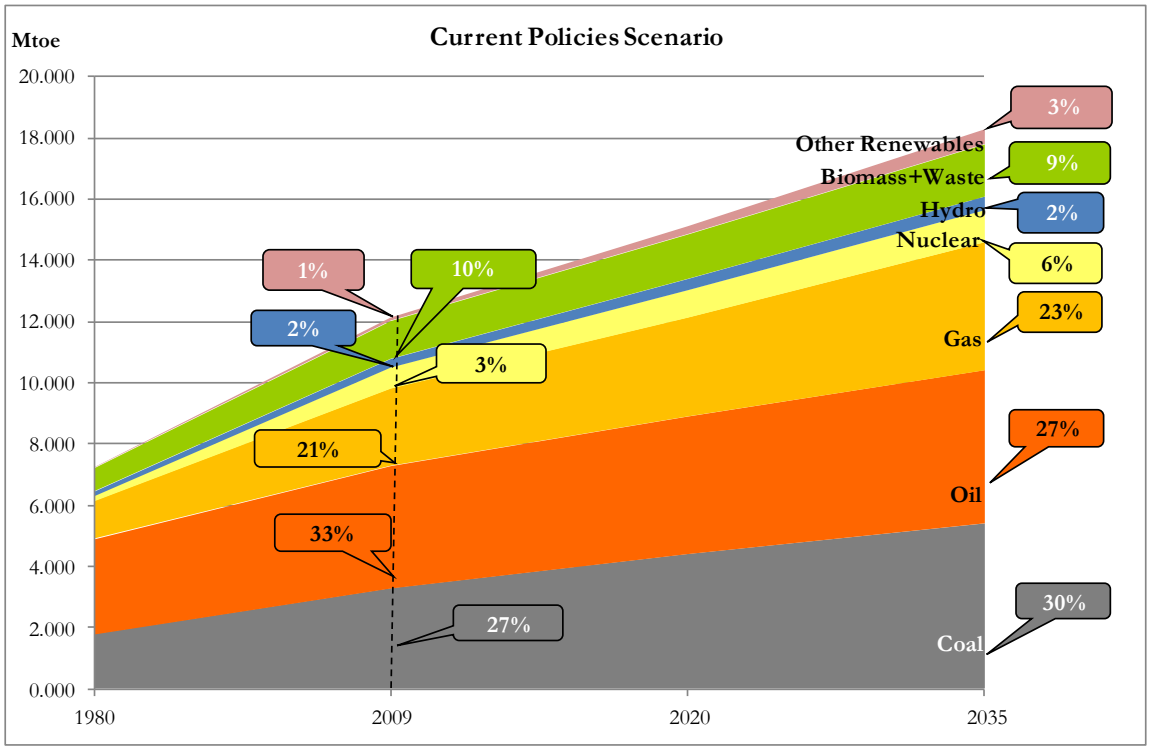

Figure 2.2 - World Primary Energy Demand Growth projected in the IEA "*Current Policies*" Scenario (WEO, 2011).

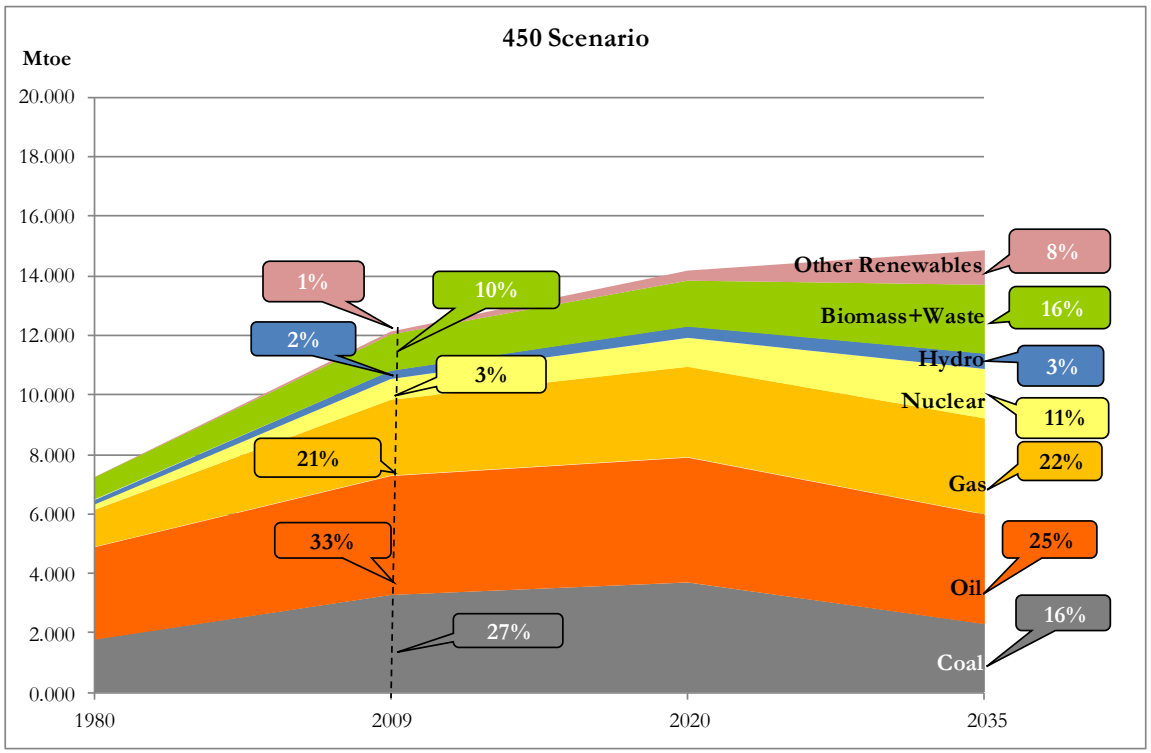

Figure 2.3 - World Primary Energy Demand Growth projected in the IEA "450 parts per million targeted" Scenario (WEO, 2011).

The share of fossil fuels decreases from 81% of world primary energy supply in 2009 to:

- 80%, in 2035, in the *Current Policies* Scenario;
- 75%, in 2035, in the *New Policies* Scenario;
- 62%, in 2035, in the "450" Scenario.

Coal is projected to account in all scenarios with more than 16%, competing strongly with other resources. However, coal use is seen worldwide as having a significant environmental impact.

From 1990 to 2006, the world carbon emissions had an increase of 30% (Rühl, 2007). The world average carbon intensity between 1971 and 1999 decreased from 0.82 to 0.745 ton carbon/ton primary energy and, in 2006, was 0.76 ton carbon/ton primary energy; over the same period, China's carbon intensity decreased from 1.02 to 0.95 ton carbon/ton primary energy.

Portugal is a country with scarce endogeneous energy fossil resources. Portugal faces a high energy dependency from foreign countries through the import of primary resources (76.6% in 2010) (DGEG, 2012). Since 2005, these imports have been decreasing through the higher contribution of renewable energy resources such as hydro, wind, solar, geothermic and biomass to the Portuguese fuel mix.

In 2010, oil still represented 49.1% of the total primary energy consumption (-0.4% than in 2009) wheras natural gas contribution rose to 19.7% in 2010 (+1.8% than in 2009). Coal's share was 7.2% and renewables rose to 23.1% (+3.1% than in 2009) (DGEG, 2012).

The installed capacity for electricity production from RES reached 9777.98 MW in 2010, with 784.5 MW being from biomass (DGEG, 2012).

In 2010, the electricity production from RES reached 29566 GWh (DGEG, 2012), distributed as presented in Figure 2.4.

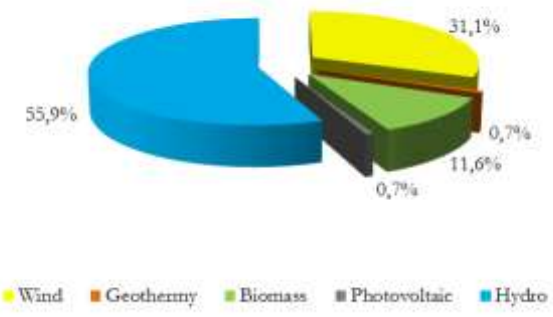

Figure 2.4 – Electricity from RES in Portugal, 2010 (from DGEG, 2012).

Looking into the Portuguese final energy consumption, it reached 17 276 ktoe in 2010 (DGEG, 2012), with the distribution of sources illustrated in Figure 2.5.

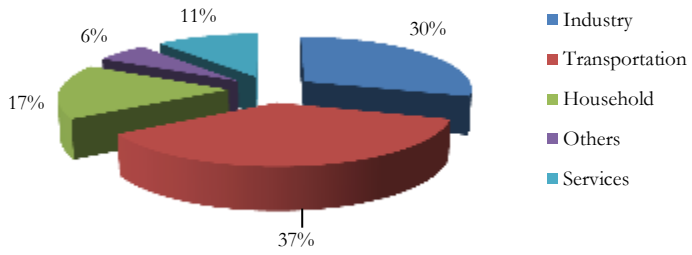

Figure 2.5 – Portuguese final energy consumption, 2010 (from DGEG, 2012).

2.2 Environmental concerns and legislation

Environmental quality has been the original driver for environmental legislation, including in Europe. In fact, the deterioration in air quality led authorities to find a way to reduce ambient concentrations of pollutants. Recently, a technology driven approach was introduced, which enables a progressive reduction in emissions resulting from the developments in improving control technologies. In Europe the concept introduced is the Best Available Technology (BAT) and in the United States of America is the Maximum Achievable Control Technology (MACT). Both mechanisms are based on a technology driven approach.

Legislation has been published around the world with the objective of eliminating environmental degradation. Most of it imposes emissions' limits for industrial processes. In accordance with the severity of the environmental impact of the various processes, countries establish their own targets and define mechanisms to guarantee a better environmental control. These can be grouped as follows (Sloss *et al.*, 2003):

Emission limits

The establishment of emissions limits are generally linked to ambient pollution concentrations. These limits are based on epidemiological data, ambient air quality and ambient air quality standards.

Cap and trade

This is a regulatory approach which recognizes that allowing the market to find its own means of emission reduction may be more cost effective than strict emission limits. The CO_2 market is an example.

Best Available Technologies (BAT) and Maximum Achievable Control Technologies (MACT)

Much of the existing legislation, such as that for SO_2 and NO_x in Europe and the United States, includes requirements for Best Available Technologies (BAT) or Maximum Achievable Control Technologies (MACT). It is generally recognized that BAT for individual sources may be different, due to the technical characteristics of the installations, the geographical location and local environmental conditions. In Europe, the European Integrated Pollution Prevention and Control Bureau (EIPPCB, 2013) exists to catalyse an exchange of technical information on BAT and to create BAT Reference documents (BREFs).

Integrated pollution prevention and control (IPPC)

This technology based approach goes further than the implementation of BAT/MACT. The main goal of the 'IPPC' is the integration and the prevention of pollution, including not only management and organization issues, but also focusing in energy efficiency. The application of the IPPC Directive to all existing plants in Europe was required by 2007, at the latest. Although, following the BAT was not mandatory, the recent recast of the IPPC is pointing to stricter emissions limits, forcing industry to apply the BAT existing in each moment, in order to achieve lower pollutant emissions to the atmosphere.

Economic mechanisms

The payment of financial penalties (fines) are commonly based on the Polluter Pays Principle, and are a way of penalizing sources for non-compliance with emission legislation.

Given the importance of international organizations' role like the United Nations, as well as the role that some countries can play like the European Union and the United States of America for their leadership and dimension, information about policies undertaken are presented below. In this context, it is also important to look at countries like India and China that can have a significant impact on the environment in terms of dimension related to their contribution within the scope of the energy sector. Information on these countries' strategies is also presented.

2.2.1 United Nations

The United Nations (UN) has several protocols and programmes considering environmental protection, which member countries decide whether or not to sign and/or to ratify on an individual basis.

The Chemicals branch of the United Nations Environment Programme (UNEP) works to protect humans and the environment from adverse effects caused by chemicals throughout their lifecycle, and includes hazardous waste. It is the focal point of UNEP activities chemicals issues and this

programme is the main catalytic force in the UN system for concerted global action on the environmentally sound management of hazardous chemicals (UNEP, 2013).

Some highlights of the work performed related to heavy metals' enissions are presented below.

In the case of mercury, in 2001, UNEP undertook a global assessment of emissions and mercury compounds. A Global Mercury Assessment report was published in December 2002 (GMA, 2002). There was sufficient evidence of significant global adverse impacts from mercury and its compounds to warrant further international action to reduce the risks to human health and to the environment. It was requested to UNEP to initiate technical assistance and capacity building activities to support the efforts of countries to take action regarding mercury pollution. In response to this request, UNEP established a mercury programme within UNEP Chemicals.

In the case of Lead and Cadmium, UNEP also undertook a number of activities related to these emissions. In 2005/2006, UNEP Chemical's work plan focused its activities towards developing reviews of scientific information on lead and cadmium, focusing especially on long-range environmental transport.

In a sectorial manner, the United Nations Economic Commission for Europe (UNECE) designs regulations to safeguard the environment and human health, whilst promoting sustainable development in its member states.

In 1979, it was launched the Convention on Long-Range Transboundary Air Pollution (CLRTAP), which since then addressed major environmental problems of the UNECE region through scientific collaboration and policy negotiation. The Convention has been extended by eight protocols, presented in Table 2.1, which identify specific measures to be taken by 51 Parties at the moment, to cut their emissions of air pollutants. The aim of the Convention is that Parties shall endeavor to limit and, as far as possible, gradually reduce and prevent air pollution including long-range transboundary air pollution. Parties develop policies and strategies to combat the discharge of air pollutants through exchanges of information, consultation, research and monitoring.

Table 2.1 - Protocols of the Convention on Long-Range Transboundary Air Pollution (CLRTAP).

Date	Protocol	N. Parties	Entrance in force
1984	Long-term Financing of the Cooperative Programme for Monitoring and Evaluation of the Long-range Transmission of Air Pollutants in Europe (EMEP)	42	28/01/1988
1985	Reduction of Sulphur Emissions or their Transboundary Fluxes by at least 30 per cent.	23	02/09/1987
1988	Control of Nitrogen Oxides or their Transboundary Fluxe	32	14/02/1991
1991	Control of Emissions of Volatile Organic Compounds or their Transboundary Fluxes	23	29/09/1997
1994	Further Reduction of Sulphur Emissions	27	05/08/1998
1998	Persistent Organic Pollutants (POPs), 1998 Aarhus Protocol on POPs	29	23/10/2003
	Protocol on Heavy Metals, known as the 1998 Aarhus Protocol on Heavy Metals	29	29/12/2003
1998	Protocol to Abate Acidification, Eutrophication and Ground-level Ozone, 1999 Gothenburg Protocol	24	17/05/2005

Within the scope of CLRTAP it was created the EMEP - European Monitoring and Evaluation Programme (EMEP, 2008), in order to "*regularly provide Governments and subsidiary bodies under the LRTAP Convention with qualified scientific information to support the development and further evaluation of the international protocols on emission reductions negotiated within the Convention*".

The EMEP Programme action includes the collection of emission data, measurements of air and precipitation quality and modelling of atmospheric transport and deposition of air pollution.

Another mechanism that is important to consider is the Intergovernmental Panel on Climate Change (IPCC) that was established to provide decision makers and others interested entities in climate change with an objective source of information about climate change (IPCC, 2013). This UN's top scientific body, set in 1988, by the United Nations Environment Programme (UNEP) and the World Meteorological Organization (WMO), is a scientific inter-governmental body.

The IPCC does not conduct any research nor monitors climate related data or parameters. Its role is to assess on a comprehensive, objective, open and transparent basis to the latest scientific, technical and socio-economic literature produced worldwide relevant to understanding the risk of human-induced climate change.

The findings of the first IPCC Assessment Report of 1990 played a decisive role in leading to the United Nations Framework Convention on Climate Change (UNFCCC), which was opened for signature in the Rio de Janeiro Summit in 1992 and entered into force in 1994. It provided the overall policy framework for addressing the climate change issue. The IPCC Second Assessment Report of 1995 provided key input for the negotiations of the Kyoto Protocol in 1997 and the Third Assessment Report of 2001, as well as the Special and Methodology Reports provided further information relevant for the development of the UNFCCC and the Kyoto Protocol.

In 2007 it was released the Fourth Assessment Report, which represents the IPCC's most comprehensive and definitive statement to date on climate change. The main conclusions are (IPCC, 2013):

a) There is strong certainty that most of the observed warming of the past half-century is due to human influences, and a clear relationship between the growth in manmade greenhouse gas emissions and the observed impacts of climate change;
b) The climate system is more vulnerable to abrupt or irreversible changes than previously thought;
c) Avoiding the most serious impacts of climate change, i.e. including irreversible changes, will require significant reductions in greenhouse gas emissions;
d) Mitigation efforts must also be combined with adaptation measures to minimize the risks of climate change.

The Fifth Assessment Report (AR5) is expected between released in four parts between September 2013 and November 2014 and will be the most comprehensive assessment of scientific knowledge on climate change since 2007.
The IPCC continues to be a major source of information for the negotiations under the UNFCCC.

2.2.2 European Union

The industrial energy sector is one of the major contributors for the emission of most atmospheric pollutants. In order to achieve a reduction of the environmental impact of the industrial energy sector, legislation initiatives have been promoted both at a National and European levels. However, legislation to be applied with success need to be both technical and economically applicable, to guarantee the environmental benefits without the need to close industrial units, which will have a very negative social impact. Flexible goals and voluntary agreements have proved to be successfull as it allows adequate adaptations of each involved partner ensuring the maintenance of their competitiveness. Alternatively, the definition of incentives also have been leading to good results in terms of compliance wit restricted emnission limits, which most likely will lead to environmental benefits.
Considering that one of the main goals of the European Union is the protection of the environment, as presented in the *Article 175 EC*, the European Parliament and Council aim at the definition of a comprehensive legal framework for the reduction of industrial emissions. The most recent approach has been the definition of a simplified model, which combines several formerly existing directives into a single document (Directive 2010/75/EC).
Setting up goals with the objective to improve ambient air quality, should also consider harmonization within Europe with the definition of common analysis methods and evaluation criteria. This can provide enough information on air quality, ensuring that the information provided on air quality status is exact, together with emergency alerts when any pollutant exceeds its predefined maximum levels.
A detailed collection of the most recent European Union directives that are related with environmental protection and improvement of air quality is presented below.

Directive 96/62/EC, 27 September 1996: Ambient air quality assessment and management

This directive was applied in the initial stage to pollutants like SO_2, NO_x, fine particulate matter, Lead and Ozone. Other air pollutants to be controlled include Benzene, Carbon monoxide, Poly-aromatic hydrocarbons and other elements like Cadmium, Arsenic, Nickel and Mercury. These limit levels must consider the specific conditions of each zone like the

population density, climatic conditions, sensitivity of flora and fauna, the possibility of long-range transport and the economic and technical feasibility.

Directive 1999/13/EC (*VOC Directive*), 11 March 1999: Limitation of emissions of volatile organic compounds due to the use of organic solvents in certain activities and installations

This Directive aims the prevention and reduction of the effects and risks to human health of emissions into air of Volatile Organic Compounds ("VOCs"). It applies to a large range of industries using solvents.

Directive 1999/30/EC, 22 April 1999: Limit values for sulphur dioxide, nitrogen dioxide and oxides of nitrogen, particulate matter and lead in ambient air

This Directive establishes the emission limits and threshold levels required to the prevention and reduction of the effects and risks to human health. It defines the maximum concentrations of each of these pollutants, with regard to different averaging periods between 1 hour and 1 calendar year.

Directive 2000/76/EC (*Waste Incineration Directive*), 4 December 2000: The incineration of waste

This Directive extends previously existing legislation on non-hazardous municipal waste, to the incineration of non-hazardous non-municipal waste (like sewage sludge, tyres and hospital waste) and hazardous wastes like waste oils and solvents.

Directive 2001/80/EC (*LCP Directive*), 23 October 2001: Limitation of emissions of certain pollutants into the air from large combustion plants

This Directive applies to combustion plants with more than 50 MW of thermal input, using solid, liquid or gaseous fuels. It contains detailed tables for limits of SO_2, NO_X and dust emissions that will be applied to new or existing plants. These limits depend mainly on the kind of fuel (solid, liquid or gaseous) or fuels obtained from other industrial processes like the gasification of coal, biomass or refinery residues. Some exceptions are also made for some European Countries and for some specific industrial units. The Directive defines also the procedures for measuring and evaluating emissions and for the determination of total annual emissions from combustion plants.

Directive 2004/107/EC, 15 December 2004: Limitation of emissions of arsenic, cadmium, mercury, nickel and polycyclic aromatic hydrocarbons in ambient air

Following previous scientific evidence on the genotoxic carcinogenic effects on humans of arsenic, cadmium, mercury, nickel and polycyclic aromatic hydrocarbons (PAHs), this directive establishes maximum levels to be accepted on ambient air.

Directive 2008/1/EC (*IPPC directive*), 15 January 2008: Codification of the existent

The codified act includes all the previous amendments to the Directive 96/61/EC and introduces some linguistic changes and adaptations. EPER, the European Pollutant Emission Register was implemented after the Directive 96/61/EC was approved, and today it is possible to consult emissions' data for the years 2001 and 2004 (EPER, 2013).

Directive 2008/50/EC (*CAFE*), 21 May 2008: Ambient air quality and cleaner air for Europe

This directive defines objectives for ambient air quality in order to avoid, prevent or reduce harmful effects on human health and the environment. It defines common methods for assessment of emission levels in Member States, providing for a continuous monitoring of air quality, while improving the results through national and Community measures.

The air quality objectives must include data on SO_2, NO_X, CO, benzene, ozone and particulate matter.

Directive 2009/28/EC, 2 April 2009: Promotion of the use of energy from renewable sources

This Directive establishes a common framework for the promotion of energy from renewable sources It sets mandatory national targets for the overall share of energy from renewable sources in gross final consumption of energy and for the share of energy from renewable sources in transport. It lays down rules relating to statistical transfers between Member States, joint projects between Member States and with third countries, guarantees of origin, administrative procedures, information and training, and access to the electricity grid for energy from renewable sources. Also establishes sustainability criteria for biofuels and bioliquids.

The Portuguese target for share of energy from renewable sources in gross final consumption of energy in 2020 was established in 31%.

Directive 2010/75/EU (*Industrial Emissions Directive*), 24 November 2010: Recast

This Directive brings together Directive 2008/1/EC (the 'IPPC Directive') and six other directives[1] in a single directive on industrial emissions.

This Directive shall cover industrial activities with a major pollution potential, defined in Annex I of the Directive, *i.e.* energy industries, production and processing of metals,

[1] Directive 1999/13/EC (*VOC Directive*), Directive 2000/76/EC (*Waste Incineration Directive*), Directive 2001/80/EC (*LCP Directive*), and Directives 78/176/EEC, 82/883/EEC and 92/112/EEC (*Titanium Dioxide Directives*).

mineral industry, chemical industry, waste management, rearing of animals, etc, containing special provisions for the following installations:

- combustion plants (≥ 50 MW);
- waste incineration or co-incineration plants;
- certain installations and activities using organic solvents;
- installations producing titanium dioxide.

In addition to the directives stated above that led to a more stringent control of pollutant emissions from combustion technologies, in 10th January 2007, the European Commission proposed a European Strategy for Energy and Climate Change, the EU Energy/Climate Package 20-20-20, with the following targets (Reference year: 1990):

- increase Renewable Energy Sources share to 20% in EU power production;
- increase by 20% the Energy Efficiency;
- decrease by 20% the GHG emissions.

2.2.3 United States

In the case of United States of America, both mining and industrial activities are very significant when considering coal combustion systems.

More than one billion tonnes of coal per year is currently mined in the United States, with well over 900 million tons used domestically. About 90% of all coal consumed in the U.S. is used for electricity generation, representing more than half of all domestic electricity production. As electricity demand is anticipated to grow by nearly 1.8% annually over the next 20 years, by the year 2025 more than 100 GW of new coal-fired steam-electric generation is expected (Feeley III, 2005). While electricity generation by advanced systems will probably increase, U. S. will continue to rely on the existing pulverized coal fired power plants. These units (nearly 320 GW capacity) currently generate over 1,900 billion kWh per year of electricity and represent the base load supply of energy.

Power generation is responsible for 63% of sulphur dioxide (SO_2), 22% of nitrogen oxides (NO_x), and 37% of mercury released to the environment by human activity. Once released, these pollutants, together with the gases and particles, can travel long distances before being deposited or can react in the atmosphere forming more hazardous compounds.

Air Pollution Control mechanisms are presented below.

Clean Air Act (CAA)

The Air Pollution Control Act of 1955 was the first federal legislation involving air pollution and gave funds for federal research in this domain. The enactment of the Clean Air Act of 1970 (1970

CAA) resulted in a major shift in the federal government role in air pollution control. This legislation allowed the development of comprehensive federal and state regulations to limit emissions from both stationary (industrial) sources and mobile sources. Four major regulatory programmes affecting stationary sources were initiated: the National Ambient Air Quality Standards (NAAQS), State Implementation Plans (SIPs), New Source Performance Standards (NSPS) and National Emission Standards for Hazardous Air Pollutants (NESHAPs). The adoption of this very important legislation occurred at approximately the same time as the National Environmental Policy Act that established the U.S. Environmental Protection Agency (EPA). EPA was created in 1971 to implement the various requirements, which included the Clean Air Act of 1970.
In 1977 and 1990 several amendments were introduced. The milestones in the evolution of the Clean Air Act (EPA CAA, 1990) are presented in Table 2.2.

Table 2.2 - Milestones in the evolution of the Clean Air Act (EPA CAA, 1990).

Title	Milestones
The Air Pollution Control Act of 1955	- First federal air pollution legislation - Funded research for scope and sources of air pollution
Clean Air Act of 1963	- Authorized the development of a national program to address air pollution related environmental problems - Authorized research into techniques to minimize air pollution
Air Quality Act of 1967	- Authorized enforcement procedures for air pollution problems involving interstate transport of pollutants - Authorized expanded research activities
Clean Air Act 1970	- Authorized the establishment of National Ambient Air Quality Standards (NAAQS) - Established requirements for State Implementation Plans to achieve the National Ambient Air Quality Standards - Authorized the establishment of New Source Performance Standards for new and modified stationary sources - Authorized the establishment of National Emission Standards for Hazardous Air Pollutants - Increased enforcement authority - Authorized requirements for control of motor vehicle emissions
1977 Amendments to the Clean Air Act of 1970	- Authorized provisions related to the Prevention of Significant Deterioration - Authorized provisions relating to areas which are non-attainment with respect to the National Ambient Air Quality Standards
1990 Amendments to the Clean Air Act of 1970	- Authorized programs for Acid Deposition Control - Authorized a program to control 189 toxic pollutants, including those previously regulated by the National Emission Standards for Hazardous Air Pollutants - Established permit program requirements - Expanded and modified provisions concerning the attainment of National Ambient Air Quality Standards - Expanded and modified enforcement authority

With this mechanism, it was possible to reduce emissions of sulphur dioxide (SO_2), nitrogen oxides (NO_x), and particulate matter (PM) from coal-fired power plants. For example, full implementation of the acid rain provision of the 1990 CAA Amendments (Title IV) provides an annual cap on power plant SO_2 emissions of 8.9 million tonnes, in comparison to the 16 million tonnes in 1970. In addition, NO_x emissions have been reduced from 6.0 million tons in 1996 to 4.2 million tonnes

in 2003. In addition, the annual emissions of particulates smaller than 10 micrometers (PM10) in 2003 were less than 250,000 tonnes, compared with early 1970 emissions that exceeded 1.6 million tons (EPA CAR, 2004).

New Source Performance Standards (NSPS)

New Source Performance Standards (NSPS) are pollution control standards issued by the United States Environmental Protection Agency (EPA), and can be found in the 40 Code of Federal Regulations (CFR) Part 60. NSPS is used in the Clean Air Act Extension of 1970 (CAA) and refer to air pollution emission standards.

Coal-fired electric utility boilers built or modified after August, 1971, must comply with a New Source Performance Standard (NSPS) limit on primary particulate emissions of 0.10 lb/million Btu (*i.e.* 0.043 mg/kJ). Plants built or modified after September, 1978, must comply with a more severe NSPS of 0.03 lb/million Btu (*i.e.* 0.013 mg/kJ), or 1 percent of the potential combustion concentration (99 percent reduction). Average primary particulate emissions from all coal fired utility boilers are about 0.043 lb/million Btu (*i.e.* 0.018 mg/kJ). Airborne particles are also regulated as "criteria pollutants" under EPA's National Ambient Air Quality Standards (NAAQS) programme, so the emissions of primary PM10 (particles smaller than 10 μm) and PM2.5 (particles smaller than 2.5 μm) from coal power plants are also subjected to limitations set forth under State Implementation Plans (SIPs) for achieving the ambient standards for these pollutants.

EPA may also consider additional restrictions on SO_2 and NO_x, as a result of their potential to form secondary fine particles. The current regulations applicable to air emissions of gaseous SO_2 and NO_x are summarized in Table 2.3 and depend on built or modifications made in the unit.

Table 2.3 - Current regulations applicable to air emissions of gaseous SO_2 and NO_x (CFR, 2013).

Unit built or modified on or after	**Pollutant**	**Emission limit ($lb/10^6$ Btu)**	**% reduction of Potential Combustion Concentration**
17/08/1971	SO_2	1.2	N/A
	NO_x derived from lignite	0.6	N/A
	NO_x derived from anthracite, bituminous, or sub-bituminous coals	0.7	N/A
	NO_x derived from ND, SD or MT lignite and burned in cyclone boilers	0.8	N/A
18/09/1978	SO_2	1.2	90
	NO_x derived from sub-bituminous coals	0.5	65
	NO_x derived from anthracite or bituminous coals	0.6	65
	NO_x derived from ND, SD or MT lignite and burned in slag tap furnaces	0.8	65
Modified After 09/07/1997	SO_2	1.2	90
	NO_x	0.15	N/A
Modified After 09/07/1997	SO_2	1.2	90
	NO_x	1.6 lb/MWh(*)	N/A

(*) Gross energy output basis

Clean Air Rules of 2004

In 2004, the Clean Air Rules present sets of actions with the global aim of improving air quality. Three of the rules specifically address the transport of pollution across state borders (the Clean Air Interstate Rule, Clean Air Mercury Rule and Clean Air Nonroad Diesel Rule). These rules are considered national tools to achieve a better air quality and the associated benefits of improved health, longevity and quality of life. The Clean Air Rules of 2004 cover the following major rules (EPA CAR, 2004):

- Clean Air Interstate Rule
- Mercury Rule
- Nonroad Diesel Rule
- Ozone Rules
- Fine Particle Rules

Clean Air Interstate Rule (CAIR)

The "CAIR" Rule, originally proposed as the Interstate Air Quality Rule, takes into consideration the pollution related to emissions of sulphur dioxide (SO_2) and nitrogen oxides (NO_x) that flows from one State to another, across 28 Eastern States and the District of Columbia Andis.

Clean Air Mercury Rule (CAMR)[2]

Mercury is a toxic, persistent pollutant that accumulates in the food chain. Mercury in air is a global problem. While fossil fuel-fired power plants are the largest remaining source of human generated mercury emissions in the United States, they contribute only to a small amount (about 1 percent) of total annual mercury emissions worldwide.

EPA issued the Clean Air Mercury Rule (originally proposed as the Utility Mercury Reductions Rule) on March, 2005 to reduce mercury emissions from coal-fired power plants. The implementation of these

Fine Particle Rules

The Clean Air Fine Particle Rules (dealing with PM 2.5 designations and implementation) appoint those areas whose air does not meet the health-based standards for fine particulate pollution. This requires States to submit plans for reducing the levels of particulate pollution in areas where the fine-particle standards are not met.

Clear Skies Initiative

[2]On February 8, 2008, the D.C. Circuit vacated EPA's rule removing power plants from the Clean Air Act list of sources

The new Clear Skies Initiative (EPA CSI, 2003) sets targets for power plant emissions reductions of sulphur dioxide (SO_2), nitrogen oxides (NO_x), and mercury by setting a national cap on each pollutant (see Table 2.4).

NO_x and SO_2 requirements affect all fossil fuel-fired power plants above 25 MW. Mercury requirements affect only coal-fired plants, also above 25 MW.

Table 2.4 - Evolution of reduction targets of Clear Skies initiative.

	Actual Emissions in 2000	**1st Phase**	**2nd Phase**	**Reduction at Full Implementation**
SO_2	11.2 million tons	4.5 million tons in 2010(1)	3 million tons in 2018(1)	73%
NO_x(2)	5.1 million tons	2.1 million tons in 2008(1)	1.7 million tons in 2018(1)	67%
Mercury	48 tons	26 tons in 2010	15 tons in 2018(1)	69%

2.2.4 India

Coal has been recognized as the most important source of energy for electricity generation in India. About 75% of the coal in the country is consumed in the power sector. By the end of March 2006, electricity generating capacity of India was 124287 MW, in which thermal power generation capacity had a share of 82411 MW, representing 66.3% of the global consumption (CEA, 2008). India's electricity sector was predominantly public and in 1991 been developed by the public sector and thegovernment opened in 1991 this sector to private participation. . In four decades, nearly 65MW of capacity were commissioned (Topper, 2003). From these, over 70% was coal-fired (Perkins, 2005).

The Particulate Matter (PM) emission limits for thermal power stations established in the Environment (Protection) Act 1986 (CPCB, 2008) were amended by MoEF (Notification of 19th May 1993) to the limits presented in Table 2.5.

Table 2.5 - Particulate Matter Emission Limits (CPCB, 2008).

Generation Capacity	**PM Emission Limit**
Generation capacity 62.5 MW or more	150 mg/Nm^3
Generation capacity less than 62.5 MW and plant Commissioned prior to 1.1.82	350 mg/Nm^3
Units located in protected area irrespective of generation capacity	150 mg/Nm^3

In India, the Central Pollution Control Board (CPCB), of the Ministry of Environment and Forests (MoEF), constituted in 1974, entrusted with the powers and functions under the Air (Prevention and Control of Pollution) Act, 1981, to improve the quality of air. In 1987 the Air (Prevention and

Control of Pollution) Act was amended but no standards were published to impose restrictions on NO_x and SO_2 by MoEF for coal/lignite fired thermal power stations. However, to ensure wider dispersal of SO_2, stack heights were notified by MoEF for different capacity units. These are presented in Table 2.6.

Table 2.6 - Minimum Stack Height (CPCB, 2008).

Generation Capacity	**Stack Height (m)**
500 MW and above	275
200 MW/210 MW and above to less than 500 MW	220
Less than 200 MW/210 MW	$H= 14(Q)^{0.3}$ where Q is emission rate of SO_2 in kg/h, and H is Stack height in meters

2.2.5 China

Most of the emissions of sulphur dioxide and particulates in China come from the power sector and from coal-fired boilers installed in most urban areas. These emissions and in the case of particulates, the fine particles (PM2.5) are responsible for major environmental problems in China. The Chinese government has developed a number of policies to address these problems, as is the case of the Total Emissions Control (TEC) policy, which restricts total SO_2 emissions in all sectors of the Economy.

China's Environmental Protection Administration (SEPA) is responsible for monitoring emissions, as well as for producing improvement notices and collecting the taxes and fiscal penalties. SEPA is also responsible for supervising the implementation of new environmental control equipment and for evaluation of its performance. In December 2003, EPA and SEPA signed a Memorandum of Understanding (MoU), establishing a Working Group on Clean Air and Clean Energy to coordinate and facilitate the implementation of the Strategy for Clean Air and Energy Cooperation (EPA China, 2004).

Under the Clean Air and Energy Strategy, EPA and SEPA are working together to reduce air pollution and greenhouse gases (GHG). The Strategy focuses on strengthening regional coordination of clean air and energy management in key regions of China and addressing priority sectors affecting air, environment, and public health. The programme focused at the beginning on the power and transportation sectors (EPA China, 2004).

Since 1985, the World Bank has been involved in the financing of nine coal fired power plants in China (Fritz, 2004), with the purpose of also assisting China to satisfy not only the growing demand for electricity but also with the objective of improving efficiency and reducing adverse environmental impacts.

In 1992, it was published the first emission standards for coal fired power plants in China (GB 13223-91), which was limited to emissions of particulates and SO_2 from existing and modified plants. Although through the standards about 90% of the plants installed or retrofitted electrostatic precipitators, air quality in many Chinese cities continued to deteriorate, demonstrating the need of tighter standards for SO_2 and NO_x levels. In 1997, new limit was imposed for NO_x (GB 13223-96) and the new standards classified power plants in 3 different categories, depending on the date of approval for original construction.

SEPA and the State Bureau of Technical Supervision, Inspection and Quarantine have jointly formulated a new emissions' standard for air pollutants in thermal power plants, GB13223-2003 (SEPA, 2003), to be enforced in 2004, January. The new emissions' standards for particulates, SO_2 and NO_x are summarized in Tables 2.7 and 2.8.

Table 2.7 - Particulates and SO_2 emission standards for thermal power plants in China (SEPA, 2003).

Time period of construction for power project	**Time-period I (Before 12/31/1996)**		**Time- period I I (1/1/1997- 1/1/2004)**		**Time- period III (After 1/1/2004)**
Date of implementation	1/1/2005	1/1/2010	1/1/2005	1/1/2010	1/1/2004
Dust for coal fired boiler (mg/m^3)	300(1) 600(2)	200	200(1) 600(2)	50 100(3) 200(4)	50 100(3) 200(4)
Dust for oil fired boiler (mg/m^3)	200	100	100	50	50
SO2 for coal and heavy oil fired boiler (mg/m^3)	2100(1)	1200(1)	2100 1200(2)	400 1200(2)	400 800(3) 1200(4)

(1) Applicable to thermal power plants located in the city area of county and higher than county.
(2) Applicable to thermal power plants located beyond the city area of county and higher than county.
(3) Applicable either to thermal power plants for which the environmental impact report of the project had been approved before this standard was implemented, or to coal mine mouth power plants burning extra low sulphur coals (S<0.5%) located in western region of china and outside of the Two Control Zones areas.
(4) Applicable to thermal power plants for which the dominant fuel is coalmine waste (heating value of the coal should be less than 12.55 MJ/kg).

Table 2.8 - NO_x emission standards (mg/Nm^3) for thermal power plants in China (SEPA, 2003).

Time period of construction for power project		**Time-period I (Before 12/31/1996)**	**Time- period II (1/1/1997- -1/1/2004)**	**Time- period III (After 1/1/2004)**
Date of implementation		1/1/2005	1/1/2005	1/1/2004
Coal fired boiler	V daf<10%	1500	1300	1100
	10%≤V daf≤20%	1100	650	650
	V daf >20%			450
Oil fired boiler		650	400	200
Gas turbine unit	Oil fired			150
	Gas fired			80

In terms of GHG, China has become the world's biggest emitter (WEO, 2011); in 2010, the total GHG emissions were 7.5 Gt $CO_{2\text{-eq}}$.

2.3 Energy Resources

2.3.1 Coal

Coal, the world's most abundant energy resource, consists in a compact, stratified mass of organic material originated from plant debris, interspersed with smaller amounts of inorganic matter and covered by sedimentary rocks (Gulyurtlu, 1989). The rank of a coal leads to its classification, depending oupon the chemical composition of coal, ranging from peat to anthracite (Table 2.9).

Table 2.9 – Coal ranks and approximate C and H contents (Gulyurtlu, 1989).

Coal Rank	Carbon (%)	Hydrogen (%)
Anthracite	93-95	3.8 - 2.8
Carbonaceous	91-93	4.25 - 3.8
Bituminous	80-91	5.6 - 4.25
Sub-Bituminous	75-80	5.6 - 5.1
Lignites	60-75	5.7-5.0

The coal deposits formation varied according to tectonic movement's characteristics, geographic location, weather and flora. During the geological history of Earth, three periods were conducive to coal formation, namely Carbonic, Permic and Jurassic (Terciary), as presented in Table 2.10.

Table 2.10 – Age of coal (Gulyurtlu, 1989).

Geological System		Aproximaded Age (million years)	Coal rank (Class)
Era	Period		
Paleozoic (Primary)	Carbonic	250	Anthracites
	Permic	210	Bituminous
Mesozoic (Secundary)	Triassic	180	Bituminous
	Jurassic	150	Bituminous
	Cretacic	100	Sub-Bituminous and Bituminous
Cenozoic (Terciary)	Paleogenic	60	Lignites and Sub-Bituminous
	Neogenic	20	Lignites
	Quaternary	1	Peat

The main known coal reserves are in the United States (28.6%), Russian Federation (18.5%), China (13.5%), Australia (9.0%), India (6.7%) and South Africa (5.7%) (BP, 2012). In terms of coal extraction, the major world producers are China (41.1%) and the United States (18.7%). Other coal producers are: Australia (6.9%), India (5.8%), South Africa (4.8%), Russian Federation (4.7%), Indonesia (3.4%), Poland (2.0%) and Germany (1.6%) (BP, 2012).

Due to both price and extent of reserves, coal is expected to continue being a significant contributor to energy production in the world, both alone or mixed with wastes. Therefore, it is of most importance to develop clean coal technologies and to increase the efficiency of energy conversion/production technologies.

2.3.2 Biomass

The term biomass describes carbonaceous materials as the following examples derived from plants: agriculture wastes, demolition plants and forestry wood waste. Biomass waste can be used as fuel, and can be converted directly to energy by:

a) direct firing;
b) co-firing;
c) indirectly by thermal or biochemical conversion.

In the case of co-firing, *i.e.* mixing biomass with coal, it has technical, economical, and environmental advantages over other options. Co-firing biomass with coal, in comparison with single coal firing, helps to reduce the total emissions per unit energy produced. However, serious slagging and fouling of heat transfer surfaces has been observed in power facilities. The major reason for this result is high alkali metal content, in particular potassium. In addition, due to the high chlorine content of MSW/RDF and some biomass, cofiring could cause high-temperature corrosion to occur on the metals inside the furnace.

In Portugal, agriculture land represents 42% of total area of Portugal. The primary sector employs 11% of active population. Temporary cultures represent 43% while permanent cultures, corresponding mainly to olive and vineyards (77%), represent 56% of the sector (COPOWER, 2007) and there is a need for infrastructures specifically created for the treatment, valorisation or elimination of agricultural residues.

The exploitation of forestry residues does not imply any changes in the management of the forests, only needing adjustments in logistic requirements for the collection of forest Biomass Residues. The principal forest species are: pines (residues: 1.5kg green/year/tree); eucalyptus (residues: 2.34kg green/year/tree); cork oak and holm oak (COPOWER, 2007). Figure 2.6 shows the distribution of Portuguese agricultural and forest biomass residues in five regions.

Figure 2.6 – Agricultural and forest biomass residues in Portugal (COPOWER, 2007).

The CO_2 emissions resulting from the combustion of renewable energy sources are considered CO_2-neutral. Thus, co-firing of biomass as secondary fuel replacing coal in power plants also results in a reduction of the CO_2 emissions.

2.3.3 Wastes

The European Union policy for waste management encourages the promotion of technologies like the integration of waste recovery processes with fluidised bed technology or the co-combustion of blends prepared using the renewable materials contained in different waste streams with conventional fuels, like coal. The co-combustion technology aims at the promotion of synergies from the simultaneous combustion of coal with other fuels, maintaining or increasing the combustion process efficiency whilst keeping pollutant emissions low.

The residues from agriculture and forest harvesting consist of biomass and are classified as primary residues (Faaij, 2006). Secondary residues are the by-products generated directly in the food, wood and paper industry; tertiary residues include various reprocessed wastes, such as the organic fraction of MSW (RDF), waste demolition wood, sludges, etc. In Table 2.11 several examples of solid biofuels are presented, based in the Large Combustion Plants BREF (LCP BREF, 2006). Availability and market prices of biomass and wastes generally depend on local and international markets demand, although for residues, elimination fees may give a negative value to organic wastes. Economical benefits of using biomass and wastes are also very dependent on local availability given the transportation costs; hence, logistic aspects are also relevant to the production of "green" electricity.

Table 2.11 – Solid biofuels from LCP BREF (Lopes *et al.*, 2006).

Type of Secondary Fuel	**Examples**
Non-woody biomass	Energy crops Agricultural residues: straw, cereal plants, grass
Wood	Wood residues, demolition wood Waste wood Forest residues Wood chips Biomass pellets/briquettes
Animal (by-) Products	Animal Meal Meat and Bone Meal Manure Chicken litter
Municipal Waste	Waste paper Packing materials Plastics RDF
Recovered Fuels	Fuels derived from high calorific waste fraction: ASR, etc
Sludge	Sewage Paper
Tyres	Shredded tyres
Chemicals	Organic acids Liquid solvents
Oily material	Tar Waste oil

It is a fact that there is steay increase in waste production around the world, most of them with a considerable energy value, which makes those suitable as a fuel. Furthermore, the Landfill Directive doesn't allow the biodegradable material deposition, which obliges authorities to dispose the waste in a different manner. As the European waste management policies promote materials recovery processes integration with Fluidised Bed technology and the co-combustion of mixtures of wastes from differents streams with conventional fuels, combustible wastes could be used as an energy resource combined with fossil fuels.

The RES Directive promotes the fossil fuel replacement by renewable energy sources. The biomass definition is very wide and includes not only the biodegradable fraction of municipal solid wastes and industrial wastes but also includes meat and bone meal and primary wastes from food and beverage production, as described in Table 2.11.

The overall CO_2 emissions of a combustion plant could decrease significantly, depending upon the degree of substitution of fossil fuel that could be achieved.

However, some wastes may exhibit high concentrations of heavy metals, such as sewage sludge and demolition wood. Some metals may remain attached to bottom ashes, whilst others are evaporated and condense in particles with the cooling of flue gases.

2.4 Fluidized bed technology

The combustion on grates is still the dominant incineration technology, mostly used in large plants. As stated above, the EU policy for waste management promotes the use of technologies for MSW with integration of material recovery processes coupled with fluidized bed technology.

Power generation using non-toxic wastes is one of the promising technologies for the utilization of MSW as an alternative to the mass-burning incineration concept.

The co-combustion technology also provides synergies from the simultaneous combustion of coal with other fuels, maintaining or increasing the combustion process efficiency whilst keeping pollutant emissions low. The option of co-firing could help to contribute to the fulfilment of the EU objectives for environmental protection and energy security, namely the reduction of the green house gases (GHG).

Fluidised Bed Combustion has become a mature technology. This has been introduced and developed in the last 20 years. The main working principle is that the fuel is combusted in a turbulent bed of sand and ash which implies good heat transfer and mixing. Fluidised bed combustors might be of bubbling type or circulating type and can be operated either at atmospheric conditions or under pressure.

The main advantage of Pressurised FBC is the low combustion temperature, which results in very low emissions of sulphur and NO_X. Furthermore, FBC units are compact in size, deal with a wide range of fuels and, due to its working principle, achieve almost instantaneously good heat and mass transfer. The main disadvantage of this technology is the price, the complexity of the system and the requirement of a low feed rate.

The gas residence time in the combustion chamber is short, only a few seconds, enough for a complete reaction due to the high gas/solid contact surface. The high turbulence in these systems allows efficient contact fuel/air, ensuring a uniform temperature distribution in the bed and high heat transfer coefficients. This allows lower reactions' temperatures when compared to other systems, usually between 750 and 900 ºC. Bed temperature is maintained by removing the heat by heat exchangers (with water, vapour or air) immersed in the bed.

<u>Advantages and disadvantages of fluidized bed combustion</u>

There are many advantages in using fluidized bed technology for the co-combustion of coal with biomass and/or non-toxic waste materials when compared with other combustion systems, as presented below (Abelha, 2005):

• the low operating temperatures (700-900°C), avoiding the volatilization of the salts and thermal NO_X formation;

• the high turbulence inside the bed provides a good level of air/fuel mixture and facilitates burning materials with low LHV;

• the high thermal transfer coefficient between the fluidized material and the immersed surface of the heat exchanger in the bed allows the use of smaller size heat recovery systems;
• due to the adsorbent action during the combustion it is possible to burn high-S and high-Cl wastes with the minimum environmental impact
• the fuel versatility allows burning different fuels, including those with high moisture content;
• the high residence times of the material in the bed, most significant in the circulating fluidized bed leads to lower levels of pollutant emissions;
• the control of temperature, excess air, mixture of the gaseous phase and residence time ensure low CO emissions;
• due to the thermal innertia and the amount of solids in the bed leads to the possibility of intermitent operation, leading to a temperature variation during stoppage of 5 ºC/h.

However, the fluidized bed technology also presents some disadvantages, which are listed below:
• high thermal inertia, due to the difficulty of response to quick load variations;
• erosion/corrosion problems in the contact surfaces with the bed;
• ash accumulation problems, due to agglomeration of material and obstruction of air inlets.

2.5 Sustainable chemistry

Paul Anastas and John C. Warner developed the 12 principles of Green Chemistry (Anastas and Warner, 1998), named Sustainable Chemistry in Europe (Table 2.12). The principles cover concepts such as:

- the design of processes to maximize the amount of raw material that ends up in the product;
- the use of safe, environment-benign substances, including solvents, whenever possible;
- the design of energy efficient processes; and
- the best form of waste disposal.

In the development of this study, focusing on the use of renewable energy sources and the use of technologies with optimisation of energy efficiency and minimizing atmospheric pollutants formation, the following principles of Green Chemistry were applied:

- Principle n. 1: Prevention;
- Principle n. 6: Design for Energy Efficiency;
- Principle n. 7: Use of Renewable Feedstocks.

Table 2.12 – The 12 Green Chemistry Principles (Anastas and Warner, 1998).

Principle	Description	Summary
1.	It is better to prevent waste than to treat or clean up waste after it is formed.	Prevention
2.	Synthetic methods should be designed to maximize the incorporation of all materials used in the process into the final product.	Atom Economy
3.	Wherever practicable, synthetic methodologies should be designed to use and generate substances that possess little or no toxicity to human health and the environment.	Less Hazardous Chemical Syntheses
4.	hemical products should be designed to preserve efficacy of function while reducing toxicity.	Designing Safer Chemicals
5.	The use of auxiliary substances (e.g. solvents, separation agents, etc.) should be made unnecessary wherever possible and innocuous when used.	Safer Solvents and Auxiliaries
6.	Energy requirements should be recognized for their environmental and economic impacts and should be minimized. Synthetic methods should be conducted at ambient temperature and pressure.	Design for Energy Efficiency
7.	A raw material or feedstock should be renewable rather than depleting wherever technically and economically practicable	Use of Renewable Feedstocks
8.	Reduce derivatives - Unnecessary derivatization (blocking group, protection/ deprotection, temporary modification) should be avoided whenever possible	Reduce Derivatives
9.	Catalytic reagents (as selective as possible) are superior to stoichiometric reagents	Catalysis
10.	Chemical products should be designed so that at the end of their function they do not persist in the environment and break down into innocuous degradation products	Design for Degradation
11.	Analytical methodologies need to be further developed to allow for real-time, in-process monitoring and control prior to the formation of hazardous substances	Real-time analysis for Pollution Prevention
12.	Substances and the form of a substance used in a chemical process should be chosen to minimize potential for chemical accidents, including releases, explosions, and fires	Inherently Safer Chemistry for Accident Prevention

3. Formation and control of pollutant emissions in combustion processes

3.1 Combustion

Combustion is a complex sequence of exothermic chemical reactions involving a fuel and an oxidizing agent, *i.e.* an oxidation process in which chemical energy is transformed to heat. The combustion process is the result of a large number of reactions, many of them involving radical species. Currently the reaction mechanisms are only partially understood, mainly due to the large number of reactions and their complex nature. Ideally, the combustion of an organic fuel results in the formation of only carbon dioxide and water (Eq. 3.1):

$$C_xH_y + (x+y/4)O_2 \rightarrow xCO_2 + (y/2)H_2O \quad (3.1)$$

A schematic illustration of different combustion stages is presented in Figure 3.1 (Aurell, 2008). Depending on the combusted fuel composition, different by-products are formed, such as sulphur oxides or hydrogen halides. Incomplete combustion conditions due to poor mixing of the flue gas or quenching of the combustion process will conduct to the formation of products of incomplete combustion (PIC).

Three main parameters affecting combustion efficiency are often referred to as 'the three Ts' (Jansson, 2008), namely: (i) Temperatures high enough to sustain the combustion reaction, (ii) Time sufficient for the reactions to occur, and (iii) Turbulence of air and combustion gases. Under normal combustion conditions, 100% combustion efficiency is never obtained and soot, uncombusted fuel fractions and products of incomplete combustion (PIC) are always generated to some extent.

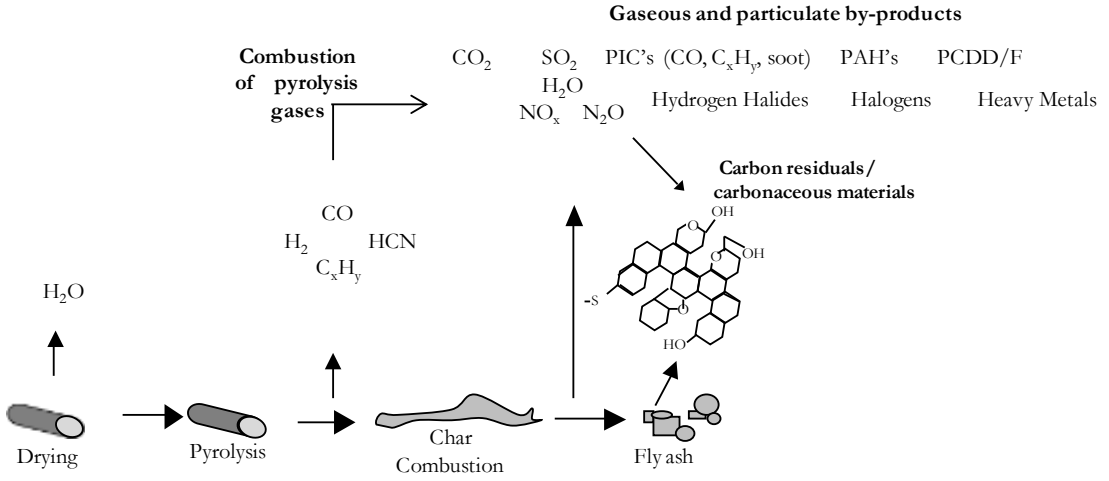

Figure 3.1 – Schematic illustration of different combustion stages (adapted from Aurell, 2008).

Carbon monoxide (CO) is also known by its toxicity and its formation needs to be well controlled especially in open coal combustion systems. CO combines with the haemoglobin the same way as the oxygen; however, one volume of CO corresponds to 210 volumes of O_2. Depending on the air concentration and the time of exposure, it could be fatal as it reaches blood saturation and, consequently asphyxiation due to the lack of oxygen.

3.2 Particulate matter

Particulate emissions are finely divided solid and liquid (other than water) substances generated by a variety of physical and chemical processes. Particulates can affect people's respiratory systems, impact local visibility and cause dust problems. Primary particulate matter is emitted to the atmosphere through combustion, industrial processes, fugitive emissions and natural sources and arises almost entirely from the mineral fraction of the fuel. A small proportion of the dust may consist of very small particles formed by the condensation of compounds volatilised during combustion. Secondary particulate matter is formed in the atmosphere from condensation of gases and is predominantly found in the fine range.

The impact of these emissions depends on granulometry and the nature of the mineral matter in terms of toxicity. Solid fuels tend to form higher amounts of ash and various studies have been performed to determine the parameters that influence the formation of different sizes of particulate matter and composition from inorganic impurities present in the fuel.

Chirone and co-workers (1991) investigated the different phenomena that contribute to the reduction of fuel particles in fluidized bed, pointing out four phenomena occurring both in series and in parallel with each other (Figure 3.2), namely (Chirone *et al.*, 1991):

i) primary fragmentation of coal;

ii) secondary fragmentation of char;

iii) fragmentation by percolation of relatively fine char; and,

iv) abrasive attrition between chars.

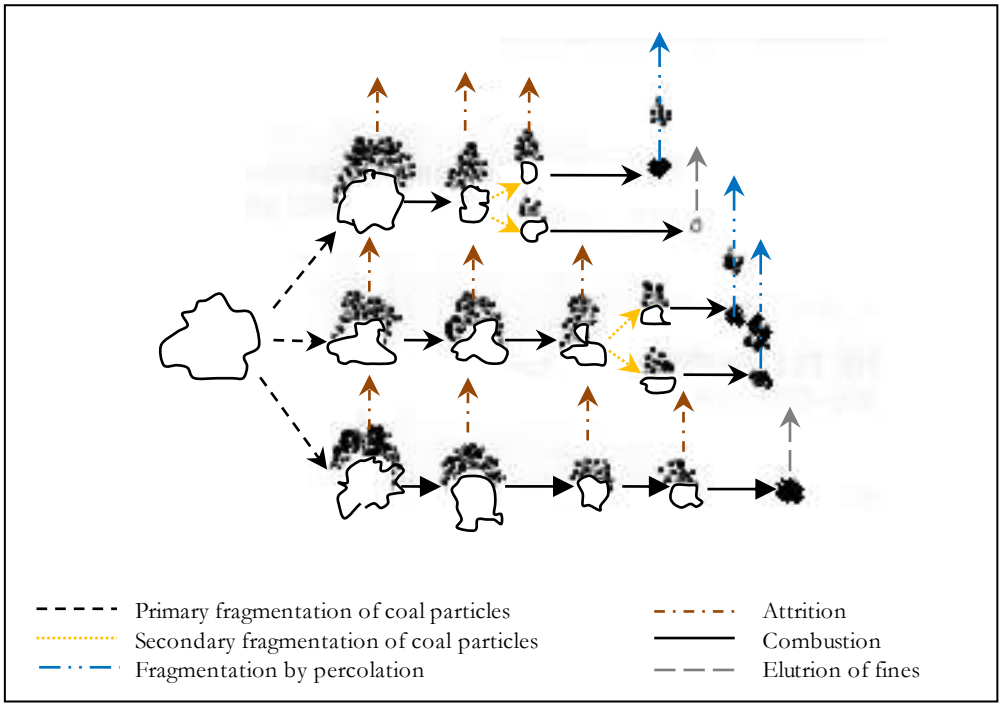

Figure 3.2 – Coal typical comminution processes (from Chirone *et al.*, 1991).

Part of the ash is discharged from the bottom of the furnace as bottom ash. The particles suspended in the flue gas are known as fly ash. Quantity and characteristics of the fly ash and particle size distribution depend on the coal mineral matter content, combustion system, and furnace operating conditions. Mineral composition of the coal and the amount of carbon in the fly ash determine the quantity, resistivity and cohesivity of the fly ash. The combustion type affects the particle size distribution in the fly ash and, hence, also affects particulate emissions. The proportion of ash entrained in the flue-gas emissions are greatly dependent on the type of combustion process used. In the case of boilers, moving grate produce a relatively small amount of fly ash (20 – 40 % of total ash), whereas pulverised coal boilers produce an appreciable amount (80 – 90 %); dry

bottom boilers produce 10-20% of bottom ash and wet bottom boilers produces 50-60% of slag. The combustion temperature may also affect the cohesivity of the fly ash. Higher operating temperatures can result in greater particle cohesivity leading to improved fly ash cake removal by reducing re-entrainment. Combustion equipment operating conditions can affect the amount of unburnt carbon in the fly ash.

Fine particulate matter may also contain higher concentrations of heavy metal elements than coarser particles. This is because fine particles have a greater total surface area available for trace elements (heavy metals), such as mercury, to condense on. Particulate matter is in general referred to as "PM", "PM10", "PM2.5" (particulate matter (PM) with an aerodynamic equivalent diameter of 10 μm or less and 2.5 μm or less, respectively).

Environmental problems can occur from particles less than 2.5 μm in diameter because they can remain suspended in the atmosphere for days or even weeks. In terms of human health, particle size is directly linked to their potential for causing health problems. Small particles, less than 10 μm, pose the greatest problems, since they can get deep into the lungs, and some may even get into the bloodstream. Particulate matter may be distinguished as fine (0.1-2.5 μm) and ultra fine particles (<0.1 μm), being the smaller ones more toxic (Castranova, 2005), as they were found to be deposit in the lungs. Enrichment of heavy metals in the smaller particles has also been reported to be responsible with the increase of asthma (Gavett *et al.*, 2003).

Environmental problems can also occur by long time agglomeration of persistent compounds in the earth or by dilution and transfer to water bodies. The distance that particles travel before they are removed from the air by settling or by precipitation depends on their physical characteristics and the weather conditions. The size, density and shape influence the rate at which particles settles. Particles larger than 10 μm in diameter settle fairly rapidly. Their impact is primarily near the source. Smaller particles less than 10 μm and especially those less than 2.5 μm can travel over hundreds of kilometres before settling. Aerosols often function as condensation nuclei for cloud formation and are washed out with rain.

A number of technologies have been developed to control particulate emissions from coal combustion and are used worldwide including: mechanical/inertial collectors (cyclones/multicyclones), wet particulate scrubbers, fabric filters (baghouses) and electrostatic precipitators (ESPs), although the primary technologies for state-of-the-art particulate control are electrostatic precipitators (ESPs) and fabric filters.

3.2.1 Mechanical/inertial collectors

Mechanical/inertial collectors' characteristics of the cyclones/multicyclones limit its use to small- or medium sized installations, and only as a pre-collection technique when combined with other

means for dust control. In the past, industrial plant operators tended to fit mainly cyclones. Cyclones are robust technologies that can deal with the cyclic operation and load changes, which is quite common in these types of plants. However, their efficiency is moderate when compared with ESP or fabric filtration. A cyclone is a cylindrical vessel, usually with a conical bottom. The flue gas enters the vessel tangentially and sets up a rotary motion whirling in a circular or conical path. The particles are 'thrown' against the walls by the centrifugal force of the flue gas motion where they impinge and eventually settle into hoppers.

3.2.2 Wet srubbers

Wet scrubbers for control of particulate emissions have been in use for several decades. The low capital cost of wet scrubbers compared to that for ESPs and fabric filters makes them potentially attractive for industrial scale use, though this may be offset by a relatively high pressure drop and operating costs. The flue-gas is cooled during wet scrubbing and requires reheating prior to emission to the atmosphere, thus incurring in higher energy costs. Partly due to such operating costs, the use of wet scrubbers for the control of particulate emissions has declined during the last decade. However, wet scrubbers have been used in some high temperature and pressure combustion applications such as integrated gasification combined cycle (IGCC) and pressurized fluidised bed combustion (PFBC).

The majority of wet scrubbers for collecting fly ash from coal-fired furnaces (industrial or utility) are installed in the US. The greatest concentration of these units is the western US, where the available low sulphur coal is so highly resistive that ESPs are less economically attractive. Many of these scrubbers are designed for combined particulate removal and control of sulphur dioxide emissions, using the alkaline fly ash as sorbent. Wet scrubbers are used to capture both particulates and sulphur dioxide by injecting water droplets into the flue gas to form a wet by-product. The addition of lime to the water helps to increase SO_2 removal. Lime is frequently added to boost SO_2 removal efficiencies.

3.2.3 Electrostatic precipitators

Electrostatic precipitators (ESP) are the most widely used particulate emissions control technology in coal-fired power plants. Flue gases are passed horizontally between collecting plates where an electrical field creates a charge on the particles. Particles in the flue gas in order to attract them to collecting plates where they are accumulated. A major limitation of ESPs is that the fractional penetration of 0.1- to 1.0-μm particles is typically at least an order of magnitude greater than for

10μm particles, so a situation exists where the particles that are of greatest health concern are collected with the lowest efficiency.

EPS efficiency is dependent on resistivity and dust particle size. Generally, ESP has a collection efficiency of 99.5-99.9% for coarse particles, but for fine particles the collection is lower. Cold side (dry) ESP is located after the air preheater and operates in a temperature range of 130-180°C. Although cold side ESP with moving electrodes is becoming more widely used, ESP with fixed/rigid electrodes is the most common type used. Hot side (dry) ESP, used mainly in the USA and Japan, is located before the air preheater. The operating temperature range is 300-450°C.

Wet ESP, a liquid film is maintained on the collection plates using spray nozzles. The process eliminates the need for rapping as the liquid film removes any deposited fly ash particles. Thus, problems with re-entrainment, fly ash resistivity and capture of fine particles become obsolete. However, wet ESP requires saturation of the flue gas stream with water, generate waste water and sludge and operate at low temperatures.

3.2.4 Fabric Filters

Fabric filters (FF) or baghouses, have been more widely used since the 1970s, especially at industrial scale. Fabric filters generally operates in the temperature range 120-180°C.

The choice between ESP and fabric filtration generally depends on coal type, plant size and boiler type and configuration. As in the case of ESP, conditioning the fly ash in the flue gas is an established technique.This is used to restore the performance of a FF in coal-fired power plants with high-resistivity fly ash resulting from burning low sulphur coals. The benefits of flue gas conditioning in fabric filters include achieving lower emissions at higher bag air to cloth ratio, reducing pressure drop and improving fly ash cake cohesivity, thus leading to better dislodgement in larger agglomerates and less re-entrainment. The main conditioning agents currently used are the same as for the ESP.

A synthesis of the main particulate removal technologies efficiency and particle size range is presented in Table 3.1 (Pinto *et al.*, 2009). Both ESPs and fabric filters are highly efficient particulate removal devices with design efficiencies above 99%.

Table 3.1 – Synthesis of the currently used particulate matter control devices (Pinto *et al.*, 2009).

Particulate removal technologies	**Removal efficiency**	**Particle size range**
Mechanical/inertial collectors	75 to 99%	1.0 to 100 μm
Wet scrubbers	90 to 99.9%	0.5 to >100 μm
Electrostatic precipitators	>99 to >99.99%	0.01 to >100 μm
Fabric Filters	>99 to >99.9999%	0.01 to >100 μm

3.2.5 Hybrids Particle Collectors

Electrostatic precipitators are inadequate for fine-particle capture, and fabric filters have high pressure drop and short lifetime because of filter blinding. Although people have been trying to combine the two mechanisms, technical challenges remain such as protection of the bags from electrically induced damage and suppression of particle reentrainment. Improvement and upgrade of is possible through flue gas conditioning, ESP replacement and enlargement or combining with FF technology.

Another possibility are hybrid devices, which attempt to integrate ESP and FF technologies into the same housing, in an effort to optimize the better of each technology, *i.e.* to improve small particles removal efficiency with a moderate increase in pressure drop. The hybrid particle collection concepts, which are at demonstration phase, will allow a higher efficiency in the collection of fines and include (Pinto *et al.*, 2009):

i) COHPAC I and COHPAC II (COmpact Hybrid Particulate Collector) systems (Chen, 1991, 1992):

The concept of COHPAC is fairly simple. A high ratio pulse jet fabric filter collector (baghouse) is installed in series with an existing, energized electrostatic precipitator, serving as the polishing or final collection device. Due to the fact that the ESP removes the majority of the ash or dust prior to entering the fabric filter, the filtration rate (air-tocloth-ratio) can be increased substantially more than conventional filtration rates, while still maintaining the same pressure drops as conventional filtration systems. It is also believed that the ESP serves as a pre-charger and helps to agglomerate the dust particles into a larger and thus more porous structure, which also aids in the filtration process. COHPAC can be either installed in a separate casing (COHPAC I) located after the ESP, or within the last 1-2 fields of the ESP's casing by replacing one or more fields of collecting plates with baghouse modules (COHPAC II). The better the performance of the remaining fields the higher the final filtration rate can be utilized.

ii) AHPC - Advanced Hybrid Particle Collector (Miller, 1999, 2003)

Advanced Hybrid™ is a new concept in particulate control that combines electrostatic precipitation with fabric filtration. The design configuration of the AHPC is unique because, instead of placing the ESP and fabric filter sections in series (as is done with other dual-mode particulate collection devices), the filter bags are placed directly between the ESP collection plates. The collection plates are perforated (45% open area) to allow dust to reach the bags; however, because the particles become charged before they pass through the plates, over 90% of the particulate mass is collected on the plates before it ever reaches the bags. When pulses of air are used to clean the filter bag surfaces, the

dislodged particles are thrown back into the ESP fields where they have another opportunity to be collected on the plates. Operating experience suggests that since the bags will not need to be cleaned as often as in typical baghouses, they will provide excellent performance over a long operating life. This leads to low operating costs since filter bag replacement is a key cost component.

iii) MSC – MultiStage Collector (Krigmont, 2003)

The Multi Stage Collector (MSC™) concept for ultra-fine particulate control offers significant improvements over current state-of-the-art technology. The new MSC™ design provides a synergistic combination of both single- and two-stage electrostatic precipitation while incorporating an additional collector-stage by filtering the gas exiting the collector through a barrier collector-zone. This arrangement ensures that essentially all dust would be detained in this final stage. The MSC™ contains multiple narrow and wide zones formed by parallel corrugated plates. Enclosed in the narrow zones are discharge electrodes. These electrodes provide a non-uniform electric field leading to corona discharge. The corona discharge causes particulate matter in the gas flow to become charged. MSC™ is a new concept for particulate control. The intent of the MSC™ is to combine the best features of the two-stage ESP and FF.

iv) Electrostatic recirculation gas cyclones (Salcedo et al., 2007):

The recent adoption of electrostatic recirculation in the same cyclone system has successfully proven to further reduce particle emissions, even in the 1-5μm particle size range, assuring future regulation compliance, particularly where legal limits are very tight, with the objective of fabric filter redundancy.

Although at demonstration stage, these systems will allow a higher efficiency in the collection of smaller particles.

3.2.6 Multipollutant control devices

There has been a trend towards developing multi-pollutant control technologies that remove two or more pollutants such as SO_X, NO_X, fine particulates, mercury and other heavy metals in one process. Some of these processes, involving effective fine particulates control, are on full-scale demonstration, while others are currently under development, and it seems likely that multi-pollutant control systems will become commercially available for coal-fired utilities in the near future.

3.3 Sulphur oxides

SO_X are composed mainly by SO_2 (90%) and in minor quantities by SO_3 (Eliot, 1981 cited by Abelha, 2005). They show some toxicity for human health and are major responsible for acid rain phenomena.

There are several options to limit its emissions from fossil fuels combustion. Primary measures for prevention of SO_2 release are the use of fuels with lower S content and the use of fuels previously cleaned. Secondary measures consist of combustion sulphur removal and post-combustion treatment. In situ combustion sulphur removal and post-combustion treatment involves the utilization of sorbent materials.

Fluidized bed combustion (FBC) systems are particularly suited for fuels containing S including waste fuels, because of their ability to burn low grade fuels as well as fuels with variable energy contents, and the ability to capture hazardous gases directly in the combustor. Sulphur removal during combustion in fluidized bed combustor (FBC), either in bubbling or circulating regime, is mainly performed with the addition of limestone ($CaCO_3$), a most worldwide available and low cost mineral. The sorbent particles are crushed and sieved and introduced to the reactor. The long residence times, at optimum temperature (~850ºC) and oxidation conditions present in FBC, calcinates $CaCO_3$ to form CaO that further reacts with the gaseous SO_X to form $CaSO_4$, through the following reactions:

$$CaCO_3 \rightleftarrows CaO + CO_2 \quad (3.2)$$

$$CaO + SO_2 + ½\ O_2 \rightleftarrows CaSO_4 \quad (3.3)$$

The calcium sulphating reaction is exothermic and extremely dependent on temperature. However, higher reaction temperatures (> 850ºC) would produce CaO with bigger pores and thus with less specific surface area for sulphatation would lead to sintering and $CaSO_4$ decomposition (<1100ºC).

According to the stoichiometry of calcium sulphating reaction, a molar ratio of Ca/S of 1 is required to capture all the SO_2 formed. However, usually molar ratios values of Ca/S around 2 are used with 80-90% of coal-S retention performances. This results from the closure of CaO pores during the sulphating process, before all the nuclei becomes saturated, since $CaSO_4$ molar volume is about 3 times higher than the CaO molar volume. For this reason, a film of $CaSO_4$ forms around the sorbent particle, blocking the access of the SO_2 to the remaining CaO. Therefore, the CaO conversion to $CaSO_4$ is typically limited to 30-40% (Xie *et al.*, 1999).

In situ desulphurization method does not introduce significant penalties in terms of energy efficiency and is a well established technology.

The partial replacement of high S content by fuels with lower S content, like most biomass or some waste materials, could be an effective way to decrease SO_2 emissions.

Furthermore, those co-fuels usually have higher Ca/S ratios than coal and, hence, their co-firing promotes increased S retention, allowing less sorbent addition (COPOWER, 2007).

During a co-combustion study, van Doorn and co-workers (1996) verified that the concentration of the SO_2 emitted in the flue gases, during waste wood co-combustion with a bituminous coal, represented about 55-70% of the fuel-S input, whereas during coal combustion runs that value ranged from 75 to 85%. The authors could observe that a significant part of the sulphur was retained in the ashes, as sulphates, during co-combustion of wood.

Helmer and co-workers (1998) reported an increase of the retention of SO_2 with increasing percentages of biomass in the fuel and verified that the particle size and the moisture content did not influence the retention degree. Gulyurtlu and co-workers (2007b), using a pilot fluidized bed combustor, have concluded that it was possible to decrease significantly the SO_2 emissions from coal combustion using different biomass species as feedstock. Analogous results were obtained by Desroches-Ducarne and co-workers (1998) and Gulyurtlu and co-workers (2006), during co-combustion of coal with RDF that demonstrated that the SO_2 capture by RDF ash could be higher than 80% of the fuel-S.

Xu and co-workers (1998) suggested that the Cl content of some fuels, like RDF, could contribute significantly to reduce SO_2 emissions during combustion in FBC systems. These authors have verified that S retention in the fuel ashes increases with the increment of Cl-fuel input.

3.4 Halogen Compounds

Halogens present in the atmosphere may result not only from natural sources, mainly from the sea, but a significant part has an anthropogenic origin, resulting from the coal combustion in large combustion plants without a flue-gas desulphurization (FDG) technology installed. The trace amounts of chlorine and fluorine present in the coal, although chlorine may reach 1% in some coals, occurs either associated with the organic matter in coal or as chlorides in the mineral matter. High-chlorine coals, found in a number of countries, are generally believed to have been formed under saline conditions. During combustion, these trace elements are released into the flue-gas and solid-waste streams. According to Liu and co-workers (2000), almost all chlorine released during coal combustion combine with hydrogen and is emitted as hydrogen chloride; in some cases elemental chorine and fluorine can be release, although to a smaller extent. The hydrogen halides combined with the air moisture produce highly soluble acidic gases which can contribute to acid rain.

The emission of halogens depends on the initial halogen content of the fuel, combustion conditions and the use of air pollution control devices to control PM, SO_x and NO_x. Halogens' emissions are indirectly controlled when using technologies to reduce other pollutants.

Flue-gas desulphurisation (FDG) technology is the most effective in retaining halogens emissions, mainly chlorine.

The sulphur-chlorine interactions during fossil fuel combustion in fluidized bed have been studied by Xie and co-workers (1999). The results obtained showed that the presence of HCl could promote SO_2 capture by the bed material and fly ash when limestone was used as adsorbent. The reaction between CaO and HCl is described by:

$$CaO + HCl \rightleftarrows CaCl_2 + H_2O \quad (3.4)$$

According to Xie and co-workers (2000), the calcium chloride trapped in the surface of limestone, after pore closure by $CaSO_4$ due to the higher molar volume, is transported from the surface into the bulk of the absorbing particle, either by diffusion or by migration of $CaCl_2$. The optimum temperature for HCl capture is 650ºC.

Matsukata and coworkers (reported by Liu and co-workers, 2000) found that the sulphurization of all size particles was markedly accelerated in the presence of HCl. In their study, the level of conversion of CaO to both $CaSO_4$ and $CaCl_2$ almost reached 100%, due to the simultaneous retention of HCl and SO_2. It was proposed that this absorption efficiency was the result of both the formation of a mobile ion-containing phase and the formation of voids playing a role in the diffusion of HCl and SO_2 towards the interior of the particle. Liu *et al.* (2000) also reported the results of Deguchi and co-workers, who tested HCl retention and the simultaneous retention of HCl and SO_2 in a bubbling fluidized bed at 850ºC. The conclusions were that there is retention of HCl by limestone and the presence of HCl results in anincrease of the efficiency of desulphurization.

Table 3.2 presents the halogens' emissions reductions achieved with different air pollution technologies in large combustion plants (BREF LCP, 2006).

Table 3.2 - Synthesis of the currently used particulate matter control devices (based in LCP BREF, 2006).

Reduction system	**Type**	**Retention of halogens**
Particulate matter	absence of sorbent	Little or no effect
	addition of sorbent	Partly captured in the particulate control systems*
FGD	wet FGD	Chlorine (HCl) 87 - 97 %
		Fluorine (HF): 43 - 97 %
		Bromine: 85 - 96 %
		Iodine: 41 - 97 %
	dry FGD	Chlorine (HCl): 87 - 97 %
		Fluorine (HF): 43 - 97 %

* There is very little information available regarding the capture of halogens by ESP and FF

3.5 Heavy Metals

Heavy metals, also known as trace metals, are natural constituents of the Earth's crust. Many of the heavy metals, in certain forms and in appropriate concentrations, are essential to life. Although some metals, like Cu, Zn or Mn, are essential to life, others like Hg, Pb, Cd or Cr could be dangerous or even fatal. Except for mercury, the heavy metals do not naturally occur in metallic form in the environment.

The definition of Heavy Metals in the 1998 Aarhus Protocol on Heavy Metals, established in the framework of CLRTAP is "*metals or, in some cases, metalloids which are stable and have a density greater than 4.5 g/cm³ and their compounds*".

Combustion and industrial processes are the predominant anthropogenic sources of emissions of heavy metals into the atmosphere with potential harmful impacts to both human health and the environment.

The aim of the 1998 Aarhus protocol on Heavy Metals was "*to control emissions of heavy metals caused by anthropogenic activities that are subject to long-range transboundary atmospheric transport and are likely to have significant adverse effects on human health or the environment*". This Protocol focuses, in particular, lead, cadmium and mercury.

As part of the 1998 Aarhus Protocol, the European Monitoring and Evaluation Programme (EMEP), delivers annually several Status Reports including one on Heavy Metals. The data collected and presented in the 2007 EMEP Status Report on Heavy Metals (EMEP 2/2007) show that the electricity and heat production sectors were the most significant contributors to the total mercury emissions in Europe (42%). The same sector contributed in second place to cadmium emissions (21%) and represented only 9% of the total lead emissions.

In Europe, the total amounts of the eight heavy metals (As, Cd, Cr, Cu, Hg, Ni, Pb, and Zn) emitted by Large Combustion Plants, reported by the EPER 2004 (EPER, 2013), are presented in Table 3.3. The percentage of the large Combustion Plants (LCP) sector to the total emissions is also presented. The following metals, Cd, Ni and Hg, are the main contributors to the total HM emissions in the 25 EU member countries. In the case of As, Cr and Cu emissions LCP are the second most important contributors to these emissions and for Pb, LCP are the third major source of emissions in Europe.

Table 3.3 - Heavy Metals emissions from LCP in the EU-25 in 2004 (EPER, 2013).

HM emissions from LCP (ton)	**N. facilities**	**As**	**Cd**	**Cr**	**Cu**	**Hg**	**Ni**	**Pb**	**Zn**
2004 EU-25	1264	25.36	13.77	41.29	24.54	12.06	170.11	94.70	96.33
% LCP sector	-	31%	46%	25%	15%	38%	42%	12%	7%

Combustion of coal in power stations can result in trace elements being released. This is due to their presence as a natural component in coal, usually in vestigial concentrations. Coal is chemically a complex substance, which may contain trace elements including mercury, selenium and arsenic. Heavy metals content in coal is normally several orders of magnitude higher than in oil or natural gas, except in the case of Ni and V in heavy fuel oil. Typical concentrations of As, Cd, Cr, Cu, Hg, Ni, Pb, and Zn in coals are shown in Table 3.4. As an example, the coal in the Guizhou province (Southwestern China), one of the major coal resources of China, has an arsenic content as high as 3.2 %(w/w) (Zhao *et al.*, 2008).

Table 3.4 - Typical concentrations of As, Cd, Cr, Cu, Hg, Ni, Pb, and Zn in coals (Raask, 1985).

Concentration range (mg/kg)	**<1**	**1-10**	**10-50**	**> 50**
Heavy Metals	Hg	Cd	As, Cr, Cu, Pb, Ni	Zn

Heavy metals are usually chemically bound in compounds like oxides, sulphates, aluminosilicates and minerals such as anhydrites and gypsum. Knowing the different modes of occurrence of trace elements in coal is fundamental to the understanding of thermal, chemical and environmental behaviour of those elements, during coal conversion processes (Davidson & Clarke, 1996; Davidson, 2000; Wang *et al.*, 2008).

The fate of trace elements has been extensively studied in both full and pilot-scale combustion processes. Heavy metals partitioning between the different streams depend on several factors. During the combustion of coal, for example, particles undergo complex changes which lead to vaporisation of volatile elements. The rate of volatilisation of heavy metal compounds depends on the fuel characteristics (*e.g.* concentrations in coal, fraction of inorganic compounds such as chlorine) and the characteristics of the technology applied (*e.g.* type of furnace, operating mode). A study performed on coal combustion by Linak and Wendt (1993) has shown that most heavy metals are firstly vapourized during combustion, then recondense to form submicron particles, or are adsorbed on the surface of fly ash particles during flue gas cooling.

Less volatile elements tend to condense onto the surface of smaller particles in the flue-gas stream. Partitioning of heavy metals during coal combustion is illustrated in Figure 3.3.

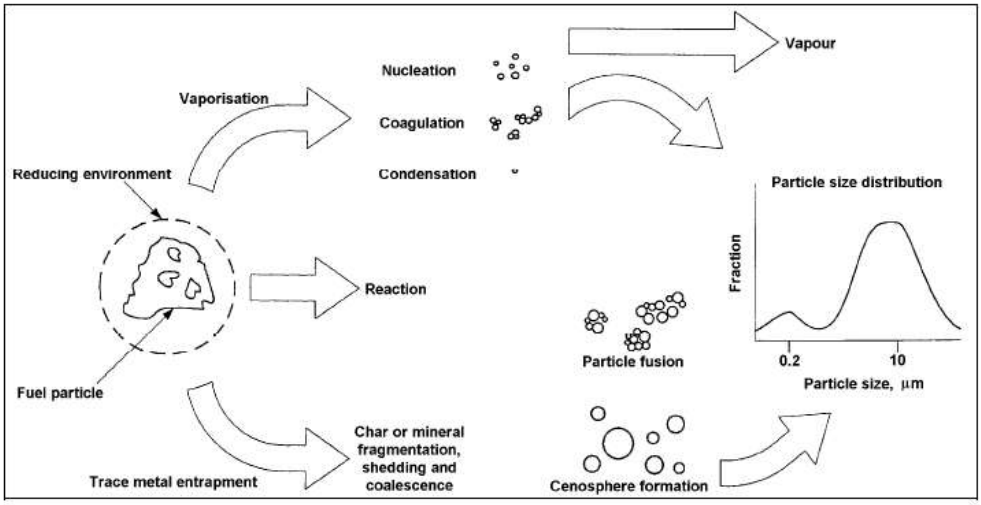

Figure 3.3 - Modes of occurrence of trace elements in coal (from Davidson, 2000).

According to Meij and co-workers (2007), the heavy metals contained in the coal can be classified in several classes, based on their behaviour during combustion This can be measured by the Relative Enrichment factor (RE). This term was introduced to describe the observed behaviour of elements and is defined by Eq. (3.5):

$$\mathrm{RE} = \frac{Conc.in\ ashes}{Conc.in\ coal} . \frac{\%\ ashes\ in\ coal}{100} \tag{3.5}$$

In Table the classification of Meij and co-workers (2007) is presented.

Table 3.5 - Classes of heavy metals (from Raask, 1985).

Class	Behaviour in installation	Fly ash RE factor	Classified elements
I	Not volatile	≈1	
IIc	Volatile in boiler	1.3 < RE < 2	Cr, Mn
IIb		2 < RE < 4	Cu, Ni
IIa		>4	As, Cd, Pb, Zn
III	Very volatile	>>1	Hg

The volatility of heavy metals is found to increase in the presence of chlorine by forming easily volatilized metal chlorides. Several authors (Frandsen *et al.*, 1994; Liu *et al.*, 2000; Ho *et al.*, 2001; Yan *et al.*, 2001) studied the specific effects of chlorine in the vapourization of trace elements and their distribution in flue gases. In a thermodynamic study that Yan and co-workers (2001) performed, he concluded that the presence of chlorine greatly affected the formation of chlorides, hence increasing the vaporization of heavy metals. Frandsen and co-workers (Frandsen *et al.*, 1994) studied the thermodynamic equilibrium of trace elements in combustion and gasification of coal, *i.e.*

in oxidant and reducing conditions and concluded that in oxidant conditions and in the presence of sulphur, Cd forms $CdSO_4$ up to temperatures of 950K (Figure 3.4).

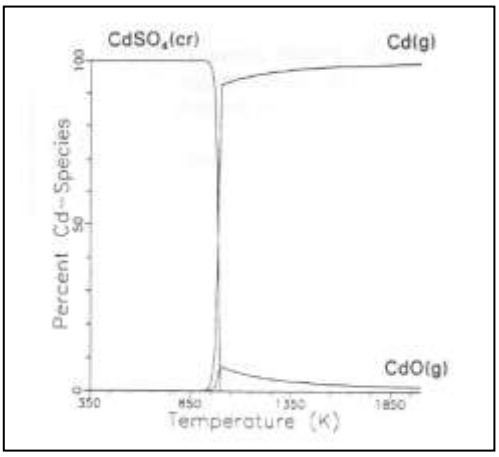

Figure 3.4 – Equilibrium distribution of Cd (%(mol Cd/mol Cd total)) at standard oxidizing conditions (in the Cd/O system) as a function of the temperature, in a flue gas from combustion of a subbituminous coal: λ=1.2 and $c_{Cd,O}$ = 0.05 ppmw (Frandsen *et al.*, 1994).

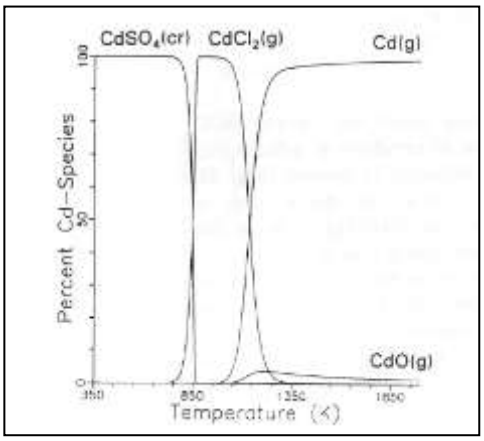

Figure 3.5 – Equilibrium distribution of Cd (%(mol Cd/mol Cd total)) at standard oxidizing conditions (in the Cd/O/Cl system) as a function of the temperature, in a flue gas from combustion of a subbituminous coal: λ=1.2 and $c_{Cd,O}$ = 0.05 ppmw and $c_{Cl,O}$ = 300 ppmw (Frandsen *et al.*, 1994).

When chlorine is present (system Cd/O/Cl), cadmium chloride ($CdCl_2(g)$) is the stable form of cadmium for a temperature range of 850-1150K (Figure 3.5); below 850K the stable form is $CdSO_4$ and above 1150K is Cd(g). Furthurmore, above 1050K, CdO(g) is formed in small amounts (< 5% (mol/mol)). In oxidant conditions and in the presence of sulphur, Pb forms $PbSO_4$ up to temperatures of 1100K (see Figure 3.6).

In the presence of chlorine (system Pb/O/Cl), lead chloride is formed ($PbCl_2(g)$) for temperatures of 950-1450K, with a maximum of 52%(mol/mol) at 1100K (Figure 3.7). It is also observed the formation of PbCl(g) between 1050-2000K, with a maximum of 5% (mol/mol) at 1200K. The quantity of gaseous chlorides formed, including $PbCl_4$, presents a strong dependency on the molar ratio Cl/Pb. Below 920K, the thermodynamic more stable form is $PbSO_4$.

Liu (2000) found that almost all the chlorine in coal was volatilized and emitted as gaseous HCl during combustion. Also, in a study conducted in a fluidized bed pilot, the presence of chlorine increased the volatility of the following metals, Cd, Cu and Pb when burning a bituminous coal (Crujeira *et al.*, 2005).

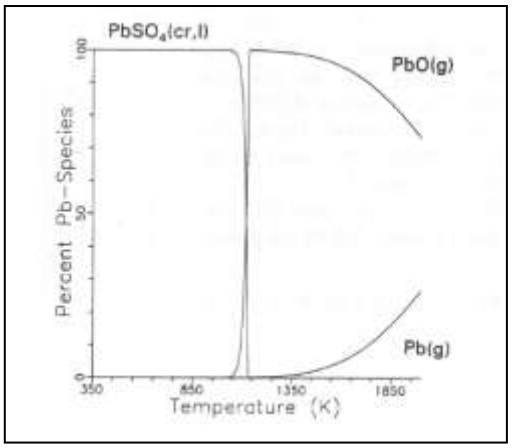

Figure 3.6 – Equilibrium distribution of Pb (%(mol Pb/mol Pb total)) at standard oxidizing conditions for a Cd/O system as a function of temperature in a flue gas from combustion of a sub-betuminous coal: λ=1.2 and $c_{Pb,O}$ = 25ppmw (Frandsen *et al*., 1994)..

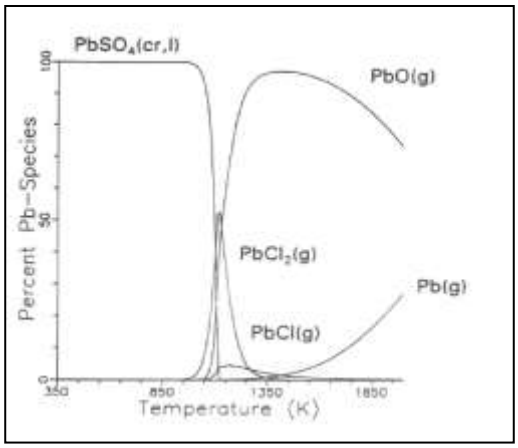

Figure 3.7 – Equilibrium distribution of Pb (%(mol Pb/mol Pb total)) at standard oxidizing conditions (in the Cd/O system) as a function of the temperature, in a flue gas from combustion of a subbituminous coal: λ=1.2 and $c_{Pb,O}$ = 25 ppmw and $c_{Cl,O}$ = 300 ppmw **(**Frandsen *et al*., 1994**)**.

Kajita and coworkers (Kajita, 1999), operating a 1.3 MW_{th} atmospheric circulating fluidized bed combustor and using RDF mixtures found that both sulphur and chlorine retention have a strong correlation with Ca/(S+0.5Cl) molar ratio.

The simultaneous presence of sulphur and chlorine enhanced the efficiency of metal capture in sorbents, according to Ho and co-workers (2000). The formation of sulphated species, which are more stable and could remain in the solid phase, could inhibit the formation of chlorinated heavy metals.

Almost all heavy metals, with the exception of Hg and Se, are associated with particulate matter. Thus the emission of these elements is highly dependent on the efficiency of the air pollution control device.

The emission of heavy metals can be reduced in three different ways:

- prior to coal combustion: by removing heavy metals from the coal
- after coal combustion:
    - removing heavy metals associated with the particulate matter by using particulate and SO_x control devices;
    - specific technologies used expressly to remove trace elements from the flue-gas.

The removal of heavy metals from coal can be achieved through several methods of cleaning processes, all based on the principle that coal is less dense than the pyretic sulphur, rock, clay, or other ash-producing impurities. Physical separation is then used to separate the impurities from coal. Another method is dense media washing, where heavy liquid solutions containing magnetite are used.

After combustion, most heavy metals are retained in the air pollution control devices, since metals have low vapour pressures at the devices operating temperatures, allowing condensation into particulate matter. In these cases, the reduction achieved for particulate matter can be extended to the metals, although with the same lower efficiency for small size particles, as described previously. The use of particulate matter control systems to reduce heavy metals emissions from coal combustion is considered the BAT for LCP, with a reduction greater than 99.5% for high performance ESP and greater than 99.95% for fabric filters.

Wet scrubber FGD systems allows an effective reduction in heavy metals emissions, due to the reduction of the flue-gas temperatures to about 50-60ºC, thus promoting the condensation of the more volatile metals. The condensed metals are mainly transferred to the wastewater stream of the wet FGD system. Special attention should be observed to the metals content of the lime, since an increase in As, Cd, Pb and Zn, might be observed if the lime used is rich in these metals.

3.6 Persistent Organic Pollutants: Polycyclic Aromatic Hydrocarbons, Dioxins & Furans and Polychlorinated Biphenyls

3.6.1 Polycyclic Aromatic Hydrocarbons

Polycyclic Aromatic Hydrocarbons (PAH) are a sub-group of Polycyclic Aromatic Compounds (PAC) that contain only carbon and hydrogen. Even though PAC can be originated from natural processes, such as volcanic eruptions and forest fires, anthropogenic activities are the main contributor to these compounds' concentration in the environment (Karunaratne, 1999), found in the atmosphere, soil, water and sediments.

The list of 18 PAH's identified as carcinogenic, mutagenic and teratogenic by the Agency for Toxic Substances and Registry (ATSDR) is presented in Table 3.6 (Lerda, 2010):

Table 3.6 – Toxic PAH's (Lerda, 2010).

▪ acenaphthene	▪ benzo[*b*]fluoranthene	▪ dibenz(a,h)anthracene
▪ acenaphthylene	▪ benzo[*ghi*]perylene	▪ fluoranthene
▪ anthracene	▪ benzo[*j*]fluoranthene	▪ fluorene
▪ benz[*a*]anthracene	▪ benzo[*k*]fluoranthene	▪ indeno(1,2,3-cd)pyrene
▪ benzo[*a*]pyrene	▪ chrysene	▪ phenanthrene
▪ benzo[*e*]pyrene	▪ coronene	▪ pyrene

High levels of PAH were found in biomass combustion, namely, coconut shell, and the effects of combustion parameters were investigated by Karunaratne (1999).

3.6.2 Dioxins and Furans

Dioxins and furans occur in the environment by natural processes, such as volcanic eruptions and forest fires, but the main contribution is from anthropogenic sources as by-products of industrial processes and in combustion. These pollutants include polycyclic aromatic hydrocarbons (PAH) as well as dioxins and furans.

Dioxins and furans are two of the twelve Persistent Organic Pollutants (POP) defined in the Stockolm Convention on Persistent Organic Pollutants which include (POPs, 2001): aldrin, chlordane, dieldrin, endrin, heptachlor, hexachlorobenzene (HCB), mirex, toxaphene, holychlorinated biphenyls (PCB) and DDT. Due to chemical similarities among the POPs or similar uses, the twelve POPs have been grouped into three main groups (POPs, 2007):

a) Pesticides (including HCB);
b) PCB, and
c) Dioxins and Furans.

The 1998 Aarhus Protocol on Persistent Organic Pollutants (POP, 1998), within the scope of the CLRTAP, with a wider range, besides the 12 POP of the Stockolm Convention also includes: lindane, chlordecone, hexabromobiphenyl and polycyclic aromatic hydrocarbons (PAHs).

Dioxins and furans is the common name for the group of chemical compounds consisting of polychlorinated dibenzo-p-dioxins (PCDD) and polychlorinated dibenzofurans (PCDF), respectively.

PCDD is a family with 75 compounds and PCDF is a family with 135 compounds. As defined in the Stockolm Convention on POP (POPs, 2001) "*PCDD and PCDF are tricyclic, aromatic compounds formed by two benzene rings connected by two oxygen atoms in polychlorinated dibenzo-p-dioxins and by one oxygen atom and one carbon-carbon bond in polychlorinated dibenzofurans and the hydrogen atoms of which may be replaced by up to eight chlorine atoms*". These compounds are structurally very similar, differing in the number and position of chlorine atoms (Figure 3.8), following international nomenclature.

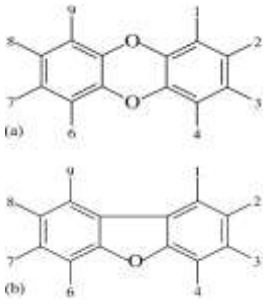

Figure 3.8 – Basic structure of (a) dibenzo-*para*-dioxin; (b) dibenzofuran.

Each individual PCDD or PCDF is named as congener, while groups of congeners with the same number of chlorine atoms are called homologues. The number of congeners in each homologue group of PCDD and PCDF are listed in Table 3.7.

Table 3.7 – Number of possible congeners and molar mass of PCCD and PCDF within each homologue group.

Homologue	Number of congeners		Molar mass (g)	
	PCDD	PCDF	PCDD	PCDF
Monochloro (M)	2	4	218.5	202.5
Dichloro (D)	10	16	253.0	237.0
Trichloro (Tr)	14	28	287.5	271.5
Tetrachloro (T)	22	38	322.0	306.0
Pentachloro (Pe)	14	28	356.5	340.5
Hexachloro (Hx)	10	16	391.0	375.0
Heptachloro (Hp)	2	4	425.5	409.5
Octachloro (O)	1	1	460.0	444.0
TOTAL	75	135		

Only seven PCDD and ten PCDF, listed in Table 3.7, are recognized as persistent, toxic and bio-accumulative compounds. All these seventeen compounds have the positions 2,3,7,8 chlorine substituted, and present different toxicity levels.

In order to evaluate the toxicological effects of PCDD/F, toxicity equivalent factors (TEF) were developed, having 2,3,7,8-TCDD, the most toxic known compound, as reference. The two most used TEF are those developed by NATO/CCMS (1988) (NATO/CCMS, 1988) and the TEF from the World Health Organization (WHO), with the last reassessment in 2005 (Van den Berg *et al.*, 1996). The NATO-TEF is worldwide accepted as the International toxicity equivalent factor (I-TEF), and these are adopted in the European Union legislation (Table 3.8).

Table 3.8 - International Toxicity Emission Factors (I-TEF) for PCCD/F.

TCDD	I-TEF	TCDF	I-TEF
2,3,7,8-TCDD	1	2,3,7,8-TCDF	0.1
1,2,3,7,8-PeCDD	0.5	1,2,3,7,8-PeCDF	0.05
1,2,3,4,7,8-HxCDD	0.1	2,3,4,7,8-PeCDF	0.5
1,2,3,6,7,8-HxCDD	0.1	1,2,3,4,7,8-HxCDF	0.1
1,2,3,7,8,9-HxCDD	0.1	1,2,3,6,7,8-HxCDF	0.1
1,2,3,4,6,7,8-HpCDD	0.01	2,3,4,6,7,8-HxCDF	0.1
OCDD	0.001	1,2,3,7,8,9-HxCDF	0.1
		1,2,3,4,6,7,8-HpCDF	0.01
		1,2,3,4,7,8,9-HpCDF	0.01
		OCDF	0.001

3.6.3 Polychlorinated Biphenyls

Polychlorinated Biphenyls (PCBs) is a group of chlorinated aromatic compounds similar to PCDD and PCDF, consisting in 209 individual substances. From these, there are 12 PCBs compounds considered toxic by the WHO. The twelve toxic PCBs, known as "dioxin-like" due to their structure, consisting of four non-ortho and eight mono-ortho PCBs, *i.e.* no chlorine atoms or only one chlorine atom in 2-, 2'-, 8- and 6'-position; all these twelve toxic PCBs have a planar or mostly planar structure (Figure 3.9).

Figure 3.9 – General structure of PCBs.

The Toxicity Emission Factors for these dioxin-like PCB were purposed by the WHO and are presented in Table 3.9. The TEF presented in Table 3.9 were revised in 2006, after a reevalution of the TEF purpose in 1998.

Table 3.9 - WHO Toxicity Emission Factors (WHO-TEF) for PCBs (Van der Berg *et al.*, 2006).

	Compound	**WHO-TEF**
Non-ortho PCB	3,3',4,4'-TetraCB (PCB 77)	0.0001
	3,4,4',5-TetraCB (PCB 81)	0.0003
	3,3',4,4',5-PentaCB (PCB 126)	0.1
	3,3',4,4',5,5'-HexaCB (PCB 169)	0.03
Mono-ortho PCB	2,3,3',4,4'-PentaCB (PCB 105)	0.00003
	2,3,4,4',5-PentaCB (PCB 114)	0.00003
	2,3',4,4',5-PentaCB (PCB 118)	0.00003
	2',3,4,4',5-PentaCB (PCB 123)	0.00003
	2,3,3',4,4',5-HexaCB (PCB 156)	0.00003
	2,3,3',4,4',5'-HexaCB (PCB 157)	0.00003

In Figure 3.10 the contribution made by different sectors to emissions of PCB, PAH and PCDD/F in Europe is presented.

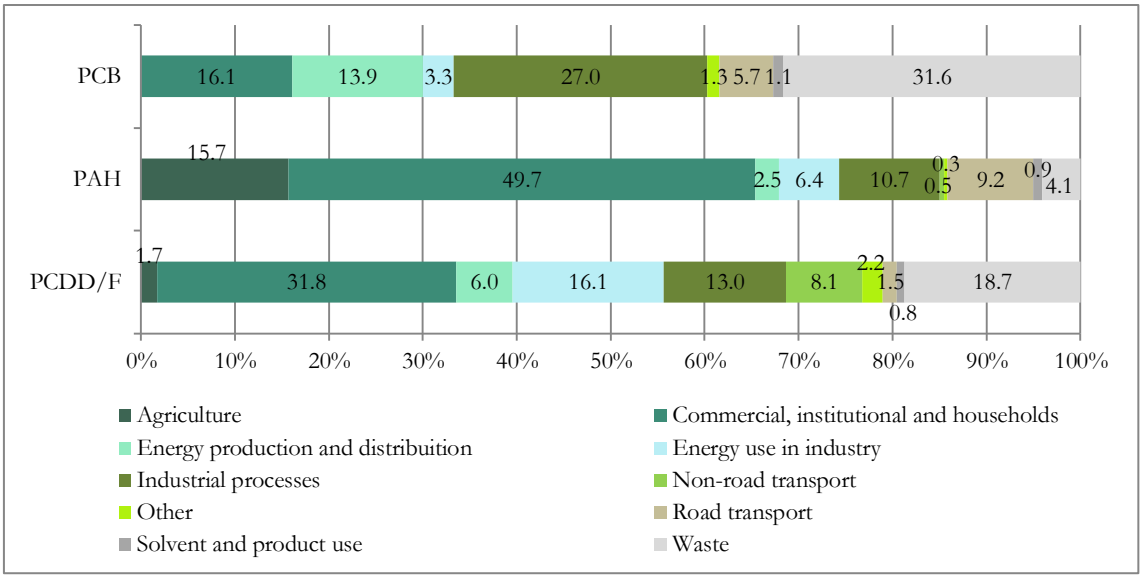

Figure 3.10 – The contribution made by different sectors to emissions of PCDD/F (from EEA, 2011).

4. Mechanisms of formation of Dioxins and Furans

The concentrations of PCDD and PCDF in the flue gas are the result of formation as well as degradation reactions (Figure 4.1). At the same time that PCDD/F are formed they are also degraded, since the degradation of PCDD/F in fly ash has been shown to occur in the same window temperature as their formation. However, the rate of their degradation increases with increasing temperature (Weber *et al.*, 1999). In a thermal system, the final result of PCDD/F will be the difference between the rates of formation and thermal destruction. Since the activation energies of the destruction reactions are higher than those of the formation reactions (Wehrmeier, 1998; Stanmore, 2004), the net rate of production has maxima at certain temperatures for both the homogeneous and heterogeneous reactions. Thus, the concentration of PCDD/F in a flue gas stream will be determined by a balance between formation and destruction reactions.

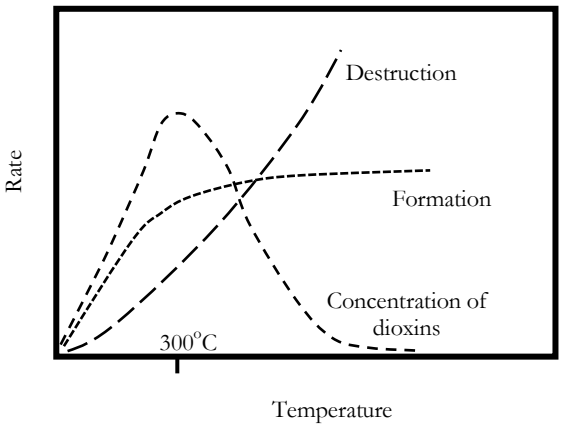

Figure 4.1 – The competing behaviour of formation and decomposition reactions (from Wehrmeier, 1998).

Several studies proposed mechanisms for PCDD/F formation in combustion systems. Dioxins and furans found in the ashes and stack gas could already be present in the fuels burned or can be the result from one of the three proposed PCDD/F formation mechanisms (Tuppurainen *et al.*, 1998):

i) pyrosynthesis, *i.e.* high temperature gas phase formation;

ii) the formation through the *de novo* synthesis from macromolecular carbon and the organic or inorganic chlorine present in the fly ash at 300-400ºC; and,

iii) through various organic precursors, which may be formed in the gas phase during incomplete combustion and combine heterogeneously and catalytically with the fly ash surface.

Both the precursor and *de novo* pathways of PCDD/F formation occur mainly at temperatures between 400°C and 250°C (Stieglitz, 1989; Milligan, 1996). Furthermore, studies have indicated that PCDFs are formed at higher rates than PCDDs at temperatures >400°C (Altwicker, 1996). Wikström and co-workers (2003) observed maximum PCDD formation rates at 300-400ºC, and maximum PCDF formation rates at 400-500ºC (Wikström *et al.*, 2003).

Several publications have identified *de novo* synthesis as the predominant formation pathway for the production of the PCDF, whereas the PCDD seem to be originated largely from precursors. Thus, the PCDD/PCDF ratio can provide indications regarding whether *de novo* or precursor formation pathway predominates in a specific case (Huang & Buekens, 1995). Generally, in MSW incineration the PCDF levels are higher than the PCDD levels (Everaert & Baeyens, 2002). Hunsinger and co-workers (2002) identifyied ratio F/D > 1 with *de novo* mechanism formation in the furnace, that could be minimized through optimization of the flue gas burnout; on the other hand, F/D ratios of ± 1 meant formation via precursor's mechanism that could be optimized with proper boiler cleaning procedure.

Formation pathways

The mechanism of formation of PCDD and PCDF from carbon is unclear and alternative routes have been proposed with wider definitions of *de novo* synthesis. The alternatives proposed (Jansson, 2008) include:

i) direct release from the carbonaceous structure (suggesting that the PCDD/F structures already exist in the carbon matrix);

ii) formation from particulate carbon via surface-bound chlorinated or non-chlorinated aromatic intermediates such as PAHs or phenolic compounds; and,

iii) formation resulting from precursor molecules that are adsorbed or chemisorbed onto the carbon surface.

Figure 4.2 summarises the PCDD/F formation pathways.

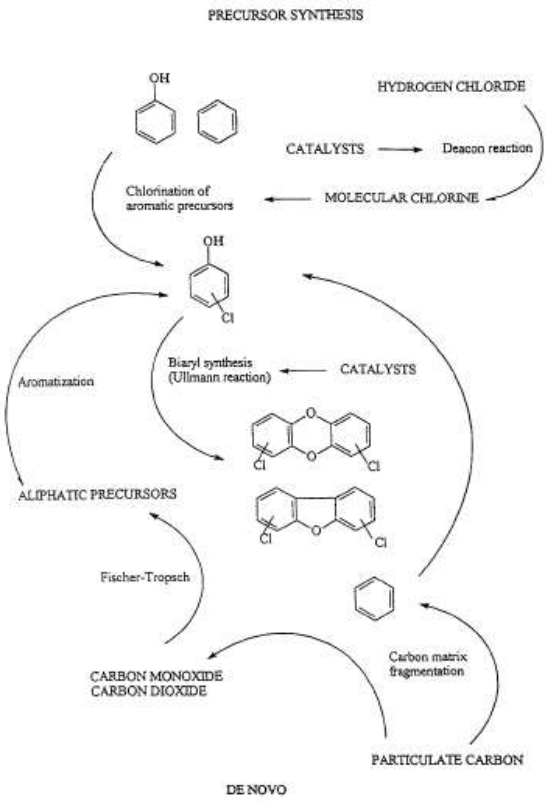

Figure 4.2 – Schematic representation of PCDD/F formation pathways (from Tuppurainen, 1998).

Precursors

A wide range of combustion by-products may act as precursors for the formation of dioxins and dioxin-like compounds. These include aliphatic compounds, monocyclic aromatics with or without functional groups and bicyclic or polycyclic aromatic compounds. Precursors may be present in the fuel and may be formed during combustion or in the post-combustion zone via multi-step reactions.

***De novo* synthesis**

De novo synthesis involves formation of dioxins and dioxin-like compounds from carbon structures in the fly ash particles entrained in the flue gas and deposited on surfaces in the post-combustion zone. Even though the distinction between precursor-mediated formation and *de novo* synthesis is not accurate, carbon in a particulate form is considered essential for the *de novo* synthesis of dioxins, and formation does not proceed via gas phase intermediates. According to Stieglitz (1998), two basic reactions are involved in the *de novo* synthesis of dioxins from carbon:

- transfer of inorganic chlorine to the macromolecular carbonaceous structure and formation of carbon-chloride bonds
- oxidative degradation of the structure

Thus, *de novo* synthesis may be defined as the chlorination and oxidation, although partial, of particulate carbon structures.

The role of chlorine

It is generally accepted that it is molecular chlorine, and not hydrogen chloride (HCl), that reacts with aromatic compounds such as phenols to produce chlorinated aromatic compounds, including chlorophenols and polychlorophenols, which are precursors of PCDD and PCDF (Xie *et al.*, 1999). The basic chemical equation for the formation of PCDD/F, commonly occurring in the temperature range between 650 and 250ºC, with a maximum value at approximately 300ºC, is the following (Tuppurainen *et al.*, 1998):

$$Cl_2 + \text{organic molecules} \rightarrow \text{chlorinated molecules (}e.g.\text{ PCDD/F)} \quad (4.1)$$

Chlorine may be present in different forms in a combustion process and gas-phase and solid-phase chlorine speciation may affect the formation of PCDD/Fs. Wikstrom and co-workers (2003) reported that while ash bound chlorine alone was a sufficient chlorine source for *de novo* formation, the addition of HCl to the system did not influence the yields of the PCDD/Fs, nor the degree of chlorination. The results of this and other work (Gullett, 1990; Wikstrom, 2000) showed that HCl is a weak chlorinating agent. Although HCl can readily react with oxidizing radicals, such as OH^- and $HO_2\cdot$, in combustion to produce $Cl\cdot$, it would be much more difficult to dissociate HCl into $H\cdot$ and $Cl\cdot$ radicals than Cl_2 into $Cl\cdot$ radicals. This is due to a much stronger H–Cl bond (430 kJ/mol) than Cl–Cl bond (240 kJ/mol) (Wikstrom *et al.*, 2003). Given that $Cl\cdot$ is a very reactive radical, it can be concluded that Cl_2 will be a strong chlorinating agent. It was observed (Wikstrom, 2003) that the yields of PCDD/Fs in the presence of only Cl_2 were similar to those with both Cl_2 and $Cl\cdot$ present. However, the concentration of HCl in incineration processes is much higher than that of Cl_2. In addition, Addink and co-workers (1995) have observed that the *de novo* formation rate in the presence of high concentrations of HCl is similar to that in the presence of high concentrations of Cl_2. In power boilers burning salt-laden hog fuel, the chlorine is introduced mainly as NaCl. Addink and co-workers (1998) found that NaCl could be a chlorinating reagent for formation of PCDF on aqueous extracted incinerator fly ash. However, PCDD were not formed, possibly because the PCDD formation catalyst had been removed through the extraction process. No difference was made by adding NaCl to the as-received incinerator ash, suggesting that NaCl was not as reactive as other chlorine sources originally present in the ash.

Kilgroe (1996) and Everaert (2001) reported that improving combustion conditions in the furnace and lowering electrostatic precipitator temperatures significantly lowered dioxin/furan emissions.

In Aurell's Ph.D. thesis (2008), who studyed the combustion of MSW in a laboratory scale fluidized bed reactor, found that the parameter that most strongly reduces PCDD/F formation is long flue gas residence time at relatively high temperatures (460ºC). A significant reduction was also found in

PCDF formation with the SO_2/HCl ratio increasing to 1.6 while PCCD showed no differences. Fluctuation in combustion process (CO peaks), high chlorine in waste (1.7%) and low temperatures in the secondary combustion zone (660°C), all tend to increase the emission levels. PCDD/PCDF ratio in the flue gas depend on chlorine level in the waste, fluctuations in the combustion process and the SO_2:HCl ratio in the flue gas. Formation pathways were found to be affected by the following parameters include:

i) quench time profiles in the post-combustion zone;
ii) fluctuations in the combustion process;
iii) addition of sulphur; and,
iii) increased levels of chorine in the waste increased the chlorination degrees of both PCDD and PCDF.

Dioxins and furans may also be formed in the presence of HCl, which can be converted to Cl_2 through the known Deacon reaction:

$$2HCl + \tfrac{1}{2}O_2 \rightleftarrows Cl_2 + H_2O \qquad (4.2)$$

The role of copper

Many copper catalysts can promote this reaction considerably, namely elemental copper (Cu), copper chlorides (CuCl, $CuCl_2$), copper oxides (CuO and Cu_2O) and copper sulphates ($CuSO_4$). In fact, the reaction might be a two-step reaction (Tuppurainen *et al.*, 1998):

$$2Cu + \tfrac{1}{2}O_2 = \rightleftarrows Cu_2O \qquad (4.2a)$$

$$Cu_2O + 2HCl = \rightleftarrows 2Cu + H_2O + Cl_2 \qquad (4.2b)$$

The role of sulphur

Another type of inhibitors are compounds that are likely to form complexes with transition metal ions that catalyze PCDD/F formation, where sulphur plays an important role. Several studies have shown that the presence of sulphur dioxide reduces the level of PCDD/F formation during incineration processes (McKay, 2002; Ogawa *et al.*, 1996, Chang *et al.*, 2006), since sulphur can capture the chlorine molecule in the presence of moisture producing SO_3 and HCl (Tuppurainen *et al.*, 1998).

In a study conducted by Xie and co-workers (2000) it was verified that dramatic decreases were observed in the major chlorine-containing products of combustion for molar ratios of S/Cl greater than 2.5. Other authors suggested different S/Cl molar ratios; Ogawa and co-workers (1996) proposed molar ratios greater than 2 and Chang and co-workers (2006) concluded that it should be

a value more than 1, in their study at laboratory scale where elemental sulphur was added to industrial wastes.

Gullett and co-workers (1992) and Chen and co-workers (1997) also proposed that sulphur could reduce the catalytic activity of Deacon Reaction catalysts, and this has experimentally been observed by Chang and co-workers (2006). A further possible mechanism is that SO_2 sulphonates the phenolic PCDD/F precursors and, consequently, either prevents chlorination and biaryl synthesis or promotes the formation of polychlorodibenzothiophenes and polychlorothianthrenes, the sulphur analogues of PCDD and PCDF (Gullett *et al.*, 1992).

In the presence of SO_2, Cl_2 may be reduced by oxidation of SO_2 according to the following reaction:

$$Cl_2 + SO_2 + H_2O \rightleftarrows SO_3 + 2HCl \quad (4.3)$$

The above reaction is thermodynamically very much favoured; SO_2 may also be oxidised by O_2:

$$SO_2 + ½\ O_2 \rightleftarrows SO_3 \quad (4.4)$$

When O_2 is present in great excess in combustion processes, reaction (4.4) should be considered to be competing with reaction (4.3) for SO_2. Equation (4.5) is the combination of reactions (4.3) and (4.4):

$$Cl_2 + 2SO_2 + H_2O + ½\ O_2 \rightleftarrows 2SO_3 + 2HCl \quad (4.5)$$

Combustion conditions

Another factor identified in the literature that affects PCDD emissions is the combustion conditions. These include combustion temperature, residence time, supplemental fuel, fuel processing, and oxygen availability. Combustion efficiency is a function of all of these factors. In order to destroy PCDDs or prevent their formation, the combustion efficiency must be high. This requires a combination of high temperatures, available oxygen, high heating value fuel, and long residence times. Even with these optimised combustion conditions end-of-pipe flue gas treatment is still required to meet the European Union PCDD/F emission limit of 0.1 ng/Nm^3.

Jansson (2008), who also studied MSW combustion in a fluidized bed installation at Umea University, Sweden, focused on the formation and chlorination pathways of dioxins and dioxin-like compounds in waste combustion flue gases in the temperature range 640-200ºC. The main conclusions from this Ph.D. study was that the contribution from homogeneous reaction is small/, or even negligible, from thermal formation in gas-phase (homogeneous reactions), at high

temperatures. The PCDD/F formation over gas- and solid-phase interface (heterogeneous reactions) occur at temperatures lower than 500°C, with two main routes: *de novo* synthesis and formation from percursors.

Particle size

The global (external) surface area appears to be a better basis for quantifying reaction rates (Stieglitz, 1997). Following an analysis of incinerator fly ash, Fängmark (1994) concluded that chlorinated organics tend to be concentrated on the smaller particles. A similar result has been reported by Ruokojärvi and co-workers (2001), where the fraction below 1.6-μm was disproportionately loaded. The distribution of PCDD/F with particle size in atmospheric dust collected at four Japanese sites was examined by Kurokawa and co-workers (1998), where the maximum size collected was 30 μm in aerodynamic diameter, and the smallest 0.1 μm. Particles less than 1.1 μm aerodynamic diameter contributed 50% of the total PCDD/F, with an almost equivalent I-TEQ proportion.

Also the homologues distribution were found to change with size, with the fraction of less chlorinated congeners in the homologue groups increasing with increasing particle size. The results of Ryan and co-workers (2000) on two carbon blacks showed that the external surface area of the spherules was the significant variable, normalised for the external (global) surface area and the carbon and chlorine contents by the empirical variable (φ)

$$\varphi = 3[\text{PCDF}]/(dp[\text{C}][\text{Cl}]) \qquad (4.6)$$

where dp is the particle diameter (μm) and [PCDF], [C], and [Cl] are the concentrations of PCDF, carbon, and chlorine, respectively.

Kinetics and thermodynamics

Most of the kinetic models available in the literature to describe PCDD/F formation rates are empirical. Mätzing (2001) proposed a kinetic model for *de novo* synthesis assuming the fly ash carbon oxidation reaction was first order in carbon and a half order in oxygen, leading to CO_X, PCDD, and PCDF. The fraction of the carbon being oxidized to PCDD/F was assumed to depend on the amount of catalyst present. It also considered further oxidation of the formed PCDD/F on fly ash surfaces. This model contained six reaction rate constants, and required two parameters, *i.e.* the pre-exponential factor and the activation energy, to be estimated for each rate constant. The kinetic model derived by Huang & Buekens (2000) for *de novo* synthesis of PCDD was based on similar mechanistic steps as those in Mätzing's model, *i.e.* carbon gasification with O_2, PCDD/F formation, desorption, and degradation. This model contained a total of eight unknown parameters.

Altwicker *et al.* (1990) developed an empirical model based on a four-step dioxin precursor formation mechanism:

solid and gas phase precursor reactions form solid phase dioxins
↓
desorption of solid phase dioxins into the gas phase
↓
solid phase dioxin dechlorination
↓
solid phase dioxin decomposition

This model contained four reaction rate constants, each with two parameters to be estimated. While the most active temperature range for *de novo* formation of PCDD/F is known to be 300–350 ºC, this model showed a maximum rate for the formation of PCDD from precursors at 250–300 ºC.

Altwicker (1996) further compared the relative rates of precursor and *de novo* formation and concluded that the precursor reactions tended to be much faster and could occur in a wider temperature range (up to 600 ºC) than those associated with the *de novo* mechanism.

It is clear that a comprehensive model should include both precursor reactions and *de novo* synthesis. Stanmore (2002) extended an empirical model for *de novo* formation on fly ash to include the precursor mechanism and a gas phase formation component. This model employed a sticking factor quantifying the adsorption potential of gaseous reactants (*e.g.* HCl, Cl_2 and/or precursors) on the ash surface. The value of the sticking factor was found to decrease exponentially with increasing sulphur concentrations in the flue gas. Since the dioxin formation rate increases linearly with an increasing sticking factor value, the model predicts that sulphur would inhibit dioxin formation.

The sulphur effect was also studied by Mueller and co-workers (1999) using a large computer model. It consisted of 199 elementary reactions to describe the C/H/O/N system, 36 more reactions involving Cl, and up to 91 additional reactions to cover sulphur interactions with O and N species. Unfortunately, this model only deals with radical chain reactions occurring at high temperatures (*e.g.* >800 ºC) in combustion and post-combustion gases. As it will be seen later, oxidation of SO_2 and HCl are not thermodynamically favored at high temperatures and, therefore, this detailed model has only limited use in explaining and predicting the effect of sulphur and chlorine on PCDD/F formation, which occurs mainly at lower temperatures.

Even the above empirical models are complicated, containing 8–12 parameters to be estimated. It would be very difficult to apply any of these models to describe dioxin formation and emissions from full-scale power boilers or incinerators. Based on test results on municipal solid waste incinerators, Everaert & Baeyens (2001) obtained a very simple correlation (Eq. 4.7) between stack PCDD/F emissions and the electrostatic precipitator (ESP) temperature:

$$\log (\text{PCDD/F})_T = (0.016T - 3.001) \quad (4.7)$$

Efforts have been made by several research groups to develop thermodynamic and kinetic models describing dioxin formation and predicting experimental results obtained on various facilities of different scales. Thus, the thermodynamics determine that PCDD/F can only be formed at localized sites as intermediate products with trace concentrations in combustion processes. The intermediate products may become "permanent" if the reaction conditions kinetically inhibit their subsequent, complete oxidation.

Given the general complexity of thermodynamic models, it is difficult to use them to interpret the overall process of dioxin formation. Also, the model developed by Tan (2001) cited by Duo & Leclerc (2007) did not include solid phase and chloride species. Studies on whether the total chlorine level was important for the formation of PCDD/Fs have led to contradictory conclusions. For instance, Yasuhara and co-workers (2002) studied the role of inorganic chlorides on the formation of PCDD/Fs in incineration processes. They found that dioxin formation increased with the NaCl content in impregnated newspapers being incinerated. Wikstrom and co-workers (1996) investigated PCDD/F formation in the combustion of an artificial fuel, containing 34% paper, 30% wheat flour, 14% sawdust, plastic materials and metals, with PVC or $CaCl_2$ added. No correlation was found between the levels of dioxin formation and the fuel chlorine content.

Duo & Leclerc (2007) applied the formation mechanisms proposed in the literature, namely precursor and *de novo*, to power boilers burning salt-laden hog fuel.

Based on test results on salt-laden hog fuel boilers, Duo & Leclerc (2007) developed a semi-empirical model relating stack PCDD/F and PAH stack emissions, [NaCl] in the hog fuel and the electrostatic precipitator (ESP) temperature:

$$[TEQ\_stack] = A + B \exp(-C/T\ ESP) + D[PAH\_stack].[NaCl]hog^2 \quad (4.8)$$

where A, B, C and D are four model parameters to be estimated with experimental data.

Poor combustion conditions in the furnace favour the formation of gas-phase precursors, such as chlorophenols and polycyclic aromatic hydrocarbons (PAHs), which lead to dioxin/furan formation through condensation and adsorption/ desorption reactions on ash particles (Leclerc, 2004). Also, high flue gas temperatures in the heat exchanging and gas cleaning zones favour dioxin/furan formation through solid-phase reactions on fly ash involving certain catalysts and unburnt carbon. A combination of the two mechanisms may be encountered in a given boiler, depending on its design and operational parameters.

Other PCDD/F Inhibitors

The emissions of PCDD/F to the atmosphere can be prevented either by the use of primary measures, through preventing the formation of those compounds, or through secondary measures in which the PCDD/F formed are removed through air pollution control devices. Primary

measures should be applied whenever it is possible, not only because preventing the formation of pollutants leads to more sustainable combustion processes but also because the installation and maintenance of secondary measures is much more expensive than applying primary measures (Pandelova *et al.*, 2005).

Lenoir and co-workers (2007) proposed the sue of primary measures to reduce PCDD/F through the Principles of Sustainable Chemistry.Primary measures in the prevention of PCCD/F formation can be achieved either by the optimisation of operational conditions, like temperature, turbulence, air flow and residence time, or through the addition of chemical compounds that inhibit or greatly reduce PCDD and PCDF formation. According to their chemical nature and structure these inhibitors are grouped as basic compounds, S-containing compounds, N-containing compounds, N- and S-containing compounds, and metal oxides.

Basic inhibitors such as NH_3, CaO, NaOH, KOH and Na_2CO_3, were the first tested under laboratory conditions, and the proposed mechanism to justify the observed decrease of PCDD/F formation was the change in the acidity of the fly ash surface (Addink, 1996).

Beyond sulphur dioxide, discussed previously, other sulphur compounds were studied as PCDD/F inhibitors namely hydrogen sulphide, sodium sulphide (Na_2S) and sodium thiosulphate ($Na_2S_2O_3$) and, in all laboratory-scale tests cases, it was found that lesser amounts of PCDD/F were formed with increasing amounts of inhibitor present (Addink, 1996).

In a 50-kW pilot plant incinerating waste, Ruokojärvi and co-workers (2004) tested four gaseous inhibitors, namely sulphur dioxide, ammonia, dimethylamine (DMA), and methyl mercaptan, observing a clear reduction in PCDD/F concentrations.

Functionalized amines such as ethylenediaminetetraacetic acid (EDTA), ethanolamine and trimethylamine can also be effective as inhibitors of PCDD/F (Samaras *et al.*, 2000). An interaction (complexation) with the (Cu) catalyst is the most likely manner in which the functionalized amines work. Addink and co-workers (1996) studied the inhibition effect of EDTA, nitrilotriacetic acid (NTA), Na_2S and $Na_2S_2O_3$, in a laboratory scale reactor, finding 80-90% reduction in PCDD/F formation when EDTA, NTA and Na_2S were used.

The studies of Samaras and co-workers (2000) and Ruokojärvi and co-workers (2004), led them to propose that the addition of inorganic S- and N-compounds to the fuel before combustion could effectively reduce PCDD/F formation. Samaras and co-workers (2000) tested five different compounds in a laboratory scale horizontal reactor: urea, amidosulphonic acid (ASA), hydroxylamine-O-sulfonic acid (HOSA), sulfamide and elemental sulphur. It was observed only a slight reduction in the emission PCDD/F when urea was added; for the other sulphur containing compounds a significant reduction was achieved.

Pandelova and co-workers (2005) tested 19 different substances as inhibitors during the co-combustion of lignite coal and waste in a laboratory scale furnace. The 19 inhibitors tested were: 3 N-containing compounds; 3 S-containing compounds; 6 N- and S-containing compounds; and 7 metal oxides. The metal oxides showed no inhibitory effect in PCDD/F formation, and the

presence of the metal oxides Cr_2O_3 and Al_2O_3 even increased the PCDD/F formation through the *de novo* mechanism. The N-containing substances showed low inhibition in PCDD/F formation while the S-containing compounds reduced the formation of dioxins and furans, as expected. The greater reduction was achieved with the N- and S-containing compounds, being the $(NH_4)_2SO_4$ and $(NH_4)_2S_2O_3$ the most efficient additives. When $(NH_4)_2SO_4$ was present at 3% of the fuel, a reduction of 90% in PCDD/F formation was achieved. The use of this inhibitor was tested by Pandelova and co-workers (2009) in a pilot scale plant during the co-combustion of wood and hospital waste, where a 50% reduction in PCDD/F formation was achieved when 5% of $(NH_4)_2SO_4$ was added as inhibitor.

Sánchez-Hervás and co-workers (2005) studied the effect of using solid urea as inhibitor in a pilot scale bubbling fluidized bed unit of 0.5 MWth in the co-combustion of coal and PVC. The results showed the prevention of PCDD/F formation due to the addition of the inhibitor, although an increase from 5 to 10% (w/w) does not seem to yield further PCDD/F reduction.

The co-combustion technology is another way of reducing PCDD/F formation through a primary measure. Co-combustion processes may combine the appliance of a primary measure in PCDD/F formation either by the positive synergies of combining different fuels or the addition of inhibitors, allowing at the same time the reduction of GHG emissions when renewable energy sources are used as fossil fuel substitutes. The replacement of coal with different materials may bring positive synergies in decreasing pollutant emissions. This was the purpose of the research carried out in this work. The experimental results and the effect of different parameters, namely, combustion temperature, chlorine, sulphur, calcium and copper contents, flue gas composition in terms of SO_2, HCl, O_2 and CO_2, and ashes composition and diemnsion, will be presented and discussed in the following chapters.

Secondary measures for the reduction in PCDD/F emissions can be achieved through several ways (Ruokojärvi *et al.*, 2004): the adsorption of PCDD/PCDF on active carbon or coke, the use of FDG technology (dry scrubbers with lime and the injection of activated carbon), or by using NO_X reduction equipment (Selective Catalytic Reduction (SCR) using a TiO_2-DeNO_X catalyst).

Interaction between fuel composition and PCDD/F formation

The complexity of the emissions resulting from a combustion process is illustrated in Figure 4.3 where the effect of the fuel composition in the different emissions pollutants is shown.

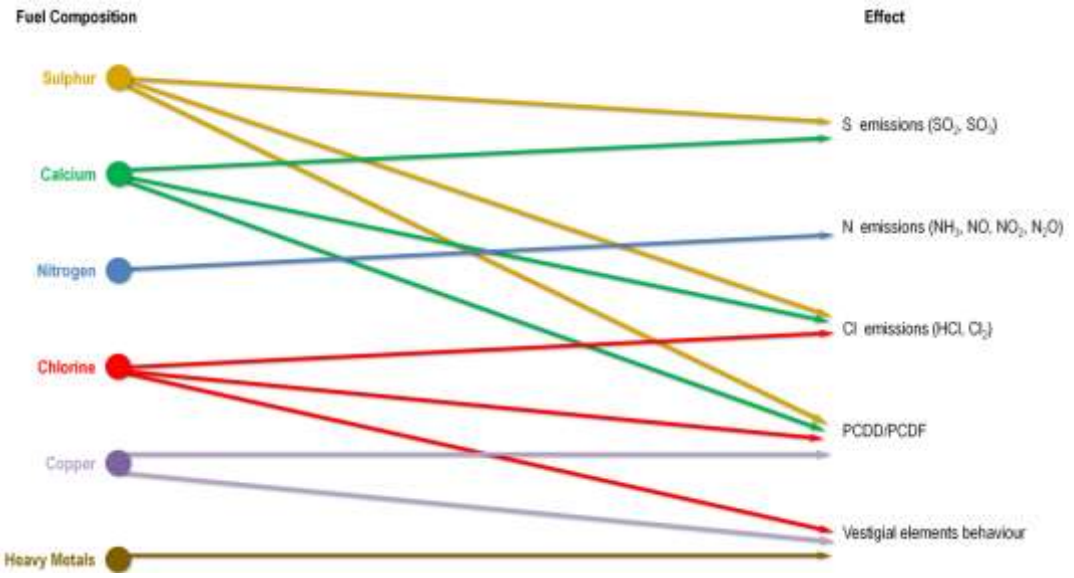

Figure 4.3 – Interaction between fuel composition and effects.

Figure 4.3 illustrate the effect of the fuel composition elements with the different emissions resulting from a combustion process.

Effect of different parameters in the PCDD/F formation

Table 4.1 summarizes the effects of the different parameters in the PCDD/F formation previously discussed.

Table 4.1 – Effect of different parameters in PCDD/F formation.

	Increased/decreased parameter	Effect(*)
Fuel	+Chlorine-Fuel	depends on S content
	+Sulphur-Fuel	depends on Ca content
	+Calcium-Fuel	-
	+Copper-Fuel	+
Operational conditions	+Combustion temperature	-
	+Cyclones temperature	+
Stack-gas	+HCl	+
	+SO_2	-
	+CO	+
	+O_2	+/0
	+NO_X	≈
Ashes	+ Fly ash diameter	-
	+Cyclone ashes diameter	-
	+Cu in Cyclone ashes	+
	+Cl in cyclone ashes	+

(1) +: increasing effect / 0: no substantial change / -: decreasing effect

5. Experimental work

5.1 Experimental Programme

Three types of materials were selected as fuels to be studied within the scope of this research: coal, biomass and non-toxic wastes. These are identified in the following Table 5.1.

Table 5.1 – Identification and codification of the monocombustion and co-combustion tests.

Fuel		**Code**	**Origin**
Coal	Colombian [3]	CC I, CC II, CC III	CTH (Chalmers)
	Polish	PC I	Duisburg
Non-toxic Waste	Meat and Bone Meal	MBM	Portugal (Rogério Leal & Filhos, SA)
Biomasses	Straw Pellets	SP	Denmark (densified wheat straw)
	Olive Bagasse	OB	Portugal (UCASUL)
	Wood pellets	WP	Sweden (densified by-products from forest industry)
	Rice Husk	RH	Italy

The Colombian coal (CC), as well as the Meat and Bone Meal (MBM) and the wood pellets (WP) were selected because these materials were actually burned in the Duisburg AG plant (one of the partners of the Copower project). The use of Polish coal (PC) and the straw pellets were decided because of their growing importance as energy source in the northern Europe. The olive bagasse (OB) and the rice husk (RH) were also selected because of its potential importance as co-firing fuel, in Mediterranean countries.

[3] Three different batchs of Colombian coal were used.

Test runs included the mono-combustion of each fuel and the co-combustion of a mixture where 5, 15 or 25% (w/w) of the coal was replaced by the same percentage of MBM, straw, olive bagasse and wood (Figure 5.1). However, only the 15% mixtures for MBM and Straw were analyzed for PCDD/F; a 100% Rice Husk test was also done.

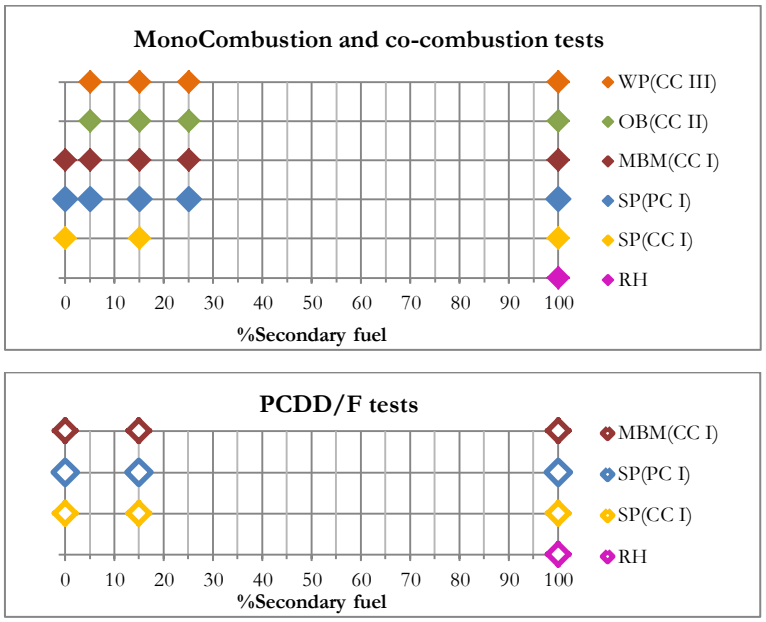

Figure 5.1 – Selected tests.

5.2 Materials used

Extensive characterization of the fuels burned in this work, was performed using the methodologies described in Table 5.2. Table 5.3 presents the results of this characterization.

The coals were selected, among the ones normally used in Portuguese power stations, in order to present different contents of sulphur and chlorine. In fact, PC coal presents four times higher content of chlorine than the CC coal although the sulphur content is 50% lower. Regarding the presence of the heavy metals listed in Table 5.2, Polish coal always presents higher contents than the Colombian coal, with the exception of Pb and Zn. The coals were crushed and sieved making use of the fraction between 0.25 and 8.0 mm.

Table 5.2 – Fuels characterization methodologies (COPOWER, 2007).

Parameter	Standard method
Proximate Analysis of Coal and Coke	ASTM D 3172
Carbon, Hydrogen and Nitrogen	ASTM D 5373
Sulphur	ASTM D 4239
Moisture	ASTM D 3173
Ash	ASTM D 3174
Volatile Matter	ISO 562
High and Low Calorific value	ASTM D 5865
Chlorine and Fluorine	ASTM D 2361; measurement by SW 846 – method 6500
Heavy Metals	EN13656 with previous ashing at 500ºC; measurement by AAS
Hg	ASTM D 6722-01

Table 5.3 - Fuels analyses (COPOWER, 2007 and INETI, 2007d).

FUELS	Coals				Waste	Biomasses			
	CC I	CC II	CC III	PC	MBM	WP	OB	SP	RH
Proximate Analysis (a.r., %wt)									
Moisture	9.3	2.5	13.5	4.7	3.2	8.6	7.9	9.1	9.2
Ash	11.4	12.0	8.0	10.5	37.3	0.4	4.9	6.3	13.4
Volatile Matter	33.6	34.7	34.0	31.5	54.1	79.0	70.6	68.5	62.4
Fixed Carbon	45.7	50.8	44.5	53.3	5.4	12.0	16.6	16.2	14.9
Elemental Analysis (d.b., %wt)									
C	66.4	68.8	69.4	69.5	32.2	45.4	46.6	41.7	38.1
H	4.7	4.6	4.5	4.8	5.0	6.3	6.4	6.2	5.8
N	1.4	1.5	1.5	1.2	8.2	<QL	1.0	0.7	0.4
S	0.95	0.92	0.68	0.5	0.4	<0.3	0.10	0.13	0.06
Cl	0.07	0.03	0.03	0.25	0.28	<0.03	0.31	0.24	0.03
Ca	0.21	0.16	0.14	0.43	12.9	0.055	0.26	0.27	0.09
Heavy Metals (mg/kg, d.b.)									
As	<10	<10	<10	<10	<10	<10	<10	<10	n.det.
Cd	<0.5	<0.5	<0.5	<0.5	<5	0.1	<5	<0.5	<1
Cr	13.8	10.7	17.1	29.8	<10	2.1	<5	5.2	<1
Cu	7.9	7.7	8.8	11.2	4.1	3.0	1.1	2.9	3
Hg	0.048	0.039	0.039	0.110	0.025	0.004	0.004	0.018	0.002
Mn	47.1	63.8	56.0	108	<10	134	0.8	19.3	101
Ni	8.5	8.8	10	30.9	<10	0.3	<5	4.5	<1
Pb	<1.0	1.8	2.4	12.0	<10	0.4	<5	<1.0	<1
Zn	25	25	26	27.2	97.5	10.5	0.9	6.5	16
LHV (d.b., MJ/kg)	28.0	26.9	28.73	29.3	14.5	18.4	18.9	16.5	15.5

ar – as received; db – dry basis; n.det. – not determined

The secondary fuels selected presented high levels of volatile matter, reaching about 70% in the case of straw pellets and olive cake. Straw was used in the form of pellets (5x30mm) and the fraction below 15mm of the olive cake was taken to be used in the combustion runs.

These materials present similar chlorine content, being about the same as the Polish coal. MBM contains high ash content due to the bones present, and consequently a high content of Ca, while straw and olive cake present only a half of the coals ash content. In Figure 5.2 the molar ratios Ca/S and S/Cl are presented.

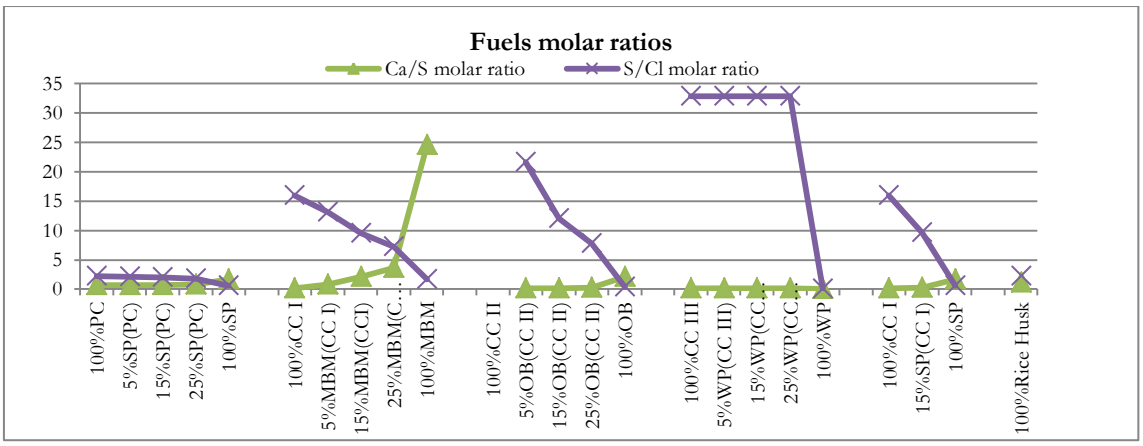

Figure 5.2 – Molar ratios for the test runs.

MBM has about eight times more nitrogen content than the other materials. Sulphur in straw pellets and in olive cake is much lower than in the other materials. As for heavy metals, the alternate fuels have lower heavy metal contents. The copper content of all fuels are of the same magnitude, from 1.1 - 11.2 mg/kg (d.b.). The low heating value of the biomasses is between half and two thirds that of the coals.

The fuels Coal Cerejon, MBM and Rice Husk were analyzed for dioxins and furans (Table 5.4). The fuels were analysed using an internal method based in EPA 1613 method.

Table 5.4 – PCCD/F content in selected fuels.

ng/kg fuel	Test Runs		
	Coal Cerejon	**MBM**	**Rice Husk**
2,3,7,8-TCDF	0.7	0.020	1.6
1,2,3,7,8-PeCDF	<QL	0.064	3.4
2,3,4,7,8-PeCDF	<QL	<QL	7.9
1,2,3,4,7,8-HxCDF	<QL	0.033	8.9
1,2,3,6,7,8-HxCDF	<QL	<QL	5.1
2,3,4,6,7,8-HxCDF	<QL	<QL	7.4
1,2,3,7,8,9-HxCDF	<QL	0.170	4.6
1,2,3,4,6,7,8-HpCDF	<QL	<QL	25.0
1,2,3,4,7,8,9-HpCDF	<QL	0.310	5.5
OCDF	<QL	0.020	45.0
2,3,7,8-TCDD	<QL	<QL	0.6
1,2,3,7,8-PeCDD	<QL	<QL	2.3
1,2,3,4,7,8-HxCDD	<QL	<QL	2.2
1,2,3,6,7,8-HxCDD	<QL	0.130	2.9
1,2,3,7,8,9-HxCDD	<QL	<QL	2.2
1,2,3,4,6,7,8-HpCDD	<QL	2.400	17.0
OCDD	9.0	11.000	110.0
Total PCDF	0.7	0.597	114.4
Total PCDD	9.0	13.530	137.2
Ratio PCDF/PCDD	0.08	0.04	0.83
Total PCDD/F	9.7	14.127	251.6

For the three selected fuels, the PCDD content is higher than the PCDF content. In terms of PCDF homologue mass distribution, both MBM and Rice Husk present significant contents of high-chlorinated isomers, the less toxic compounds (Table 3.6); coal cerejon contain only the TCDF isomer. As for PCDD, all analyzed fuels present more than 80% of OCDD, thus a lower toxicity.

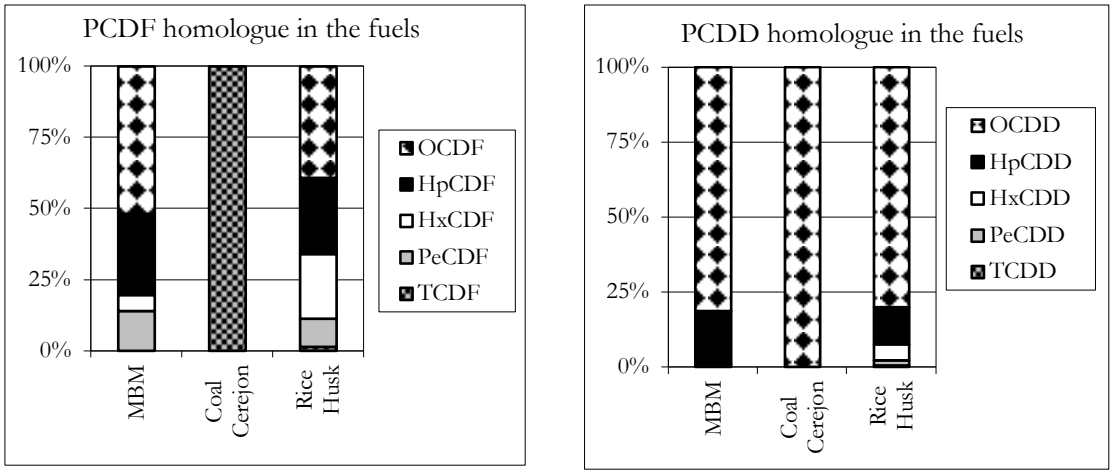

Figure 5.3 – PDCF and PCDD homologue mass distribution in the fuels.

5.3 Experimental Installation Description

The combustion studies were carried out in two pilot installations of INETI - National Institute of Engineering, Technology and Innovation (restructured to LNEG – National Laboratory of Energy and Geology). The smaller size installation was built some years ago and is called in this work as "Old installation", with a nominal capacity of 70kW$_{th}$; the "New installation", built around 2006, is a larger installation and has a nominal capacity of 100kW$_{th}$.

Figure 5.5 describes schematically the pilot installations used for the tests. Figure 5.6 presents two photographic views of the new installation.

Both installations have square cross sections and the combustor body were made of refractory steel and were externally insulated. Air staging was done in both installations between the bed and the freeboard to deal with high volatile fuels. Bed and freeboard temperatures were continuously monitored (Figure 5.4).

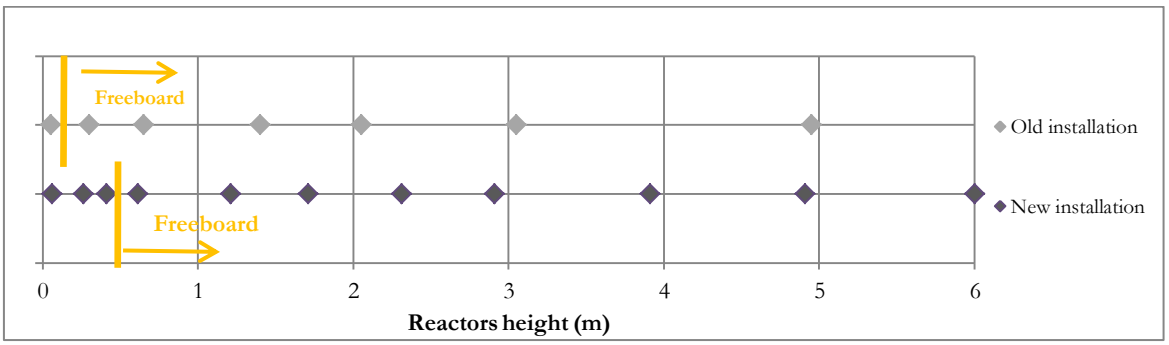

Figure 5.4 – Temperature measurement points along the reactor.

There are two independent gas/water heat exchangers in the reactor, one immersed in the bed and another in the freeboard, which allows the temperature control.

Ashes were separated from the flue gases through two cyclones installed in series and the gases were then released to the atmosphere through a stack after the second cyclone. For feeding the fluidised bed combustor, coals were crushed and sieved to separate out the fraction between 0.25 and 8.0 mm. Fluff materials such as straw, wood and sewage sludge, were prepared as pellets in order to increase their density and improve the fuel feeding to the reactor. The MBM/Colombian Coal and Straw/Polish Coal tests were performed in this old reactor.

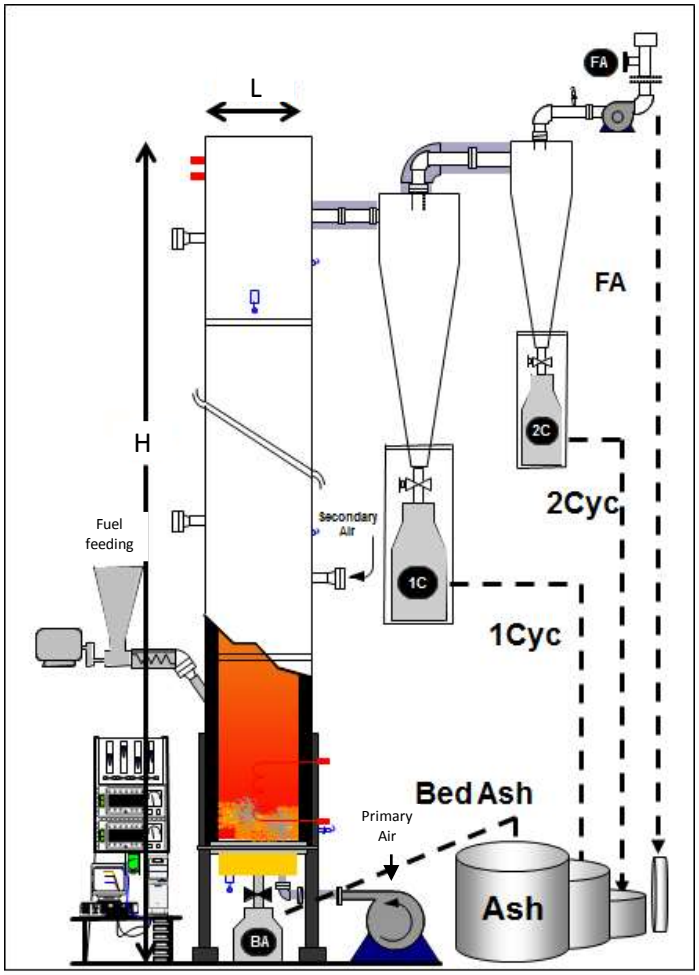

- **Stainless Steel**
- **Height (H): 5m (Old); 6m (New)**
- **Side (L): 0.30m (Old); 0.35m (New)**
- **External insulation**
- **Water coil refrigeration**
- **Bed material-Sand**
- **Air Staging between bed and freeboard**
- **2 Cyclones for fly ash separation**
- **Sampling Probes along the Reactor for gas measurements**
- **Sampling Probes in the stack for particles, metals, HCl and PCDD/F**
- **Computerized Control (T, P, air and Fuel flow)**

Figure 5.5 – Schematic view of the pilot fluidised bed combustors.

The new combustor has 6.0 m height and it has a 0.35 m size of square section. The bed was operated in bubbling regime, with a static height of about 0.5 m and its temperature was maintained by means of nine water-cooled gas sampling probes, immersed with the desired length. Secondary air could be fed at two levels, at 1.1 and 1.6 m respectively. There are two cyclones placed in series, at the combustor exit, for particulate matter removal, which was not recirculated but was collected for analysis. The combustor was operated in the bubbling regime.

The Olive Bagasse/Colombian Coal and Wood/Colombian Coal tests were performed in the new reactor, as well as the Straw/Colombian coal and the 100% Rice Husk test.

During combustion tests, the temperatures, pressures and gaseous pollutants were continuously monitored. There is a heated filter and sample line, located after the 2nd cyclone, attached to a continuous gas analyzer system to on-line measures of O_2, CO_2, CO, NO_x and SO_2. There are also several sampling points along the reactor through water-cooled gas sampling probe extraction if desired (Abelha, 2005).

The bed material was composed of washed silica sand (99.4 %wt) extracted from the river. The average particle diameter was 0.33mm and d_{SV} was 0.36mm, with a density of 2650 kg/m^3. The static bed bulk density was about 1580 kg/m^3.

Figure 5.6 – Views of the LNEG pilot fluidised bed "New installation".

5.3.1 Experimental Installation Operation

The installation is pre-heated with propane, introduced in the reactor in an appropriate mixture with primary air, until the bed temperature reaches 700-800ºC, which takes about 45 minutes. Then the fuel is gradually added until the desire flow rate and simultaneously the propane feed is reduced

until is cut. This process takes about 10 minutes, after which the fuel feed is regulated for the desired value as well as the air flow rate and air partition. Then the combustion will stabilize, which may take up to 2 hours. When the bed and freeboard temperatures are stable, the test characterization is started.

Data collection was taken after stabilization of bed temperature, which occurs usually after 2 to 3 hours of start-up. Figure 5.7 shows the test run for the 100%Straw Pellets.

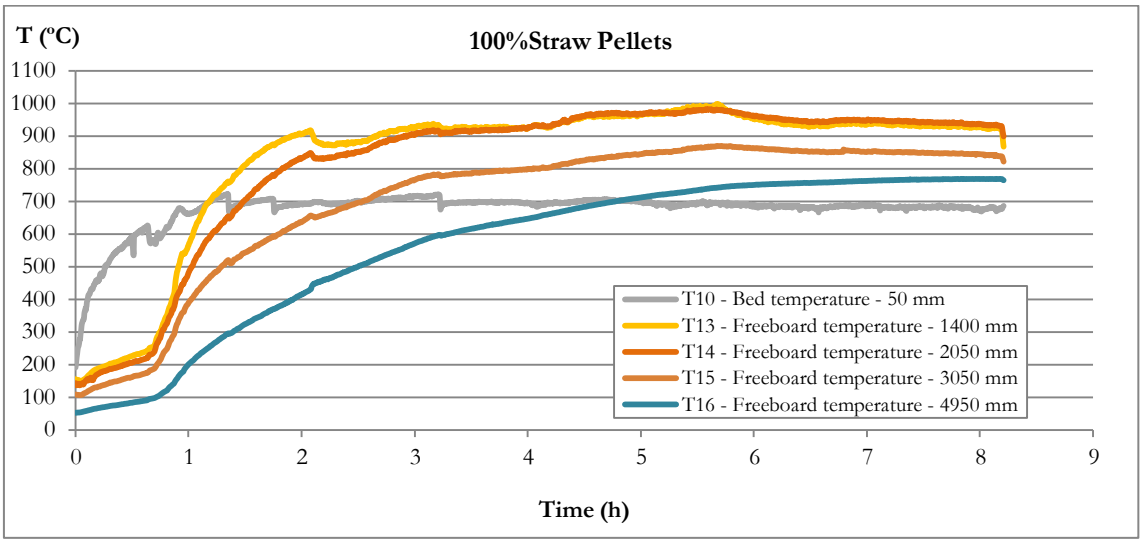

Figure 5.7 – Temperature profile evolution in the heating and test run periods of the 100%Straw pellets test.

5.3.2 Fluidized bed characteristics

The minimum fluidization velocity at 20ºC was experimentally determined by Abelha (2005) and was found to be U_{mf} = 0.12 m/s (Abelha, 2005). A theorical calculation, valid for low Reynolds numbers, found U_{mf} = 0.11 m/s, a difference of ca. 10%. Using the same calculation for the average bed temperature, 850ºC, the minimum fluidization velocity was found to be 0.05 m/s.

The selected fluidisation velocity was 1.0 m/s, *i.e.* 20-fold the minimum fluidisation velocity.

The terminal velocity of the bed material, U_t = 2.1 m/s, was also calculated by Abelha (2005), in order to guarantee that the bed material wouldn't be elutriated from the bed. Thus, with the selected fluidisation velocity being half the terminal velocity of the bed material, it is not expected significant bed material transport and it is assured that the operation regime remains at bubbling bed.

5.4 Flue gases characterization

Flue gas characterization is most complex task from all the combustion resulting fluxes and may be the main source of the uncertainty associated with combustion systems.

Pollutants species may be analysed through several processes, mainly by continuous processes or discontinuous processes (manual methods). In this study, flue gas sampling was performed by automatic equipments for the parameters CO, CO_2, O_2, NO_x e SO_2, and by manual methods through isokinetic sampling for Particulate Matter (PM), inorganic chloride compounds (HCl and Cl_2), heavy metals (Cd, Cr, Cu, Hg, Mn, Ni, Pb, Zn), Dioxins and Furans (PCDD/F) and granulometric classification.

The location of the sampling plane and the determination of the sampling points were extensively described (Crujeira, 2004).

Particulate matter as well as the pollutants associated with particulate matter, such is the case of the heavy metals and PCDD/F, are the most difficult parameters to measure since particles with dimensions higher than 3 μm are subjected to inertia phenomena due to the changing of direction and intensity of velocity flux. Thus, particulate matter sampling has to be done under isokinetic conditions, *i.e.* sampling at such a flow rate that the velocity and the direction of the gas entering the sampling nozzle are the same as in the duct (Figure 5.8).

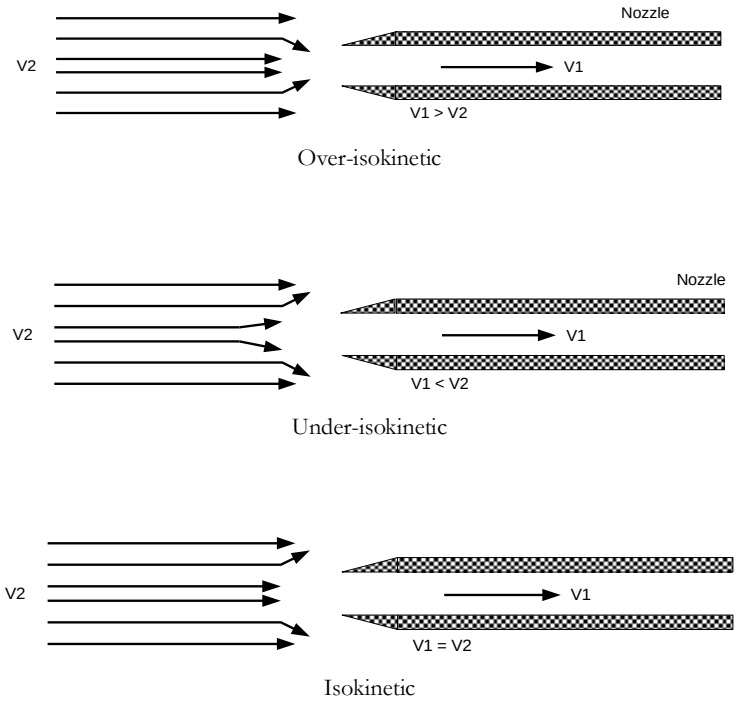

Figure 5.8 – Over-isokinetic, under-isokinetic and isokinetic sampling.

The sampling validation is given by the isokinetic factor, I, which is the ratio between the sampling velocity and the stack velocity. A stack-gas sampling is considered representative for 90% < I < 110% or 95% < I < 115%, depending on the standard/method criteria.

The methods and techniques that should be applied in the determination stack-gas emissions for combustion and co-combustion processes should be CEN (Comité Européen de Normalisation) standards. If these are not available, ISO (International Organization for Standardization) or other national or international recognized methodologies should be used, such as the U.S. Environmental Protection Agency methods (U.S. EPA).

In this study, the selected methodologies for stack-gas sampling were mainly U.S. EPA methodologies, since at the beginning of the test runs not all the European Standards were already approved and published, with the exception the PCDD/F standard which was first published in 1998.

For full stack gas emissions characterization flux parameters should be determined: pressure, velocity, average gas temperature, volumetric flow rate, and gas moisture and gas density. Table 5.5 summarizes the methodologies and standards used for flue gas characterization.

Table 5.5 - Summary of the flue gas sampling methodologies.

Parameter	Method/Standard
Localization of the sampling area	NP 2167:2007
Sampling points	EPA 1:2000
Velocity and volumetric flow rate	EPA 2:2000
Molecular weight	EPA 3:2000
CO, CO_2 O_2 SO_2 NO_x	NP ISO 10396:1998
Gas moisture	EPA 4:2000
PM – Particulate Matter	EPA 5:2000
Particulate Granulometric Classification	Internal Method CG [4]
Inorganic halide compounds	Internal Method HX [5]
Heavy metals	EPA 29:2000
PCDD/F	EN 1948-1: 2006

5.4.1 CO, CO_2, O_2, SO_2 and NO_x analysis

The gases were analysed through an electrochemical cell, with a TESTO 350 and TESTO 350XL. The analyzers were calibrated for the analysed gases and verification was periodically carried out.

[4] Cascade Impactor (ANDERSEN Mark III Particle Sizing) with EPA5 sampling.

[5] Internal method based in EPA 26A:2000: the reference method of EPA 26A is ionic chromatography; electrophoresis methodology was validated.

5.4.2 Particulate matter: total particulate matter and granulometric classification

Total particulate matter (PM) were sampled simultaneously with heavy metals, under isokinetic conditions, in accordance with U.S. EPA method 29 (CFR, 2013), with a NAPP sampling train.

Granulometric classification of the particulate matter was performed by connecting a cascade impactor ANDERSEN Mark III Particle Sizing (Figure 5.9a) to the probe and performing an isokinetic sampling following method EPA 5. The particulate matter is separated by aerodynamic size in eight classes of diameter ranges; a detail of one classification level is shown in Figure 5.9b. A more detailed description was made by Salema (2008).

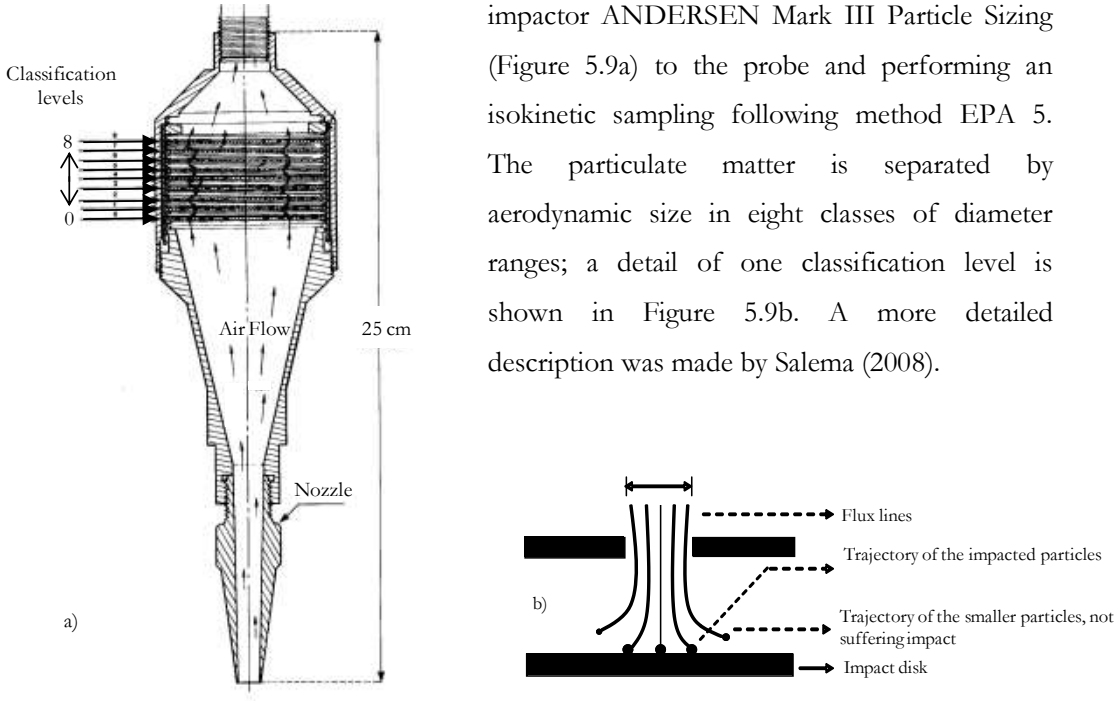

Figure 5.9 – Granulometric classification: a) Andersen Mark III Sampler, b) a classification level detail (adapted from Salema, 2008).

5.4.3 Chlorinated compounds

Chlorinated compounds were sampled under isokinetic conditions, in accordance with an internal method based in U.S. EPA method 26 A (CFR, 2013), with a NAPP sampling train. The flue gas passes through a heated filter to remove the particulate matter and both chlorine and hydrogen chloride are retained in water. The analysis was made through capillary electrophoresis.

5.4.4 Heavy Metals

Heavy metals were sampled under isokinetic conditions in accordance with U.S. EPA method 29 (CFR, 2013), with a NAPP sampling train. For heavy metals sampling, particulate matter is collected in a heated fibre glass filter and the gas passes through a series of bubblers containing the absorption solutions: HNO_3/H_2O_2 for all metals including mercury and an additional acidic

solution of $KMnO_4$ for the mercury. These methods are described in more detail by Crujeira (2004).

5.4.5 Dioxins and Furans

PCDD/F in the stack gases were sampled for 6 hours under isokinetic conditions in accordance with the European Standard EN 1948-1:2006 (CEN, 2006). The method used was the filter/condensation system, using the XAD-2 resin and the dioxin recovery test was performed in the heated filter, spiked with ^{13}C PCDD/F.

A scheme of the selected configuration is presented in Figure 5.9 and a view of the PCDD/F sampling is shown in Figure 5.10.

The extraction, clean-up and analysis of the samples were made by high resolution gas chromatography/ high resolution mass spectrometry (HRGC/HRMS), following the European Standard EN 1948-2,3:2006 (CEN, 2006), in the Portuguese National Environmental Reference Laboratory (Laboratório de Referência do Ambiente).

The preparation of the glass material, *i.e.* the decontamination with toluene p.a. and subsequent thermal treatment, was carried out at INETI;

The results of PCDD/F sampling were validated when the spiking recovery is higher than 50% and the field blank is below the detection limit of the method.

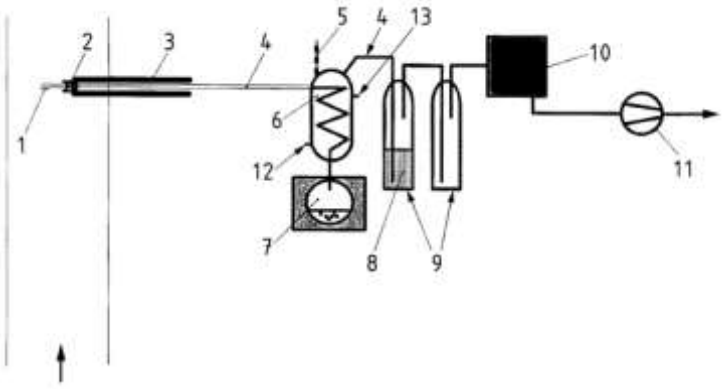

Key

1 – nozzle	6 - condenser	10 – silica
2 – filter	7 – condensate flask	11 – suction device
3 – heated probe	8 – diethylene glycol (optional)	12 – cooling water inlet
4 – connections (glass)	9 – bubbler	13 - cooling water outlet
5 – temperature control		

Figure 5.10 – EN 1948-1 filter/condensator sampling train (EN 1948-1).

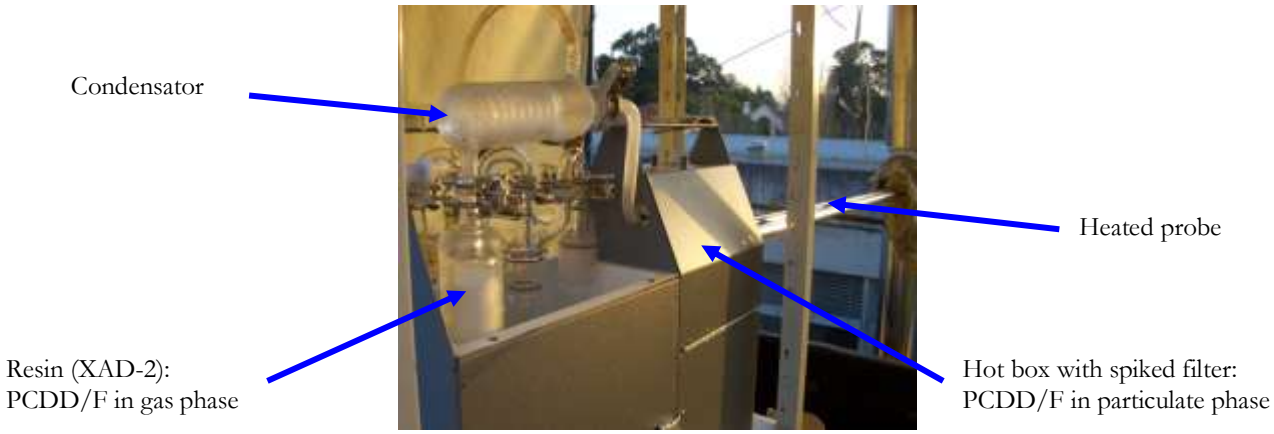

Figure 5.11 – View of the PCDD/F sampling assembly.

5.5 Ashes characterization

Bed ashes, 1st and 2nd cyclone ashes (BA, Cyc1 and Cyc2) were collected after the system cooling. The ashes characterization consisted in granulometric analysis, chloride and heavy metals analyses.

5.5.1 Granulometric analysis

Bed ashes and 1st cyclone ashes were analysed through dry sieving, with ASTM sieves, in accordance with the standard ISO 1953:1994. The bed ashes sieves range was 0-3150 µm; for the 1st cyclone the sieves range was 0-335 µm.

The 2nd cyclone ashes granulometric analysis were made by laser diffraction in a Malvern Series 2600-Droplet and Particle Sizer.

5.5.2 Carbon, hydrogen, nitrogen and sulphur content in the ashes

The content of carbon, sulphur and nitrogen in the three ash streams was measured with automatic analyzers (LECO CHN 2000 and LECO SC 144DR).

5.5.3 Heavy metals analysis in the ashes

The content of heavy metals in the ashes was measured in accordance with EN 13656:2002 and Hg in accordance with ASTM D 6722-01. The organic matter is completely destroyed by oxidation and acid digestion. The inorganic constituents are solubilised and the metals of the resulting solution are analyzed by atomic absorption spectrometry or ICP.

6. Experimental Results

6.1 Operational conditions

6.1.1 Fluidization velocity

The freeboard fluidization velocity is given by

$$v_{freeboard} = Q_{v\ freeboard} / A_{reactor} \quad (6.1)$$

where $Q_{v\ freeboard}$ is the volumetric flow of the gas in the freeboard at the average freeboard temperature and $A_{reactor}$ is the section of the reactor.

6.1.2 Gases residence time

The volumetric flow of the gas is given by

$$Q_v = dV/dt \quad (6.2)$$

thus the time the gas stays in the equipment with the volume V is defined as residence time and given by

$$\tau = V/Q_v \quad (6.3)$$

Freeboard residence time

The volume of the freeboard is given by

$$V_{freeboard} = A_{reactor}.h_{freeboard} \quad (6.4)$$

where

$$h_{freeboard} = h_{reactor} - h_{expanded\ bed} \quad (6.5)$$

It is assumed that the height of the expanded bed is 15% higher than the static bed height (Abelha, 2005). Replacing Eqs. 6.3, 6.4 and 6.5 in Eq. 6.1, results in the residence time of the gases in the freeboard:

$$\tau_{freeboard} = (h_{reactor} - h_{expanded\ bed})/v_{freeboard} \quad (6.6)$$

Table 6.1 presents the results obtained for the PCDD/F test runs. The residence time of the combustion gases in the freeboard at temperatures higher than 600ºC ranged from 3.1 to 4.9s and at temperatures higher than 750ºC ranged from 1.3 to 4.0s.

Table 6.1 – Freeboard residence time of the gases for the PCDD/F tests.

$\tau_{freeboard}$ (s)	100%PC	15%SP(PC)	100%SP	100%CC	15%MBM(CC)	100%MBM	15%SP(CC)	100%RH
T>600ºC	3.8	4.0	3.3	4.3	3.3	3.1	4.9	4.0
T>700ºC	2.7	3.5	3.3	2.6	2.2	2.9	4.1	4.0
T>750ºC	1.5	2.4	1.9	1.7	1.3	1.8	3.0	4.0

Cyclones residence time

The volume of the Cyclone 1 was calculated as 0.180 m^3 and Cyclone 2 as 0.039 m^3. The residence time of the gases in each cyclone is given by Eqs. 6.7 and 6.8 and is presented in Table 6.2.

$$(\tau_{Cyc\ 1} = 0.180/Q_v)_{TCyc1} \quad (6.7)$$

$$(\tau_{Cyc\ 2} = 0.039/Q_v)_{TCyc2} \quad (6.8)$$

Table 6.2 – Residence time of the gases in Cyclones 1 and 2 for the PCDD/F tests.

	100%PC	15%SP(PC)	100%SP	100%CC	15%MBM(CC)	100%MBM	15%SP(CC)	100%RH
$\tau_{Cyc\ 1}$ (s)	2.0	2.2	2.0	2.3	2.2	1.7	1.8	1.5
$\tau_{Cyc\ 2}$ (s)	0.5	0.5	0.5	0.6	0.5	0.4	0.5	0.4

6.1.3 Cyclones temperature

The range of temperatures of operation of the 1st and 2nd cyclones is presented in Figure 6.1. The first two campaigns were carried out in the "Old" installation. In the 2nd cyclone was observed a smaller temperature range.

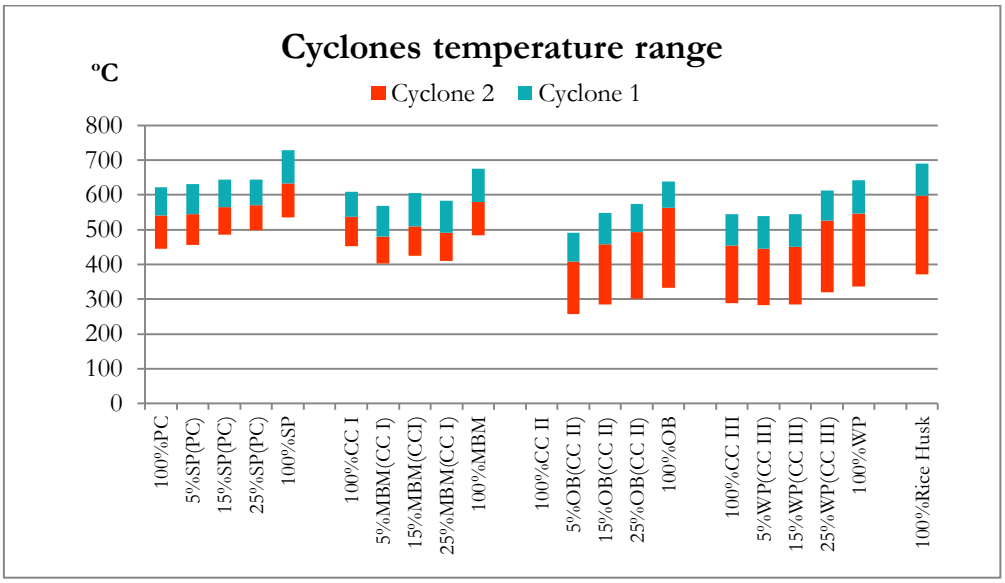

Figure 6.1 – 1st and 2nd cyclone temperature range for the different campaigns.

The 2nd cyclone exit temperature for the monocombustion of coals was lower, when compared with the monocombustion of the secondary fuels. The rise in the freeboard temperature due to the higher input of fuels with higher volatile matter content is reflected in the temperature of the dedusting equipment. In all cases, it was not possible to carry out rapid cooling of the flue gas from higher temperatures to 200 ºC, due to constraints of the installation.

6.1.4 Combustion efficiency

The combustion efficiency in terms of carbon conversion, *i.e.*:

$$\eta = (\text{C mass converted to } CO_2/\text{C input})*100\% \quad (6.9)$$

was indirectly calculated based on the unburned carbon collected in the ashes (bed, cyclones 1 and 2 and fly ash) as well as the CO measured:

$$\eta = (100 - \%C_{\text{bed ash}} - \%C_{\text{Cyc 1}} - \%C_{\text{Cyc 2}} - \%C_{\text{Fly ash}} - \%C_{\text{converted to CO}})*100\% \quad (6.10)$$

The combustion efficiency was determined to be respectively 91.3 and 92.8% for Polish and Colombian coals, during monocombustion tests, significantly lower than those determined for SP, MBM and RH monocombustion tests which were found to be 100%, 99.4% and 100%, respectively. All the combustion efficiency results are presented in Figure 6.2.

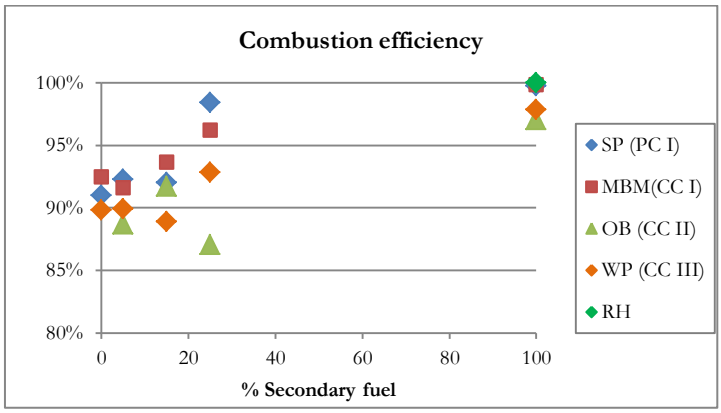

Figure 6.2 – Combustion efficiency for the different campaigns (COPOWER, 2007).

The use of higher excess air and greater degree of air staging for the combustion of 100% SP/MBM/RH tests were believed to contribute to such high combustion efficiency. For both coals it was observed greater amounts of unburned carbon collected in cyclones. The unburned carbon content decreased with the addition of other fuels and hence, the replacement of 15% of SP/MBM in the Polish/Colombian coal led to an increase of the combustion efficiency to 92.0 and 93.7%, respectively. This will be discussed later, in section 6.4.3.

6.2 Operational conditions synthesis

In Table 6.2 are summarized the operational conditions of the tests and the temperature profiles along the reactor are presented in Figure 6.3.

Results obtained indicate that the co-feeding of the secondary fuels did not present any problem and ensured stable combustion conditions together with a high thermal efficiency in fuel conversion. However, for temperatures above 800 ºC, bed agglomeration was observed for all biomass origin materials studied, when burned alone. The bed temperature was kept between 700-770ºC for the biomass origin burning tests and no agglomeration problems were detected during test period. In contrary to coal, most of the combustion of biomass origin material was observed to take place in the freeboard, where the temperature was 150-250 ºC above that of the bed (Figure 6.3). Another observation was that there were higher amounts of fuel fraction released as volatile matter, by the biomasses than by coal, which evolved near the feeding point (approximately 0.5 m above distributor plate). This contributed for the higher burning rates observed in the freeboard, where the secondary air had also to be fed more intensely, in higher proportions, to maintain the

CO at low levels. The fact that the bed temperature had to be kept in lower and controlled values also contributed to the values reported for the temperature difference.

Table 6.3 – Operational conditions for the test runs (INETI, 2005a, 2005b, 2007a, 2007b, 2007c).

Old FB Pilot	New FB Pilot	Fuel feed rate (kg/h)	Energy Input (MJ/h)	Bed height (m)	Bed temperature (ºC)	Bed Gas velocity (m/s@$T_{bed\_average}$)	Freeboard Gas velocity (m/s@$T_{freeboard\_average}$)	Excess air level (%)	Secondary air (%)
100%CCI		9.8	245	0.16	830	1.0	1.1	40	20
5%MBM(CCI)		10.0	245	0.17	785	0.9	1.1	40	20
15%MBM(CCI)		10.4	244	0.18	763	0.9	1.1	40	21
25%MBM(CCI)		10.8	242	0.18	752	0.9	1.1	39	26
100%MBM		15.4	215	0.20	739	0.8	1.6	83	46
100%CPI		9.6	266	0.17	818	1.0	1.2	35	18
5%SP(CPI)		9.8	265	0.17	813	1.0	1.2	31	20
15%SP(CPI)		10.4	269	0.18	813	1.0	1.2	36	21
25%SP(CPI)		10.6	260	0.17	769	0.9	1.2	31	23
100%SP		15.7	233	0.16	701	0.9	1.5	52	35
	100%CCII								
	5%OB(CCII)	12.4	318	0.50	845	0.9	1.1	40	25
	15%OB(CCII)	12.9	321	0.50	840	0.9	1.1	35	25
	25%OB(CCII)	14.0	334	0.50	831	0.9	1.2	35	25
	100%OB	20.3	353	0.50	766	1.1	1.5	45	25
	100%CCIII	11.5	281	0.50	850	0.8	0.9	36	23
	5%WP(CCIII)	12.4	300	0.50	843	0.8	1.0	37	25
	15%WP(CCIII)	13.4	313	0.50	842	0.8	1.1	36	28
	25%WP(CCIII)	13.8	313	0.50	841	0.8	1.1	36	30
	100%WP	18.3	316	0.50	831	0.8	1.3	38	32
	100%Rice	20.4	288	0.50	821	0.8	1.6	85	25

To deal with the higher volatile matter of the secondary fuels, the air staging was amplified and a higher excess air level was used in the run tests of 100%SP/MBM/OB/WP/RH. For example, MBM presents a much higher ratio of volatile matter and low fixed carbon (VM_{MBM}/FC_{MBM}=10.0; $VM_{CC\ I}/FC_{CC\ I}$ =0.7). Hence, the combustion intensity is lower in the bed and most of the combustion of MBM occurs in the gas phase and proceeds in the freeboard region, justifying the rise in the freeboard temperature as observed when the amount of MBM was increased (Figure 6.3). Another parameter that was varied in the test runs was the excess air. In order not to vary too much the aerodynamic conditions, the MBM was burned with higher excess air ratio than in other tests. The higher air staging ratio served to enable the efficient combustion of volatile matter and also to control the formation of nitrogen oxides, given the very high N content in MBM.

In the case of SP, the bed temperature was reduced to prevent agglomeration as it was observed in the MBM campaign. However, in this case, it was observed that the bed temperature had to be maintained at lower values, around 700ºC, when using 100% SP (Figure 6.3).

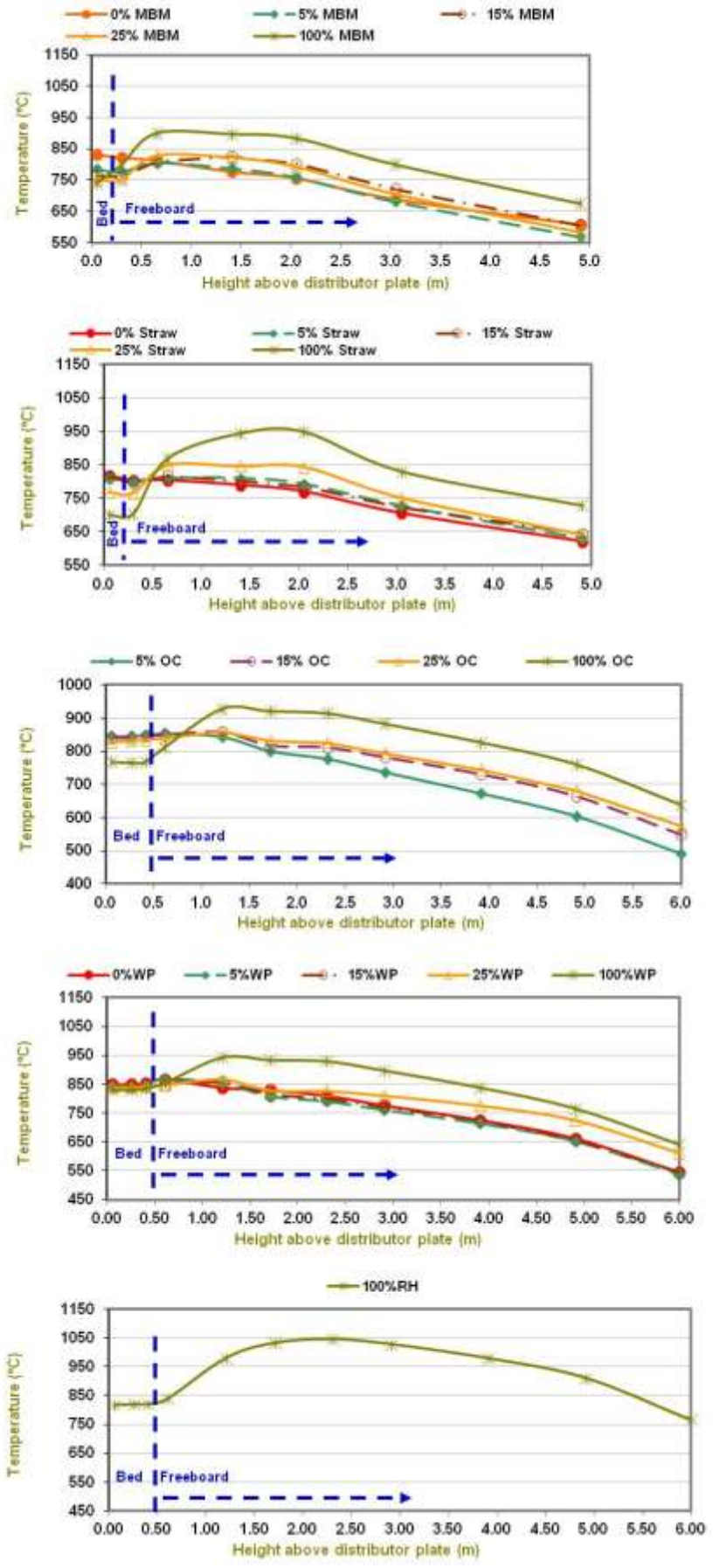

Figure 6.3 – Temperature profile along the combustor height for the test runs (COPOWER, 2007; INETI, 2007c).

The SP presents a much higher ratio of volatile matter/fixed carbon than coal (VM_{SP}/FC_{SP}=4.2; VM_{PC_I}/FC_{PC_I} =0.6); hence, the combustion intensity is lower in the bed for the SP and most of the combustion of SP occurs in the gas phase along the freeboard region, justifying the rise in the freeboard temperature, observed when the amount of SP in the fuel was increased. In the 100% SP test, the gases leaved the reactor with a 100ºC temperature difference from the Polish coal test.

The excess air was maintained between 30-35%, except for the run with 100% SP. In this case, it was needed about 50% of air excess to control the temperature and in order not only to maintain the aerodynamic conditions in the bed, but also to deal with the higher volatile burning rate in the freeboard. This resulted in a higher air staging ratio, to enable the efficient combustion of volatile matter and also to control the formation of nitrogen oxides.

In the Olive Bagasse/Cerejon campaign, the bed temperature was reduced to 750-770 ºC during the 100% OB combustion run in order to avoid the agglomeration tendency due to the presence of alkalis in significant amounts in the OB. In addition, the air excess was raised to 45% and the bed velocity was increased to 1.1 m/s (Table 6.3). When compared to coal, OB presents a much higher ratio of volatile matter/fixed carbon (VM_{OB}/FC_{OB}=4.3; VM_{CC_II}/FC_{CC_II}=0.7); hence, the combustion intensity in the bed was also lowered with the increasing share of the OB in the fuel.

In the case of the Wood Pellets, to deal with the higher volatile matter content of the WP (VM_{WP}/FC_{WP}=6.6; VM_{CC_III}/FC_{CC_III}=0.8), there was a need to use greater amounts of excess air and, more importantly, staging the air was necessary to ensure complete combustion of VM for the 100% WP test.

In the case of Rice Husk, only the 100%RH was tested. The temperature profile is similar to the 100% OB and 100%WP, although freeboard temperature reached *ca.* 1100 ºC. For this fuel VM_{RH}/FC_{RH}=4.2.

Beyond the Straw+Polish Coal tests, carried out in the "Old" installation, it was also tested the 15%Straw+85%Colombian Coal mixture in the "New" installation. In Figure 6.4 it is presented the temperature profiles of the SP/CC tests, presented in terms of relative height of the reactor due to the height difference between both installations.

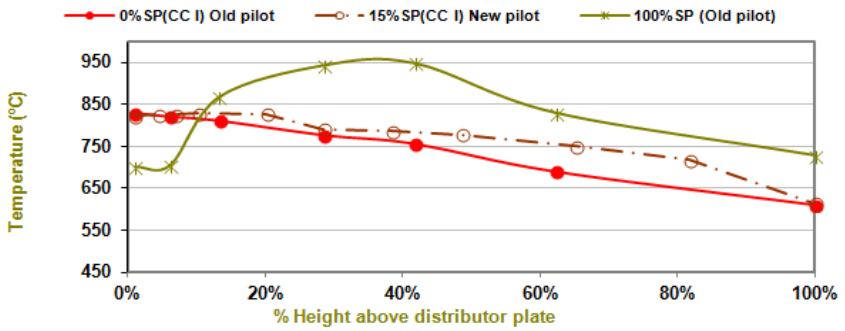

Figure 6.4 – Temperature profile along the combustor height for the test Straw/CC I test runs (COPOWER, 2007; INETI, 2007d).

The relative temperature profile of the 15%SP/CC I test is similar to the one of the SP/PC campaign (Figure 6.3), thus showing a good reproductibily between both installations.

6.3 Flue gas composition

Table 6.4 summarize the conditions during the isokinetic samplings.

Table 6.4 – Characterization of isokinetic test runs for PM, GC, HM and Halogens sampling (INETI, 2005a, 2005b, 2007a, 2007b, 2007c and Lopes *et al*., 2009).

Old FB Pilot	New FB Pilot	O_2 (%) (V/V)	Moisture (%) (V/V)	Molecular weight (w.b.) (g/mol)	Stack-gas Temperature (ºC)	Stack-gas Velocity (m/s)	Volumetric Flow Rate (Nm^3/h)	Isokinetic Index (%)
100%CCI		13.2	4.4	28.9	176	3.3	122	90
5%MBM(CCI)		12.8	4.5	29.0	164	3.1	122	98
15%MBM(CCI)		12.7	4.4	29.0	186	3.2	122	97
25%MBM(CCI)		13.1	4.5	28.9	191	3.4	122	96
100%MBM		13.6	6.8	28.6	203	3.7	117	95
100%CPI		13.5	3.8	29.0	125	3.4	138	99
5%SP(CPI)		14.0	3.8	28.8	120	3.7	138	97
15%SP(CPI)		13.3	3.8	29.0	133	3.5	140	91
25%SP(CPI)		14.1	3.7	29.0	136	3.7	136	104
100%SP		13.9	5.9	28.9	173	3.8	127	101
	100%CCII							
	5%OC(CCII)	9.2	5.8	29.6	141	3.2	170	92
	15%OC(CCII)	7.9	6.2	29.6	185	3.2	180	100
	25%OC(CCII)	8.3	6.8	29.0	199	3.6	190	95
	100%OC	8.6	9.5	29.2	240	4.4	194	96
	100%CCIII	7.6	7.1	29.6	178	2.6	141	95
	5%WP(CCIII)	7.9	2.3	30.1	169	2.6	151	95
	15%WP(CCIII)	7.9	4.7	29.9	175	2.9	157	97
	25%WP(CCIII)	7.4	6.3	29.7	171	2.8	157	97
	100%WP	7.2	10.3	29.2	208	3.1	181	103
	100%RiceHusk	14.1	8.4	28.4	257	3.3	153	98

(*) Lopes *et al*., 2009

The emission range of CO, NO_x, SO_2 and HCl in the flue gas is presented in Table 6.5. In the case of RH, the results correspond to the test 100%RH. The results for each test are discussed below.

Table 6.5 – Range of the gaseous emissions for the tested fuels (INETI, 2005a, 2005b, 2007a, 2007b, 2007c).

$mg/Nm^3@11\%O_2$	CO	NO_x	SO_2	HCl
SP(PC)	10 – 437	133 – 199	4 – 380	222 – 307
SP(CC I)	10-408	199 -253	17 - 995	20 - 307
MBM(CC I)	80 – 408	146 – 342	44 – 995	15 – 239
OB (CC II)	7 – 168	99 - 148	21 – 980	17 – 93
WP (CC III)	2 – 407	89 – 113	5 – 841	5 – 12
RH	16	522	68	50

6.3.1 CO emissions

The CO emissions (Figure 6.5) tend to decrease with the increment of the secondary fuel fraction in the inlet fuel, independently of the material type. This can be explained by a more effective mixture with combustion air. The higher temperatures developed in the freeboard of the reactor and the more intense air staging contributed to that result, having also a positive effect in the combustion conversion efficiency, which was improved from about 90% with the coals, to values higher than 99.5% with the biomass origin materials (Figure 6.2). Furthermore, the higher amounts of coal in the fuel mixture led to greater fixed carbon entering the combustor which decreased the combustion rate of solid particles.

Most of char particles is burned in the bed section and some of char particles may lead to reduction of gases formed and in addition, the gases leaving the bed may not have mixed well with oxygen in the freeboard due to plug flow nature. The burning of greater level of volatile matter of the biomass origin fuels also gives rise to higher freeboard temperatures (Figure 6.3) just above the bed, which accelerates the CO combustion.

It was also observed that there was a considerable difference in CO levels measured in combustion gases leaving the combustor and the second cyclone when coal was used. This could be due to further oxidation of unburned cyclones in the cyclones.

6.3.2 NO_X emissions

Another positive synergy observed in the co-combustion of coal with these biomass origin materials was the significant decrease in the NO_X emissions when compared with the combustion of the individual fuels (Figure 6.5). For example, although the nitrogen mass in the MBM is about six times higher than that in coal (Table 5.3), the NO_X emissions decrease about 36% when adding just up to 5% of MBM to the coal combustion.

This level was maintained when increasing the MBM fraction up to 25%. However, the Fuel-N conversion to NO_X was found to decrease with the increase of MBM share in the fuel to 100%, from 8.1 to 1.2%.

It is believed that a significant part of the N-fuel was released as NH_i (with i varying from 0 to 3), mostly to the freeboard during the devolatilization stage, by thermal decomposition of amino acid or other amine groups of the biomass structures. These NH_i-species could then react with NO_X formed in the bed by reducing it to N_2 through the known De-NOx mechanism (Cabrita, 1981).

6.3.3 SO_X emissions

The biomass origin materials have only 10 to 50% of the S content of the respective mixture with coal (Figure 6.6).

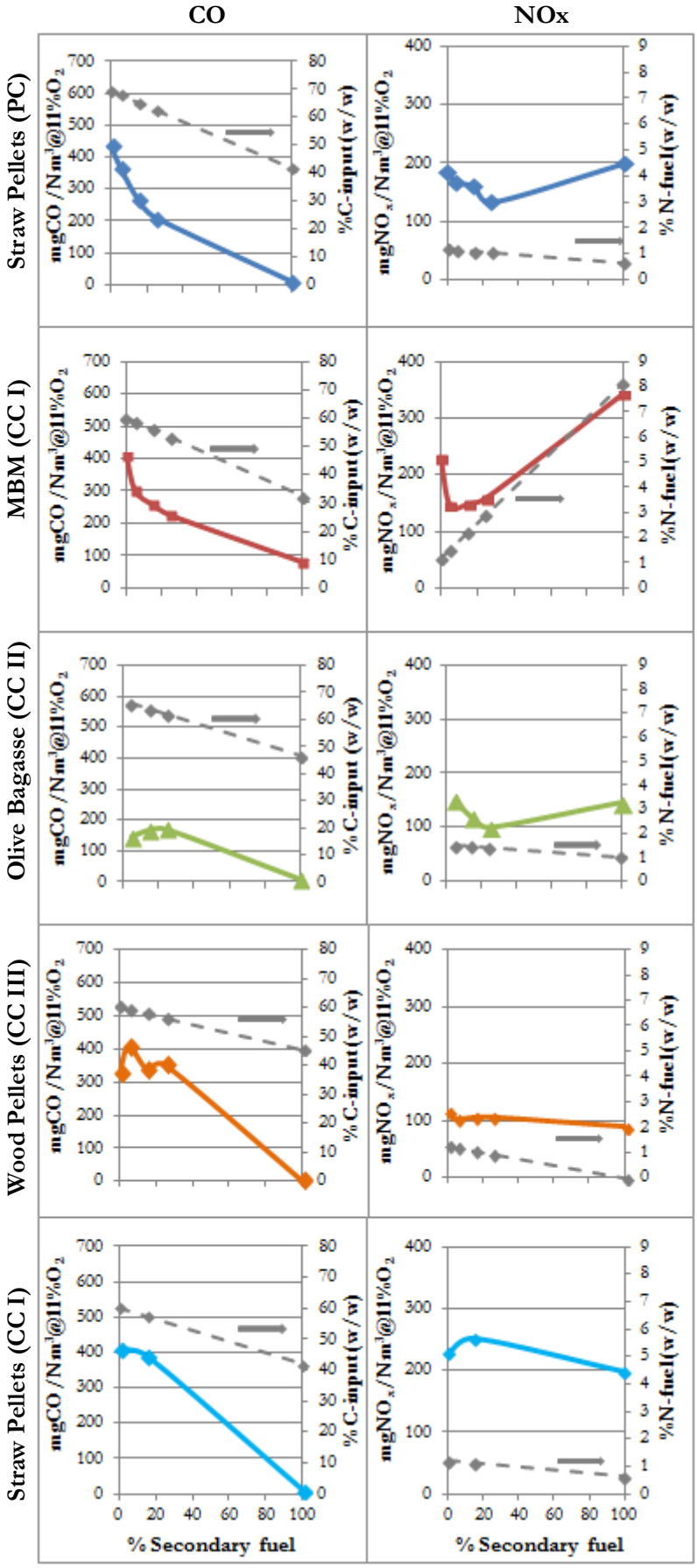

Figure 6.5 – CO and NO_x emissions obtained for the five campaigns (INETI 2005a, 2005b, 2007a, 2007b, 2007d).

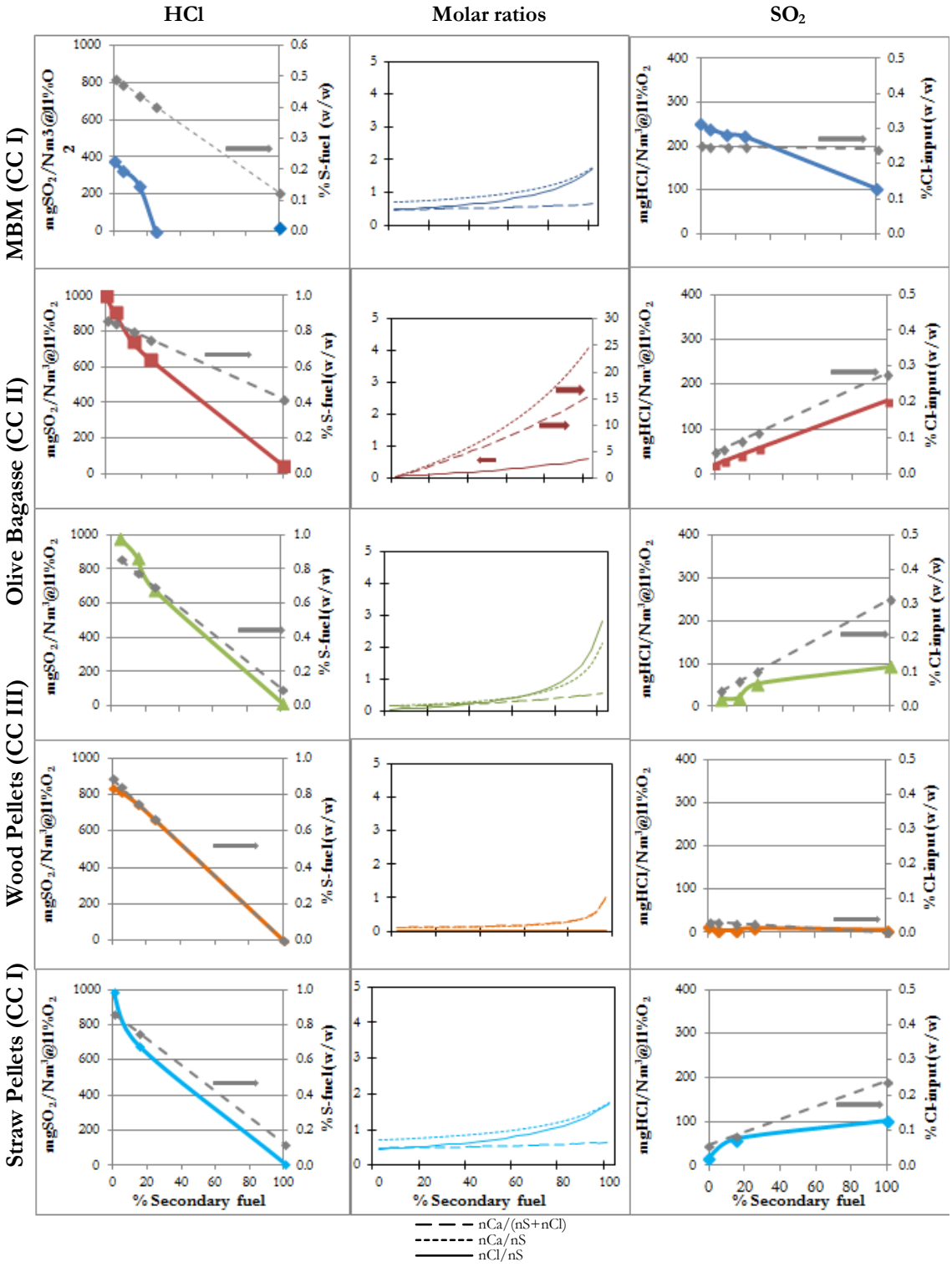

Figure 6.6 – HCl, SO_2 and molar ratios for the five campaigns (INETI 2005a, 2005b, 2007a, 2007b, 2007d).

For this reason, it is not surprising that the SO_2 emissions decreased with the increment of the fuel biomass share. However, the level of decrease observed is not proportional to the decrease of S-fuel input, being much higher than expected. The proportion of the Ca to S content, of these biomasses, is to a great extent superior than that in the coals, and the presence of Ca in the fuel has a significant influence in SO_2 emissions.

MBM presents a very Ca/S molar ratio of 24.6. SP had a Ca/S molar ratio of about 1.8, for olive bagasse this was 2.1 and for RH is 2.5, whereas for WP is very high (S-Fuel <QL); in the case of coals, CC and PC presented lower ratios: 0.2 and 0.7 respectively (Figure 5.2). This means that by adding increasing proportions of those alternative fuels to the combustion of these coals, in addition to lowering S input, an increasing fraction of the SO_2 formed may be retained in the ashes as $CaSO_4$. This explains why the SO_2 emissions decreased below what could be expected when increasing the share of straw, wood or olive bagasse in the fuel blend. The impact of this retention is that, while in the coal combustion about 80-85% of the Fuel-S is emitted as SO_2, in the case of biomass monocombustion, a maximum of 15% was observed during the tests to be emitted as SO_2. However, the decresase in SO_2 for the MBM mixtures was much lower than expected for the Ca/S molar ratios of 2.1 and 3.6 for the 15% and 25% mixtures, respectively. Since the higher calcium content was due to the quantity of bones present in MBM, it is possible that Ca from the bones was not reactive for sulphur capture (Gulyurtlu *et al.*, 2007a, 2007c). All SO_2 emissions of all tests, in both installations, were ploted as can be seen in Figure 6.7.

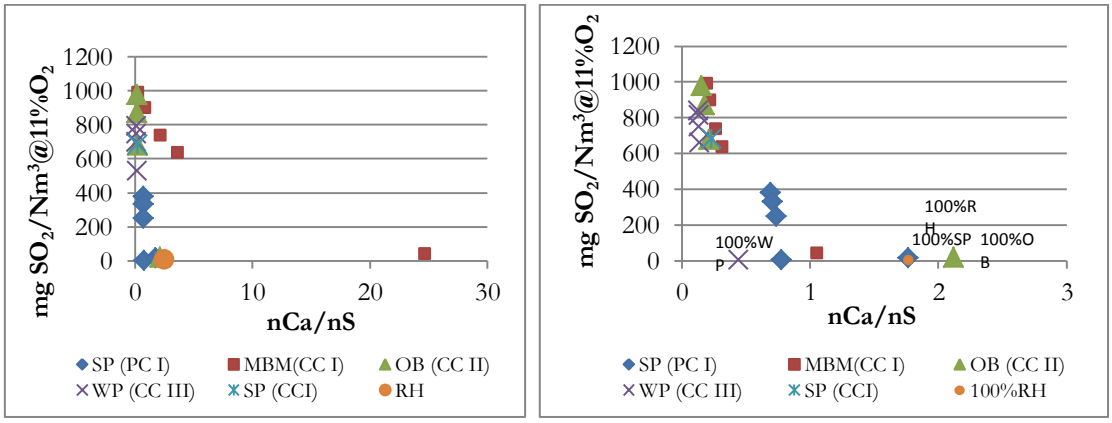

Figure 6.7 – Plot of SO_2 emissions *versus* nCa/nS (left: with all MBM tests; right: tests without MBM).

From Figure 6.7 it is clear that for molar ratios above 0.8, *i.e.* below the stoichometric ratio of 1, the SO_2 emissions were negligible. However, in same cases, this also could be a consequence of low sulphur content in the mixture. To verify that aspect, another plot was made (Figure 6.8) where becames clear that the low emissions observed in Figure 6.7 are due to low sulphur content instead of the high Ca/S molar ratio.

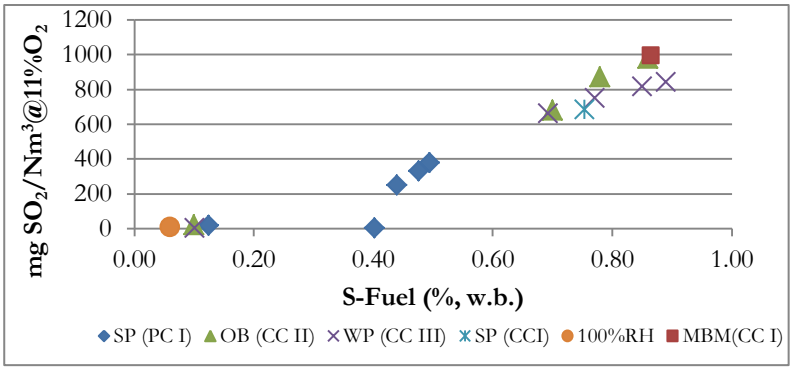

Figure 6.8 – Relation between SO_2 emisisons and the sulphur content of the mixtures.

This means that in this study the negligle SO_2 emissions in the 100%RH, 100%OB, 100%WP and 100%SP were due to low sulphur content (S<0.4%w/w, d.b.) whereas the 25%SP(PC) was clearly affected by the presence of calcium. Since n_{Ca}/n_S=0.77, the absence of SO_2 reflects that some phenomena occurred with this test. Since the 25%MBM/CC test was carried out after the 100%MBM, and although the measures taken to clean the reactor from any material from the previous test, it becames clear that some calcium contamination took place.

In order to analyse the emissions of sulphur it is necessary to simultaneously evaluate the presence of both chlorine and calcium, since the emissions of SO_2 and HCl are interrelated by these three elements. Figure 6.9 presents the sulphur and chlorine contents of the tested fuels.

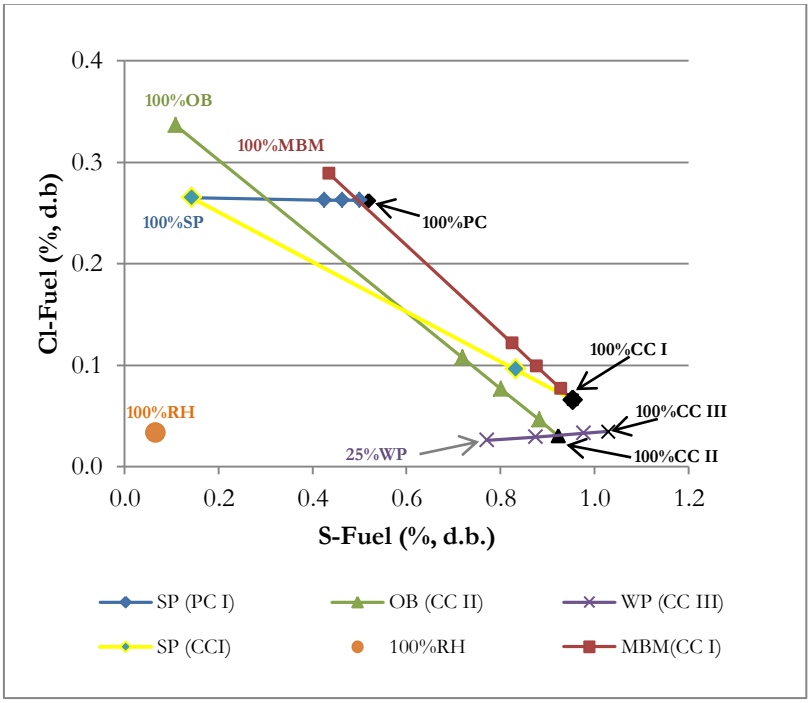

Figure 6.9 - Sulphur and chlorine content of the tested mixtures and fuels.

Since sulphur is correlated with the molar ratio nCa/(nS+nCl), a plot of of the SO_2 emissions were made (Figure 6.10) *vs.* S-Fuel (%, w.b.)/[nCa/(nS+nCl).

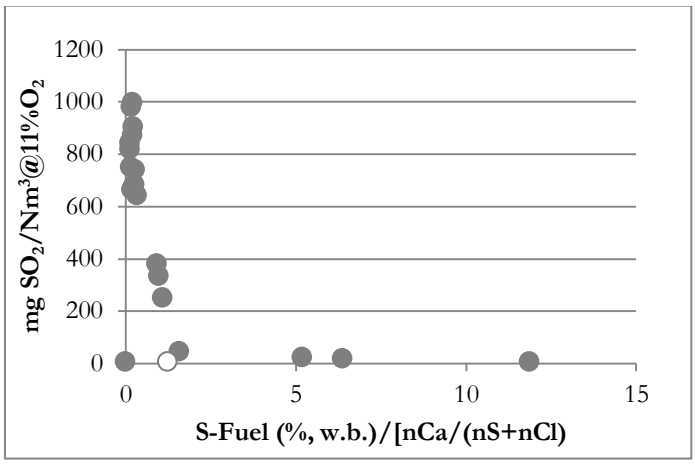

Figure 6.10 -Sulphur emissions vs. the sulphur, calcium and chlorine content of the tested mixtures.

Here it was possible to identify two tests that were not fitting. A closer inspection revealed that the fuel mixtures contain Cl<0.03. Removing those tests (marked as white circle), a correlation of measured SO_2 *vs.* [nCa/(nS+nCl)]/(%Cl-Fuel,db)/(%S-Fuel,db) was done (Figure 6.11).

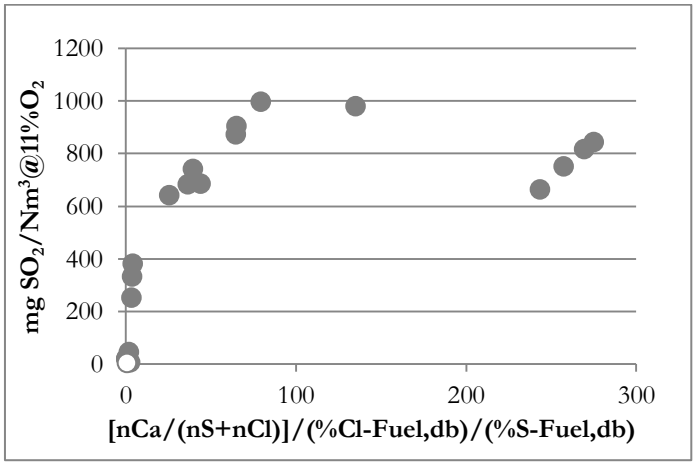

Figure 6.11 – Relation between SO_2 emisisons and the sulphur content of the mixtures.

In order to interprete the results, SO_2 emissions were plotted in two different ranges of the factor [nCa/(nS+nCl)]/(%Cl-Fuel,d.b.)/(%S-Fuel,d.b.). The obtained correlations are presented in Figures 6.12 and 6.13.

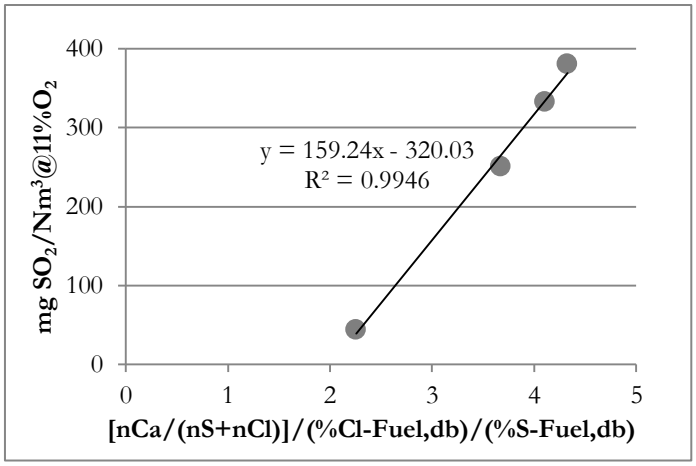

Figure 6.12 – Plot of SO_2 emissions *versus* [nCa/(nS+nCl)]/(%Cl-Fuel,db)/(%S-Fuel,db) < 20.

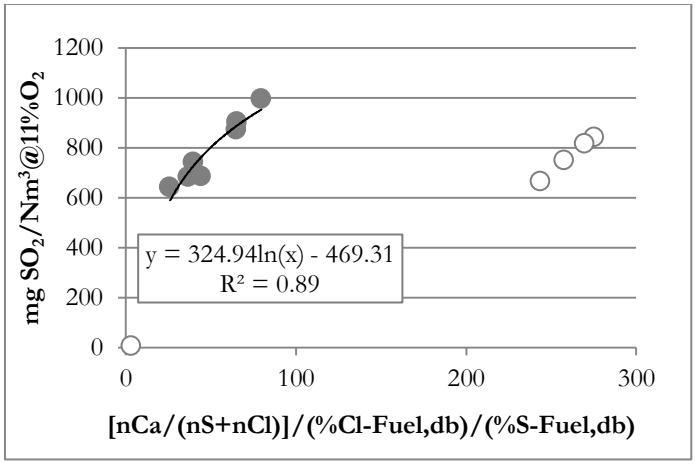

Figure 6.13 – Plot of SO_2 emissions *versus* [nCa/(nS+nCl)]/(%Cl-Fuel,db)/(%S-Fuel,db) > 20.

As can be seen, very good correlations were found for each range. The blank data in Figure 6.13 belong to the WP/CC III tests that do not fulfil the criteria of %Cl>0.03 in order to apply these correlations.

From the correlation found for [nCa/(nS+nCl)]/(%Cl-Fuel,db)/(%S-Fuel,db)>20 it is possible to estimate SO_2 through Eq. 6.11:

$$mgSO_2/Nm^3@11\%O_2\ (dry) = 324.94 * \ln[nCa/(nS+nCl)/\%Cl\text{-}Fuel(d.b.)/\%S\text{-}Fuel(d.b.)] - 469.31 \quad (6.11)$$

Figure 6.14 represents the plot of the predicted SO_2 emissions *vs.* the experimental data, showing very good consistency.

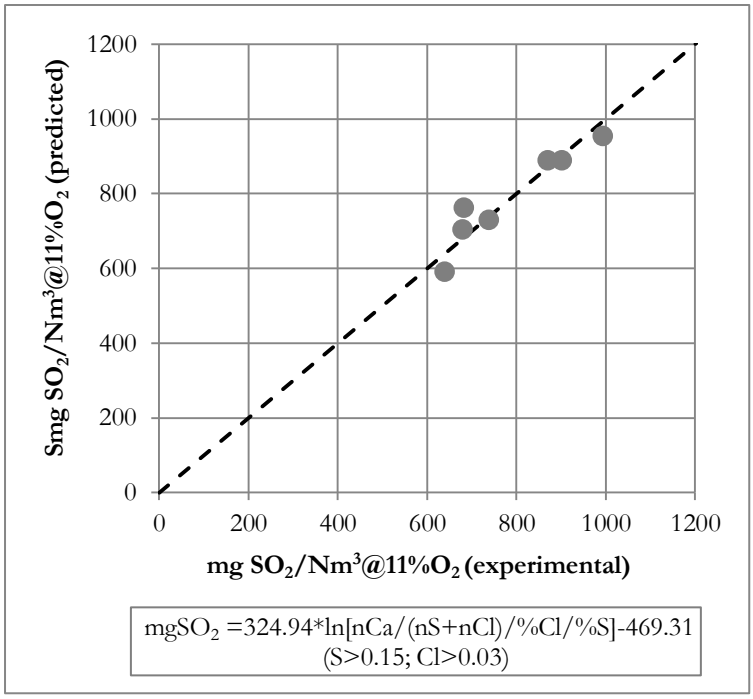

Figure 6.14 – Plot of the predicted *vs.* experimental SO_2 emissions.

From Eq. 611 and the measured value of SO_2 in the 100%MBM test, it was possible to estimate $Ca_{reactive}$-Fuel of MBM. The result obtained was 0.58% (w/w, d.b). The effective nCa_{eff}/nS for sulphur retention was recalculated and plotted to SO_2 emissions (Figure 6.15).

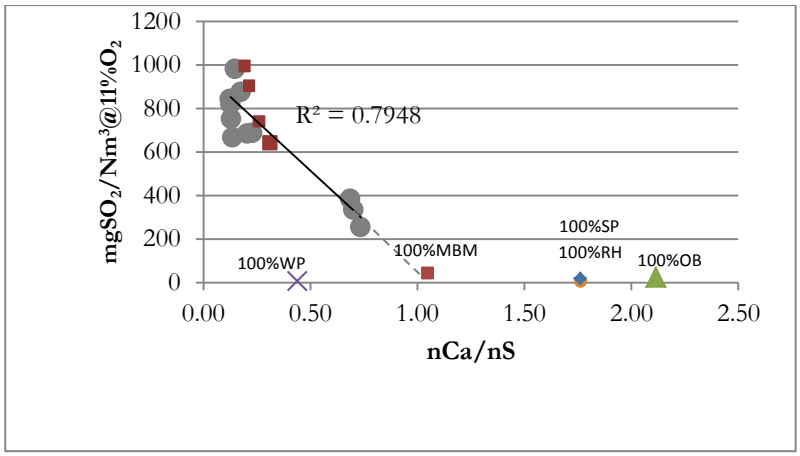

Figure 6.15 – Plot of SO_2 emissions *versus* nCa/nS (recalculated for MBM/CC tests).

The obtained results are in agreement with the observed high levels of SO_2 measured in those MBM tests. Furthermore, although the correlation between measured SO_2 and n_{Ca}/n_S has only R^2=0.79, the equation leads to zero emissions for n_{Ca}/n_S=1, which is the stoichometric ratio.

In conclusion, in both fluidized bed pilots where the experimental tests were carried out, sulphur retention was achieved for molar ratios higher than 1, lower than the 2.5 proposed by Xie and co-workers (1999).

6.3.4 Chlorine emissions

Chlorine emissions are presented in Figure 6.5. Such as in the case of sulphur, chlorine is also correlated with the molar ratio nCa/(nS+nCl) present in the fuel mixtures. A plot of the HCl emissions *vs.* Cl-Fuel (%, w.b.)/[nCa/(nS+nCl) is presented in Figure 6.16.

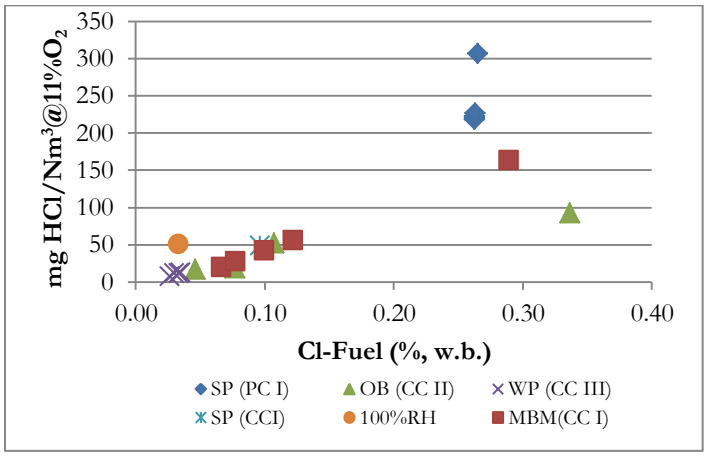

Figure 6.16 - Relation between HCl emisisons and the sulphur content of the mixtures.

Chlorine emissions are also correlated with the molar ratio nCa/(nS+nCl); a plot of of the HCl emissions *vs.* S-Fuel (%, w.b.)/[nCa/(nS+nCl) were made (Figure 6.10).

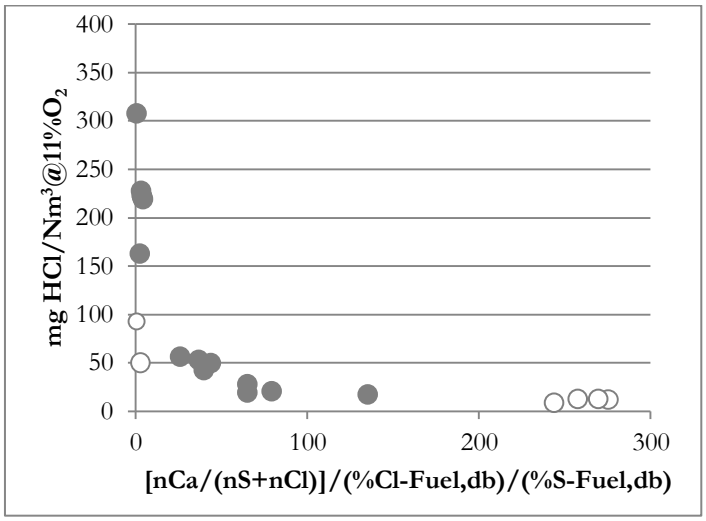

Figure 6.17 – Plot of HCl emissions *versus* [nCa/(nS+nCl)]/(%Cl-Fuel,db)/(%S-Fuel,db).

As in the case of sulphur, two different ranges were identified of the factor [nCa/(nS+nCl)]/(%Cl-Fuel,d.b.)/(%S-Fuel,d.b.). Figures 6.18 and 6.19 present those correlations.

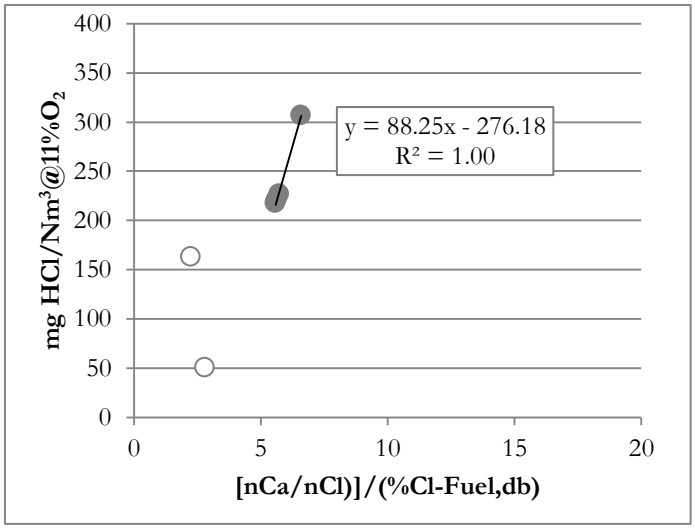

Figure 6.18 – Plot of HCl emissions *versus* [nCa/(nS+nCl)]/(%Cl-Fuel,db)/(%S-Fuel,db) < 20.

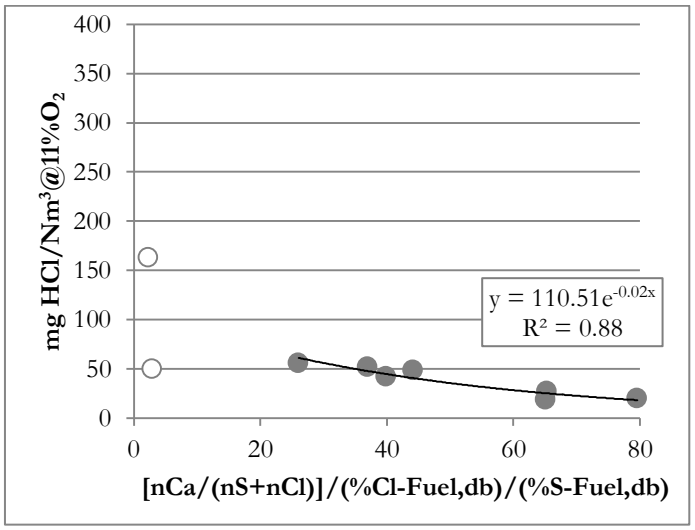

Figure 6.19 – Plot of HCl emissions *versus* [nCa/(nS+nCl)]/(%Cl-Fuel,db)/(%S-Fuel,db) > 20.

Estimation of SO_2 and HCl

From the experimental data it was possible to identify what mechanism was driving the realease of each pollutant. Analysing the results, it was possible to define the following diagram (Figure 6.20), identifying the controlling parameters for SO_2 and HCl, depending on the fuel composition.

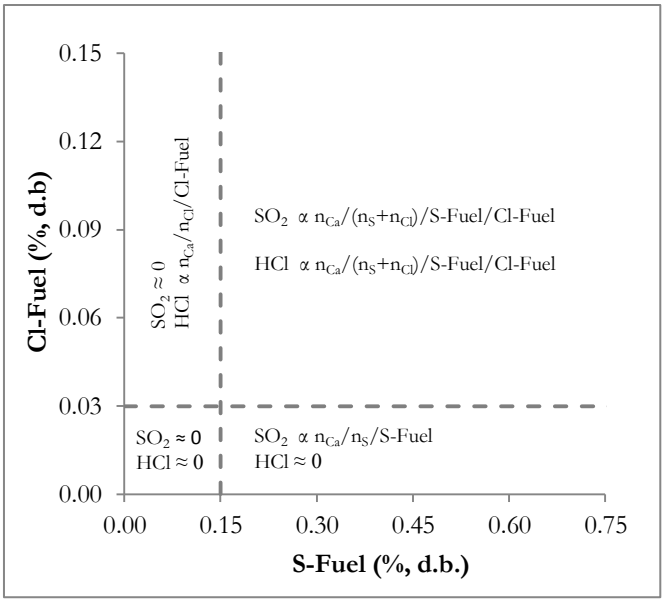

Figure 6.20 – Dependence of SO_2 and HCl emissions of the S-Fuel and Cl-Fuel content.

The equations are presented in Figure 6.21.

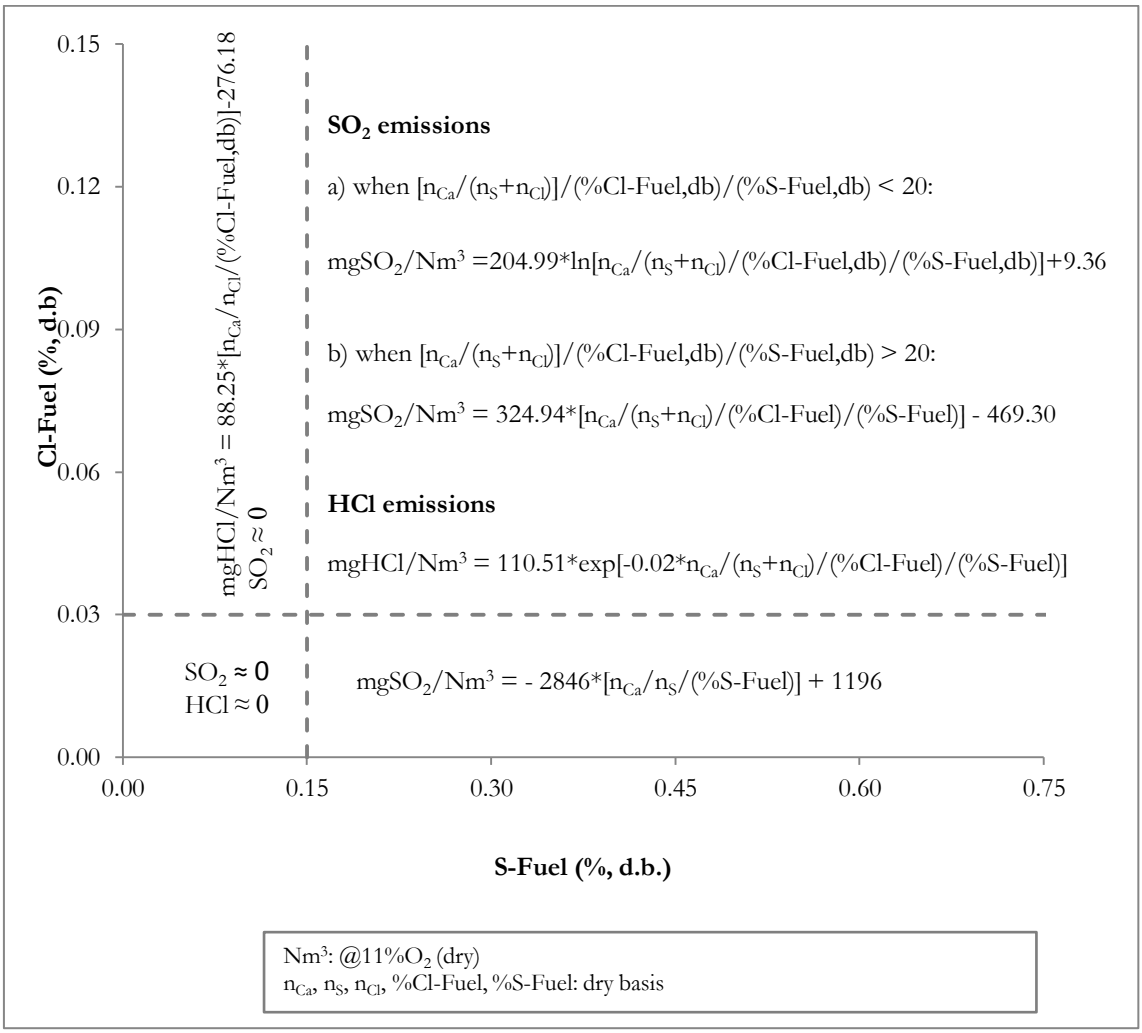

Figure 6.21 – Predicted emissions of SO_2 and HCl from the knowledge of Ca, S and Cl fuel content.

6.3.5 Particulate matter emissions

6.3.5.1 Total Particulate Matter emissions

The amount of particulate matter emitted is presented in Figure 6.22, with the distinction between the mineral and the unburned carbon contents. As discussed previously, the rise of the combustion efficiency for higher percentages of the secondary fuel is well demonstrated in Figure 6.22, with the diminishing level of unburned carbon in the particle matter emitted by the stack.

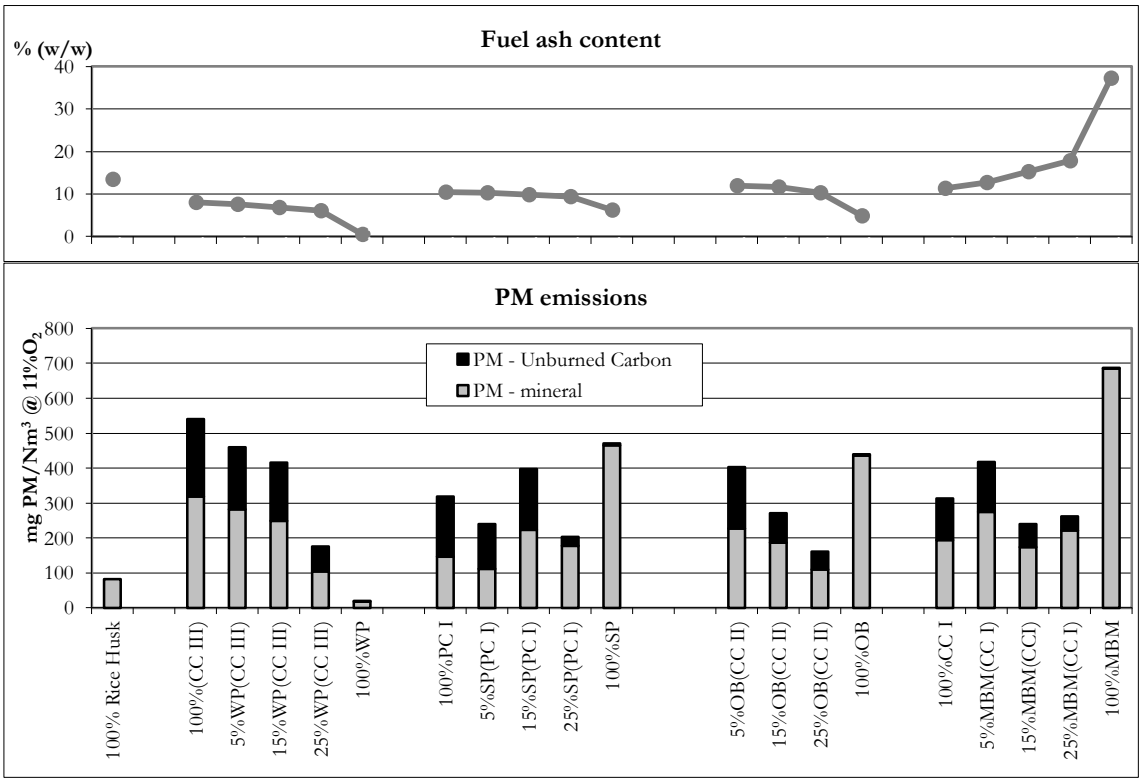

Figure 6.22 – PM stack-gas emissions and fuel ash content for the test runs (based in COPOWER, 2007).

The amount of particles emitted was not found to present a clear correlation with the amounts of MBM and SP used in the fuel blends. For SP, OB and MBM, a clear increase is seen for monocombustion tests, indicating a certain tendency to produce finer particles (Figure 6.23). In the case of the Wood Pellets, the lower emission of PM is associated with low ash content in the fuel. Since most of the metals are released associated with the fly ashes, the higher emission level of some of the mixtures (*e.g.* 5%MBM(CC I) or 15%SP(PC I)) will imply higher levels of heavy metal emissions.

6.3.5.2 Granulometric Classification of Particulate Matter emissions

In Figure 6.23 is presented the mean diameter (d_{50}) of particles collected in the stack during the combustion tests performed with MBM and Coal El Cerejon and the diameters d_{10} and d_{90}, as determined by Salema (2008). It is also marked the diameters of PM1, PM2.5 and PM4, dimensions of the particles that can reach the pulmonary alveoli and enter the blood circulation (Gavett *et al.*, 2003; Castranova, 2005).

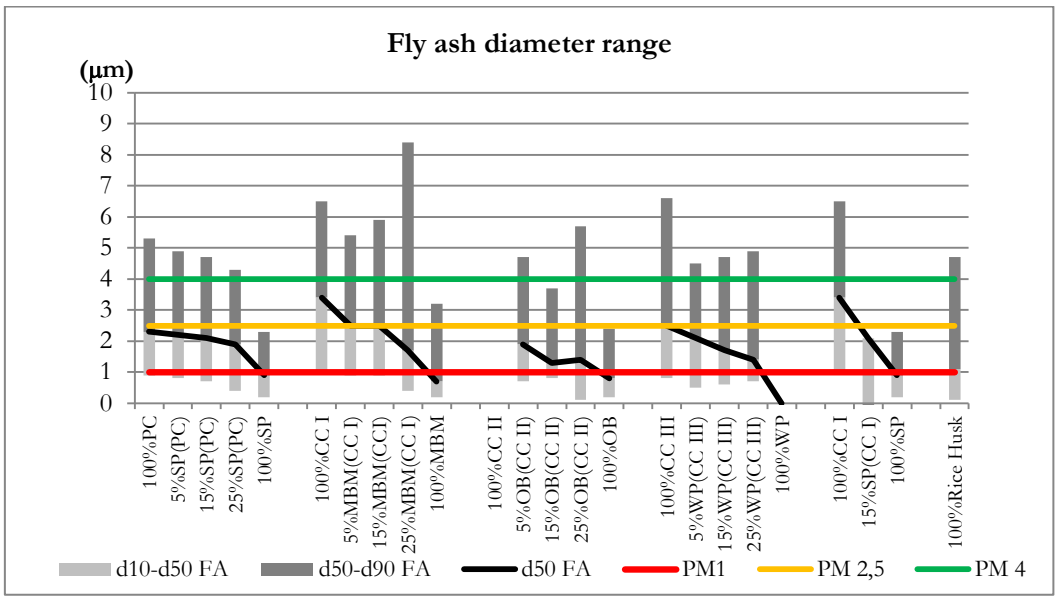

Figure 6.23 – Fly ash diameter range for the five campaigns (based in COPOWER, 2005 and 2007).

The ashes of the coals are essentially particles of micron size while the secondary fuels carried out with the flue gases are in the submicron range. Ashes of co-combustion present intermediate sizes, decreasing for higher amounts of secondary fuel addition. Ashes of co-combustion present intermediate behaviour, showing an increase of the amount of submicron particles and a decrease of the mean diameter of micron range.

6.3.6 Heavy metal emissions

Table 6.6 summarizes the heavy metals emissions for the test runs. Results will be presented below separately for the different mixtures used in the test runs and some conclusions will be withdrawn based on these results.

MBM/CC I

In terms of heavy metals emissions it was observed that the emissions of arsenic, cadmium and mercury, were below the quantification limits (QL) of the method. In the case of As and Cd, these elements were not detected in both fuels (Table 5.3); for Hg, despite its presence in both fuels, it was not possible to detect it in the flue gases.

Although the presence of Pb was below the QL in the fuels (Table 5.3), it was detected in the flue gas emissions, mainly in the 100%CC I test, most probably because the high volatility of this element.

The higher Cu content in Cerejon coal (Cu=7.9 mg/kg, d.b.) is reflected in the higher emissions of this element in the 100% coal test. In the co-firing tests the substitution of coal with different percentages of MBM, which has half of the Cu content (Cu=4.1 mg/kg, d.b.), lead to similar Cu emissions in all cases. This may be justified by the rising input of chlorine with MBM, and the resulting higher level of HCl in the gas phase, thus leading to higher volatility of the Cu present.

Table 6.6–Heavy metals emissions (INETI, 2005a, 2005b, 2007a, 2007b, 2007c).

mg/Nm³@11%O_2		% Secondary fuel				
		0%	5%	15%	25%	100%
MBM/CC I	As	< QL	< QL	< QL	< QL	< QL
	Cd	< QL	< QL	< QL	< QL	< QL
	Cr	0.05	0.13	0.07	0.05	0.31
	Cu	0.02	0.04	0.03	0.04	0.09
	Hg	0.0020	0.0031	0.0013	0.0016	0.0007
	Mn	0.12	0.12	0.07	0.10	0.50
	Ni	0.04	0.11	0.06	0.04	0.06
	Pb	0.01	0.02	0.01	0.02	0.21
SP/PC I	As	< QL	< QL	< QL	< QL	< QL
	Cd	< QL	< QL	< QL	< QL	< QL
	Cr	0.10	0.07	0.08	0.06	0.10
	Cu	0.09	0.06	0.09	0.03	0.06
	Hg	< QL	< QL	< QL	< QL	< QL
	Mn	0.12	0.09	0.13	0.05	0.03
	Ni	0.17	0.10	0.14	0.05	0.01
	Pb	0.06	0.04	0.05	0.06	0.25
OB/CC II	As		< QL	< QL	< QL	< QL
	Cd		< QL	< QL	< QL	< QL
	Cr		0.093	0.067	0.308	0.077
	Cu	—	0.025	0.027	0.084	<QL
	Hg		0.003	0.003	0.002	0.004
	Mn		0.148	0.066	0.014	0.155
	Ni		0.058	0.028	<QL	0.077
	Pb		0.029	0.020	0.028	0.022
WP/CC III	As	<QL		<QL	<QL	<QL
	Cd	<QL		0.005	0.004	0.005
	Cr	0.189		0.104	0.139	(*)
	Cu	0.054	Contamination	0.015	0.021	<QL
	Hg	0.005		0.007	0.002	0.003
	Mn	0.291		0.341	0.536	0.492
	Ni	0.102		0.134	0.038	0.039
	Pb	0.075		0.029	0.025	0.079
RH	As					< QL
	Cd					0.016
	Cr					1.060
	Cu					0.217
	Hg	< ----------	not tested		--------- >	< QL
	Mn					0.197
	Ni					< QL
	Pb					1.731

QL – Quantification Limit (*) - Contamination

In terms of Cr, Mn and Ni emissions, it was observed that higher inputs from the coal led to higher emissions of these metals; replacing coal with MBM promoted the reduction of these emissions.

It was also observed a similar profile between the PM and the heavy metals emitted by the stack. Figure 6.24 presents the cases of two volatile metals, Cu and Pb, which are volatilized in the presence of chlorine and condense at the small particles surface, leaving the stack.

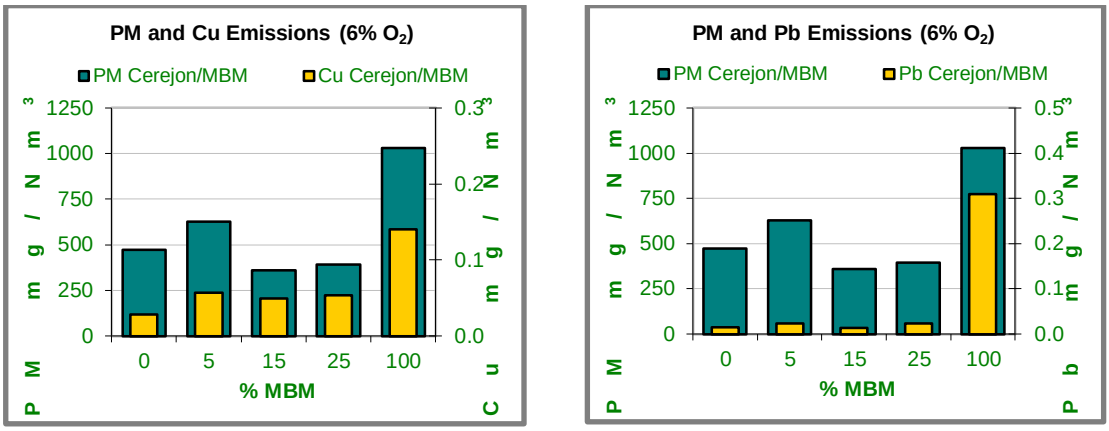

Figure 6.24 – Comparison between the PM emissions and Cu and Pb emissions for the MBM/CC I test.

Straw Pellets/PC

The Polish Coal presents higher Cr and Cu contents, being around 6 and 4 times higher, respectively, than in the SP. As the Polish coal was replaced with 5 and 25% SP a reduction in these metals emissions was obtained, as expected. On the contrary, for the 100% SP test, these metals' emissions were of the same order of magnitude as for the 100% Polish Coal. This, however, is not consistent with the input amounts of these metals. It seems that some contamination occurred with these elements, as it happened in the case of lead.

In terms of Mn and Ni emissions, it was observed that higher inputs from the coal led to higher emissions of these metals; again, replacing coal with SP promoted the reduction of these emissions.

The analysis on these results does not include the 15% SP test run, since the raise observed in the metals emission is justified by the raise of the particulate matter collected in this trial.

Although the presence of lead was below the QL in the SP, it was detected in the flue gas emissions of the 100% SP trial. Although this element is highly volatile the results found are extremely improbable and could be due to contamination during the analysis process.

As for the MBM/Cerejon tests it was observed in these tests that the emissions of arsenic, cadmium and mercury were below the quantification limits (QL) of the method. In the case of As and Cd, these elements were not detected in both fuels (Table 5.3); for Hg, despite its presence in both fuels, it was not possible to detect it in the flue gases.

Although the presence of lead was below the QL in the SP, it was detected in the flue gas emissions of the 100% SP trial. Although this element is highly volatile the results found are extremely improbable and could be due to contamination during the analysis process.

The Polish Coal presents higher Cr and Cu contents, being around 6 and 4 times higher, respectively, than in the SP. As the Polish coal was replaced with 5 and 25% SP a reduction in these metals emissions were obtained, as expected. On the contrary, for the 100% SP trial these metals emissions were of the same order as for the 100% Polish Coal, which is not very consistent with these metals input unless some contamination occurred for these elements as it is suspected it happened for lead.

In terms of Mn and Ni emissions it was observed that higher inputs from the coal led to higher emissions of this metals; the replacing of coal with SP promoted the reduction of these emissions.

As was the case of MBM/CC I, it was also observed a similar profile between the PM and the heavy metals emitted by the stack for the SP/PC I test. Figure 6.25 presents the cases of two volatile metals, Cu and Pb, which are volatilized in the presence of chlorine and condense at the small particles surface, thus leaving the stack.

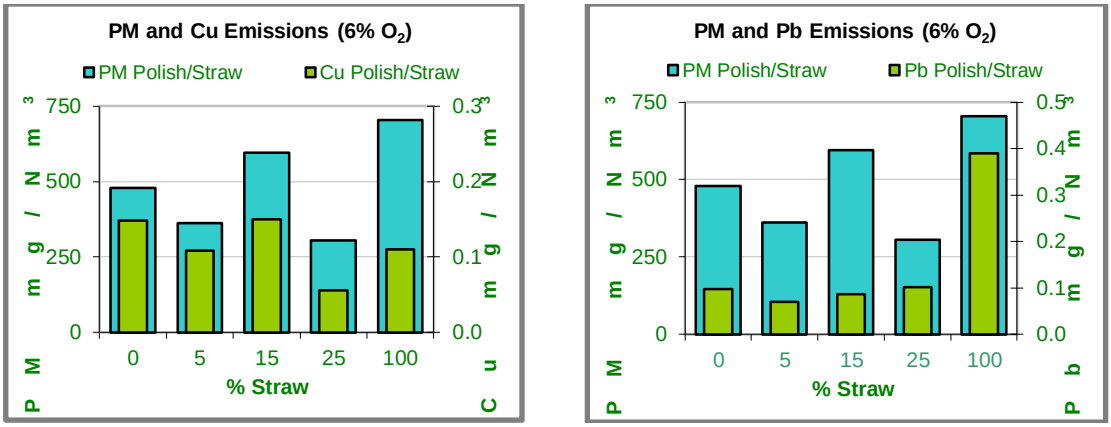

Figure 6.25 – Comparison between the PM emissions and Cu and Pb emissions for the SP/PC test.

Olive Cake/CC II

In Table 6.5 is presented the Heavy Metal Emissions for the OB/CC II tests. It was observed in these tests that the emissions of arsenic and cadmium were below the quantification limits (QL) of the method, and were also not detected in both fuels (Table 5.3).

Olive cake contains lesser amounts of Cr, Cu, Mn, Ni and Pb, hence it was expected a decrease in the stack gas emissions of these metals for higher % of coal substitution. This was generally verified, including not finding Ni in the 100% OC test, since this metal was not found in the fuel. For the 100% OB test, a contamination probably occurred since it was measured a significant level of Cr, higher than for the other test runs, when this metal was not detected in the fuel. Although the Pb content in the OB was below the quantification limit

(QL=5 mg/kg dry fuel), this metal was measured in the stack-gas emissions for the 100% OB test run. It is believed that the level of chlorine present in the stack gas, promotes the volatility of lead and its condensation on the surface of the smaller particles, which are emitted with the combustion gases.

Wood Pellets/CC III

In Table 6.5 the Heavy Metal Emissions for the WP/CC III tests is presented. The emission of arsenic was below the quantification limit (QL) of the method, and was also not detected in both fuels (Table 5.3). For all the other heavy metals present in the stack emissions studied, the wood pellets presented higher contents of Cd and Mn than the Colombian coal (CC III).

The results of the heavy metal emissions for the 5% WP are not presented, since they are directly correlated with the particulate matter emitted and for this test the particles emitted were much below the expected.

The 100% WP test run resulted in very low levels of particle emissions, *i.e.* 30 $mg/Nm^3@6\%O_2$ (Figure 6.6). It is noted that in this case experimental errors have more impact on results. However, the increase in the Cd and Mn emissions with the higher input of these metals with the wood pellets was clearly observed.

In the case of Cr it is believed that some contamination occurred in the 100%WP test run, however, the presence of Cr has no influence on the formation of PCDD/F.

For Cu and Ni the replacement of coal by wood pellets reduces these metals input in the combustion system, thus reducing these metals emissions.

Hg emissions were almost the same in all tests, although the Colombian coal contains almost 8 times more Hg than the WP (Table 5.3). The fact that Hg is not measured in the stack gases can be explained by its retention by the unburned carbon in the cyclones.

6.4 Emission Limit Values

Heavy Metals

In terms of fulfilment of the Emission Limit Values (ELV), in accordance with the existing Directives, the results obtained for each type of campaign are discussed below.

Hg emission was below the ELV of 0.05 $mg/Nm^3@6\%O_2$, for all the blends tested (Figure 6.26). For the sum of the heavy metals studied, all the mixtures of olive bagasse with this Colombian coal presented emissions lower than the ELV of 0.5 $mg/Nm^3@6\%O_2$, as shown in Figure 6.27. The use of air pollution control devices to reduce the particulate matter emissions will reduce furthermore these heavy metal emissions.

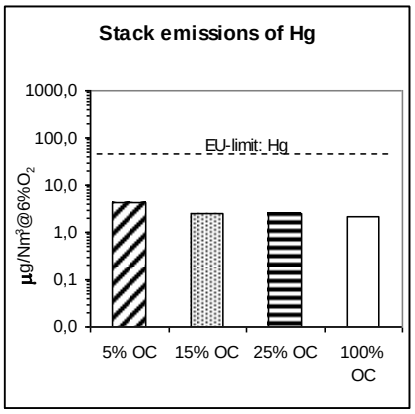

Figure 6.26 – Stack emissions of Hg for CC II/OB tests.

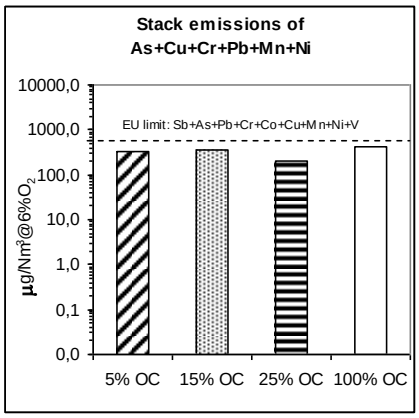

Figure 6.27 – Stack emissions of As+Cu+Cr+Pb+Mn+Ni for CC II/OB tests.

Both Hg and Cd emissions for the wood pellets combustion tests were below the ELV of 0.05 mg/Nm³@6%O_2 (Figures 6.28 and 6.29). For the other heavy metals studied, the emissions were always greater than the ELV of 0.5 mg/Nm³@6%O_2 (Figure 6.29).

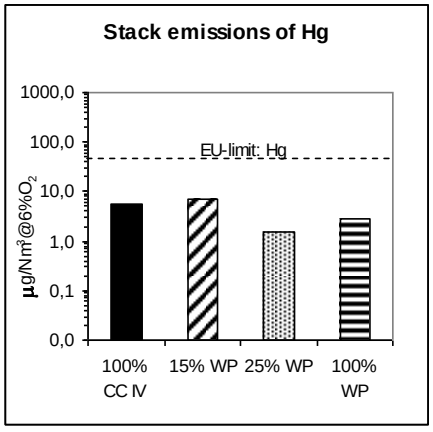

Figure 6.28 – Stack emissions of Hg for CC III/WP tests.

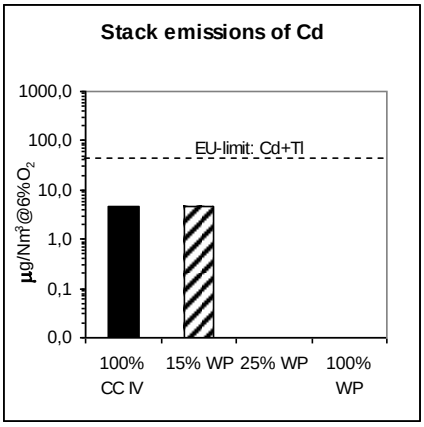

Figure 6.29 – Stack emissions of Cd for CC III/WP tests

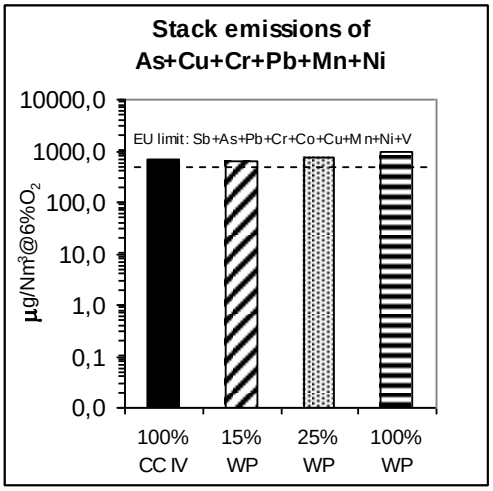

Figure 6.30 – Stack emissions of As+Cu+Cr+Pb+Mn+Ni for CC III/WP tests.

The use of a disposal for cleaning the stack gas in terms of particulate matter will reduce the heavy metals emissions.

6.5 Ash streams

6.5.1 Ash yields

The fluidized-bed combustor has four output streams of material: the bed material, including the bed ashes (BA) formed during the combustion, the ashes collected in the 1st cyclone, (Cyc1) and 2nd cyclone (Cyc2) and the material emitted by the stack.

In fluidized bed systems, bed ashes (BA) are highly diluted in the bed material (sand). In order to achieve a mass balance to the combustor the amount of sand should be taken in account. The ashes emitted in the stack are identified as PM (Particulate Matter). The partitioning of the ashes in the different streams is represented by Eq. 6.12:

$$X_{Output\_iAsh} = \frac{M_{Output\_iAsh}}{M_{Input\_FuelAsh} + M_{Input\_Sand}} \quad (i=BA,\ Cyc1,\ Cyc2,\ and\ PM) \tag{6.12}$$

Since in some streams there are high levels of unburned carbon, especially significant in the 1st and 2nd cyclone ashes, the carbon content of each ash was analysed and the ash amounts collected in each stream was corrected. For the PM emitted in the stack it was assumed the same carbon content as found in the 2nd cyclone.

MBM/Colombian Coal

The partitioning pattern of ashes produced in the MBM/Coal El Cerejon tests (Figure 6.31) is highly coherent with the increasing substitution with MBM. Production of bed ashes increased about 16% of the total to 77%, varying the substitution of MBM from 0 to 100%.

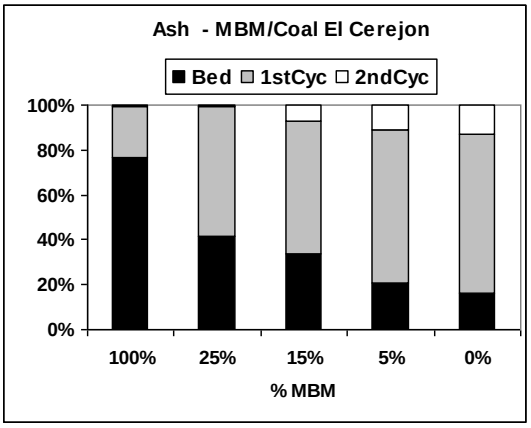

Figure 6.31 - Ash Partitioning in MBM/Cerejon Coal tests (COPOWER, 2007).

Ashes percentage collected in the cyclones decreased with the addition of MBM, from 23 to 70% and 0.3 to 13% respectively for the first and second cyclone. This behaviour is related with the nature of mineral matter present in MBM which is mainly composed of bone fragments of varying size, which do not undergo any significant shrinkage during combustion and hence remain in the bed zone. In addition, with the decrease of bed ash amount for lower MBM addition during co-firing, the increase of cyclone ash share is also explained by the presence of unburned carbon in coal ashes.

Straw Pellets/Polish Coal

Ashes accumulated in the bed during combustion of 100% Straw that was followed by co-combustion of Straw with Polish coal demonstrated difficulties in combustion of Straw under the conditions employed. During combustion of 100% Straw, the material collected from the bed contained agglomerated sand particles, which then gave very inconsistent results regarding the ash accumulated in the bed (Figure 6.32). It is believed that the bed was not completely cleaned in between the subsequent tests. This then gave higher quantity of bed material collected with co-firing. In theory, without sintering, bed accumulation should be less for higher Straw additions, while cyclone ash should increase.

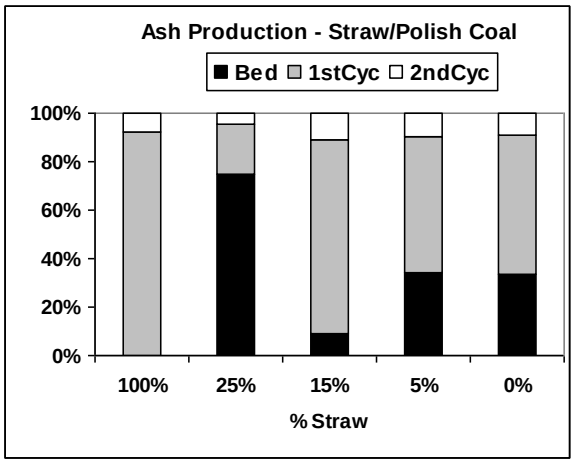

Figure 6.32 - Ash Partitioning in Straw/Polish Coal Tests (COPOWER, 2007).

6.5.2 Ashes size analysis

Ashes were collected from the 2 cyclones with different ranges of granulometries (Figure 6.33).

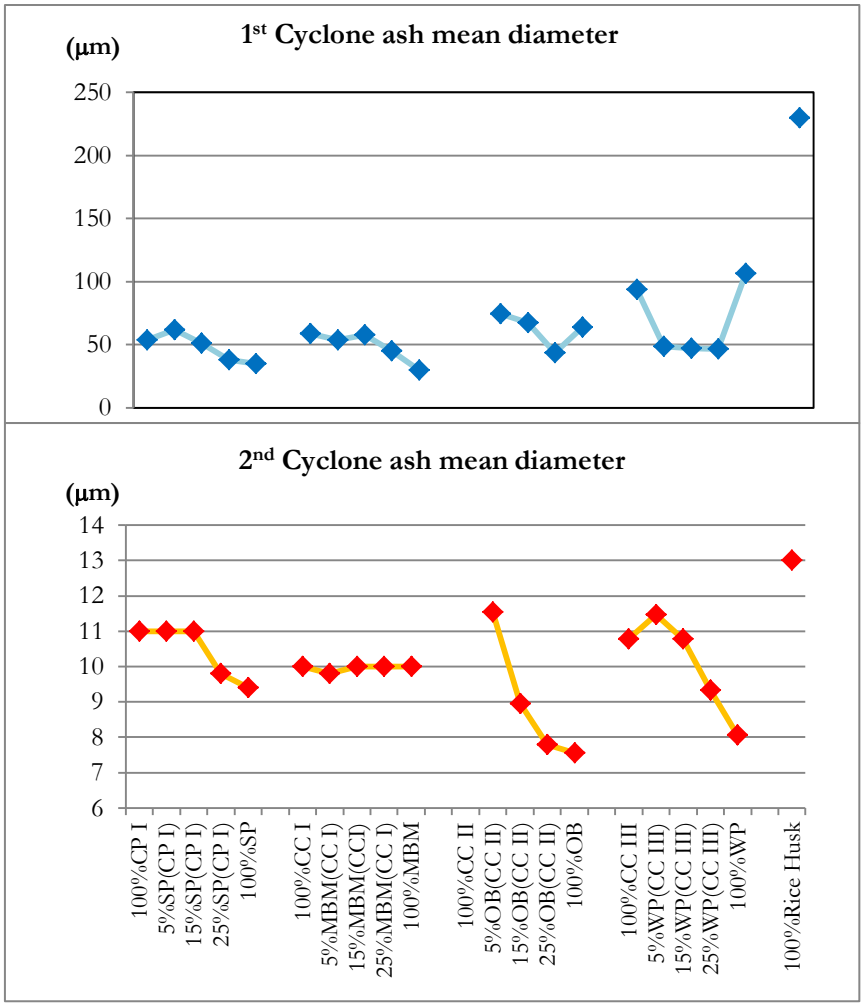

Figure 6.33 – Mean diameter d50 for the 1st and 2nd cyclone ashes (COPOWER, 2007; INETI, 2007c).

Ashes collected in the first and second cyclones present diameters between 5 and 500 µm and 2 to 60 µm, respectively. Ash from coal collected in the first cyclone present higher sizes than those of Straw. This shows that increasing addition of Straw leads to a decrease of particle diameters. Similar tendency, although less pronounced, is seen for ashes collected in the second cyclone. The ashes from coal are darker and the change to grey colour with the Straw blends indicates that increasing amount of unburned matter may influence the ash granulometry.

6.5.3 Carbon and Sulphur ashes characterization

The content of carbon and sulphur in the three ash streams is presented in Figure 6.34. The content of unburned carbon in cyclone ashes decreases for higher proportions of MBM, being in trace amounts for mono-combustion of MBM. This is related with higher level of fixed carbon in coal, and tendency for elutriation of char particles in fluidized bed systems.

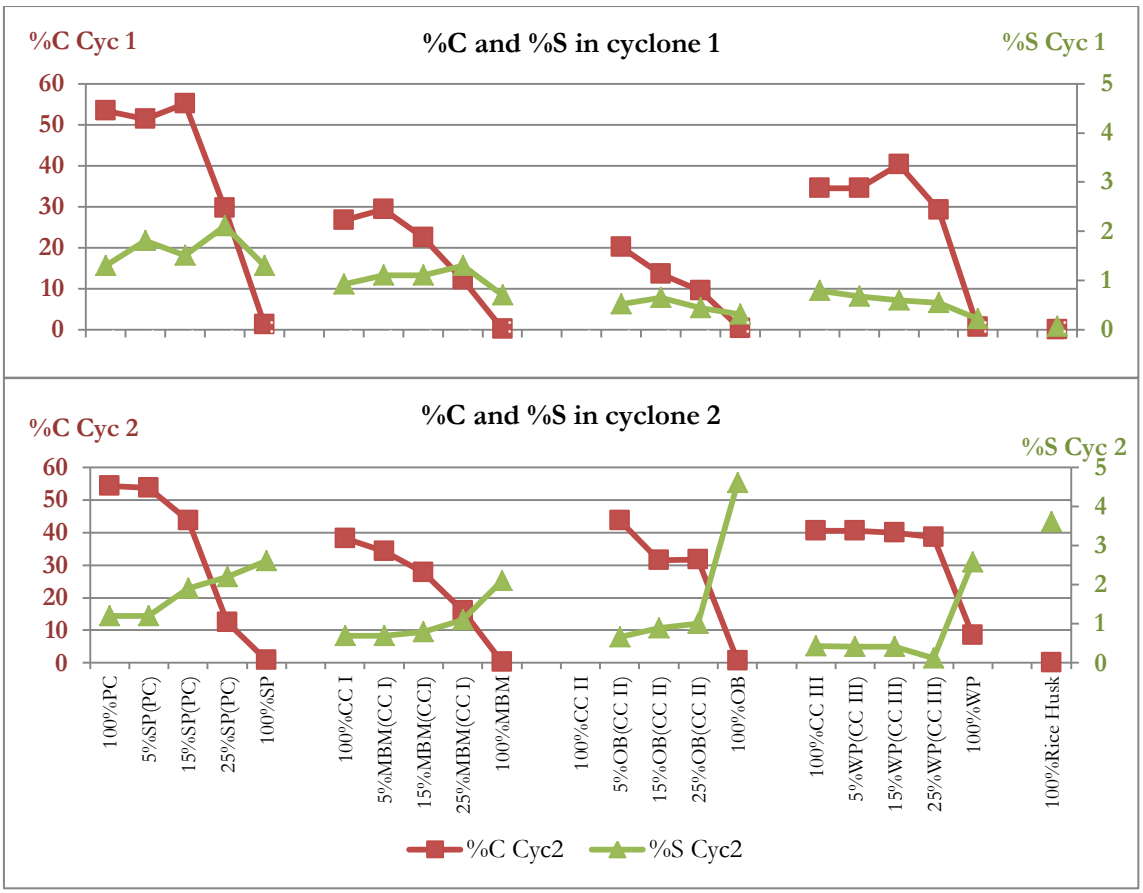

Figure 6.34 – Carbon and sulphur content for the 1st and 2nd cyclone ashes (COPOWER, 2007).

Sulphur displays the inverse tendency. Although in coal El Cerejon, S content is higher than that in MBM, the concentration of S is higher in ashes from runs of MBM co-combustion and mono-combustion. This may be due to several facts higher content of alkali elements and Ca in MBM ashes that may capture S, dilution effects due to unburned matter and higher ash amounts produced.

As mentioned before, the content of unburned carbon in cyclone ashes decreases for higher proportions of Straw, being negligible for mono-combustion of Straw. This is also related with higher level of fixed carbon in coal, and tendency for elutriation of char particles in fluidized bed systems. Sulphur displays the inverse tendency. Although in Polish coal, the S content is higher than in Straw, the concentration of S is higher in ashes during the runs of Straw co-combustion and mono-combustion. This may be due to several facts: higher content of alkali elements in straw ashes that may capture S, which is also reflected in the S appearing in bed ashes, dilution effects due to unburned matter and higher ash amounts produced.

6.5.4 Heavy metals in ashes

The concentrations of Cu and soluble chlorine in the cyclone ashes are presented in (Figure 6.35). It may be observed that, although the concentration of metals were lower in MBM than in the coal El Cerejon, metal concentrations in ashes from MBM mono-combustion were generally higher than those from co-combustion or mono-combustion of coal.

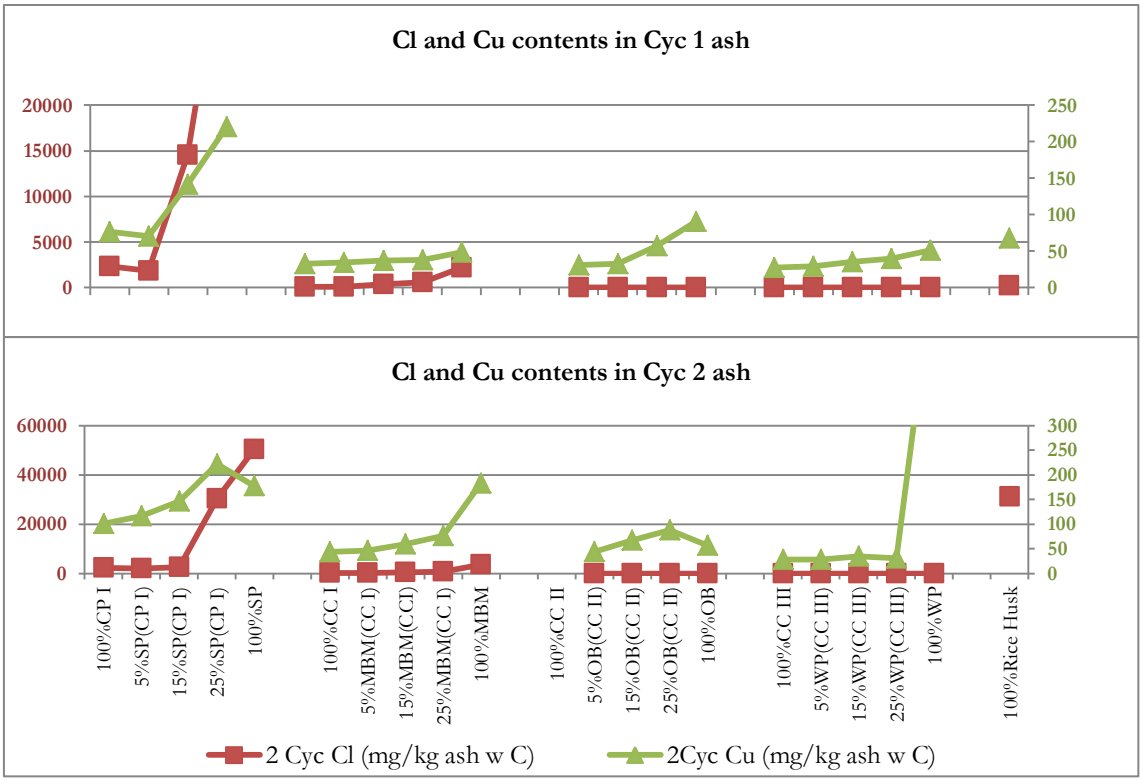

Figure 6.35 – Chlorine and copper content for the 1st and 2nd cyclone ashes.

Another important aspect is the evaluation of the ashes Relative Enrichment (RE) in heavy metals, mainly the more volatile ones, such as Cd, Pb and Cu, which is obtained using Eq. (3.5). Figure 6.36 summarize the RE for Cu and Pb in the SP/PC, MBM/CCI, OB/CC II and WP/CC III campaigns. As for the 100%RH test, the Relative Enrichment for Cu was even higher: $RE_{Cyc\ 1}$=2.7, $RE_{Cyc\ 2}$=353 $RE_{Fly\ Ash}$=89. In the case of Pb it was not possible to calculate the RE since the fuel content of Pb was below the quantification limit. As can be seen from Figure 6.25, the RE of Cu and Pb was higher than 1, which is in accordance with the classification of Raask (Table 3.5) as volatile elements. The RE higher than 1 are associated with the levels of chlorine.

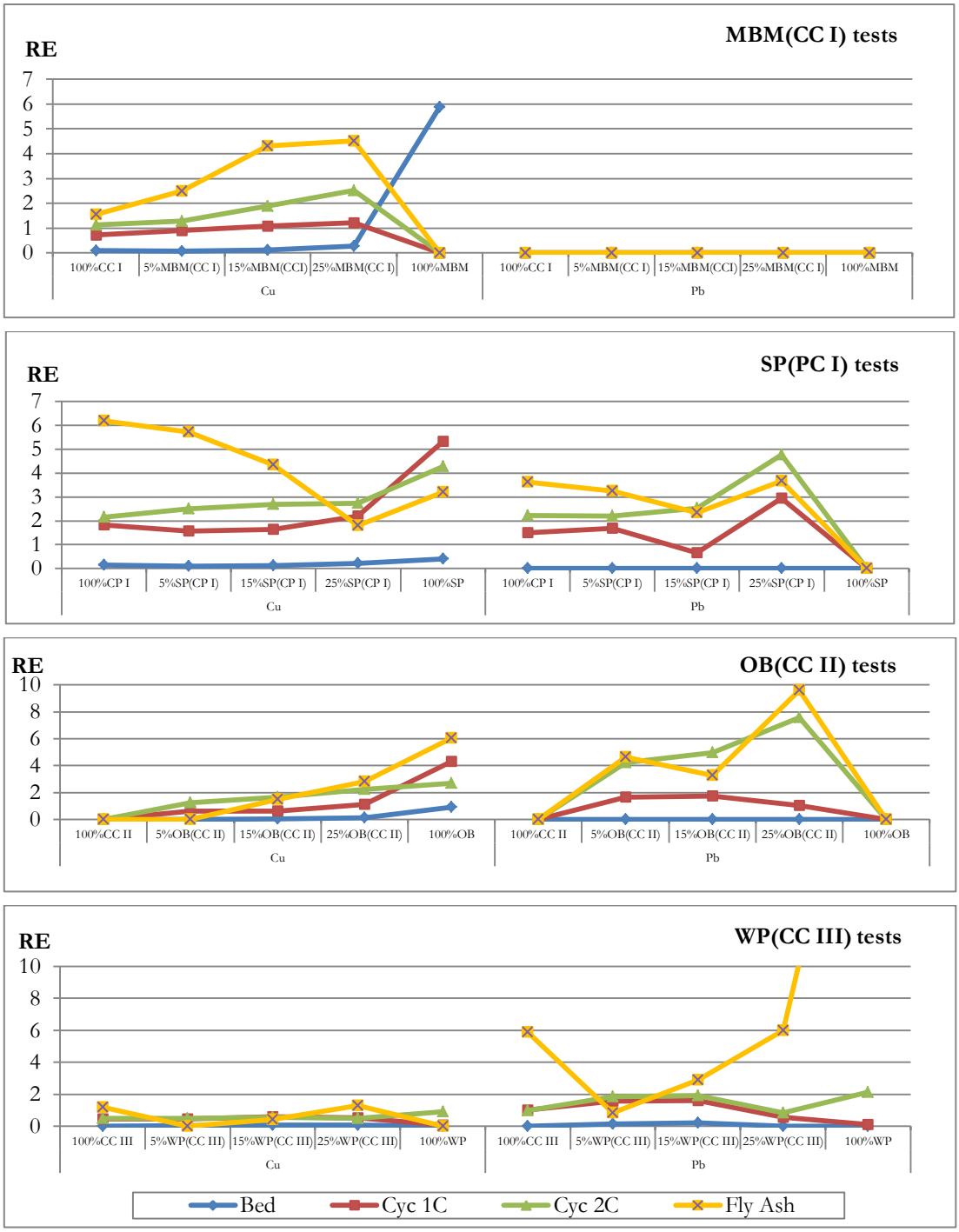

Figure 6.36 – Relative enrichment of the ashes streams, corrected for the carbon content.

This increase is due to the higher chlorine content present in the gases that led to higher the volatility of both Cu and Pb. This is in accordance with the results of other authors (Liu *et al.*, 2000; Lopes, 2002; Crujeira *et al.*, 2005).

6.6 Dioxins and Furans

6.6.1 PCDD/F tests characterization

The test runs where PCDD/F was measured were selected from the MBM/Cerejon coal and Straw/Polish coal campaigns, and were carried out in the "Old installation" described in Figure 5.5. Further tests were made in the "New installation", combining the Cerejon coal with the Straw pellets, and 100% Rice husk test, a new biomass material used. Table 6.7 summarizes the operational conditions of the PCDD/F tests.

Table 6.7 – Operational conditions for the PCDD/F test runs (INETI, 2005a, 2005b, 2007c, 2007d).

Fuel composition	pRES fuels			Mixtures			Coals	
	100% MBM	100% SP	100% RH	15%MBM 85%CCI	15%SP 85%CCI	15%SP 85%PCI	100% CCI	100% PCI
Feed rate (kg/h)	15.2	16.1	20.4	10.4	13.1	10.1	9.8	10.0
Energy Input (MJ/h)	212	238	288	244	310	260	246	277
Bed height (m)	0.20	0.16	0.50	0.18	0.50	0.18	0.16	0.17
Bed temperature (ºC)	759	688	819	774	823	830	836	816
Bed gas velocity@$T_{bed\_average}$ (m/s)	0.8	0.8	0.8	0.7	0.9	1.0	1.0	1.1
Freeboard velocity@$T_{freeboard\_average}$ (m/s)	1.5	1.5	1.3	1.2	1.1	1.2	1.1	1.3
Excess air (%)	83	41	40	43	45	31	39	36
Secondary air (%)	46	35	30	46	25	21	19	18
Ratio Ca/S (mol/mol)	24.6	1.8	1.1	2.1	0.2	0.7	0.2	0.7
Ratio Ca/(S+Cl) (mol/mol)	15.4	0.6	0.8	1.9	0.2	0.5	0.2	0.5
Ratio S/Cl (mol/mol)	1.7	0.6	2.2	9.5	9.6	2.0	16.0	2.2

The molar ratios between S, Cl and Ca, for the PCDD/F tests are summarized in Table 6.8.

Table 6.8 - Molar ratios between S, Cl and Ca, for the PCDD/F tests.

	100%PCI	15%SP(PCI)	100%SP	100%CCI	15%MBM(CCI)	100%MBM	15%SP(CCI)	100%Rice
nCa/nS	0.7	0.7	1.8	0.2	2.1	24.6	0.2	1.1
nCa/nCl	1.5	1.4	1.0	3.1	20.2	41.0	2.2	2.5
nCa/(nS+nCl)	0.5	0.5	0.6	0.2	1.9	15.4	0.2	0.8
nS/nCl	2.2	2.0	0.6	16.0	9.5	1.7	9.6	2.2

In Table 6.9 the copper content in cyclones and fly ashes is presented whereas in the Table 6.10 the total amount of copper are summarized.

Table 6.9 – Copper concentration in the cyclones and fly ashes for the PCDD/F tests.

mg Cu/kg ash	100%PCI	15%SP(PCI)	100%SP	100%CCI	15%MBM(CCI)	100%MBM	15%SP(CCI)	100%Rice
Cyc 1	87	71	221	33	37	49	43	68
Cyc 2	101	146	178	44	60	183	228	8962
Fly Ash	288	236	133	61	137	136	n.det.	2255

n. det. – not determined

Table 6.10 - Copper mass in the cyclones and fly ashes for the PCDD/F tests.

mg Cu	100%PCI	15%SP(PCI)	100%SP	100%CCI	15%MBM(CCI)	100%MBM	15%SP(CCI)	100%Rice
Cyc 1	496	320	141	280	260	216		279
Cyc 2	88	88	10	66	54	18	320	359
Fly Ash	81	76	46	16	21	55	n.det.	100

n. det. – not determined

6.6.2 PCDD/F stack-gas emissions

Table 6.11 summarize the characterization of the isokinetic runs for PCDD/F sampling. The test runs were much longer than the ones for the other parameters sampled; nevertheless, the experimental conditions were kept as similar as possible as those of the other test runs.

Table 6.11 – Characterization of isokinetic test runs for PCDD/F sampling (INETI, 2005a, 2005b, 2007c, 2007d).

Fuels	Old FB Pilot	New FB Pilot	O_2 (%) (V/V)	Moisture (%) (V/V)	Molecular weight (w.b.) (g/mol)	Stack-gas Temperature (ºC)	Stack-gas Velocity (m/s)	Volumetric Flow Rate (Nm^3/h)	Isokinetic Index (%)
Coals	100%CCI		13.1	4.0	29.0	160	3.3	122	98
	100%PCI		12.1	6.6	28.7	155	3.3	144	96
Mixtures	15%MBM(CCI)		12.9	4.1	29.0	171	3.1	122	97
		15%SP(CCI)	10.1	4.7	29.9	241	3.9	156	114
	15%SP(PCI)		13.0	4.3	29.0	183	3.6	135	106
pRES	100%MBM		12.4	6.3	28.8	246	3.7	117	96
	100%SP		13.5	6.6	28.7	202	4.0	130	106
		100%Rice	8.7	9.9	29.5	257	3.6	150	112

The range of temperatures of operation of the 1st and 2nd cyclones along PCDD/F sampling tests is presented in Figure 6.37.

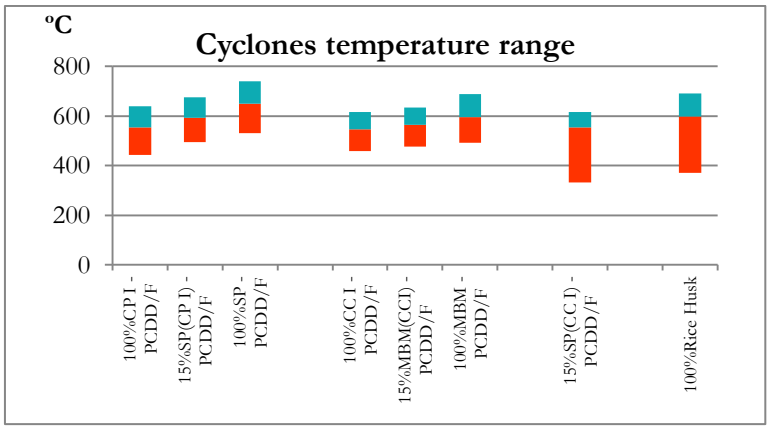

Figure 6.37 – 1st and 2nd cyclone temperature range for the different PCDD/F campaigns (Old pilot: SP/CC I and MBM/CC I tests –; New pilot: 15SP(CC I) + 100%Rice Husk tests).

The first two campaigns were carried out in the "Old installation". In the 2nd cyclone was observed a smaller temperature range, within the same range as for the tests for other pollutants samplings (Figure 6.1).

MBM/Cerejon coal

The stack gas emissions from the MBM co-combustion campaign are presented in Table 6.12 (ng/Nm³@11%O_2).

Table 6.12 – PCCD/F Stack gas emissions of MBM/Colombian Coal Tests (ng/Nm³@11%O_2).

ng/Nm³@11%O_2	**Test Runs**		
	100% CC I	**15% MBM(CC I)**	**100% MBM**
2,3,7,8-TCDF	0.0047	0.0098	1.6981
1,2,3,7,8-PeCDF	< QL	< QL	0.2658
2,3,4,7,8-PeCDF	< QL	< QL	0.2997
1,2,3,4,7,8-HxCDF	< QL	< QL	0.3756
1,2,3,6,7,8-HxCDF	< QL	< QL	0.1786
2,3,4,6,7,8-HxCDF	< QL	< QL	0.1589
1,2,3,7,8,9-HxCDF	< QL	< QL	0.0532
1,2,3,4,6,7,8-HpCDF	< QL	< QL	0.3705
1,2,3,4,7,8,9-HpCDF	< QL	< QL	0.0726
OCDF	< QL	< QL	0.1916
Total PCDF	0.0047	0.0098	3.6645
2,3,7,8-TCDD	< QL	< QL	< QL
1,2,3,7,8-PeCDD	< QL	< QL	0.1153
1,2,3,4,7,8-HxCDD	< QL	< QL	0.0725
1,2,3,6,7,8-HxCDD	< QL	< QL	0.0922
1,2,3,7,8,9-HxCDD	< QL	< QL	0.0486
1,2,3,4,6,7,8-HpCDD	< QL	< QL	0.2746
OCDD	< QL	< QL	0.2473
Total PCDD	< QL	< QL	0.8505
Total PCDD/F	**0.0047**	**0.0098**	**4.5150**

In the coal mono-combustion test only 2,3,7,8-TCDF congener is emitted. In the 100%MBM test all toxic congeners are present except 2,3,7,8-TCDD; when these are mixture with 15% of MBM is added to the mixture 2,3,7,8-TCDF is also the only congener emitted, although in higher concentration.

In all cases, the 2,3,7,8-TCDF congener presents the higher value in emissions, being the only contribution for the 0% and 15% MBM test runs. For the 100% MBM case almost all the congeners are present, although it was not detected the most toxic of all, the 2,3,7,8-TCDD.

The overall values obtained for dioxin/furan emissions appear to prove that the combustion of 100%MBM may lead to significant PCDD/F emissions. The result obtained for the mixture of

15% MBM does not differ very significantly from that obtained for coal combustion alone. Two reasons could explain this fact:

a) one is the higher Cl content of MBM, which be the main cause of greater dioxin formation,

b) and the other reason is the presence of higher amounts of S when coal is present, as SO_2 formed from S in the fuel may have reduced the activity of Cl in forming dioxins. This inhibitory effect of sulphur was previously discussed by several authors (Addink, 1996; Samaras *et al.*, 2000; Ruokojärvi *et al.*, 2004; Pandelova *et al.*, 2005).

A comparison of the total PCDD/F emissions identifying each congener is shown in Figure 6.387.

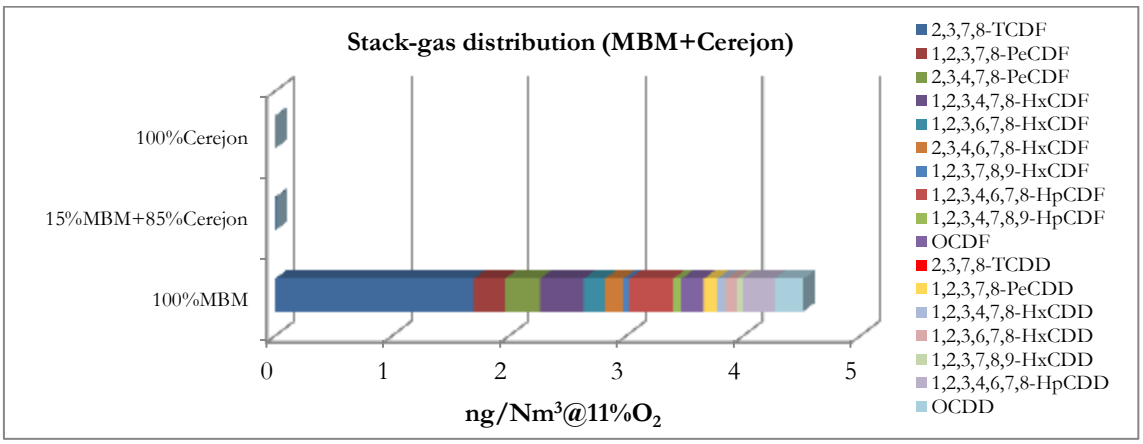

Figure 6.38 – PCDD/F distribution in the stack-gas emissions of the MBM/Coal Cerejon tests.

Straw Pellets/Polish coal

The stack gas emissions from the SP co-combustion with Colombian coal campaign is presented in Table 6.13 (ng/Nm³@11%O_2). As for the PCDD/F emissions for the test runs of MBM/CC it is clear that no synergy in this case was achieved.

Although the chlorine content of the fuels were similar the presence of higher quantities of Ca introduced by the SP reduced the SO_2 formation and for the 100%SP test SO_2 was not detected (Figure 6.17). As a result, chlorine activity was not reduced by the SO_2, as was previously observed as being necessary to produce positive synergy in reducing PCDD/F levels, thus resulting in PCDD/F emissions far above the limits allowed. In fact, the S/Cl molar ratios for these tests were always lower than 2.5, which is the minimum molar ratio necessary to prevent PCDD/F formation (Chang *et al.*, 2006).

Table 6.13 – PCCD/F Stack gas emissions of Straw/Polish Coal Tests (ng/Nm³@11%O_2).

ng/Nm³@11%O_2	Test Runs		
	100% PC I	**15% SP(PC I)**	**100% SP**
2,3,7,8-TCDF	<LQ	1.8647	11.2820
1,2,3,7,8-PeCDF	0.1274	0.8269	18.3896
2,3,4,7,8-PeCDF	0.1336	0.3496	15.3059
1,2,3,4,7,8-HxCDF	0.0854	0.0407	7.7094
1,2,3,6,7,8-HxCDF	0.0832	0.0463	7.6341
2,3,4,6,7,8-HxCDF	0.0702	0.0264	6.9948
1,2,3,7,8,9-HxCDF	<LQ	0.0292	2.6513
1,2,3,4,6,7,8-HpCDF	0.2459	0.0264	8.0854
1,2,3,4,7,8,9-HpCDF	0.0209	0.0179	1.3463
OCDF	0.0461	0.0179	0.7183
Total PCDF	0.8121	3.2459	80.1172
2,3,7,8-TCDD	<LQ	0.0961	2.0420
1,2,3,7,8-PeCDD	0.0288	0.0396	4.2119
1,2,3,4,7,8-HxCDD	0.0180	0.0235	1.5155
1,2,3,6,7,8-HxCDD	0.0278	0.1224	1.6321
1,2,3,7,8,9-HxCDD	0.0137	0.0452	0.9778
1,2,3,4,6,7,8-HpCDD	0.0846	0.7282	2.7114
OCDD	0.0828	0.6378	1.2297
Total PCDD	0.2557	1.6928	14.3206
Total PCDD/F	**1.0682**	**4.9387**	**94.4378**

A comparison of the total PCDD/F emissions identifying each congener is shown in Figure 6.39.

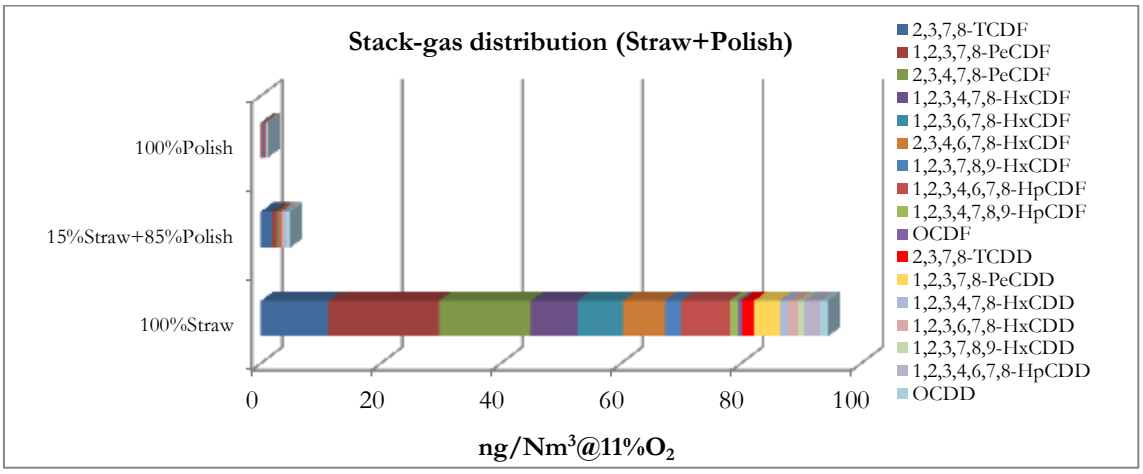

Figure 6.39 – PCDD/F distribution in the stack-gas emissions of the Straw Pellets/Polish coal tests.

Straw Pellets/Cerejon coal

In order to evaluate the importance of the chlorine and sulphur contents of coal in the formation and emission of PCDD/F from the co-combustion of straw pellets, a mixture of 15%SP with Cerejon coal was tested. This new test run was carried out in the new installation; the

monocombustion tests of each fuel were carried out in the old installation. In Table 6.14 the emissions of the 17 dioxin and furans congeners are presented, as well the total emission of the PCDD/F.

Table 6.14 – PCCD/F Stack gas emissions of Straw/Cerejon coal tests (ng/Nm³@11%O_2).

ng/Nm³@11%O_2	**Test Runs**		
	100% CC I[1]	**15% SP(CC I)**	**100% SP[2]**
2,3,7,8-TCDF	0.0047	0.0002	11.2820
1,2,3,7,8-PeCDF	< QL	0.0006	18.3896
2,3,4,7,8-PeCDF	< QL	0.0007	15.3059
1,2,3,4,7,8-HxCDF	< QL	0.0008	7.7094
1,2,3,6,7,8-HxCDF	< QL	0.0010	7.6341
2,3,4,6,7,8-HxCDF	< QL	0.0016	6.9948
1,2,3,7,8,9-HxCDF	< QL	0.0010	2.6513
1,2,3,4,6,7,8-HpCDF	< QL	0.0034	8.0854
1,2,3,4,7,8,9-HpCDF	< QL	0.0012	1.3463
OCDF	< QL	0.0024	0.7183
Total PCDF	0.0047	0.0129	80.1172
2,3,7,8-TCDD	< QL	0.0001	2.0420
1,2,3,7,8-PeCDD	< QL	0.0004	4.2119
1,2,3,4,7,8-HxCDD	< QL	0.0003	1.5155
1,2,3,6,7,8-HxCDD	< QL	0.0007	1.6321
1,2,3,7,8,9-HxCDD	< QL	0.0002	0.9778
1,2,3,4,6,7,8-HpCDD	< QL	0.0034	2.7114
OCDD	< QL	0.0046	1.2297
Total PCDD	< QL	0.0097	14.3206
Total PCDD/F	**0.0047**	**0.0226**	**94.4378**

[1] – From Table 6.14; test in the old installation.
[2] – From Table 6.15; test in the old installation.

As for the PCDD/F emissions for the test runs of Straw/Polish coal, all the 17 toxic congeners are emitted for the 15%SP(CC I) test.

In this case, the amount is more than 5 times the amount of the 15%SP(PC I), with higher content of the more toxic congeners. Since in this test a lower chlorine content coal was used in the mixture, the differences between the Ca/S and S/Cl molar ratios were different. On the other hand, the test was carried out in a different installation, and this fact might justify the difference found in the results obtained.

A comparison of the total PCDD/F emissions identifying each congener is shown in Figure 6.40.

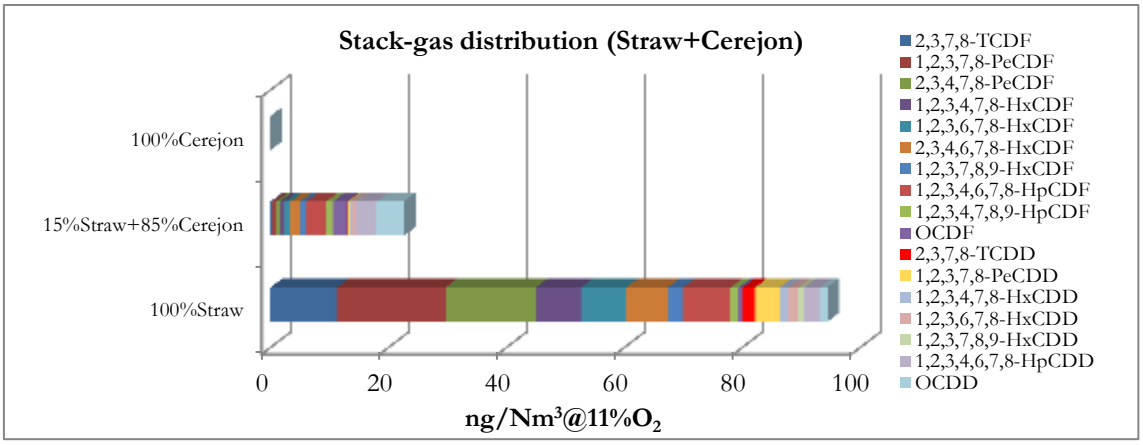

Figure 6.40 – PCDD/F distribution in the stack-gas emissions of the Straw Pellets/Cerejon coal tests.

Rice Husk

The stack gas emissions when using 100%Rice Husk in the tests are presented in Table 6.15 (ng/Nm³@11%O_2), as well the total emission of the PCDD/F.

Table 6.15 – PCCD/F Stack gas emissions of Rice Husk test (ng/Nm³@11%O_2).

ng/Nm³@11%O_2	100% Rice Husk
2,3,7,8-TCDF	5.1852
1,2,3,7,8-PeCDF	12.6518
2,3,4,7,8-PeCDF	14.3111
1,2,3,4,7,8-HxCDF	11.6148
1,2,3,6,7,8-HxCDF	15.5555
2,3,4,6,7,8-HxCDF	25.3037
1,2,3,7,8,9-HxCDF	12.6518
1,2,3,4,6,7,8-HpCDF	39.4074
1,2,3,4,7,8,9-HpCDF	15.7630
OCDF	30.074
Total PCDF	182.5183
2,3,7,8-TCDD	2.2815
1,2,3,7,8-PeCDD	4.5630
1,2,3,4,7,8-HxCDD	6.0148
1,2,3,6,7,8-HxCDD	8.0889
1,2,3,7,8,9-HxCDD	4.1481
1,2,3,4,6,7,8-HpCDD	40.2370
OCDD	33.1852
Total PCDD	98.5184
Total PCDD/F	**281.0367**

The PCDD/F emissions for the test runs of Rice Husk are the highest found in this study. All the toxic congeners were found, with a significant amount of the most toxic congener, 2,3,7,8-TCDD. Since PCDD/F are destroyed at temperatures higher than 600ºC, it was expected that all PCDD/F contained in the fuel were destroyed, since the residence time of the gases in the freeboard at a temperature above 600ºC was 4.0 seconds (Table 6.1).

Iin order to identify the large amount of PCDD/F emitted in the stack-gas, a comparison was made between the congener's contents in the fuel and in the stack-gas (Figure 6.41).

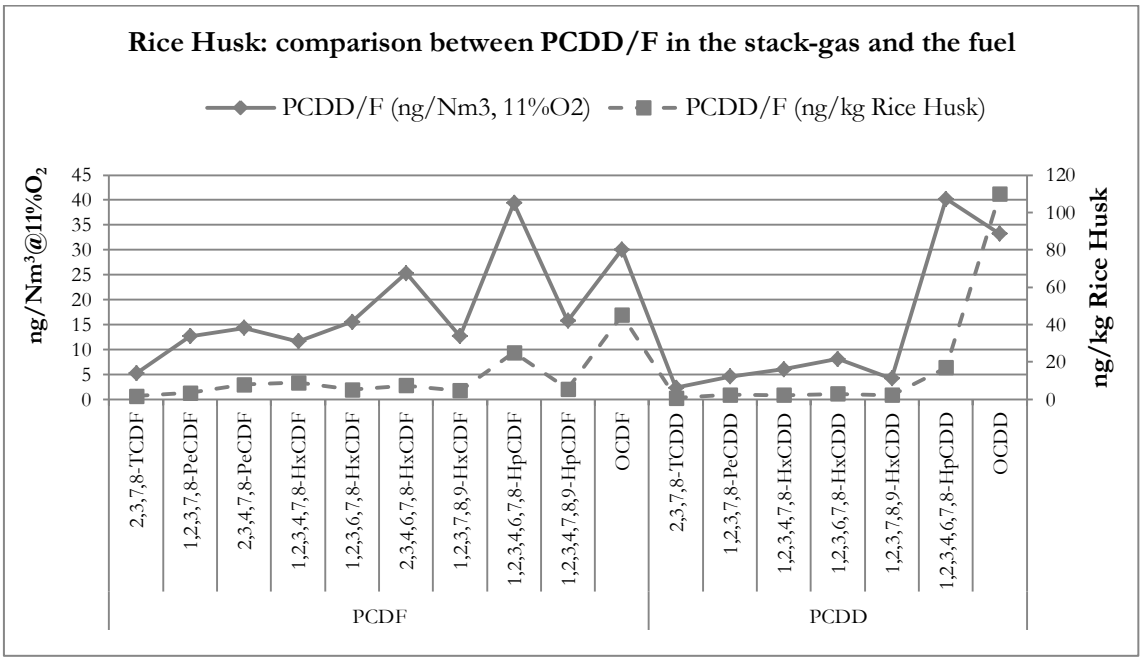

Figure 6.41 – Comparison between PCDD/F stack-gas emissions congeners with the Rice Husk fuel congeners.

As it can be seen, the emissions show a similar profile with the fuel congener distribution. This could be explained by incomplete combustion conditions leading to a significant amount of unburned Rice Husk with small dimensions (in the stack d50=1.1 µm) that was elutriated from the reactor prior to combustion. However, the amount of PCDD/F found in the stack-gas is several orders of magnitude higher than in the fuel inlet. It is probably the structure of Rice Husk that acts as precursor to PCDD/F formation levels found in this test.

A comparison of the total PCDD/F emissions identifying each congener of the 100% combustion tests is shown in Figure 6.42.

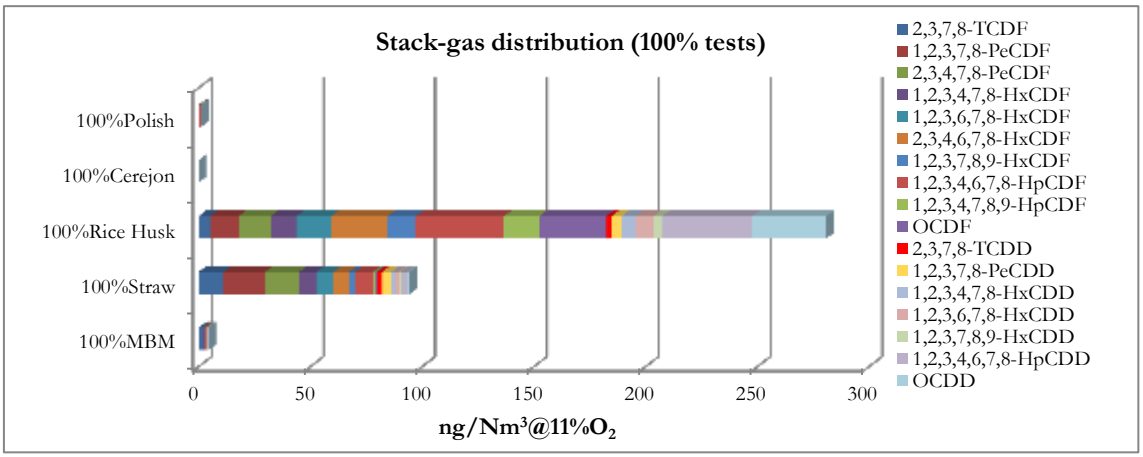

Figure 6.42 – PCDD/F distribution in the stack-gas emissions of the Rice Husk test and comparison with the other 100% combustion tests.

As can be seen from Figure 6.41, the emissions of PCDD/F in both 100% tests with biomass present remarkably high emissions when compared with the coals emissions. Although in the case of the coal tests there were some PCDD/F retained in the cyclones ashes (as will be presented and discussed next), the total PCDD/F formed with coals are significantly lower than with the biomass origin materials tested. To note that the emissions here presented have different toxicity and that not reflect the total PCDD/F in terms of I-TEQ, which will be discussed above.

Emission Limits

A comparison of the total PCDD/F emissions of all PCDD/F tests, in terms of ng I-TEQ (calculated with the I-TEF of Table 3.7) is presented in Table 6.16.

Table 6.16 – PCCD/F Stack gas emissions (ng I-TEQ/Nm^3@11%O_2).

ng I-TEQ/Nm^3@11 % O_2	100%PCI	15%SP(PCI)	100%SP	100%CCI	15%MBM(CCI)	100%MBM	15%SP(CCI)	100%Rice
PCDD	0.10	0.42	12.3	0.0005	0.001	0.41	0.91	15.4
PCDF	0.02	0.14	4.6	n.d.	n.d.	0.08	0.43	6.8
Total PCDD/F	**0.12**	**0.56**	**16.9**	**0.0005**	**0.0010**	**0.50**	**1.34**	**22.2**

n.d. – not detected

In terms of ng I-TEQ, even the Polish coal monocombustion presents PCDD/F emissions of 0.121 ng I-TEQ/Nm^3@11% O_2, higher than the ELV of the European Directive of 0.1 ng I-TEQ/Nm^3@11% O_2. This can be attributed to the significant content of chlorine and relatively low sulphur amount in both fuels. As the straw content increased in the SP/PC tests, there was a significant rise in the PCDD/F emissions, being almost 140 times higher for the 100%SP test run when compared to the 100%PC test.

The 15%SP(CCI) test presents PCDD/F emissions of 1.34 ng I-TEQ/Nm^3@11% O_2, more than 13-fold higher than the ELV.

In the 100%RH test all the toxic congeners were found, with a significant amount of the most toxic congener, 2,3,7,8-TCDD, with 200-fold higher than the European Union 0.1 ng I-TEQ/Nm^3@11% O_2 emission limit value.

6.6.3 Content of PCDD/F in ashes

MBM/Cerejon coal

For the MBM/Cerejon campaign, the dioxins and furans content in the ashes collected in both cyclones are presented in Table 6.17.

Table 6.17 – PCCD/F Content in the cyclone ashes from MBM/Cerejon Coal Tests.

ng/kg ash	Test Runs					
	1st Cyclone			2nd Cyclone		
	100% Coal Cerejon	15% MBM	100% MBM	100% Coal Cerejon	15% MBM	100% MBM
2,3,7,8-TCDF	13.0	3.5	6.85	0.2	<QL	8.0
1,2,3,7,8-PeCDF	<QL	<QL	<QL	<QL	<QL	4.0
2,3,4,7,8-PeCDF	<QL	<QL	<QL	<QL	<QL	4.0
1,2,3,4,7,8-HxCDF	<QL	<QL	<QL	<QL	1.5	2.7
1,2,3,6,7,8-HxCDF	<QL	<QL	<QL	<QL	1.5	3.0
2,3,4,6,7,8-HxCDF	<QL	<QL	1.22	<QL	1.5	2.7
1,2,3,7,8,9-HxCDF	<QL	<QL	<QL	<QL	2.4	1.2
1,2,3,4,6,7,8-HpCDF	<QL	<QL	1.70	<QL	7.3	6.2
1,2,3,4,7,8,9-HpCDF	<QL	<QL	1.20	<QL	3.9	<QL
OCDF	<QL	<QL	2.90	<QL	11.4	5.2
Total PCDF	13.0	3.5	13.87	0.2	29.5	37.0
2,3,7,8-TCDD	<QL	<QL	<QL	<QL	<QL	1.5
1,2,3,7,8-PeCDD	<QL	<QL	<QL	<QL	<QL	2.2
1,2,3,4,7,8-HxCDD	1.3	<QL	<QL	<QL	<QL	1.5
1,2,3,6,7,8-HxCDD	1.5	<QL	1.22	<QL	1.5	1.7
1,2,3,7,8,9-HxCDD	<QL	<QL	1.47	<QL	<QL	<QL
1,2,3,4,6,7,8-HpCDD	4.2	2.0	6.60	2.2	12.8	9.7
OCDD	4.7	4.7	8.60	5.9	42.8	24.1
Total PCDD	11.7	6.7	17.89	8.1	57.1	40.7
Total PCDD/F	**24.62**	**10.2**	**31.76**	**8.3**	**86.6**	**77.7**
Average T_{inlet} (ºC)	615	634	689	546	564	595
Average T_{outlet} (ºC)	546	564	595	476	476	491

For the 1st cyclone, the retention is higher for the 100% fuel tests; for the blend there was a significant decrease. For the 2nd cyclone the behaviour was an increasing concentration with the increase of MBM.

Figure 6.43 presents a comparison between the emission of each congener for the 1st and 2nd cyclones.

In terms of total PCDD/F mass retained in the ashes (Table 6.18) the retention is not linear with the blends proportion and other correlations should be explored in order to understand these results.

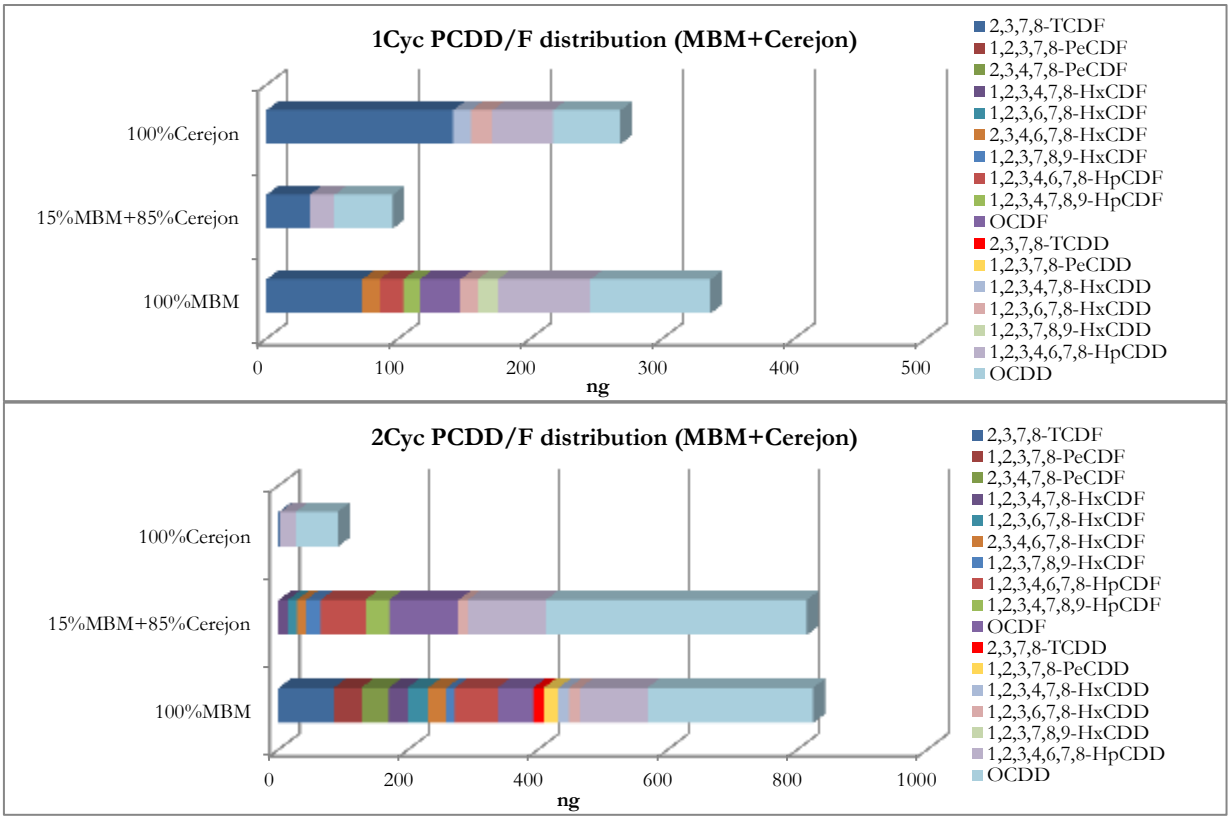

Figure 6.43 – PCDD/F distribution in the 1st and 2nd Cyclone ashes of the MBM/Coal Cerejon tests.

The lower retention in the cyclones as well as the lower emitted PCDD/F occurs in the co-combustion test (Table 6.18). In the 100% Cerejon test more than 93% of the formed PCDD/F was retained in the 1st cyclone. This might be due to the high unburned carbon present in the ash material.

Table 6.18 – PCCD/F distribution for the MBM/Cerejon Coal Tests.

Total PCDD/F Mass (ng)	**Test Runs**		
	100%CC I	**15%MBM(CC I)**	**100%MBM**
1st Cyclone	268	96	337
2nd Cyclone	14.8	106	32
Stack gas	4.8	9.0	3996
TOTAL	288	211	4365

Straw Pellets/Polish coal

The dioxins and furans content in the ashes collected in both cyclones for the Straw/Polish coal tests are presented in Table 6.19.

Table 6.19 – PCCD/F Content in the cyclones ashes from Straw/Polish Coal Tests.

ng/kg ash	Test Runs					
	1st Cyclone			2nd Cyclone		
	100% Polish Coal	15% SP	100% SP	100% Polish Coal	15% SP	100% SP
2,3,7,8-TCDF	58.90	36.5	103.0	1152.0	742.0	213.0
1,2,3,7,8-PeCDF	31.3	7.4	33.1	199.0	273.0	186.0
2,3,4,7,8-PeCDF	35.6	9.2	35.5	377.0	363.0	300.0
1,2,3,4,7,8-HxCDF	21.1	1.7	12.8	189.0	94.0	141.0
1,2,3,6,7,8-HxCDF	21.1	1.7	15.7	182.0	87.0	129.0
2,3,4,6,7,8-HxCDF	16.9	2.2	17.9	147.0	72.0	131.0
1,2,3,7,8,9-HxCDF	5.5	<LQ	5.6	42.0	23.0	45.0
1,2,3,4,6,7,8-HpCDF	42.0	3.0	30.2	461.0	87.0	178.0
1,2,3,4,7,8,9-HpCDF	3.2	<LQ	5.6	32.0	12.0	35.0
OCDF	8.5	5.7	23.9	60.0	13.0	59.0
Total PCDF	244.1	67.4	283.3	2841.0	1766.0	1417.0
2,3,7,8-TCDD	5.7	<LQ	13.5	150.0	40.0	15.0
1,2,3,7,8-PeCDD	10.4	8.7	13.5	115.0	72.0	52.0
1,2,3,4,7,8-HxCDD	5.5	7.7	7.2	35.0	67.0	25.0
1,2,3,6,7,8-HxCDD	7.2	8.4	10.1	40.0	65.0	45.0
1,2,3,7,8,9-HxCDD	4.0	5.0	7.7	24.0	30.0	23.0
1,2,3,4,6,7,8-HpCDD	17.2	26.3	56.7	117.0	214.0	446.0
OCDD	21.9	33.8	90.3	125.0	92.0	1273.0
Total PCDD	71.9	89.9	199.0	606.0	580.0	1879.0
Total PCDD/F	**316.0**	**157.3**	**482.3**	**3447.0**	**2346.0**	**3296.0**
Inlet Temperature (ºC)	638	674	740	554	592	649
Outlet Temperature (ºC)	554	592	649	444	495	530

For the 1st cyclone the retention is higher for the 100% fuel tests; for the blend there was a significant decrease. For the 2nd cyclone the behaviour was an increasing concentration with the increase of MBM.

A comparison between the emissions of each congener is made in Figure 6.44 for the 1st and 2nd cyclone ashes.

The total PCDD/F mass retained in the ashes (Table 6.20) decreased with the increase of SP in the blends.

Table 6.20 – PCCD/F distribution for the SP/Polish Coal Tests.

Total PCDD/F Mass (ng)	Test Runs		
	100%PC I	15%SP(PC I)	100%SP
1st Cyclone	1770	661	289
2nd Cyclone	4841	2053	893
Stack gas	1109	5763	91130
TOTAL	7720	8476	92312

This decrease was compensated with the higher PCDD/F emissions observed for this trial (Table 6.13). This might be due to the high unburned material present in both cyclone ashes for combustion and co-combustion of coal. In fact, the content of these ashes in carbon was higher than 40% (Figure 6.34).

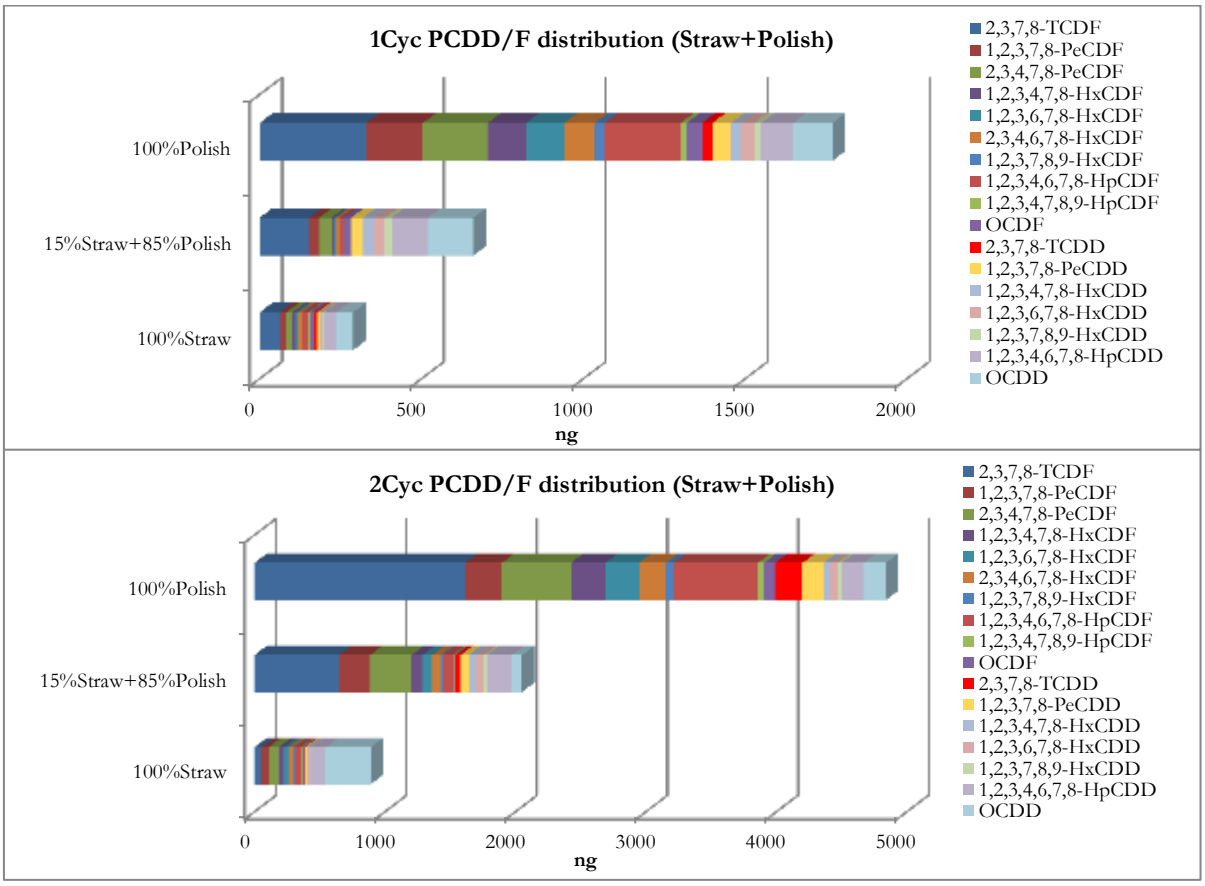

Figure 6.44 – PCDD/F distribution in the 1st and 2nd Cyclone ashes of the Straw/Polish Coal tests.

Straw Pellets/Cerejon coal

The dioxins and furans content in the ashes collected in both cyclones for the Straw/Cerejon coal tests are presented in Table 6.21. The 15%SP(CC I) combustion test was carried out in the new installation. The cyclone ashes concentrations presented a different behaviour than the ones of the Straw Pellets/Polish coal mixture. On that case, the 1st cyclone ashes contained 8 Furans congeners (except 1,2,3,7,8,9-HxCDF and 1,2,3,4,7,8,9-HpCDF) and 6 Dioxin congeners (except 1,2,7,8-TCDD); in the 15%SP(CC I) test, only 3 Furan congeners were found. For the 2nd cyclone ashes, in both tests all the 17 toxic compounds were found.

In terms of amounts, *i.e.* taking into account the mass of each cyclone stream mass, the total amount of the PCDD/F collected in the cyclone ashes are presented in Figure 6.45.

Table 6.21 – PCCD/F Content in the cyclones ashes from Straw/Cerejon Coal Tests.

ng/kg ash	Test Runs					
	1st Cyclone			2nd Cyclone		
	100% CC I(1)	15% SP(CC I)	100% SP(2)	100% CC I(1)	15% SP(CC I)	100% SP(2)
2,3,7,8-TCDF	13.0	<QL	103.0	0.2	54.0	213.0
1,2,3,7,8-PeCDF	<QL	<QL	33.1	<QL	43.0	186.0
2,3,4,7,8-PeCDF	<QL	<QL	35.5	<QL	70.0	300.0
1,2,3,4,7,8-HxCDF	<QL	1.0	12.8	<QL	40.0	141.0
1,2,3,6,7,8-HxCDF	<QL	<QL	15.7	<QL	44.0	129.0
2,3,4,6,7,8-HxCDF	<QL	<QL	17.9	<QL	57.0	131.0
1,2,3,7,8,9-HxCDF	<QL	<QL	5.6	<QL	22.0	45.0
1,2,3,4,6,7,8-HpCDF	<QL	4.1	30.2	<QL	98.0	178.0
1,2,3,4,7,8,9-HpCDF	<QL	<QL	5.6	<QL	24.0	35.0
OCDF	<QL	4.3	23.9	<QL	71.0	59.0
Total PCDF	13.0	9.4	283.3	0.2	523.0	1417.0
2,3,7,8-TCDD	<QL	<QL	13.5	<QL	6.5	15.0
1,2,3,7,8-PeCDD	<QL	<QL	13.5	<QL	13.0	52.0
1,2,3,4,7,8-HxCDD	1.3	<QL	7.2	<QL	6.2	25.0
1,2,3,6,7,8-HxCDD	1.5	<QL	10.1	<QL	6.9	45.0
1,2,3,7,8,9-HxCDD	<QL	<QL	7.7	<QL	4.6	23.0
1,2,3,4,6,7,8-HpCDD	4.2	<QL	56.7	2.2	37.0	446.0
OCDD	4.7	<QL	90.3	5.9	76.0	1273.0
Total PCDD	11.7	<QL	199.0	8.1	150.2	1879.0
Total PCDD/F	**24.62**	**9.4**	**482.3**	**8.3**	**673.2**	**3296.0**

(1) – From Table 6.18; test in the old installation.
(2) – From Table 6.20; test in the old installation.

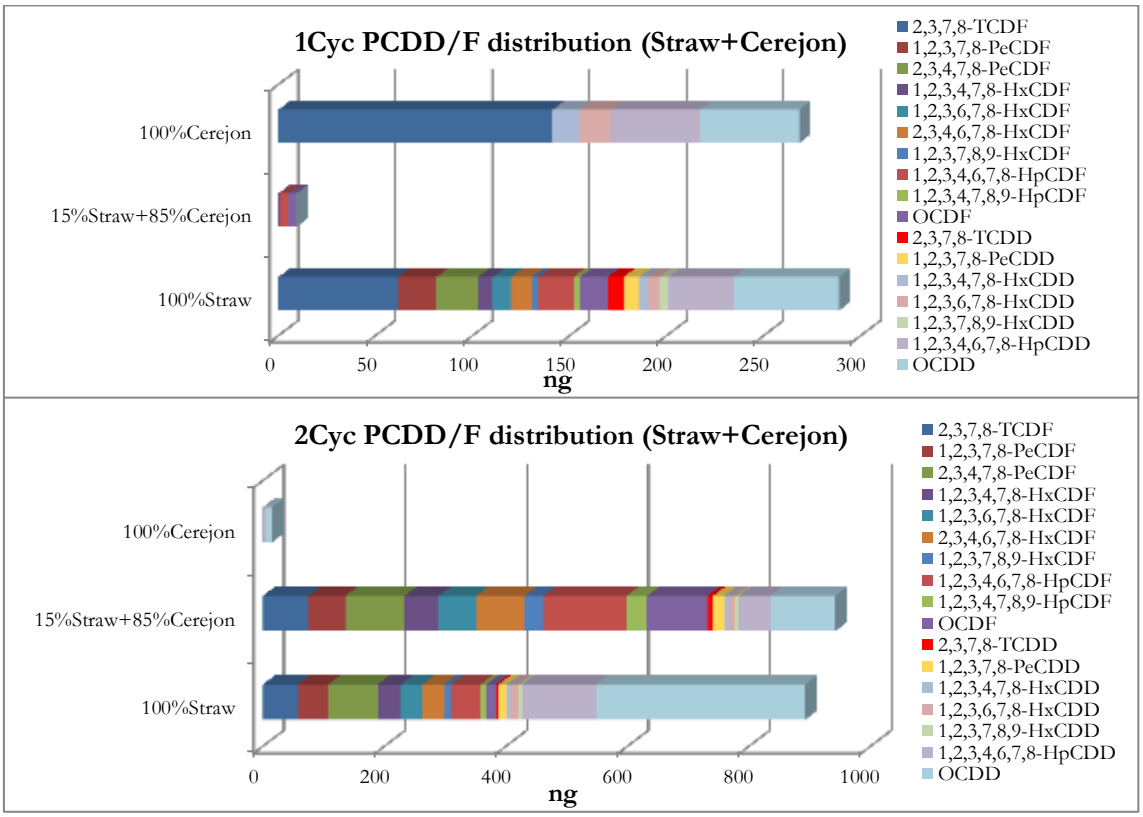

Figure 6.45 – PCDD/F distribution in the 1st and 2nd Cyclone ashes of the Straw/Cerejon coal tests.

In terms of 1st cyclone ash, the total amount of PCDD/F is significantly lower than the ones of the monocombustion test. As for the 2nd cyclone ash, the total amount of PCDD/F was slightly higher than for the 100%SP test.

The total amounts of PCDD/F in the cyclone ashes are much lower than for the Straw Pellets/Polish coal campaign, where the 100%SP represented the better situation.

When Cerejon coal was used in the mixture, the total PCDD/F mass retained in the 2nd cyclone ashes (Table 6.22) decreased; in the 1st cyclone it was observed a significant reduction in the total PCDD/F amount.

Table 6.22 – PCCD/F distribution for the SP/Cerejon Coal Tests.

Total PCDD/F Mass (ng)	**Test Runs**		
	100%CC I	**15%SP(CC I)**	**100%SP**
1st Cyclone	268	57	289
2nd Cyclone	14.8	942	893
Stack gas	4.8	25610	91130
TOTAL	288	26609	92312

Rice Husk

The 1st and 2nd cyclone ash content for the 100%Rice Husk test are presented in Table 6.23.

Table 6.23 – PCCD/F Content in the cyclones ashes from Straw/Polish Coal Tests.

ng/kg ash	**1st Cyclone**	**2nd Cyclone**
2,3,7,8-TCDF	7.1	840
1,2,3,7,8-PeCDF	13.0	1000
2,3,4,7,8-PeCDF	29.0	2300
1,2,3,4,7,8-HxCDF	14.0	1500
1,2,3,6,7,8-HxCDF	13.0	1700
2,3,4,6,7,8-HxCDF	17.0	2800
1,2,3,7,8,9-HxCDF	12.0	1100
1,2,3,4,6,7,8-HpCDF	50.0	5600
1,2,3,4,7,8,9-HpCDF	19.0	1400
OCDF	270.0	6700
Total PCDF	444.1	24940
2,3,7,8-TCDD	2.8	90
1,2,3,7,8-PeCDD	23.0	380
1,2,3,4,7,8-HxCDD	11.0	250
1,2,3,6,7,8-HxCDD	17.0	350
1,2,3,7,8,9-HxCDD	11.0	200
1,2,3,4,6,7,8-HpCDD	180.0	2700
OCDD	700.0	6400
Total PCDD	944.8	10370
Total PCDD/F	**1388.9**	**35310**

As for the stack-gas emissions, the cyclone ashes profiles were compared with the PCDD/F-fuel concentration (Figure 6.46).

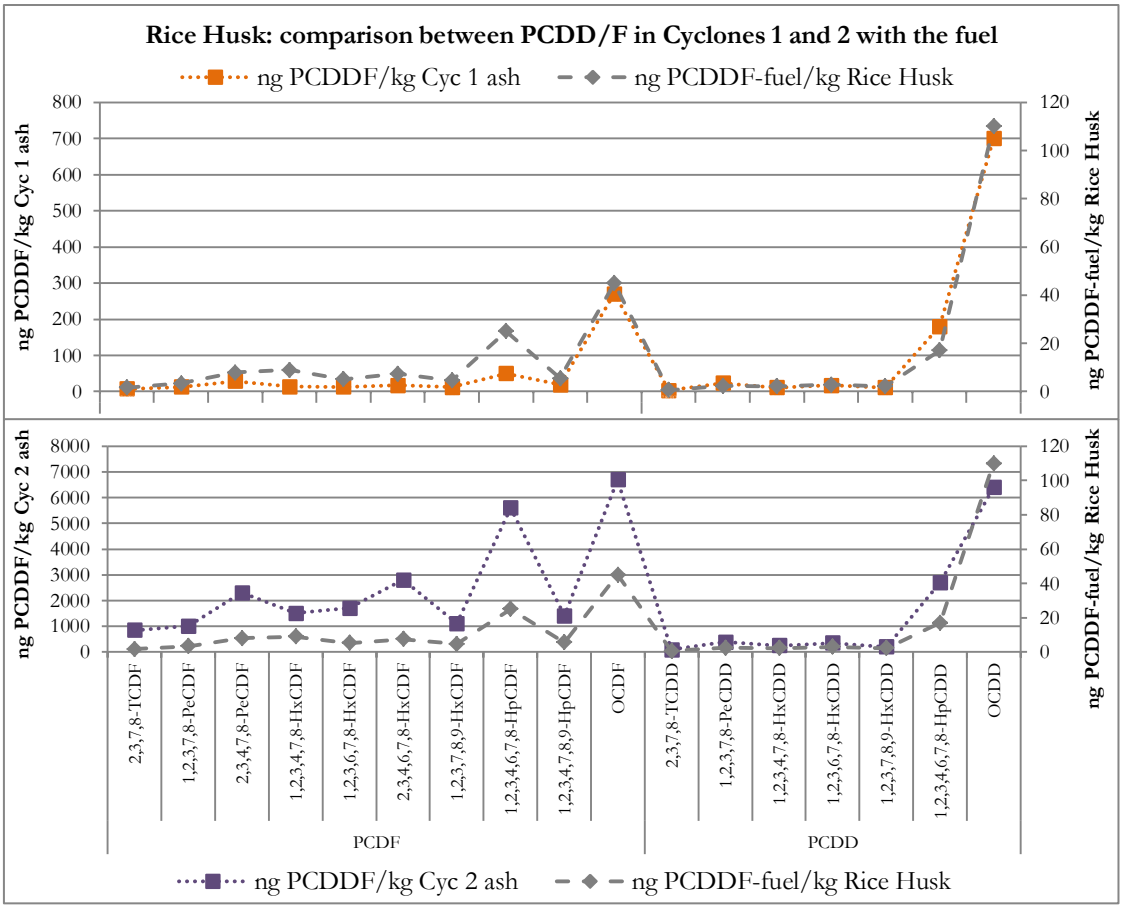

Figure 6.46 – PCDD/F congener distribution in the 1st and 2nd Cyclone ashes of Rice Husk test.

Once again, similar profiles were found between the cyclone ashes and the Rice Husk, although for some congeners it can be seen that a higher proportion was found (*eg.*: 1,2,3,4,6,7,8-HpCDF in the 1st cyclone; 2,3,4,7,8-PeCDF, 2,3,4,6,7,8-HxCDF, 1,2,3,4,6,7,8-HpCDF, OCDF and 1,2,3,4,6,7,8-HpCDD in the 2nd cyclone) probably resulting from PCDD/F formation. Once again, the similar profiles of the cyclone ashes with the fuel congener distribution.

The total amount of the PCDD/F collected in the cyclone ashes is presented in Figure 6.47. Rice Husk ashes contain very high amounts of PCDD and PCDF. When comparing all the 100% tests it is possible to identify the Polish coal as the other fuel that contains high amounts of PCDD/F. Although these ashes are highly contaminated, the formed PCDD and PCDF were not emitted to the atmosphere, thus preventing the release of these highly toxic pollutants.

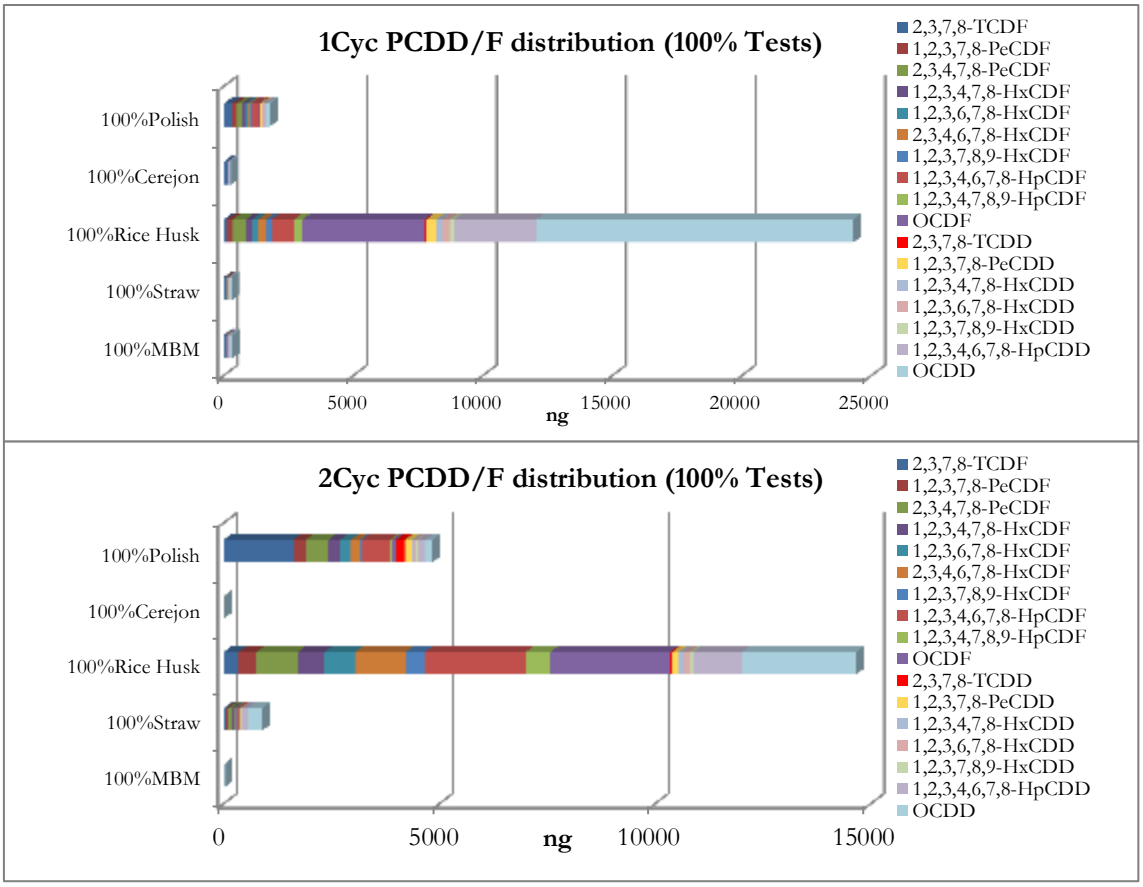

Figure 6.47 – PCDD/F distribution in the 1st and 2nd Cyclone ashes of the 100%RH test and comparison with the other 100% combustion tests.

Table 6.24 summarizes the mass distribution of the formed PCDD/F among the different streams. Note that the results are presented in µg.

Table 6.24 – PCCD/F distribution for the 100%RH test.

Total PCDD/F Mass (µg)	100%RH
1st Cyclone	24.3
2nd Cyclone	14.7
Stack gas	318.7
TOTAL	357.7

For this test, over 89% of the formed PCCD/F was released in the stack-gas. Since this fuel presents the smaller fly ash mean diameter (1.1 µm), the PCDD/F associated with the particulate matter were not collected in the cyclones and were released to the atmosphere. Hence, the use of a very efficient particle collector for small fly ash, such as a hybrids particle collector, will be absolutely necessary in order to fulfil the ELV for PCDD/F.

6.6.4 PCDD/F Homologue Profiles

In order to evaluate the degree of chlorination of the PCDD/F, the homologue profiles of the cyclone ashes and stack-gas emission were evaluated. Jansson and co-workers (2009a, 2009b) e valuated the isomers distribution patterns of PCDD/Fs formed during MSW combustion.

MBM/Cerejon coal

For the MBM and Cerejon coal, the fuels homologue profiles are presented in Figure 6.48.

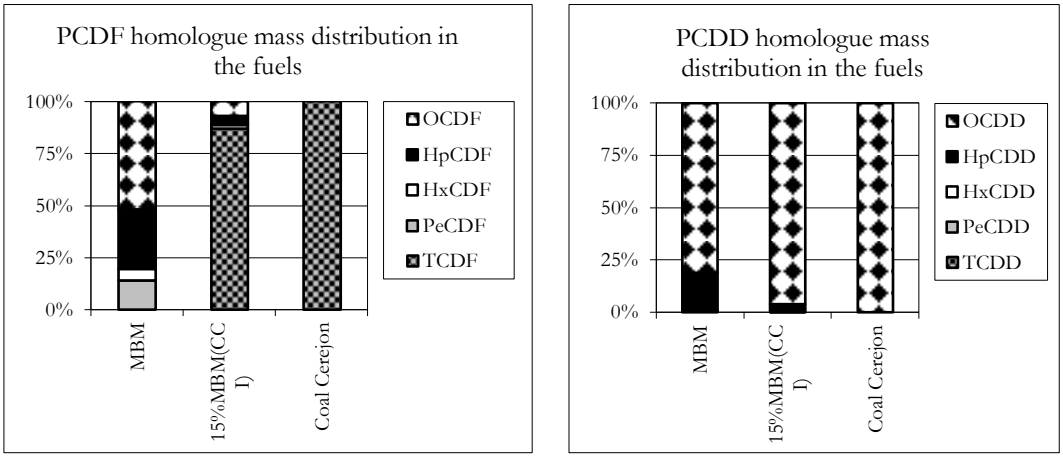

Figure 6.48 – Homologue distribution in MBM and Coal Cerejon (ng $_{PCDD/F}$/kg fuel).

The cyclones ashes and stack-gas emissions are presented in Figures 6.49 and 6.50.

In terms of PCDF, the 1st cyclone presents lower chlorination degree whereas the PCDD present are the higher chlorinated congeners, with a chlorination degree (CD) of 7.1 -7.5. The PCDD collected in the 2nd cyclone present high chlorination degrees (CD=7.2-7.7).

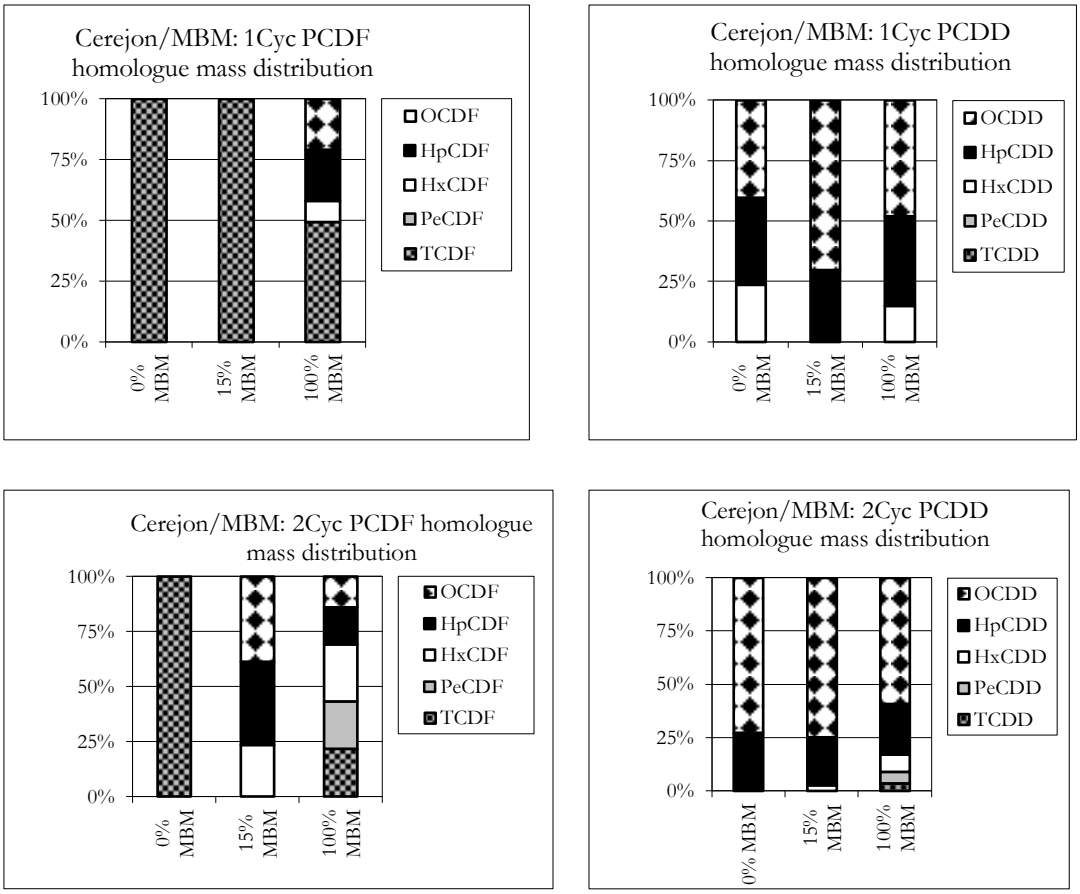

Figure 6.49 – Homologue distribution in the 1st and 2nd cyclone ashes for the MBM(CC I) tests (as measured, ng $_{PCDD/F}$).

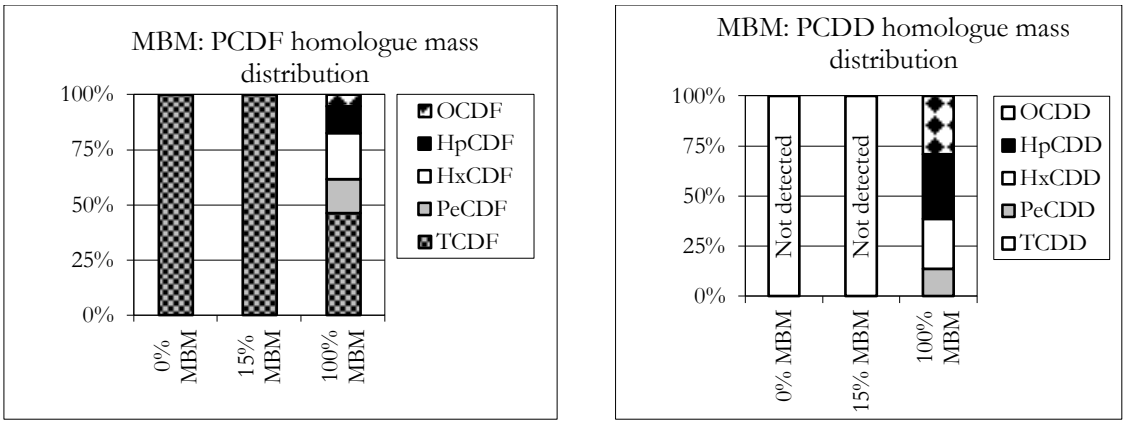

Figure 6.50 – Homologue distribution in the stack-gas emissions of the MBM/Coal Cerejon tests (ng $_{PCDD/F}$/Nm³).

The different homologue distribuition of PCDD/F in the cyclone ashes and in the stack gas with the fuels distribution led to the conclusion that the PCDD/F introduced with the fuels were destroyed during combustion.

Straw Pellets/Polish coal

For the Straw Pellets and Polish coal, the cyclones ashes and stack-gas emissions are presented in Figures 6.51 and 6.52.

In the case of furans the chlorination degree is lower than in the dioxins emitted. Nevertheless, in the 15% Straw and 100% Straw tests, significant amounts of 2,3,7,8-TCDD are emitted corresponding to almost 70% and 45% of the total PCDD/F emitted.

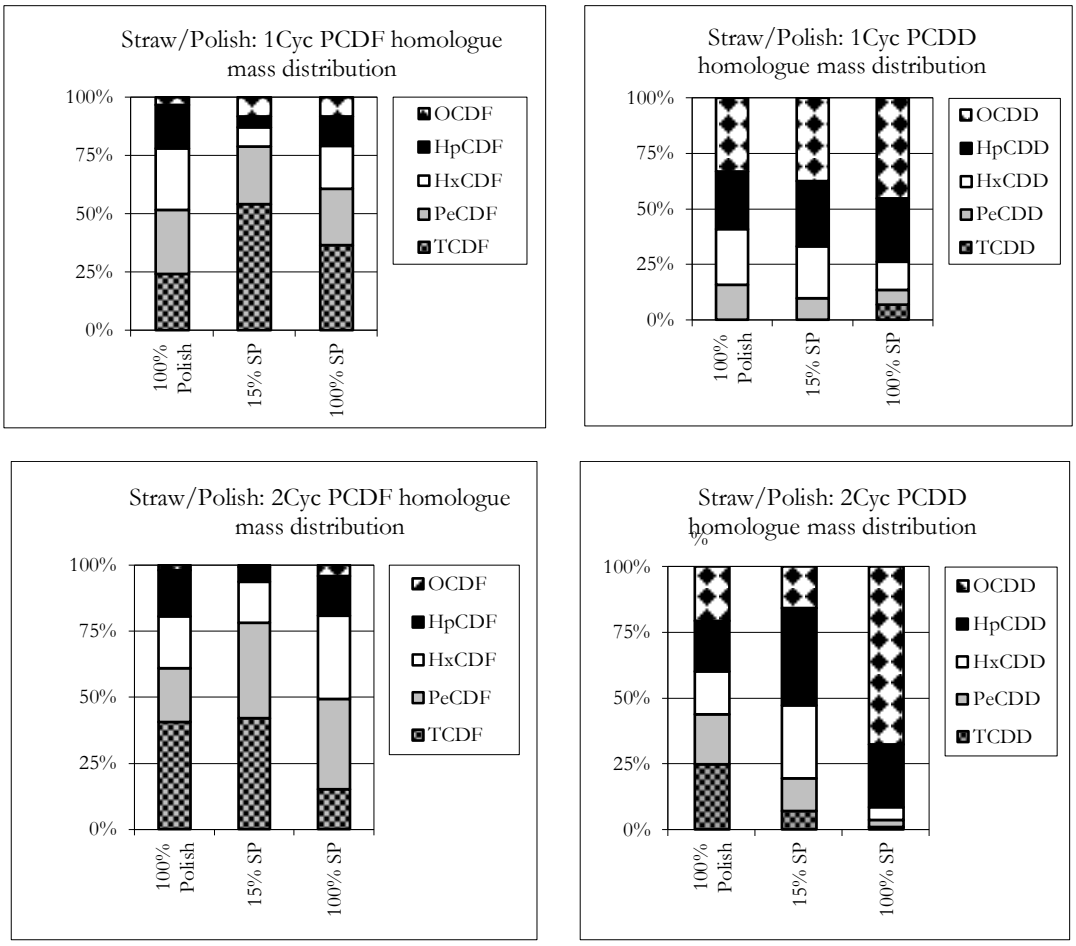

Figure 6.51 – Homologue distribution in the 1st and 2nd cyclone ashes for the SP(PC I) tests (as measured, ng $_{PCDD/F}$).

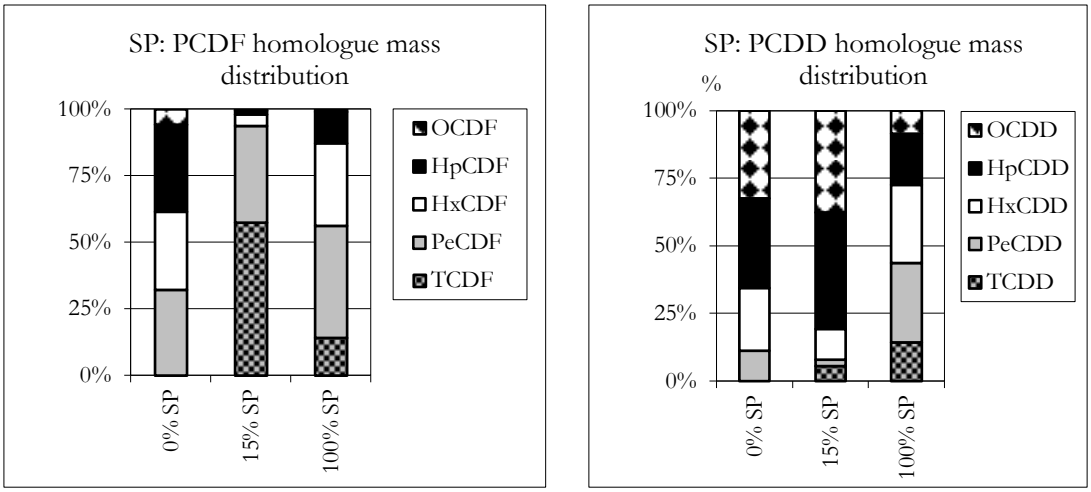

Figure 6.52 – Homologue distribution in the 1st and 2nd cyclone ashes and in the stack gas emitted for the SP(PC I) tests (as measured, ng $_{PCDD/F}$).

Straw Pellets/Cerejon coal

For the Straw Pellets and Cerejon coal, the cyclones ashes and stack-gas emissions are presented in Figures 6.53 and 6.54.

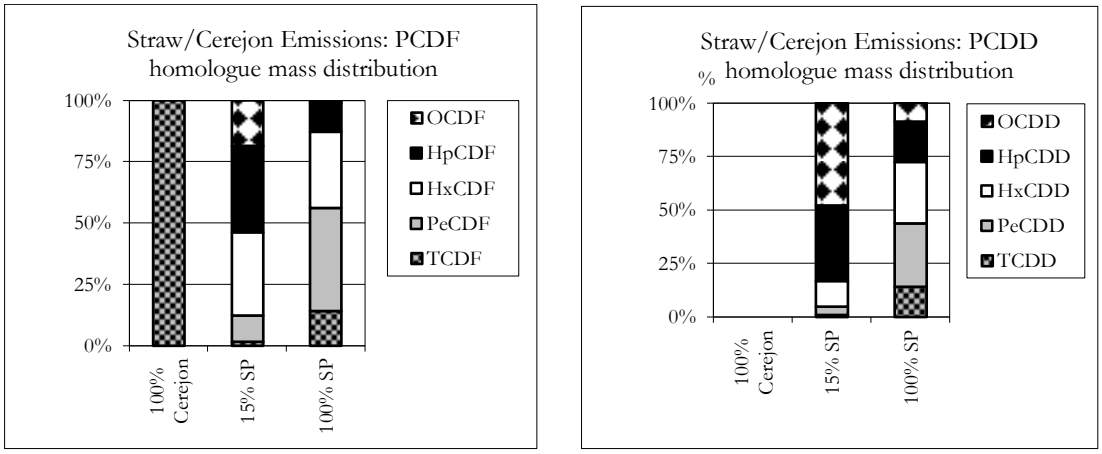

Figure 6.53 – Homologue distribution in the 1st and 2nd cyclone ashes for the SP(CC I) tests (as measured, ng $_{PCDD/F}$).

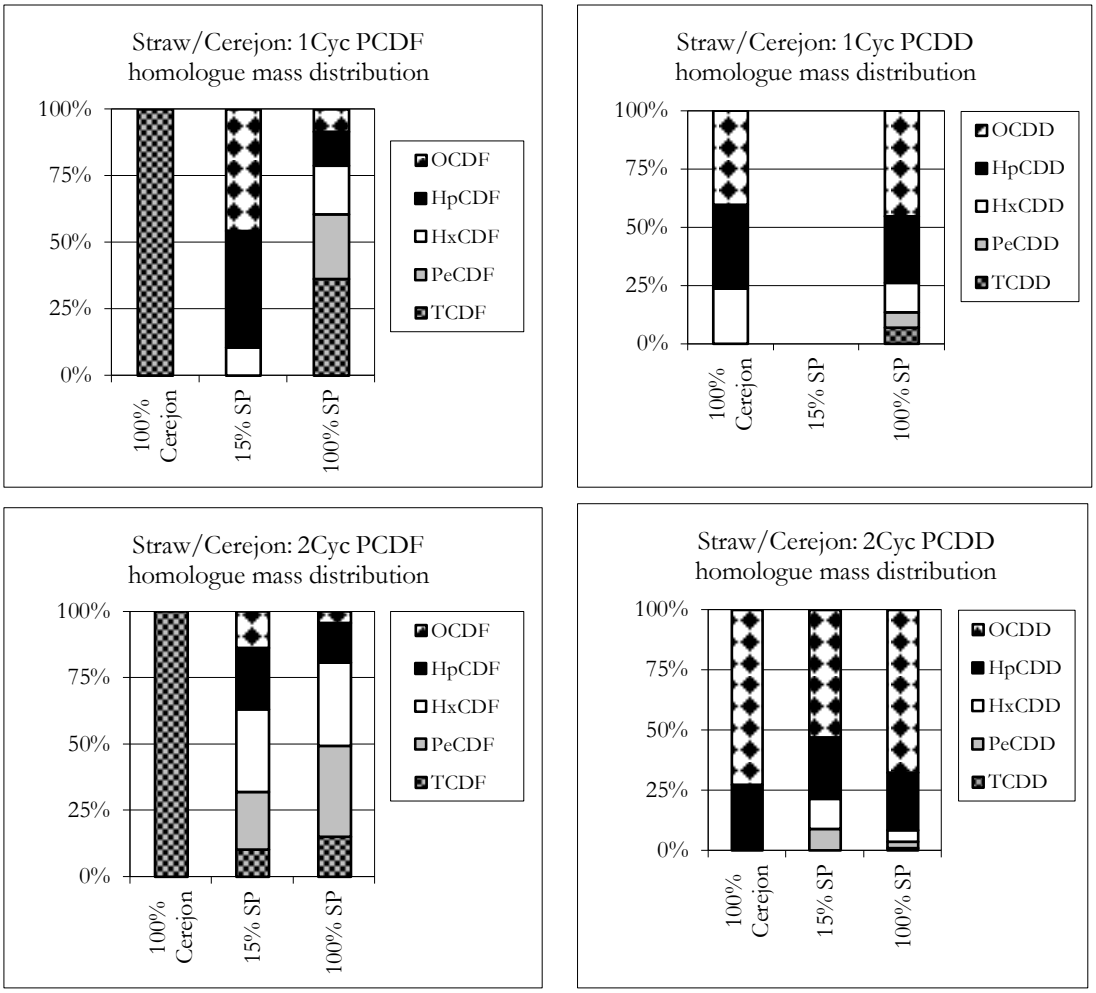

Figure 6.54 – Homologue distribution in the 1st and 2nd cyclone ashes and in the stack gas emitted for the SP(PC I) tests (as measured, ng $_{PCDD/F}$).

Rice Husk

For the 100% Rice Husk test, the cyclones ashes and stack-gas emissions are presented in Figure 6.55.

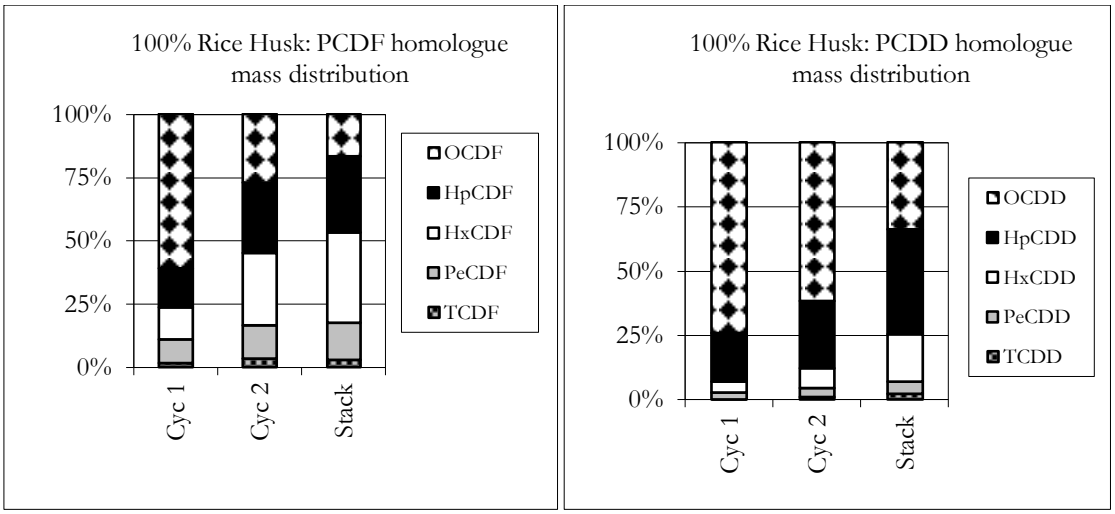

Figure 6.55 – Homologue distribution in the 1st and 2nd cyclone ashes and in the stack gas emitted for the 100%RH test (as measured, ng $_{PCDD/F}$).

6.6.5 PCCD/F distribution synthesis

In Figure 6.56 the PCDD and PCDF distribution are shown. As can be seen in Figure 6.44, the emissions of PCDD and PCDF for the pRES fuels is higher than 90% of the total PCDD/F formed in the process. This may be explained by the smaller fly ash diameter of these materials (Figure 6.13) and by the absence SO_2 during combustion, due to low S-Fuel materials, such as SP and RH, or through S retention by Ca, as in the case of MBM. It was also verified that the option of co-firing these pRES materials with coal reduced the PCDD/F emissions, at least *ca.* 35% for a high-S and high-Cl coal whereas with a high-S and low-Cl coal the PCDD/F emissions could be reduced by *ca.* 95%.

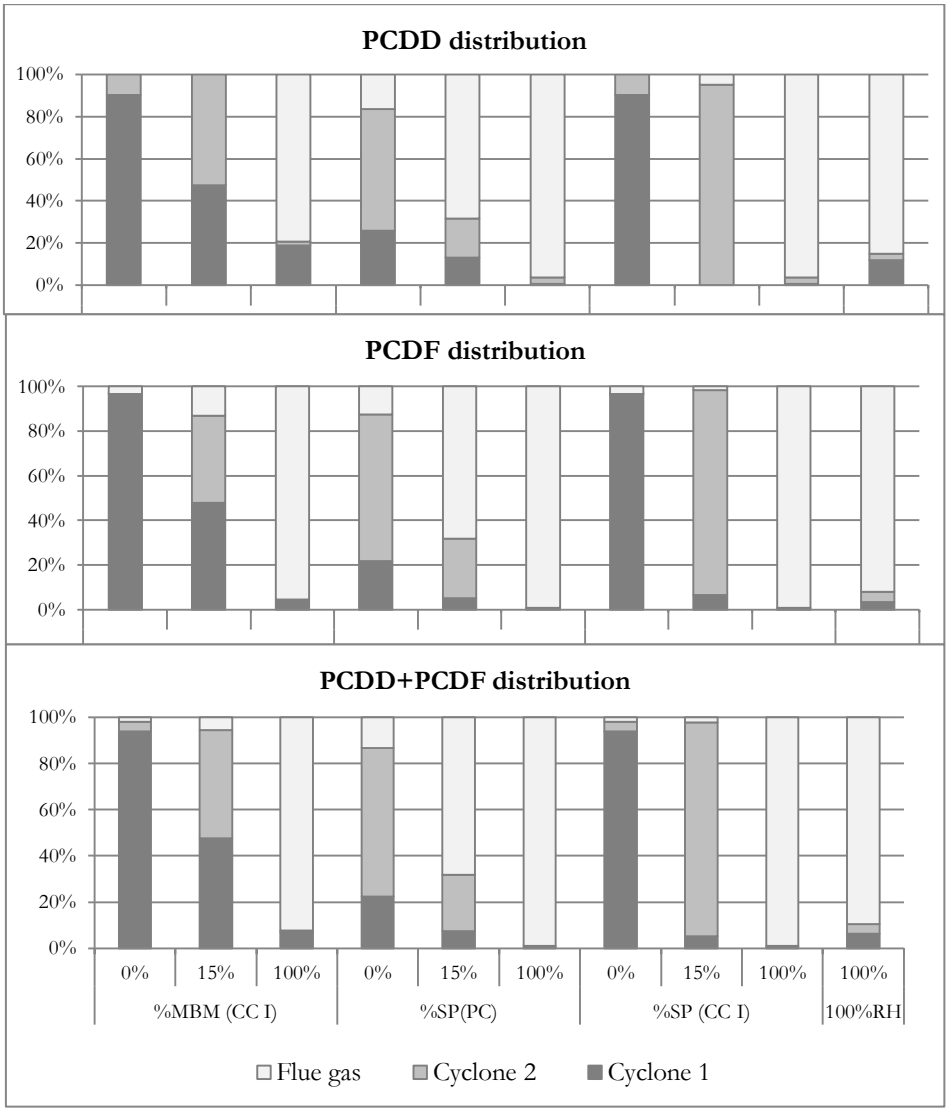

Figure 6.56 – PCDD and PCDF distribution between the 1st and 2nd cyclone ashes and the stack gas emitted (in terms of measured $mol_{PCDD/F}$).

6.7 Statistical analysis

A statistical analysis was performed in order to identify the factors that affected the total emission of PCDD/F in the different streams of the system, *i.e.* 1st Cyclone, 2nd Cyclone and stack gas. The results obtained were correlated with different parameters/descriptors, as listed in Table 6.25.

Table 6.25 – Tested parameters.

Parameter	Units	Parameter	Units
N. of moles PCDD	mol PCDD	Molar ratio nS/nCl	mol S/mol Cl
M. of moles PCDF	mol PCDF	Molar ratio nCl/nCu	mol Cl/mol Cu
N. of moles PCDD+PCDF	mol PCDD+mol PCDF	Fuel Cl content	mol Cl-Fuel/mol Fuel
Molar ratio PCDD/PCDF	mol PCDD/mol PCDF	Fuel S content	mol S-Fuel/mol Fuel
PCDD content	mol PCDD/mol Fuel	Fuel Cu content	mol Cu-Fuel/mol Fuel
PCDF content	mol PCDF/mol Fuel	Oxygen content	% (V/V)
PCDD+PCDF content	mol PCDD+PCDF/mol Fuel	CO concentration in the flue gas	mg CO/Nm^3@11%O_2
Ash d50 (mean diameter)	µm	SO_2 concentration in the flue gas	mg S/Nm^3@11%O_2
Ash Cu content	mol Cu-Ash/mol Fuel	HCl concentration in the flue gas	mg Cl/Nm^3@11%O_2
Ash Cl content	mol Cl-Ash/mol Fuel	Residence time	s
Molar ratio nCa/nS	mol Ca/mol S	Average temperature	K
Molar ratio nCa/(nS+nCl)	mol Ca/(mol S + mol Cl)		

To facilitate the identification of the sum of the toxic PCDF and PCDD, this parameter will hereafter be referred as D+F. Table 6.26 presents the molar fractions of total formed PCDD/F (y_{D+F}) and the molar fraction of the selected elements (x_i), in terms of the total mol of fuel.

Table 6.26 – Molar fractions of selected parameters.

Test runs	y_{D+F}	x_{Cu}	x_{Ca}	x_S	x_{Cl}
	(10^{15}mol/mol)	(10^6mol/mol)	(10^3mol/mol)	(10^3mol/mol)	(10^3mol/mol)
100%RH	66120	0.61	0.24	0.21	0.10
100%CC	108	1.24	0.57	2.97	0.19
15%MBM/85%CC	73	1.20	6.00	2.83	0.30
100%MBM	1474	0.88	45.20	1.84	1.10
100%PC	3298	1.84	1.17	1.69	0.77
15%SP/85%PC	3016	1.62	1.10	1.50	0.76
100%SP	22938	0.44	0.73	0.41	0.72
15%SP/85%CC	7465[6]	1.12	0.60	2.57	0.27

To establish a possible relationship between the molar fraction of the formed PCDD/F (yD+F) and the molar fraction of the several analyzed elements (x_i), standard multiple linear regressions (MLR) were performed, using the Data Analysis add-in, available in Microsoft Excel. In addition, a statistical validation test was done to ensure the reliability of the model. A log-log basis was used for the regressions to deal with the different orders of magnitude of y_D quantities.

All the four uniparametric regressions possible to compute with each descriptor, *i.e.* $\log y_{D+F} = a_0 + a_1 \log x_i$, were tested. The obtained results were not satisfactory; the calculated regression coefficients (r^2) for Ca, Cu, Cl and S were 0.20, 0.28, <0.01 and 0.66, respectively.

[6] This value was reanalysed and found incorrect; the corrected value was 3-magnitude orders lower.

With regard to the sulphur's results, it was observed that one of the values was considerably deviated from the predicted linear trend. Excluding that point ("New Installation": 15%SP/85%CC) and considering only the data for the first seven results, the fit was substantially improved. The determination coefficient for the uniparametric model obtained with log x_S was higher than the threshold value of 0.80, usually considered an acceptable result. The other three uniparametric models didn't show any significant improvement.

Considering seven experimental results available, all possible six biparametric relations were tested. The independency of the chosen descriptors was guaranteed since the value of r^2 for each pair of descriptors was low, as shown in Table 6.27.

Table 6.27 – Correlation coefficients between descriptors.

r^2	Cu	Cl	S
Ca	0.02	0.34	0.28
Cu		0.04	0.56
Cl			0.10

Of the tested biparametric relations only the model equations which included log x_S descriptor showed a determination coefficient (R^2) higher than 0.80.

The biparametric models obtained presented a low significance level (SL) for the descriptors log x_{Cu} or log x_{Ca}; a SL > 95% is a common statistical requirement.

The two following models (Eqs. 6.13 e 6.14) were the only ones considered statistically appropriate. The standard deviation of the fit, s_{fit}, and Fisher's F values were also computed and analysed. These are presented below.

$$\log y_{D+F} = \underset{(SL>99\%)}{-18.42_{\pm 1.29}} - \underset{(>99\%)}{2.30_{\pm 0.44}} \log x_S \qquad (6.13)$$

($s_{fit} = 0.470$, $R^2 = 0.847$, $N = 7$, $F = 28$)

$$\log y_{D+F} = \underset{(SL>99\%)}{-16.11_{\pm 1.34}} - \underset{(>99\%)}{2.55_{\pm 0.33}} \log x_S + \underset{(92\%)}{0.90_{\pm 0.38}} \log x_{Cl} \qquad (6.14)$$

($s_{fit} = 0.337$, $R^2 = 0.937$, $N = 7$, $F = 30$)

As expected, the results confirmed that the presence of sulphur inhibits the formation of PCDD/F and the presence of chlorine promotes its formation. Since the tested descriptors were orthogonal, the tested models do not seem to indicate the statistical relevance for the calcium or copper's fuel contents on PCDD/F formation.

As the equations were computed on a log-log basis, they are consistent with the empirical model $y_{D+F} \propto x_{Cl} / x_S^{2.5}$. This relationship was further tested (on a log-log basis) and the result was satisfactory (Eq. 6.15).

$$\log y_{D+F} = \underset{(SL>99\%)}{-15.70_{\pm 0.49}} + \underset{(>99\%)}{1.02_{\pm 0.12}} \log(x_{Cl}/x_S^{2.5}) \quad (6.15)$$

($s_{fit} = 0.306$, $R^2 = 0.935$, $N = 7$, $F = 72$)

Internal validation strategies were used to test the attained model. The value of Q^2, a cross-validated *leave-one-out* correlation coefficient, was calculated, exhibiting a high value (0.939). This fully ensures the robustness of the model (Golbraikh and Tropsha, 2002; Tropsha *et al.*, 2003). Figure 6.57 illustrates the goodness-of-fit.

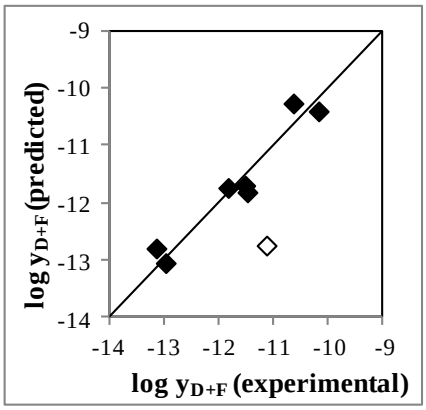

Figure 6.57 – Predicted vs. Experimental log $_{yD+F}$ (◊ - data for 15%SP/85%CC).

The strong correlation between PCDD/F formation and the sulphur and chlorine content is partly in accordance with the work of Thomas and McCreight (2008). This empirical model should be further tested with more experimental data. A summary of these conclusions were presented by Crujeira and co-workers (2013).

The outliner value was reanalysed and the group found that the (15%SP/85%CC) value was 3-magnitude orders lower. In that case, the correct value fits the previously found correlation (Eq. 6.15). Previously, the fitting of only one of the tests on the "New Installation" (100%RH) seemed to indicate that there was not reproductibily between the two installations used. However, after the reanalyse of the results and the correction of the 15%SP/85%CC test, not only increased the confidence between the correlation between PCDD/F formation and the sulphur and chlorine content of the fuels but also the reproductibility of the results from both installations was verifyed.

Figures 6.58 and 6.59 present the found correlations between the tested parameters and PCDD/F, which were plotted as the Total PCDD+PCDF in the test but also disaggregated by the different streams, *i.e.* 1st Cyclone, 2nd Cyclone and Stack gas. In each stream, Dioxins and Furans were tested separately and also as the sum (PCDD+PCDF).

6.7.1 Flue gas PCDD/F formation

The best fit obtained for both PCDD and PCDF in the stack gas was with $n_{Ca}/(n_S + n_{SCl})/x_S*x_{Cl}$.

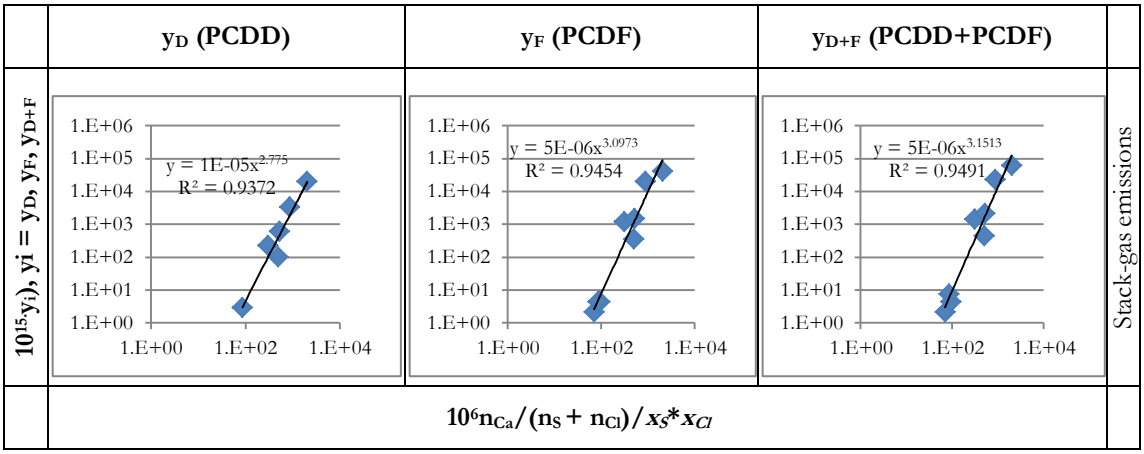

Figure 6.58 – Correlation between the different fractions of PCDD and PCDF and the factor $x_{Cl}/10^3.x_S$.

As it can be seen, all experimental data fitted with a good value for R^2 (0.94) for both PCDD and PCDF. The fitted factor included only fuel composition data, *i.e.* the Ca, S and Cl content. Thus, it was possible to conclude that:

> It is possible to estimate the stack emissions of PCDD/F from a fluidized bed combustor simply through the knowledge of the mixture fuel composition in terms of Cl, S and Ca.

Furthermore, the results were obtained in two different fluidized bed pilots, and the good correlation indicates the reproducibility of the results in different installations, with different nominal thermal capacity.

6.7.2 Cyclone 1 and Cyclone 2 PCDD/F formation

For the PCDD/F in the cyclone ashes, of all the tested parameters, the best fit occurred with the factor $Cu_{ash}*Cl_{ash}$ $\%C_{ash}$, where $Cu_{ash}*Cl_{ash}$ $\%C_{ash}$ are the copper, chlorine and carbon content in the fly ash and d50 is the mean diameter of each cyclone ash.

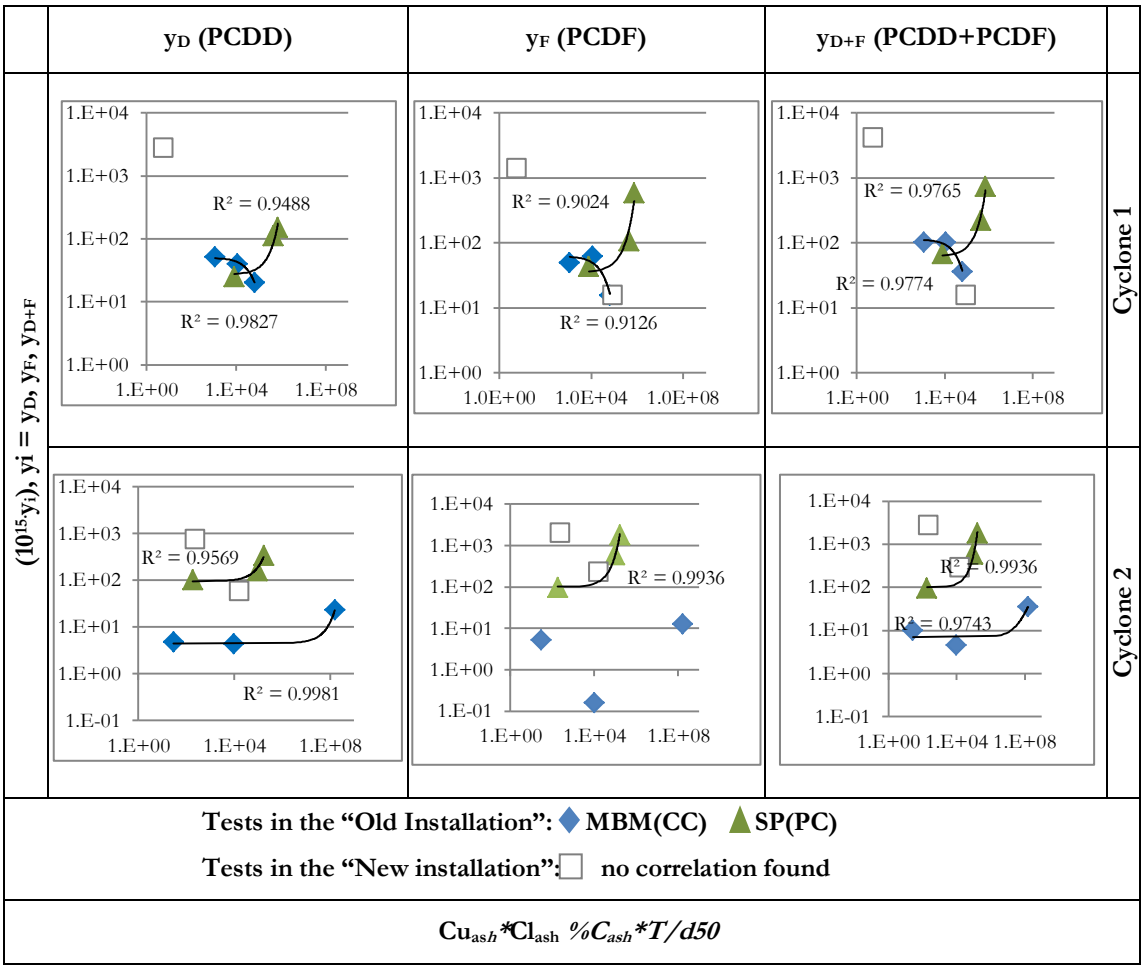

Figure 6.59 – Correlation between the different fractions of PCDD and PCDF and the factor Cu_{ash}*Cl_{ash} %C_{ash}*T/d_{50}.

As it can be seen, for each series of tests in the "Old Installation", it was generally found an acceptable correlation (R^2>0.90) within each series. The plots done separately for each parameter did not present a good correlation with the experimental results. In the case of the d50, the mean particle diameter, these results were not in accordance with the results observed by other authors (Stieglitz, 1997; Ruokojarvi *et al.*, 2001; Kurokawa *et al.*, 1998) As for the factor Cu_{ash}*Cl_{ash}/d50, proposed by Ryan and co-workers (2000), the correlation was significantly good. However, the best fit was achieved for the factor Cu_{ash}*Cl_{ash} *%C_{ash}*T/d50*, which also takes into account the cyclones' temperature as well as the high levels of unburned carbon present in the cyclones for the tests of mixtures with coal. In the SP/CC I series, no relationship was found in any situation. These results indicate, as expected, that the differences introduced in the "New installation" do not make possible the comparison between the formation of PCDD and PCDF in the cyclone ashes.

6.8 Inhibition of PCDD/F formation

In order to prevent PCDD/F emissions from the combustion of pRES and being sulphur an inhibitor to those pollutants formation, it was necessary to establish what was the SO_2 concentration above which the formation of PCDD/F were minimized.

In Figures 6.8 and 6.18, SO_2 and HCl emissions were plotted against the ratio factor [nCa/(nS+nCl)]/S-fuel (%, d.b.)*Cl-fuel (%, d.b.) that represents the relation between those pollutants release and their presence in the fuel mixtures. The goal was to find out what is the minimum SO_2 that allow the fulfilment of the ELV of PCDD/F (Figures 6.60 and 6.61).

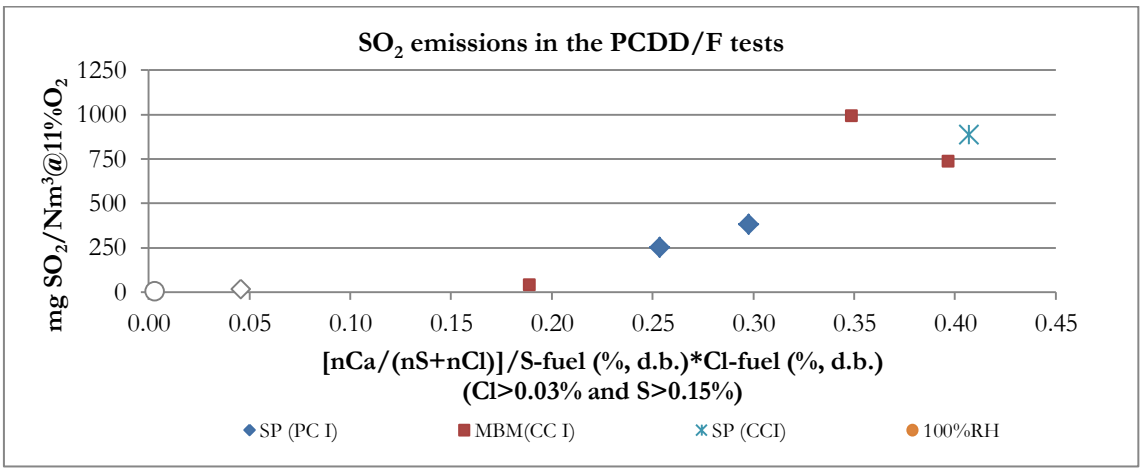

Figure 6.60 – SO_2 emissions in the PCDD/F tests *vs.* [nCa/(nS+nCl)]/S-fuel (%, d.b.)*Cl-fuel (%, d.b.).

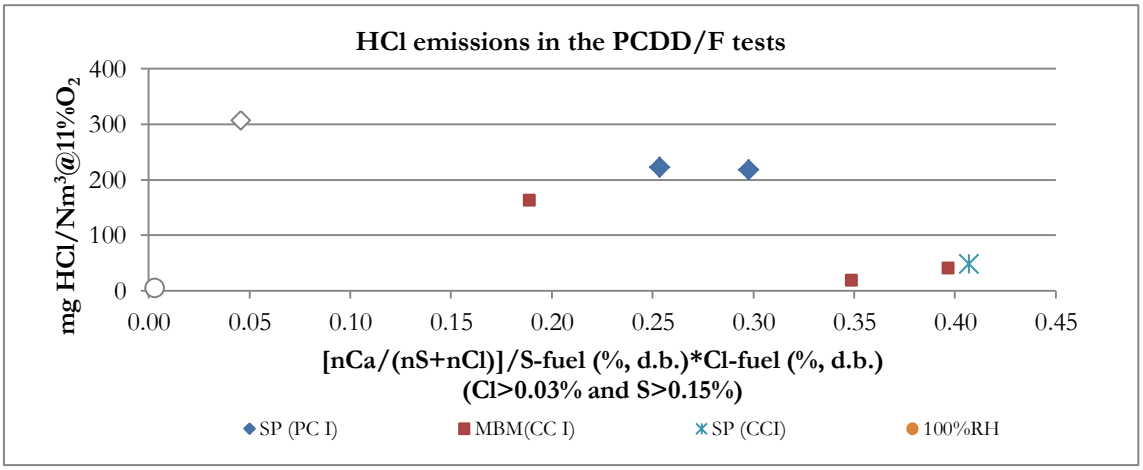

Figure 6.61 - HCl emissions in the PCDD/F tests *vs.* [nCa/(nS+nCl)]/S-fuel (%, d.b.)*Cl-fuel (%, d.b.).

In order to be comparable, PCDD/F emissions were also plotted against the same ratio factor. Figure 6.62 presents the measured emissions whereas in Figure 6.63 PCDD/F emissions are expressed as ng I-TEQ.

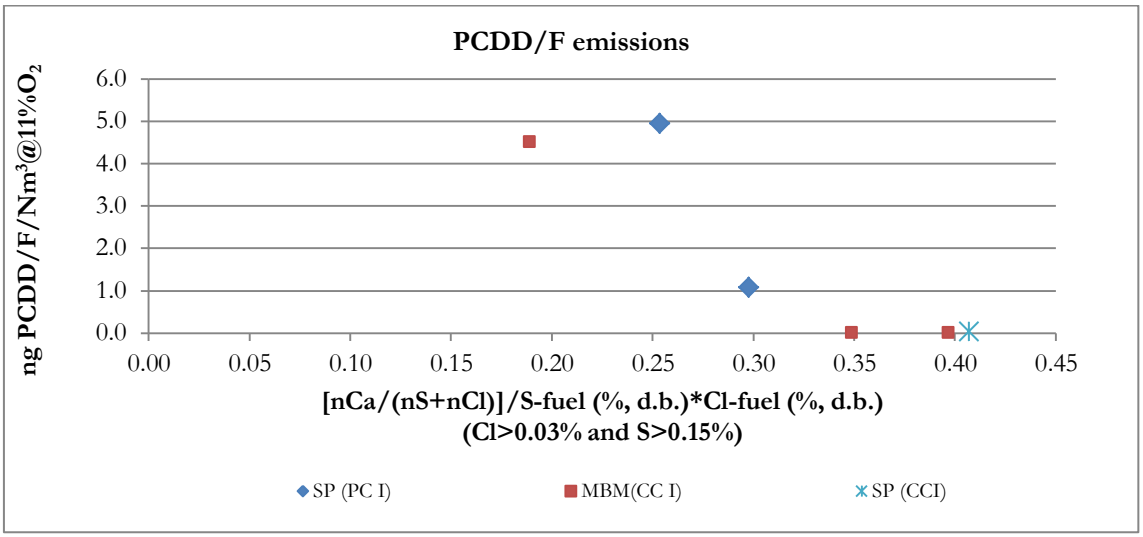

Figure 6.62 - PCDD/F emissions *vs.* [nCa/(nS+nCl)]/S-fuel (%, d.b.)*Cl-fuel (%, d.b.).

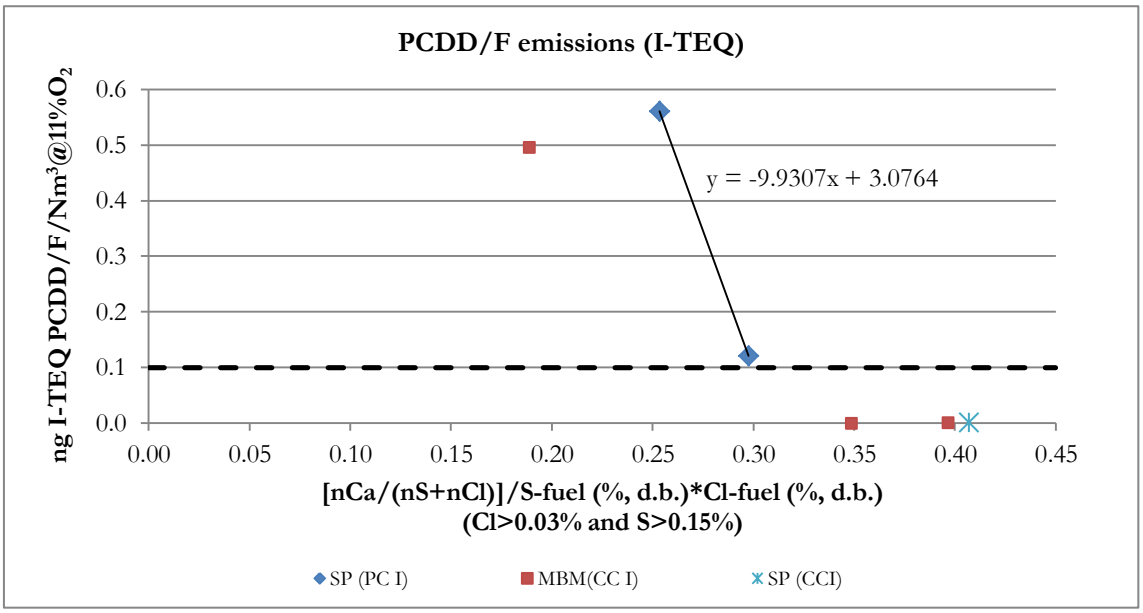

Figure 6.63 - PCDD/F emissions in ng I-TEQ*vs.* [nCa/(nS+nCl)]/S-fuel (%, d.b.)*Cl-fuel (%, d.b.)

Luckily, there was a test where PCDD/F was at the same order of the ELV. That means that the SO_2 content necessary in the stack gas that inhibits the emissions of PCDD/F is slightly higher than the 380 mg $SO_2/Nm^3@11\%O_2$ (dry) that was measured in the 100%PC test. Assuming a safety margin of 10%, *i.e.* maximum of 0.09 ng I-TEQ/$Nm^3@11\%O_2$ (dry), it is plausible to consider that 450 mg $SO_2/Nm^3@11\%O_2$ (dry) is the minimum SO_2 concentration.

As a conclusion, it is possible to state that:

> It is possible to achieve PCDD/F emissions lower than the ELV in a bubbling fluidized bed combustor for SO_2 in the stack gases higher than 450 mg $SO_2/Nm^3@11\%O_2$ (dry).

Since it is possible to estimate the SO_2 emissions of a specific mixture as a function of its composition, *i.e.* the sulphur, chlorine and calcium contents, it is possible to combine different fuels in a mixture so that PCDD/F emissions are lower than the ELV, based on the following criteria that must be met simultaneously:

Conditions to achieve PCDD/F emissions < 0.1 ng I-TEQ/$Nm^3@11\%O_2$ (dry)	
Fuel composition	S>0.15% (d.b.) and Cl>0.03% (d.b.)
Relative ratio	[nCa/(nS+nCl)]/(%Cl-Fuel,db)/(%S-Fuel,db) > 4.84

From this result is possible to conclude that the combustion of fuels from biomass origin, with sulphur content below 0.15% (d.b.), will lead to the exceeding of PCDD/F emissions ELV and the need to use a cleaning gas system.

Instead, a primary measure should be applied in preventing these toxic pollutants formation. The use of the technology of co-combustion of these biomass origin materials with other fuels with high S content in fluidized bed will allow the desired combination. Furthermore, in the case of fuels with low calcium content, the addition of limestone is an easy and cheap way of guarantying the adequate [nCa/(nS+nCl)]/(%Cl-Fuel,d.b.)/(%S-Fuel,d.b.) ratio value.

6.9 Percursor vs. *de novo* mechanism formation

As described previously, the PCDF/PCDD ratio may indicate the main formation mechanism, *i.e.* which is the predominant formation mechanism. According to Huang & Buekens (1995) a *de novo* synthesis is associated with PCDF/PCDD ratios >1 while the precursors mechanism is associated with ratios of PCDF/PCDD <1. Luijk and co-workers (1993) found PCDF/PCDD ratios of 10, also associated with the *de novo* mechanism. Hunsinger and co-workers (2002) also identifyied that a PCDF/PCDD ratio>1 was associated with the *de novo* mechanism.

As a qualitative approach, PCDF/PCDD ratios might indicate which mechanism is subjacent to the PCDD/F formation obtained in the tests with MBM/Cerejon coal and Straw/Polish coal. Tables 6.27 present the PCDF/PCDD ratios in the cyclones and stack gas (expressed as ngPCDF/ngPCDD).

As it can be seen in Table 6.28, there were no PCDD formed when mistures with 0% MBM and the 15% MBM/Cerejon were tested.

The cyclone ashes ratios differ between the two cases studied (MBM/Cerejon and straw/Polish coal): For the MBM tests, a PCDF/PCDD ratio of ≈ 1 for the cyclone ashes, indicate the predominance for the *de novo* mechanism. In the case of Straw/Polish coal tests, the behaviour is not so clear. It was observed a higher PCDF ratio for both cyclone ashes when using 100% Polish Coal. In the case of mixtures, it seems that both mechanisms are acting simultaneously. The study on the ashes obtained from the 1st cyclone, for the mixture 15% Straw/Polish Coal, indicate *de novo* mechanism as the main formation pathway, while in the 2nd cyclone the formation from precursors seems the main formation pathway. For the cyclone ashes of the 100% Straw test the conclusions are inverse, *i.e.* precursors mechanism for the 1st cyclone ashes and *de novo* mechanism for the 2nd cyclone ashes.

Table 6.28 – Mass ratio PCDF/PCDD in the cyclones and stack gas (ng_{PCDF}/ng_{PCDD}).

Ratio F/D		**Test Runs (old installation)**		
		100% Coal	**85% Coal**	**0% Coal**
MBM/Colombian Coal	1st Cyclone	1.1	0.5	0.8
	2nd Cyclone	0.025	0.5	0.9
	Stack gas emissions	>>1	>>1	4.3
Straw/Polish Coal	1st Cyclone	3.7	0.7	1.4
	2nd Cyclone	4.7	3.0	0.8
	Stack gas emissions	3.2	1.9	5.6
Straw/Colombian Coal	1st Cyclone	1.1	>>1 (1)	1.4
	2nd Cyclone	0.025	3.6 (1)	0.8
	Stack gas emissions	>>1	1.4 (1)	5.6
Rice Husk	1st Cyclone	-	-	0.5 (1)
	2nd Cyclone	-	-	2.4 (1)
	Stack gas emissions	-	-	1.9 (1)

(1) – new installation

The formation pathway of PCDD/F of the 15%Straw/Cerejon test, is clearly the *de novo* mechanism, more significant in the cyclone ashes than in stack gas emissions.

Another test made in the new reactor was the 100% rice husk: the 1st cyclone ash presents F/D ratio<1, thus indicating the precursor's mechanism, wheras the 2nd cyclone ash denotes the *de novo* mechanism.

7. Kinetic mechanism for the formation and destruction of PCDD/F

7.1 Model basic assumptions

The objective of this chapter is to present the FB-OWL model, developed within the scope of this thesis, with the aim of identifying the mechanism associated with the PCDD/F formation in a pilot-fluidised bed combustor.

The development of the FB-OWL[7] model was carried out by adapting to the experimental conditions the model proposed by Duo & Leclerc (2007) to simulate the PCDD/F emissions from salt-laden hog fuel combustion boiler. Table 7.1 summarizes the main differences between the model obtained in this work and the one found in the literature reported above. The assumptions made for development of the FB-OWL model are the following:

i) Dioxins and furans formation occur downstream, at lower temperatures. This is based on the observation that PCDD/F contained in the fuel were completely destroyed at high temperatures in the fluidized bed combustor; the residence time of the combustion gases in the freeboard at temperatures higher than 600ºC is higher than 3.1 seconds for all the test runs (Table 6.1).

[7] In Portuguese, "OWL" is *Coruja* from which cames the surname *Crujeira*.

ii) PCDD/F precursors were formed in combustion from chlorine and fuel organic compounds (OC). These compounds were not measured; the total amount of precursors is referred to as PREC:

$$OC + Cl \rightarrow PREC \quad (7.1)$$

iii) Products of Incomplete Combustion (PIC) are formed in combustion processes from hydrocarbons (HC) and are not destroyed in the downstream flue gas:

$$HC \rightarrow PIC \quad (7.2)$$

iv) Precursor reactions lead primarily to PCDD and *de novo* reactions to PCDF. PCDD/F's are formed in the flue gas via precursor (7.3) and *de novo* (7.4) reactions:

Precursor: $$PREC + M \rightarrow PCDD+PCDF \quad (7.3)$$

de novo: $$PIC + Cl + O_2 + M \rightarrow PCDF+PCDD \quad (7.4)$$

where M represents active catalysts (solid) and Cl could have as sources chlorine NaCl(g), HCl, Cl_2 and/or $Cl^{\bullet}$. It is likely that the most reactive chlorine species is in the form of $Cl^{\bullet}$ for reaction (7.1) and Cl_2 for reaction (7.4).

v) Both reactions take place in a plug flow reactor. Since the gas and solids residence times in the effective zone are short (1.7-2.6 seconds for Cyclone 1 and 0.4-0.6 seconds for Cyclone 2, as shown in Table 6.2), the decomposition of PCDD/F is not considered.

vi) The reactions are assumed to be first order relative to the reactants in the above reactions.

vii) Only the formation of the 10 toxic PCDF and 7 toxic PCDD isomers is considered.

Table 7.1 –Comparison between FB-OWL and Duo models.

FB-OWL model	**Duo & Leclerc (2007) model**
Fluidised bed	Combustion boiler
Coal, biomass and non-toxic wastes	Salt-laden hog fuel
PCDD/F contained in the fuel were completely destroyed at high temperatures	
PCDD/F precursors were formed in combustion from chlorine and fuel organic compounds	
PIC are formed from hydrocarbons (HC)	PAH are formed from hydrocarbons (HC)
PCDDs are formed via precursor reactions PCDFs are formed via *de novo* reactions	PCDD/Fs are formed via precursor and *de novo* reactions
The reaction takes place in a plug flow reactor	
The reactions are assumed to be first order relative to the reactants	
Only 10 toxic PCDF + 7 toxic PCDD is considered	--
Variable formation of PCDD/F from precursors	Constant formation of PCDD/F from precursors
Non-excess catalyst (Cu)	Excess catalyst (Cu)
Specific area for catalytic reactions	--
Excess SO_2	Absence of excess SO_2
Presence of an effective absorbent for HCl (Ca)	Absence of an effective absorbent for HCl

7.2 Kinetic formula

$PCDD/F_{toxic}$ represents the total PCDD/F formed, and then the $PCDD/F_{toxic}$ formation rate, in the downstream flue gas, may be expressed as:

$$d[PCDD/F_{toxic}]/dt = k_{prec}[PREC][M] + k_{de\ novo}[PIC][Cl_2][M] \quad (7.5)$$

In the above expression it is assumed that oxygen content was in excess (5.5-10.1 $\%O_2$ in the considered runs).

The presence of the catalyst (copper) and the number of active sites at the ash surface are related by the following correlation:

$$[M] = PM_{s\_a}.\alpha_{Cu}M_{Cu} \quad (7.6)$$

where PM_{s_a} is the specific area of the cyclones' particulate matter and α_{Cu} is the fraction of the copper mass M_{Cu} (Table 6.22) available for the reaction (4.2).

Both [PIC] and [PREC] are functions of combustion conditions and symbolically expressed as follows:

$$[PREC] = f_1(T_c, t_c)[Cl^{\bullet}] \quad (7.7)$$

$$[PIC] = f_2(T_c, t_c)[CO] \quad (7.8)$$

where T_c and t_c represent combustion temperature and time, respectively. Inserting Eq. (7.7) into Eq. (7.5) leads to the following equation:

$$d[PCDD/F_{toxic}]/dt = k_{prec}[f_1(T_c, t_c)][Cl^{\bullet}].PM_{s\_a}.\alpha_{Cu}M_{Cu} + k_{de\ novo}[PIC][Cl_2].PM_{s\_a}.\alpha_{Cu}M_{Cu} \quad (7.9)$$

Replacing Eq. (7.8) in Eq. (7.9), the PCDD/F_{toxic} formation rate is obtained:

$$d[PCDD/F_{toxic}]/dt = (k_{prec}[f_1(T_c, t_c)].[Cl^{\bullet}].\ PM_{s\_a}.\alpha_{Cu}M_{Cu} + \\ + k_{de\ novo}[f_2(T_c, t_c)].[CO].[Cl_2]\ ).PM_{s\_a}.\alpha_{Cu}M_{Cu} \quad (7.10)$$

7.3 PCDD/F formation model

Once formed in the flue gas, the PCDD/F would either be removed together with fly ash or emitted from the stack.

The total PCDD/F_{toxic} formation rate may be determined by combining the ash and stack PCDD/F_{toxic} flow rates (*e.g.* in ng/h). The amount emitted depends not only on the amount formed but also on the removal efficiency of the dedusting equipment.

In the absence of added sorbents, such as activated carbon, PCDD/F removal is mainly by condensation and adsorption onto ash particles and then separation of the particles from the flue gas in the cyclones.

A kinetic model for stack PCDD/F_{toxic} emissions may be developed from the formation and emission concept:

$$[PCDD/F_{toxic}]_{stack} = X.\{[PCDD/F_{toxic}]_{prec} + [PCDD/F_{toxic}]_{de\ novo}\} \quad (7.11)$$

where [PCDD/F_{toxic}] represents the concentration of PCDD/F in flue gas (ng/m^3), the subscript "de novo" indicates formation by *de novo* synthesis, and the subscript "prec" indicates formation from precursors. The parameter X represents the fraction of formed PCDD/F emitted by the stack. The fraction being removed through the ashes in the cyclones is, therefore, (1 –X), where X=X1+X2, *i.e.* the fractions collected in the 1st and 2nd cyclones, respectively.

The sum of $[PCDD/F_{toxic}]_{prec}$ and $[PCDD/F_{toxic}]_{de\ novo}$ gives the total formation and may be obtained by integrating Eq. (7.10). Since the reactions took place in the cyclones, a non-isothermal zone, the integration of Eq. (7.10) requires the knowledge of the relationship between the reaction time and temperature.

In order to predict the equilibrium composition of the several species of the equations (4.4) to (4.7), the equilibrium constants, represented by K_p, were calculated using the thermodynamic data in Table 7.2 through the following equations:

$$\Delta G^{o}_{f} = \Delta H^{o}_{f} - T\Delta S^{o}_{f} \quad (7.12)$$

$$K_p = \exp(-\Delta G^{o}_{f} / RT) \quad (7.13)$$

where: ΔG^{o}_{f} is the standard Gibbs free energy for the reaction;

ΔH^{o}_{f} is the standard reaction enthalpy;

ΔS^{o}_{f} is the standard entropy of the reaction;

T is the absolute temperature; and,

R is the ideal gas constant.

Table 7.2 – Thermodynamic data (Atkins, 1991).

@298.15K	ΔH^{o}_{f} (kJ/mol)	ΔS^{o}_{f} (J/K/mol)
$Cl_{2\,(g)}$	0	223.07
$HCl_{\,(g)}$	-92.31	186.91
$H_2O_{\,(g)}$	-241.82	188.83
$O_{2\,(g)}$	0	205.138
$SO_{2\,(g)}$	-296.83	248.22
$SO_{3\,(g)}$	-395.72	256.76

The standard reaction enthalpy and entropy for reactions (4.2) to (4.5) are presented in Table 7.3.

Table 7.3 – Thermodynamic equilibrium constants for reactions (4.2) to (4.5).

	Equation	ΔH^{o}_{f} (J/mol)	ΔS^{o}_{f} (J/K/mol)
(4.2)	$2HCl + \frac{1}{2}O_2 \rightleftarrows Cl_2 + H_2O$	-5.72E+04	-6.45E+01
(4.3)	$Cl_2 + SO_2 + H_2O \rightleftarrows SO_3 + 2HCl$	-4.17E+04	-2.95E+01
(4.4)	$SO_2 + \frac{1}{2}O_2 \rightleftarrows SO_3$	-9.89E+04	-9.40E+01
(4.5)	$Cl_2 + 2SO_2 + H_2O + \frac{1}{2}O_2 \rightleftarrows 2SO_3 + 2HCl$	-1.41E+05	-1.24E+02

The thermodynamic equilibrium constants of the reactions (4.2) to (4.5) are presented in Table 7.4.

Table 7.4 – Calculated thermodynamic equilibrium constants for reactions (4.2) to (4.5).

T (ºC)	Equilibrium constant for reactions			
	(4.2)	(4.3)	(4.4)	(4.5)
0	3.7E+07	2.7E+06	1.0E+14	2.7E+20
25	4.5E+06	5.8E+05	2.6E+12	1.5E+18
100	4.4E+04	2.0E+04	8.5E+08	1.7E+13
200	8.8E+06	1.1E+03	1.0E+06	1.2E+09
300	7.0E+01	1.8E+02	1.3E+04	2.3E+06
400	1.2E+01	4.9E+01	5.8E+02	2.8E+04
500	3.1E+00	1.9E+01	5.9E+01	1.1E+03
600	1.1E-00	8.9E+00	1.0E+01	9.0E+01
700	5.0E-01	5.0E+00	2.5E+00	1.2E+01
800	2.6E-01	3.1E+00	8.0E-01	2.4E+00
900	1.5E-01	2.1E+00	3.1E-01	6.4E-01
1000	9.5E-02	1.5E+00	1.4E-01	2.1E-01
1100	6.4E-02	1.1E+00	7.1E-02	7.8E-02
1200	4.6E-02	8.6E-01	3.9E-02	3.4E-02
1300	3.4E-02	6.9E-01	2.4E-02	1.6E-02

Thermodynamic data shows that the Deacon Reaction - reaction (4.2) - is favoured over the range of temperatures from 273 to 1273K and is exothermic at 25ºC.

An increase in temperature will cause the equilibrium to move towards the reactants, which will lower the conversion of HCl to Cl_2. Before the equilibrium is reached, however, the reaction is predominantly kinetic-controlled.

The concentration of Cl_2 in the flue gas depends on the thermodynamics and kinetics of reaction (4.2), which is a gas phase reaction at high temperatures, leading to a low equilibrium Cl_2 concentration, as illustrated in Fig. 7.1. The darker area in Fig. 7.1 corresponds to the temperature range for maximum PCDD and PCDF reaction rates.

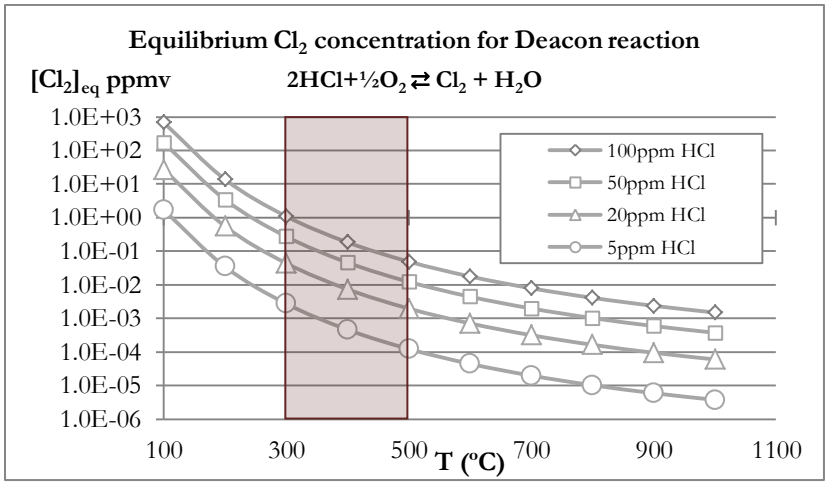

Figure 7.1 – Equilibrium gas concentrations calculated for the reaction (4.2), at 20% H_2O and 10% O_2.

At low temperatures, it is known as the Deacon process, a heterogeneous catalytic reaction. For a given HCl concentration, the equilibrium Cl_2 concentration could be four or five orders of magnitude higher at lower temperatures than at higher temperatures. Figures 7.2 and 7.3 present

the different equilibrium concentration of Cl_2 for each test conditions, as described before in chapter 6.

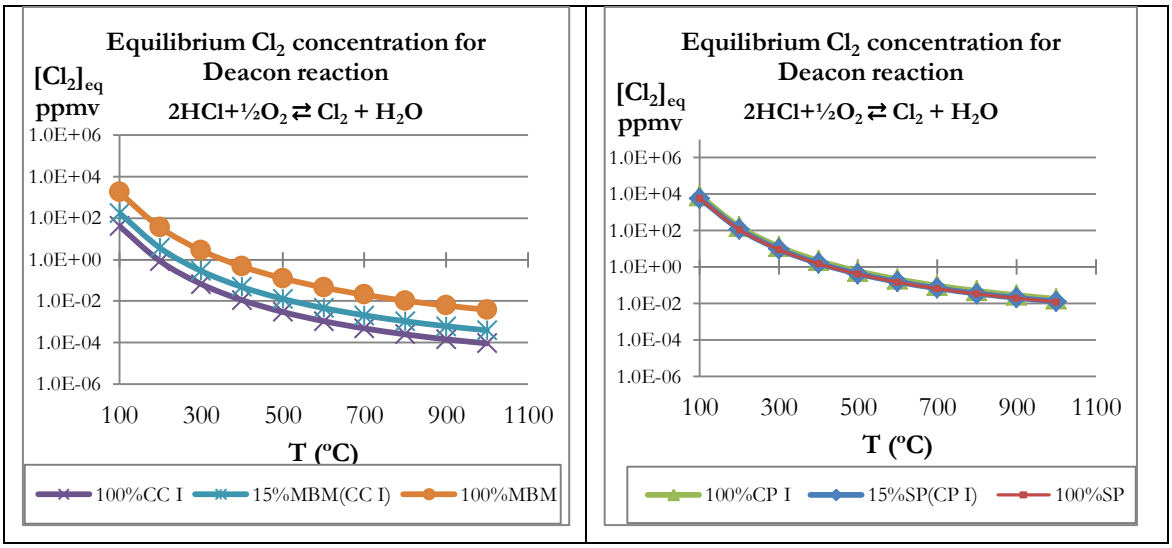

Figure 7.2 – Equilibrium gas concentrations calculated for the reaction (4.2) for the MBM/CC and SP/PC experimental test conditions.

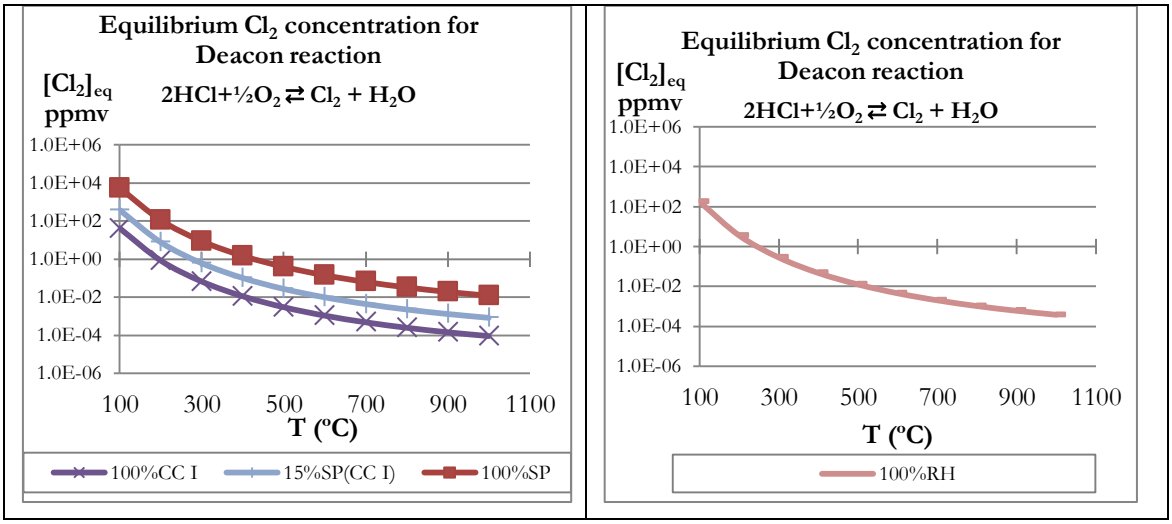

Figure 7.3 – Equilibrium gas concentrations calculated for the reaction (4.2) for the SP/CC and Rice Husk experimental test conditions.

In the presence of SO_2, Cl_2 may be reduced by oxidation of SO_2 according to the reaction (4.3), which is thermodynamically very much favoured. Furthermore, SO_2 may also be oxidized by O_2 through reaction (4.4).

At atmospheric pressure and fluidised bed typical operating temperatures, the concentration of SO_3 not very significant; *e.g.* at 850ºC, and in the presence of 5.5% O_2, the equilibrium concentration of SO_3 calculated from the data presented in Table 7.3 is 10% of SO_2 concentration being *ca.* 10% of SO_2 (Figure 7.4). This is in accordance with Tarelho (2001).

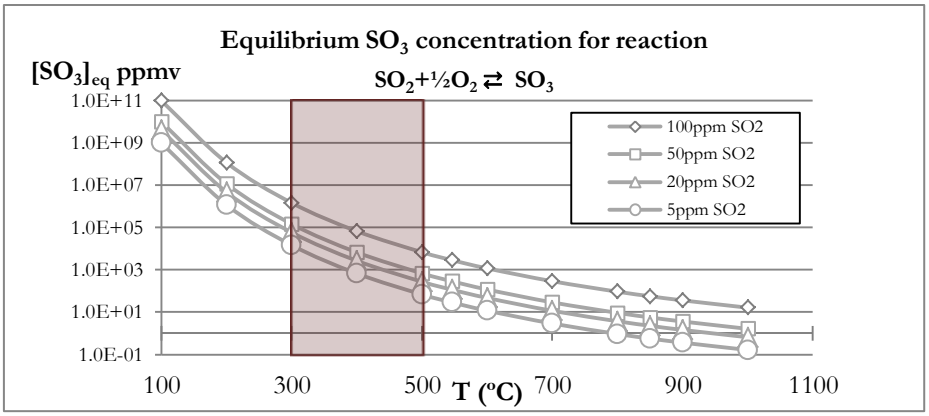

Figure 7.4 – Equilibrium gas concentrations calculated for the reaction (4.4), at 5.5% O_2.

However, at the temperatures of PCDD/F maximum formation rates, the ratio of $[SO_3]/[SO_2]$ may reach 3.000-fold.

Since O_2 is present in excess in combustion processes, reaction (4.6) should be considered to be competing with reaction (4.3) for SO_2.

Equation (4.5) is the combination of reactions (4.3) and (4.4). As shown in Fig. 7.5, the thermodynamics of the Eq. (4.5) remain highly favoured at temperatures below 600ºC. As in Figure 7.4, the darker area corresponds to the temperature range for maximum PCDD and PCDF reaction rates.

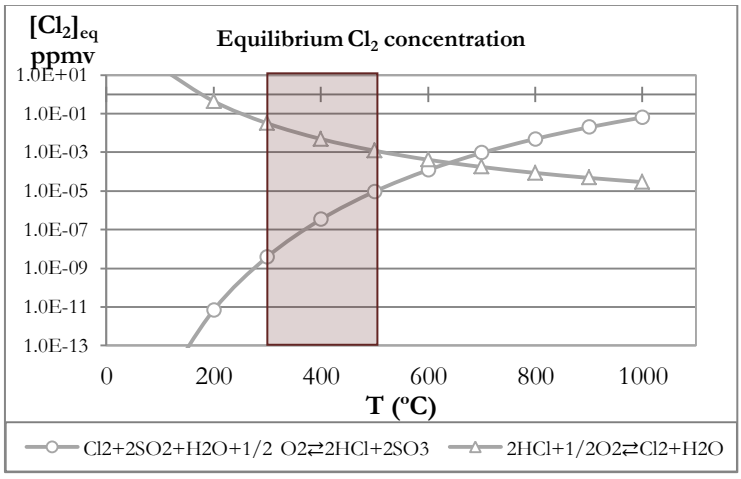

Figure 7.5 – Equilibrium Cl_2 concentration calculated for the sulphur reaction and the Deacon reaction at 20% H_2O, 10% O_2, with 20 ppm HCl, and with $P_{SO_2}=10.P_{SO_3}$.

The real Cl_2 concentration depends on the determining step between reactions (4.3) and (4.2). The rate of the heterogeneous reaction (4.2) depends on the levels of effective catalysts present in the process.

The concentration of Cl_2 is determined by the equilibrium of reaction (4.5), in the presence of excess SO_2:

$$[Cl_2] = \frac{1}{K_c}.\frac{[HCl]^2[SO_3/SO_2]^2}{[H_2O].[O_2]^{0.5}} = \frac{(RT)^{-0.5}}{K_p}.\frac{[HCl]^2[SO_3/SO_2]^2}{[H_2O].[O_2]^{0.5}} \quad (7.14)$$

where K_c is the equilibrium constant in terms of concentration, which is related to K_p by

$$K_c = (RT)^{-\Delta n}.K_p \quad (7.15)$$

and Δn is the change in the number of gas molecules between products and reactants of reaction (4.5); K_p is given by Eq. (7.13).

For a given stable operation, the oxygen and moisture contents do not change much in the downstream flue gas. In the absence of significant quantities of an effective absorbent for HCl, which is the case for all runned tests except for de 100%MBM (Table 6.20), the concentration of Cl_2 would only depend on temperature.

Therefore:

$$Q = \frac{[HCl]^2[SO_3/SO_2]^2}{[H_2O].[O_2]^{0.5}} \quad (7.16)$$

Q may be treated as a constant in the precursor and *de novo* reaction zones for a specific test and may be replaced in Eq. (7.14):

$$[Cl_2] = Q.\ \frac{(RT)^{-0.5}}{\exp(-\Delta G_{4.5}/RT)} \quad (7.17)$$

The Arrhenius equation for the rate constants of reactions (7.3) and (7.4) may be expressed as follows:

Precursor: $$k_{prec} = A_{prec}.\exp(-E_{prec}/RT) \quad (7.18)$$

de novo: $$k_{de\ novo} = A_{de\ novo}.\exp(-E_{de\ novo}/RT) \quad (7.19)$$

where E_{prec} and $E_{de\ novo}$ represents the activation energy for both reactions and $A_{prec}/A_{de\ novo}$ and $E_{prec}/E_{de\ novo}$ are independent of temperature. Replacing Eqs. 7.17 and 7.18 in the precursor component of Eq. (7.10) the following equation is obtained:

$$d[PCDD/F_{toxic}]_{prec} = A_{prec}.Q.(RT)^{-0.5}.PM_{s\_a}.\alpha_{Cu}M_{Cu}.\ exp\left(\frac{E_{prec}}{\Delta G_{4.5}}\right)dt \quad (7.20)$$

The concentration of CO is mainly determined by upstream combustion conditions and may be considered constant in the *de novo* zone. Replacing Eqs. 7.17 and 7.19 in the *de novo* component of Eq. (7.10) results as follows:

$$d[PCDD/F_{toxic}]_{dc\ novo} = A_{de\ novo} .[CO].Q.(RT)^{-0.5}. PM_{s\_a}.\alpha_{Cu}M_{Cu}. exp\left(\frac{E_{de\ novo}}{\Delta G_{4.5}}\right)dt \quad (7.21)$$

The magnitude of E_{prec} and $E_{de\ novo}$ are not known and the combined reaction rates are temperature independent. Integrating Eqs. 7.10 results in:

$$\int d[PCDD/F_{toxic}] = A_{prec} .Q.(RT)^{-0.5}. PM_{s\_a}.\alpha_{Cu}M_{Cu}. \int exp\left(\frac{E_{prec}}{\Delta G_{4.5}}\right)dt +$$
$$+ A_{de\ novo} .[CO].Q.(RT)^{-0.5}. PM_{s\_a}.\alpha_{Cu}M_{Cu}. \int exp\left(\frac{E_{de\ novo}}{\Delta G_{4.5}}\right)dt \quad (7.22)$$

Considering $\int dt=\tau$, being τ the residence time of flue gas in the equipment in which the reactions occur, and that $\int d[PCDD/F_{toxic}] = \Delta[PCDD/F_{toxic}] = PCDD/F_{toxic}$, since all the PCDD/F present in the fuels were destroyed in the combustion chamber, Eq. 7.22 may be simplified as:

$$[PCDD/F_{toxic}] = A_{prec} .Q.(RT)^{-0.5}. PM_{s\_a}.\alpha_{Cu}M_{Cu}.\exp\left(\frac{E_{prec}}{\Delta G_{4.5}}\right).\tau +$$
$$+ A_{de\ novo} .[CO].Q.(RT)^{-0.5}. PM_{s\_a}.\alpha_{Cu}M_{Cu}.\exp\left(\frac{E_{de\ novo}}{\Delta G_{4.5}}\right).\tau \quad (7.23)$$

Furthermore, let $k_{prec'}$ and $k_{de\ novo'}$ be the apparent reaction rate constants:

Precursor: $$k_{prec'} = A_{prec}.\exp\left(\frac{E_{prec}}{\Delta G_{4.5}}\right) \quad (7.24)$$

de novo: $$k_{de\ novo'} = A_{de\ novo}.\exp\left(\frac{E_{de\ novo}}{\Delta G_{4.5}}\right) \quad (7.25)$$

and T_m is the average temperature at which the reactions occur. Then Eqs. (7.20) and (7.21) may be simplified into

Precursor:

$$[PCDD/F_{toxic}]_{prec} = k_{prec'}.\tau.(RT_m)^{-0.5}. PM_{s\_a}.\alpha_{Cu}M_{Cu}.[SO_3/SO_2]^2.[HCl]^2/[H_2O]/[O_2]^{0.5} \quad (7.26)$$

de novo:

$$[PCDD/F_{toxic}]_{de\ novo} = k_{de\ novo'}.\tau.[CO].(RT_m)^{-0.5}. PM_{s\_a}.\alpha_{Cu}M_{Cu}.[SO_3/SO_2]^2.[HCl]^2/[H_2O]/[O_2]^{0.5} \quad (7.27)$$

where the ratio $[SO_3/SO_2]$ is given by the following expression:

$$[SO_3/SO_2] = \exp(\ln K_{c(4.4)@298.15} - \Delta H_{(4.4)@298.15}/R*(1/T_m - 1/298.15))*[O_2]^{0.5} \quad (7.28)$$

Equations (7.26) and (7.27) may be simplified as

Precursor:

$$[PCDD/F_{toxic}]_{prec} = k_{prec'}.\Psi \quad (7.29)$$

de novo:

$$[PCDD/F_{toxic}]_{de\ novo} = k_{de\ novo'}.[CO].\Psi \quad (7.30)$$

where the factor Ψ is:

$$\Psi = \tau.(RT_m)^{-0.5}.\ PM_{s\_a}.\alpha_{Cu}M_{Cu}.[SO_3/SO_2]^2.[HCl]^2/[H_2O]/[O_2]^{0.5} \quad (7.31)$$

and the variables in equation (7.31) refer to measured data obtained during the combustion tests.

7.4 FB-OWL model for PCDD/F stack emission

The contribution due to gas phase emissions is determined by the volumetric flow rate of the flue gas and the PCDD/Fs vapour partial pressure:

$$[PCDD/F_{toxic\ G}]_{stack} = P_{PCDD/Ftoxic}.Qv_{stack} \quad (7.32)$$

where $P_{PCDD/Ftoxic}$ represents the partial pressure of PCDD/Fs in the flue gas and Qv_{stack} is the flue gas flow rate.

The PCDD/F partial pressure may be estimated assuming that equilibrium is established in the cyclones between the vapourized PCDD/Fs and the PCDD/Fs condensed or adsorbed on the solid particles due to the long retention times (six hours). The equilibrium vapour pressure increases with the cyclones' temperature according to the following thermodynamic equation:

$$P_{PCDD/Ftoxic} = \exp(-\Delta G^o_{PCDD/Ftoxic}/RT_{Cyclone}) \quad (7.33)$$

where $\Delta G^{o}_{PCDD/Ftoxic}$ is the free energy change at the standard state for desorption of PCDD/Fs from ash particles and $T_{Cyclone}$ is the 2nd cyclone's outlet temperature. Replacing Eq. (7.33) in (7.32) results in

$$\ln([PCDD/F_{toxic\ G}]_{stack}/Qv_{stack}) = (-\Delta G^{o}_{PCDD/Ftoxic}/RT_{Cyclone}) \quad (7.34)$$

Eq. 7.34 is the simplified equation derived in this work to determine the amount of PCDD/F emitted through the stack.

7.5 Model validation, data correlation and discussion

7.5.1 PCDD and PCDF collected in the cyclones

The correlation of the test results with Eqs. (7.29) and (7.30) is shown in Figures 7.6 (Cyclone 1) and 7.7 (Cyclone 2). Plotting the results obtained in the two pilot installations together, one can observe that scattering is significant, meaning that combustion is influenced by the equipment characteristics.

Old and New installations data	Old installation data
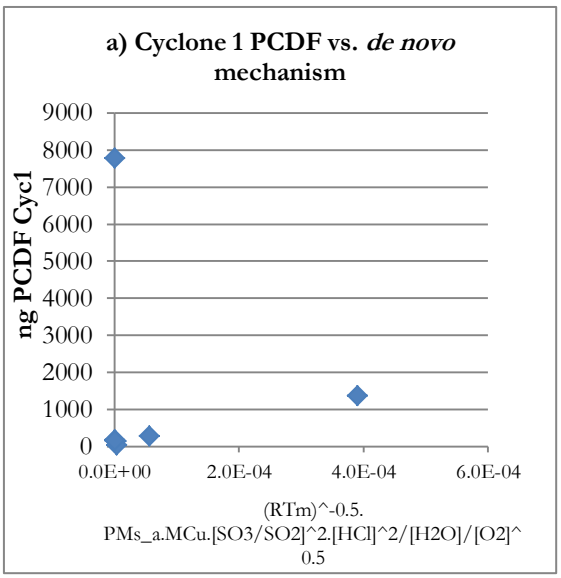	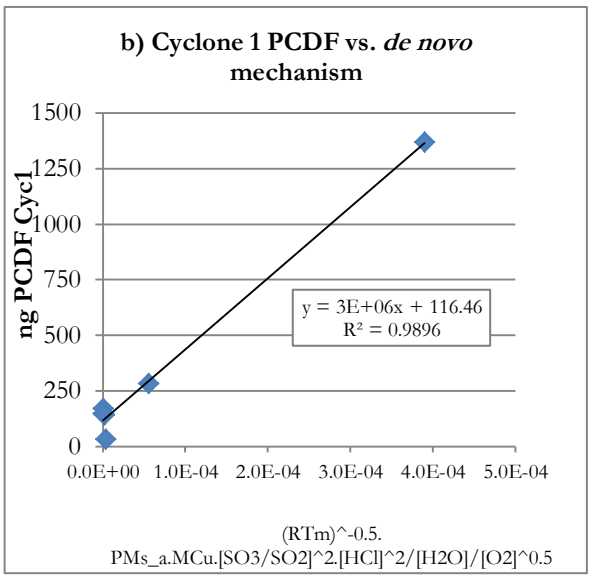

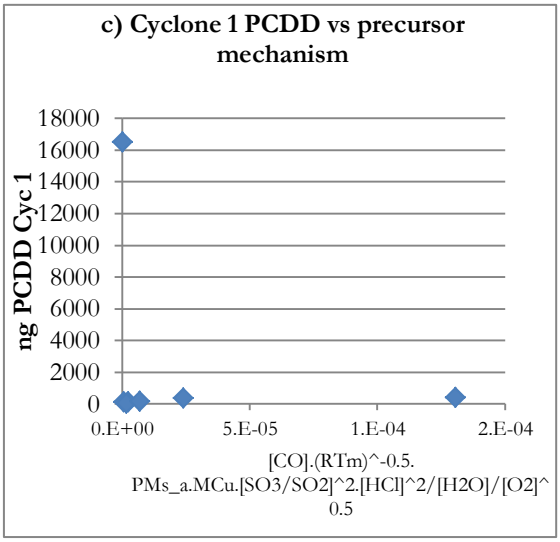

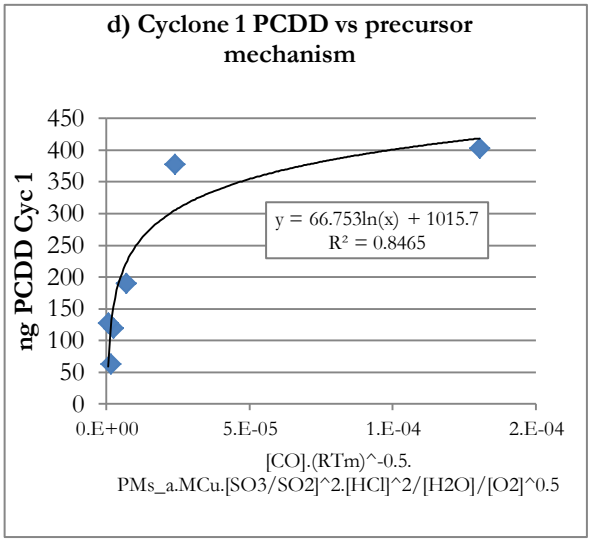

Figure 7.6 – Correlation between FB-OWL model for precursor and *de novo* mechanisms and experimental PCDD/F data obtained in Cyclone 1.

Hence, the data was analysed first in the old installation as more tests were run (figures b) and d) in Figs. 7.6 and 7.7).

Old and New installations data	Old installation data

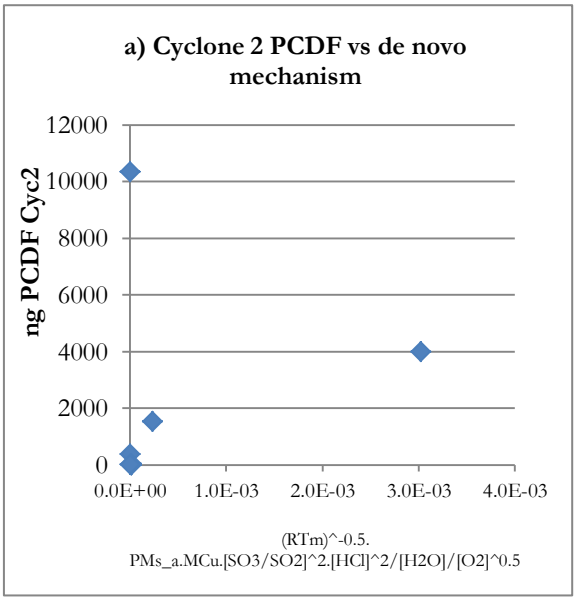

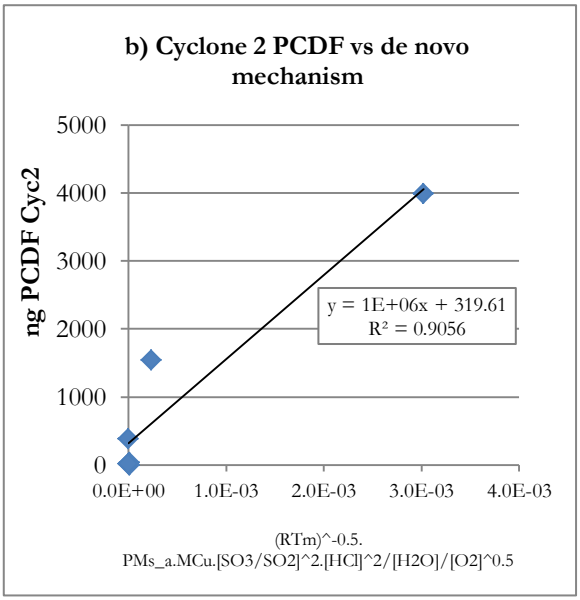

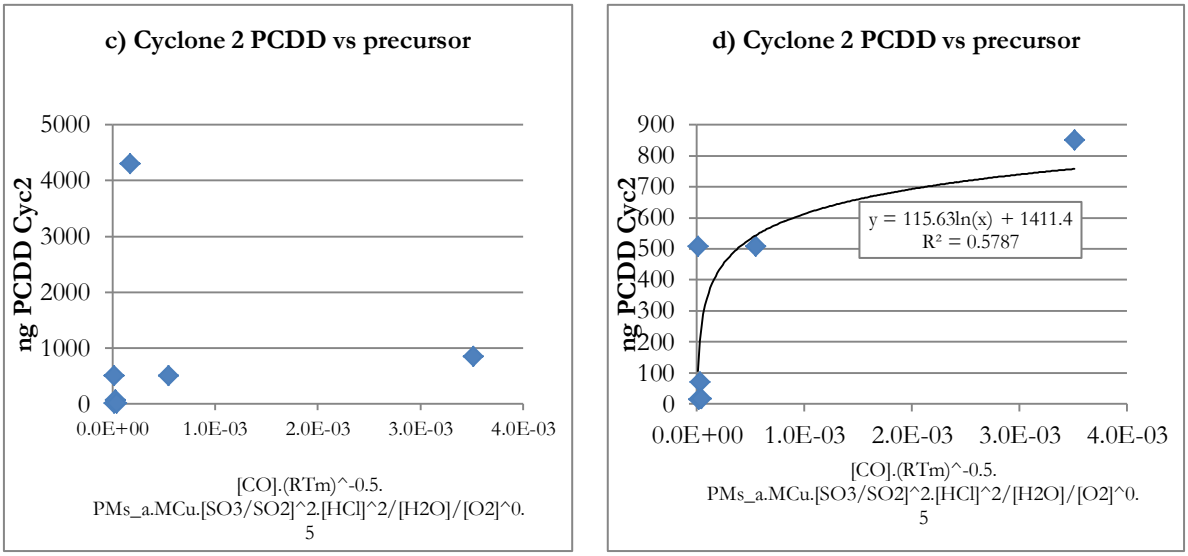

Figure 7.7 – Correlation between FB-OWL model for precursor and *de novo* mechanisms and experimental PCDD/F data obtained in Cyclone 2.

Given the nature of the tests on the pilot-scale fluidised bed and all the simplifications made in the model development, the correlation obtained for the PCDF collected in both cyclones can be accepted as being fairly good. Furthermore, it is possible to conclude that each installation has a characteristic rate constant.

However, for the PCDD collected in both cyclones, the FB-OWL model does not fit with the measured data, thus indicating that both precursor and *de novo* mechanisms are associated with the formation of these compounds.

7.5.2 PCDD and PCDF emitted by the stack

Figure 7.8 presents the correlation of the results of the stack gas emissions through Eq. (7.3), considering the tests of the Old installation (R^2=0.704).

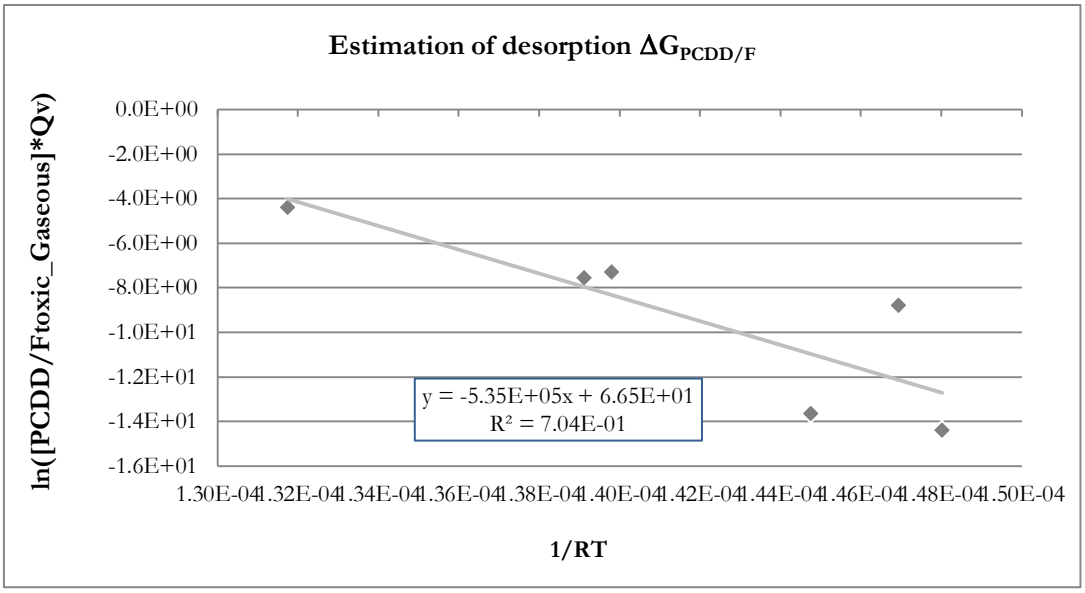

Figure 7.8 – Estimation of PCDD/F desorption free Gibbs energy from the experimental data.

The desorption free Gibbs energy, $\Delta G^{o}_{PCDD/Ftoxic}$, obtained is -5.35E^{+02} J/kmol, which is of the magnitude expected.

8. Conclusions and Future Work

8.1 Conclusions

Co-combustion of coals with biomass and wastes could contribute to reduce fossil CO_2 emissions, as well as CO levels and obtain less reactive unburned char particles to improve fuel conversion efficiencies.

In the studies developed within the scope of the present work, it was observed that most of the combustion of pRES occurred in the gas phase due to the release of high levels of volatiles, which constitute about 70% of the mass of the fuel.

The emissions of SO_2 may be decreased when low sulphur pRES is co-fired with coal, as was the case of olive cake.

Both the partitioning and the characterization of ashes produced are affected by the addition of pRES, depending on their nature and percentages used.

It was demonstrated that with controlled temperatures and air staging the co-combustion may result in positive synergies for NO_X and SO_2 emissions and retaining the SO_2 coming from the coal by the calcium introduced with the biomass origin material.

In general, with the exception of dioxins and furans, the emissions resulting from biomass combustion are expected to be lower than those observed for conventional fossil fuels, like coal. The studies carried out within the scope of this work proved that the level of PCDD/F could be quite high when burning biomass like straw and rice husk, materials with low sulphur content. For

straw combustion, particulate matter as well as PCDD/F levels were found to be high. In the case of PCDD/F, this is due to high Cl content in the fuel, confirming that high concentrations of chlorine and low concentrations of SO_2 promote PCDD/F formation.

This observation confirms that, when high chlorine and low sulphur content fuel combinations are used, PCDD/F emissions are expected to be higher.

In the case of co-combustion of MBM and Colombian coal, it was observed a significant reduction of PCDD/F formation, where the total PCDD/F formed was lower than the results obtained from monocombustion of each fuel. Furthermore, the co-combustion of MBM and Colombian coal could achieve the emission limits set by the European Directive for PCDD/F, which is 0.1 ng I-TEQ/Nm^3@11%O_2.

In this case, only the *de novo* mechanism was identified. It is possible in this situation to reduce further the level of emissions if flue gas burnout is used.

The presence of SO_2 directly influences PCDD/F emissions, as the reduction in SO_2 was found to lead to higher PCDD/F emissions. It was also found that the chlorine and sulphur feed ratio is not directly related with the PCDD/F emissions.

For fuels of similar chlorine content approximately the same HCl amounts were observed, although PCDD/F emissions varied very differently. This shows the influence of sulphur in the HCl emissions. It was also found that the Cu concentration in the cyclones' ashes was not directly correlated with the final PCDD/F emissions.

Lower fly ash d50 implies greater superficial area for catalysis, thus greater levels of PCDD/F were measured both in the gas phase and adsorbed on particle surfaces. In addition, higher concentrations of Cu were found in these smaller size particles due to the presence of chlorine, because it improves Cu volatility, enhancing further the conditions for PCDD/F formation.

The kinetic mechanism derived in this work, the "FB-OWL" model, correlates well with the precursor's mechanism and can be used to estimate possible PCDD/F emissions from the co-combustion of renewable fuels mixed with coal in a bubbling fluidized bed.

It was also possible to establish that to achieve PCDD/F emissions lower than the ELV in a bubbling fluidized bed combustor, SO_2 in the stack gases should be higher than 450 mg SO_2/Nm^3@11%O_2 (dry).

Finally, the following matrix of feeding materials was obtained for decision-making support when selecting feeding mixtures for low levels of potential PCDD/F in Fluidized Bed combustion systems:

$$\begin{cases} \text{Fuel composition: } S>0.15\% \text{ (d.b.) and } Cl>0.03\% \text{ (d.b.)} \\ \text{Molar ratio factor: } [nCa/(nS+nCl)]/(\%Cl\text{-Fuel,d.b.})/(\%S\text{-Fuel,d.b.}) > 4.84 \end{cases}$$

It is noted that the above conditions, obtained with this work, have to be fulfilled simultaneously to ensure low Dioxins and Furans emissions. Additionally, the attained mathematical model can be used to adjust fuel mixtures with appropriate sulphur and chlorine input in order to maintain PCDD/F emissions below the legal limits.
It was possible to identify primary measures in order to avoid SO_2, HCl and PCDD/F emissions through the application of the Sustainable Chemistry principles n. 1 and n. 7.

8.2 Future Work

As future work, further tests are needed to validate the reproductibility of some of the results obtained, as well as more extensive characterization of the different fractions of fly ashes.

Another important goal will be to obtain a generalization of the matrix obtained to include the fulfilment of the SO_2 and HCl Emission Limit Values.

Another important work to develop will be the modelling of the PCDD/F formation mechanism so that the identification of the main mechanism, *i.e. de novo* or precursors', is the main one present in the combustion of mixtures of biomass origin materials and coal in a fluidized bed system.

Following the development of this Thesis, a Life Cycle Assessment (LCA) would give a perspective about the impacts that the co-combustion of RES may have in terms of sustainability.

Life Cycle Assessment (LCA) is becoming an effective tool for evaluating the potential environmental impacts, since it applies an overall view to detect those phases of the product life cycle where major environmental effects occur.

An economic analysis of this co-combustion system should be made in order to predict how successful is expected to be the technology transfer to the industrial sector.

9. Epilogue

The conclusions obtained in this Thesis were only possible due to the high quality of experimental work obtained by the COPOWER team, coordinated by Professor Ibrahim Gulyurtlu.
The author, Cláudia Sargaço ("Old Installation" tests) and David Salema (M.Sc.), carried out the stack-gas sampling as well as the glassware preparation and decontamination (in the case of heavy metals and PCDD/F) and the analysers verifications.
Pedro Abelha (Ph.D.) runs the FB pilot; some of them alone (even in the case of the PCDD/F tests). Due to the lack of technical personnel P. Abelha also had to do some of the fuels preparation, such as coal crushing and sieving.
The Laboratory team (Márcia Freire, Paula Teixeira and Margarida Galhetas) was coordinated by M. Helena Lopes (Ph.D.), who validated all the analytical data.
The author validated all the stack-gas samplings with the exception of the Granulometric Classification of fly ashes, which was carried out by M. H. Lopes.

The success of the present work was not possible to achieve if there was not an excellent team work, which is the four Principles of Girl Guiding and Boy Scouts. As Lord Baden-Powell, said in his last letter:

"Try and leave the world a little better than you found it"

(Baden-Powell, 1941)

I hope I've made it!

10. References

A

Abelha P, Gulyurtlu I, Boavida D, Seabra Barros J, Cabrita I, Leahy J, *et al*., 2003, "Combustion of poultry litter in a fluidised bed combustor", Fuel 82, pp. 687-692.

Abelha P., 2005, "Gaseous emissions during the co-combustion of coal with wastes" (in Portuguese), Ph.D. Dissertation, FCT/UNL, Lisbon, Portugal.

Abelha P., Gulyurtlu I., Crujeira T., Cabrita I., 2008, "Co-Combustion of Several Biomass Materials with a Bituminous Coal in a Circulating Fluidised Bed Combustor", Proceedings of 9th International Conference on Circulating Fluidized Beds, May 13–16, Hamburg, Germany.

Addink R., Paulus R., Olie K., 1993, "Inhibition of PCDDyF formation during de novo synthesis on fly ash using N- and S-compounds", Organohalogen Compd, 12, pp. 27 –30.

Addink R., Paulus R., Olie K., 1996, "Prevention of polychlorinated dibenzo-*p*-dioxins/Ddibenzofurans formation on municipal waste incinerator fly ash using nitrogen and sulfur compounds", Env. Sci. Technol., 30, pp. 2350 –2354.

Altarawneh, M., Dlugogorski, B.Z., Kennedy, E.M.; Mackie, J.C., 2009, "Mechanisms for formation, chlorination, dechlorination and destruction of polychlorinated dibenzo-p-dioxins and dibenzofurans (PCDD/Fs)", Prog. Energ. Comb. Sci., 35, pp. 245-274.

Altwicker E. R., 1996a, "Relative rates of formation of polychlorinated dioxins and furans from precursor and de novo reactions", Chemosphere, 33, 1897-1904.

Altwicker, E.R., 1996b, "Formation of PCDD/F in municipal solid waste incinerators: laboratory and modelling studies", J. Hazard. Materials, 47, pp. 137-161.

Amaral, L.M., 2008, "*O 3º choque petrolífero e a evolução dos sistemas energéticos: O caso português", Conferência Parlamentar "Energia e sustentabilidade, um novo desígnio*"(in Portuguese), 27th October.

Anastas, P. T.; Warner, J. C.; 1998, "Green Chemistry: Theory and Practice, Oxford University Press: New York", p.30.

Anthony, E.J., 1995, "Fluidized bed combustion of alternative solid fuels: status, successes and problems of the technology", Prog. Energy Combust. Sci., Vol. 21, pp. 239-268.

Atkins P. 1991, "Physical Chemistry", 4th Ed., Oxford University Press.

Aurell, J, 2008, "Effects of Varying Combustion Conditions on PCDD/F Formation", Ph.D. Dissertation, Umeå University, Sweden.

Aurell J., Fick J., Haglind P., Marklund S., 2009a, "Effects of sulphur on PCDD/F formation under stable and transient combustion conditions during MSW incineration", Chemosphere 76, pp. 767-773.

Aurell J., Marklund S., 2009b, "Effects of varying combustion conditions on PCDD/F emissions and formation during MSW incineration", Chemosphere 75, pp. 667-673.

B

Baden-Powell, 1941, "Baden-Powell's Last Message" (available at:

http://www.scout.org/sites/default/files/library_files/B-P%27s%20Last%20Message.pdf)

BP, 2012, "BP Statistical Review of World Energy 2011", June.

Blumenstock M, Zimmermann R, Schramm KW, Kettrup A., 2000, "Influence of combustion conditions on the PCDD/F, PCB-,PCBz and PAH-concentrations in the post-combustion chamber of a waste incineration pilot plant" Chemosphere, 40(9-11), pp. 987-993.

Buekens A, Huang H. 1998, "Review Comparative evaluation of techniques for controlling the formation and emissions of chlorinated dioxins/furans in municipal waste incineration", Journal of Hazardous Material, 62, pp.1-33.

C

Cabrita I., 1981, "Formation of nitric oxides in flames", Ph.D. Thesis, University of Sheffield, UK.

Cabrita I., Gulyurtlu, Pinto F., Boavida D., Costa P., Racha L., 2003, "Formação e Destruição de Dioxinas em Processos de Combustão e Co-Combustão" (in Portuguese), presented at the 1st National Meeting on Dioxins and Similar compounds, published in Revista da Faculdade de Medicina de Lisboa, July/August 2003; Série III; 8 (4): pp. 225-235.

Castranova, V., 2005, "Toxicity of Ultrafine Particles", NIOSH, Centers for Disease Control and Prevention,
[http://usachppm.apgea.army.mil/doem/particle/apnds/appendix%20e,%20castranova.pdf]

CEA, 2008, "Performance Review of Thermal Power Stations 2005-06", Central Electricity Authority, India.

(available at http://www.cea.nic.in/god/opm/thermal_performance_review/0506/thermal

%20performance%20review%20_eng_0506_pdf/SECTION-14.pdf).

CEN, 1996, EN 1948-1:1996 "Stationary source emissions – Determination of the mass concentration of PCDDs/PCDFs – Part 1: Sampling", CEN, 1996.

CEN, 2006, EN 1948-1:2006 -"Stationary source emissions - Determination of the mass concentration of PCDDs/PCDFs and dioxin-like PCBs. Sampling of PCDDs/PCDFs", CEN.

CFR, 2013, "40 Code of Federal Regulations (CFR), Part 60, Appendix A".

(available at http://www.epa.gov/ttnemc01/promgate.html)

Chang M, Cheng Y, Chi K., 2006, "Reducing PCDD/F formation by adding sulfur as inhibitor in waste incineration processes", Sci. Total Enviro., 366, pp. 456-465.

Chen, R., 1991, "Compact Hybrid particulate collector", US Patent N.º 5,024,681.

Chen, R., 1992, "Compact Hybrid particulate collector (COHPAC)", US Patent N.º 5,158,580.

Chen J-C, Wey M-Y, Yan M-H, 1997, "Theoretical and experimental study of metal capture during incineration process", J. Environ. Eng., 123, pp. 1100–1106.

Chi, K.H., Chang, M.B., Chang, S.H., 2006, "Evaluation of PCDD/F partitioning between vapor and solid phases in MSWI flue gases with temperature variation"; J. Hard. Materials, B138, pp. 620-627.

Chirone R., Massimilla L., Salatino P., 1991, "Comminution of carbons in fluidized bed combustion", Progress in Energy and Combustion Science, Volume 17, Issue 4, pp. 297-326.

CLRTAP, 2008, "Convention on Long-Range Transboundary Air Pollution".

(available at www.unece.org/env/lrtap/)

COPOWER, 2007, "European Project", SES6-CT-2004, Final Report.

(available at http://www.copowerproject.com)

Coulson J.M., Richardson J.F., 1978, "Tecnologia Química II: Operações Unitárias" (in Portuguese), 3rd Ed., FCG.

Coutinho, M., Rodrigues, R., Borrego, C., 2003, "Caracterização das Emissões Atmosféricas de Dioxinas e Furanos em Portugal: 1999-2003", (in Portuguese), presented at the 1st National Meeting on Dioxins and Similar compounds, published in Revista da Faculdade de Medicina de Lisboa, July/August; Série III; 8 (4): pp. 245-257.

CPCB, 2008, "Indian Thermal Power Plant: Emission Standards".

(available at http://www.cpcb.nic.in/Industry-Specific-Standards/Effluent/ThermalPowerPlant.pdf).

Crujeira, T., 2004, "Fluidised bed combustion of coal and Refuse Derived Fuel: the influence of adsorbent addition in heavy metals and chlorine compounds distribution" (in Portuguese), Dissertation for access to the Investigation Assistant category, INETI, Lisbon, Portugal.

Crujeira, T., Lopes, H., Abelha P., Sargaço, C., Gonçalves, R., Freire, M., Cabrita, I. & Gulyurtlu, I., 2005, "Study of toxic metals during combustion of RDF in a fluidized bed pilot", Environmental Engineering Science, Volume 22, Number 2, pp. 241-250.

Crujeira T., Lopes H., Abelha P., Cabrita I., Gulyurtlu I., 2007, "Minimization of Flue Gas Emissions Produced by Co-combustion with Biomass and Wastes" (in Portuguese), Proceedings of the 9th National Environmental Conference, April 18 – 20, Aveiro, Portugal, Ed. Borrego, C. *et al.*, pp. 723-731; ISBN 978-972-789-230-3.

Crujeira, T., Gulyurtlu, I., Lopes, H., Abelha, P., Cabrita, I., 2008, "Bioenergy originating from biomass combustion in a fluidized bed", Proceedings of the International Conference and Exhibition on Bioenergy - Bioenergy: Challenges and Opportunities, April 6 – 9, Minho University, Guimarães, Portugal.

Crujeira T., Moreira L., Cabrita I., Gulyurtlu I., 2013, "PCDD/F formation in the co-combustion of biomass and coal: the influence of chlorine, copper, calcium and sulphur", Proceedings of the 1st International Congress on Bioenergy, 23-25 May, Portalegre, Portugal, ISBN 978-989-98406-2-1.

D

Davidson RM, Clarke LB.,1996, "Trace elements in coal", IEAPER/21. London, UK: IEA Coal Research.

Davidson RM., 2000, "Modes of occurrence of trace elements in coal" CCC/36, London, UK: IEA Coal Research.

Debecker D.P. Delaigle R., Hung P.C., Buekens A., Gaigneaux E.M., Chang M.B., 2011, "Evaluation of PCDD/F oxidation catalysts: Confronting studies on model molecules with tests on PCDD/F-containing gas stream", Chemosphere 82, pp. 1337–1342.

Desroches-Ducarne E., Marty E., Martin G., Delfosse L., 1998, "Co-combustion of coal and municipal solid waste in a circulating fluidized bed", Fuel, Vol. 77(12), pp. 1311-1315.

DGEG, 2012, Direcção Geral de Energia e Geologia, Ministério da Economia e do Emprego (*in Portuguese*)

(available at http://www.dgeg.pt/)

Directive 96/62/EC; Ambient air quality assessment and management, European Commission; Luxembourg; 27 September 1996; OJ L 296, 21.11.1996.

Directive 1999/13/EC; Limitation of emissions of volatile organic compounds due to the use of organic solvents in certain activities and installations ("Solvents Directive"); European Commission; Luxembourg; 11 March 1999; OJ L 85, 29.3.1999.

Directive 1999/30/EC; Relating to limit values for sulphur dioxide, nitrogen dioxide and oxides of nitrogen, particulate matter and lead in ambient air; European Commission; Luxembourg; 22 April 1999; OJ L 163, 29.6.1999.

Directive 2000/76/EC; The incineration of waste ("Waste Incineration Directive"); European Parliament and Council; Luxembourg; 4 December 2000; OJ L 332, 28.12.2000.

Directive 2001/80/EC; Limitation of emissions of certain pollutants into the air from large combustion plants ("LCP Directive"); European Parliament and Council; Luxembourg; 23 October 2001; OJ L 309, 27.11.2001.

Directive 2004/107/EC; Arsenic, cadmium, mercury, nickel and polycyclic aromatic hydrocarbons in ambient air; European Parliament and Council; 15 December 2004; OJ L23, 26.01.2005.

Directive 2008/1/EC; Concerning integrated pollution prevention and control ("IPPC Directive"); European Parliament and Council; 15 January 2008; OJ L24, 29.01.2008.

Directive 2008/50/EC; Ambient air quality and cleaner air for Europe; European Parliament and Council; 21 May 2008; OJ L152, 11.06.2008.

Directive 2009/28/EC; On the promotion of the use of energy from renewable sources and amending and subsequently repealing Directives 2001/77/EC and 2003/30/EC; European Parliament and Council of 23 April 2009; OJ L140, 05.06.2009.

Directive 2010/75/EU; Concerning the on industrial emissions (integrated pollution prevention and control) (Recast); European Parliament and Council; 24 November 2010; OJ L334, 17.12.2010.

E

EEA, 2011, "Data aggregated and gap-filled air emission dataset, based on 2011 officially reported national total and sectoral emissions to UNECE LRTAP Convention, the EU NEC Directive and EU-MM/UNFCCC".

(available at http://www.eea.europa.eu/data-and-maps/data/national-emissions-reported-to-the-convention-on-long-range-transboundary-air-pollution-lrtap-convention-5)

EIPPCB, 2013 - European Integrated Pollution Prevention and Control Bureau European Integrated Pollution Prevention and Control Bureau, Institute for Prospective Technological Studies, Joint Research Centre, European Commision.

(available at: http://eippcb.jrc.ec.europa.eu/).

EMEP, 2007, "EMEP Status Report 2/2007, Heavy Metals: transboundary pollution of the environment".

(available at http://www.emep.int/publ/common_publications.html#2007)

EMEP, 2008 - Co-operative Programme for Monitoring and Evaluation of the Long-range Transmission of Air pollutants in Europe (available at http://www.emep.int/index_facts.html).

EPA CAA, 1990 – EPA Clean Air Act, 1990

(available at http://www.epa.gov/air/caa/index.html).

EPA CAMR, 2005 - EPA Clean Air Mercury Rule, 2005.

(available at http://www.epa.gov/air/mercuryrule/).

EPA CAR, 2004, "EPA Clean Air Rules", 2004 (available at http://www.epa.gov/cleanair2004/).

EPA China, 2004, "Strategy for Clean Air and Energy Cooperation between the Environmental Protection Agency of the United States of America and the State Environmental Protection Administration of the People's Republic of China", 2004.

(available at http://www.epa.gov/oia/regions/Asia/china/2004_sca_eng.pdf).

EPA CSI, 2003, "EPA Clear Skies Initiative", 2003.

(available at http://www.epa.gov/air/clearskies/basic.html).

EPER, 2013, "European Pollutant Emission Register".

(available at http://www.eea.europa.eu/data-and-maps/data/eper-the-european-pollutant-emission-register-4).

E-PRTR, 2006, "Guidance Document for the implementation of the European PRTR", European Commission, 31 May 2006.

(available at http: http://prtr.ec.europa.eu/docs/EN_E-PRTR_fin.pdf)

Everaert K., Baeyens J., 2002, "The formation and emission of dioxins in large scale thermal processes", Chemosphere 46, pp. 439-448.

F

Faaij APC, 2006, "Bio-Energy in Europe: changing technology choices", Energy Policy, 34, pp. 322-342.

Fängmark I., Strömberg B., Berge N., Rappe C., 1994, "Influence of small fly ash particles on the post-combustion formation of PCDDs, PCDFs, PCBzs and CPs in a pilot incinerator", Chemosphere 29, pp. 1903–1909.

Feeley III T. J., 2005, "Enhancing the Environmental Performance of Coal-Fired Power Plants – Doe's Innovations for Existing Plants Program", February 2005, National Energy Technology Laboratory, Office of Fossil Energy, U.S. Department of Energy.

Frandsen, F., Dam-Johansen, K., Rasmussen, P., 1994, Trace elements from combustion and gasification of coal – an equilibrium approach. Prog. Energy Comb. Sci., 20(2), pp. 115-38.

Fritz J., 2004, "Environmental Performance of Coal-Fired Power Plants Financed by the World Bank", Proceedings of the Symposium Urbanization, Energy, and Air Pollution in China: The Challenges Ahead, The National Academies Press, pp. 187-204.

G

Gavett S., Haykal-Coates N., Copeland L. B., Heinrich J., Ian Gilmour M., 2003, "Metal Composition of Ambient PM2.5 Influences Severity of Allergic Airways Disease in Mice", Environmental Health Perspectives, Vol. 111, N. 12, pp. 1471-1477.

GMA, 2002, "Global Mercury Assessment", Issued by UNEP Chemicals, Geneva, Switzerland, December 2002 [http://www.chem.unep.ch/mercury/Report/GMA-report-TOC.htm].

Golbraikh A., Tropsha A., 2002, "Beware of q^2!" Journal of Molecular Graphics and Modelling, 20, pp. 269-276.

Griffin R.A, 1986, "New theory of dioxin formation in municipal waste combustion", Chemosphere, 15, pp. 1987–1990.

Gullett B.K., Bruce K.R., Beach L.O., 1992, "Effect of sulfur dioxide on the formation mechanism of polychlorinated dibenzodioxin and dibenzofuran in municipal waste combustors", Enviro. Sci Techno., 26 (10), pp. 1938 –1943.

Gullett B.K., Raghunathan K., 1997, "Observations on the effect of process parameters on dioxin/furan yield in municipal waste and coal systems", Chemosphere 34, pp. 1027–1032.

Gulyurtlu, I., 1989, "Coal technology", INETI, Portugal.

Gulyurtlu I, Boavida D, Abelha P, Miranda M, Cabrita I., 1999, "Combustion of cork waste in a circulating fluidised bed combustor", Circulating Fluidized Bed Technology VI, pp. 697-704.

Gulyurtlu I, Boavida D, Abelha P, Lopes H, Cabrita I., 2002, "Co-combustion of waste with coal in a circulating bed combustor", Circulating Fluidized Bed Technology VII; pp. 693-700.

Gulyurtlu, I., Abelha, P., Gregório, A., García-García, A., Boavida, D., Crujeira, T., Cabrita, I., 2004, "The emissions of VOCs during co-combustion of coal with different waste materials in a fluidized bed", Energy & Fuels, Vol. 18, 3, pp. 605-610.

Gulyurtlu I., Crujeira T., Lopes M. H., Abelha P., Boavida D., Seabra J., Gonçalves R., Sargaço C., Cabrita I., 2006, "The study of combustion of municipal waste in a fluidised bed combustor", JERT (Journal of Energy Resources Technologies), Special Issue on Advances in Fluidized Bed Combustion, June, Vol. 128, pp. 123-128.

Gulyurtlu I., Lopes H., Crujeira T., Boavida D., Abelha P., 2007a, "COPOWER - Co-Firing of Biomass and other Wastes in Fluidised Bed Systems", Proceedings of the International Conference on Coal Science and Technology, August 28 – 31, Nottingham, United Kingdom.

Gulyurtlu I., Abelha P., Lopes H., Crujeira A., Cabrita I., 2007b, "Considerations on Valorization of Biomass Origin Materials in Co-combustion with Coal in Fluidized Bed", Proceedings of the 3rd International Conference on Clean Coal Technologies for Our Future, May 15 – 17, Sardinia, Italy.

Gulyurtlu I, Crujeira A. T., Abelha P., Cabrita I., 2007c, "Measurements of dioxin emissions during co-firing in a fluidised bed", Fuel 86, pp. 2090–2100.

H

Hagenmaier H., Kraft M., Brunner H., Haag R., 1987, "Catalytic effects of fly ash from waste incineration facilities on the formation and decomposition of polychlorinated dibenzo-p-dioxins and polychlorinated dibenzofurans", Environmental Science & Technology (21), pp. 1080-1084.

Hasselriis, F.; Licata, A., 1996, "Analysis of heavy metal emission data from municipal waste combustion", Journal of Hazardous Materials, Vol. 47, 77-102.

Ho, T.C., Chuang, T.C., Chelluri, S., Lee, Y., Hopper, J.R., 2001, "Simultaneous capture of metal, sulphur and chlorine by sorbents during fluidised bed incineration", Waste Management, Vol. 21(5), 435-441.

Huang, H.; Buekens, A., 1995, "On the mechanisms of dioxin formation in combustion processes", Chemosphere, 31 (9), pp. 4099-4117.

Huang, H.; Buekens, A., 2000, "Chemical kinetic modelling of PCDD formation from chlorophenol catalysed by incinerator fly ash", Chemosphere, 41, pp. 943-951.

Hunsinger H., Jay K., Vehlow J., 2002, "Formation and destruction of PCDD/F inside a grate furnace", Chemosphere, 46, pp. 1263–1272.

I

IEA, 2010, "Energy Technology Perspectives'. Scenarios and Strategies to 2050", International Energy Agency, OECD/IEA, Paris. ISBN 987-92-08597-8.

IEA, 2012, "Key World Energy Statistics", International Energy Agency, OECD/IEA Paris.

Iino F., Takasuga T., Touati A., Gullett B.K., 2003, "Correlations between homologue concentrations of PCDD/Fs and toxic equivalency values in laboratory-, package boiler-, and field-scale incinerators", Waste Management 23, pp. 729–736.

INETI, 2005a, Salema D., Sargaço C., Pacheco R., Crujeira A.T., Gulyurtlu I., "Caracterização de Efluentes Gasosos: Queima de Farinha de carne em reactor de Leito Fluidizado" (in Portuguese), DEECA 03/05, April 2005.

INETI, 2005b, Salema D., Sargaço C., Pacheco R., Crujeira A.T., Gulyurtlu I., "Caracterização de Efluentes Gasosos: Combustão de "Straw pellets" em reactor de Leito Fluidizado" (in Portuguese), DEECA 04/05, May 2005.

INETI, 2007a, Salema D., Pereira R.P., Crujeira A.T., Gulyurtlu I., "Caracterização de Efluentes Gasosos: Combustão de Bagaço de azeitona em reactor de Leito Fluidizado" (in Portuguese), DEECA 05/07, March 2007.

INETI, 2007b, Salema D., Pereira R.P., Crujeira A.T., Gulyurtlu I., "Caracterização de Efluentes Gasosos: Combustão de "Wood Pellets" em reactor de Leito Fluidizado" (in Portuguese), DEECA 06/07, April 2007.

INETI, 2007c, Salema D., Pereira R.P., Crujeira A.T., Gulyurtlu I., "Caracterização de Efluentes Gasosos: Combustão de "Rice Husk" em reactor de Leito Fluidizado" (in Portuguese), DEECA 07/07, April 2007.

INETI, 2007d, Salema D., Pereira R.P., Crujeira A.T., Gulyurtlu I., "Caracterização de Efluentes Gasosos: Combustão de "Straw pellets" e carvão colombiano em reactor de Leito Fluidizado" (in Portuguese), DEECA 08/07, April 2007.

IPCC, 2013 - Intergovernmental Panel on Climate Change.

(available at http://www.ipcc.ch/)

J

Jansson, S., 2008, "Thermal Formation and Chlorination of Dioxins and Dioxin-Like Compounds", Ph.D. Dissertation, Umeå University, Sweden.

Jansson S., Fick J., Tysklind M., Marklund S., 2009a, "Post-combustion formation of PCDD, PCDF, PCBz, and PCPh in a laboratory-scale reactor: Influence of dibenzo-p-dioxin injection", Chemosphere 76, pp. 818-825.

Jansson S., Antti H., Marklund S., Tysklind M., 2009b, "Multivariate relationships between molecular descriptors and isomer distribution patterns of PCDD/Fs formed during MSW combustion", Environ. Sci. Technol., 43, pp. 7032-7038.

K

Karunaratne, D.G.G.P., 1999, "Formation of Polycyclic Aromatic Hydrocarbons from coconut biomass combustion"; Ph.D. Dissertation, FCT/UNL, Lisbon, Portugal.

Kajita, A.; Tanaka, T.; Narukawa, K.; Kobayashi, N.; Nishiyama, A.; Oide, M; 1999, "Combustion test for RDF and coal in the 1.3 MWth ACFB", Proceedings of the 15th International Conference on Fluidized Bed Combustion, (FBC99-0160).

Korzun, E.A., Heck, H.H., 1990, "Sources and fates of lead and cadmium in municipal solid waste", J. Air Waste Manage. Assoc., 40(9), 1220-1226.

Krigmont H.V., 2003, "Multi-Stage Collector (MSC™) Development", Proceedings of the 20th Annual International Coal Conference, The Westin - Convention Center in Downtown Pittsburgh, September 15-19, Paper 95.

Kurokawa Y., Takahiko M., Matayoshi N., Sato T., Kazumi F., 1998, "Distribution of polychlorinated dibenzo-p-dioxins and dibenzofurans in various sizes of airborne particles", Chemosphere 37, pp. 2161–2171.

L

Lasagni M., Collina E., Grandesso E., Piccinelli E., Pitea D., 2009, "Kinetics of carbon degradation and PCDD/PCDF formation on MSWI fly ash", Chemosphere 74, pp. 377–383.

LCP BREF, 2005, Integrated Pollution Prevention and Control, Reference Document on Best Available Techniques for Large Combustion Plants, May 2005. European Commission, Directorate-General Joint Research Centre, Institute for Prospective Technological Studies, European IPPC Bureau.

(available at: http://eippcb.jrc.ec.europa.eu/reference/BREF/lcp_bref_0706.pdf)

LCP BREF, 2013, Integrated Pollution Prevention and Control, Reference Document on Best Available Techniques for Large Combustion Plants, J Draft 1 (June 2013), European Commission, JRC, Institute for Prospective Technological Studies, Sustainable Production and Consumption Unit, European IPPC Bureau.

(available at: http://eippcb.jrc.ec.europa.eu/reference/BREF/LCP_D1_June_online.pdf).

Lemieux PM, Lee CW, Ryan JV, Lutes CC. Bench-scale studies on the simultaneous formation of PCBs and PCDD/Fs from combustion systems. Waste Management 2001; 21(5): 419- 425.

Lenoir D., Feicht E.A., Pandelova M., Schramm K.-W., 2007, "Methods and Reagents for Green Chemistry: An introduction", Ed. Tundo P., Perosa A. & Zecchini F., John Wiley & Sons, Inc.

Lenoir D., Klobasa O., Pandelova M., Henkelmann B., Schramm K.-W., 2012, "Laboratory studies on formation and minimisation of polychlorinated dibenzodioxins and -furans (PCDD/F) in secondary aluminium process", Chemosphere 87, pp. 998–1002.

Lerda D., 2010, "Polycyclic Aromatic Hydrocarbons (PAHs) Factsheet", 3rd Ed., irmm, JRC 60146, European Union, 2010.

Li X.-D., Zhang J., Yan J.-H., Cen K.-F., Ryan S.P., Gullet B.K., Lee C., 2007, "Experimental and modeling study of de novo formation of PCDD/PCDF on MSW fly ash", Journal of Environmental Sciences 19, pp. 117-122.

Linak, W., Wendt, J., 1993, "Toxic metal emissions from incineration: mechanisms and control" Progr. Energy and Combustion Science, 19, pp. 145-85.

Lindbauer R.L., Wurst F., Prey T., 1992, "Combustion dioxin suppression in municipal solid waste incineration with sulfur additives", Chemosphere, 25, pp. 1409–1414.

Liu, K., Pan, W.-P., Riley, J.T., 2000, "A study of chlorine behavior in a simulated fluidised bed combustion system", Fuel 79, pp. 1115-1124.

Liu, G.-Q.; Itaya, Y.; Yamazaki, R.; Mori, S.; Yamaguchi, M.; Kondoh, M.; 2001, "Fundamental study of the behavior of chlorine during the combustion of single RDF", Waste Management, Vol. 21 (5), pp. 427-433.

Liu W., Zheng M., Zhang B., Qian Y., Ma X., Liu W., 2005, " Inhibition of PCDD/Fs formation from dioxin precursors by calcium oxide", Chemosphere 60, pp. 785–790.

Lopes M.H., 2002, "Study of the behaviour of Heavy Metals in the combustion of Sewage Sludge in Fluidised Bed" (in Portuguese), Ph.D. Dissertation, FCT/UNL, Lisbon, Portugal.

Lopes H., Abelha P., Lapa N., Oliveira J.S., Cabrita I., Gulyurtlu I., 2003, The behaviour of ashes and heavy metals during the co-combustion of sewage sludges in a fluidised bed, Waste Management 23, pp. 859–870.

Lopes M.H., Gulyurtlu I., Abelha P., Teixeira P., Crujeira T., Boavida D., Marques F., I. Cabrita, 2006, "Co-combustion for Fossil Fuel Replacement and Better Environment", Proceedings of the 7th European Conference on Industrial Boilers and Furnaces, April, Porto, Portugal, Paper Infub_92; ISBN 972-99309-1-0.

Lopes H., Gulyurtlu I., Abelha P., Crujeira T., Salema D., Freire M., Pereira R., Cabrita I., 2009, "Particulate and PCDD/F emissions from coal co-firing with solid biofuels in a bubbling fluidised bed reactor", Fuel 88, pp. 2373-2384.

Luijk R., Dorland C., Kapteijn F., Govers H. A. J., 1993, "The formation of PCDDs and PCDFs in the catalysed combustion of carbon: implications for coal combustion", Fuel, 72, pp. 343-347.

M

Mätzing, H., 2001a, "A simple kinetic model of PCDD/F formation by de novo synthesis", Chemosphere 44, pp. 1497-1503.

Mätzing, H., Baumann W., Becker B., Jay K., Paur H.-R., Seifert H., 2001b, "Adsorption of PCDD/F on MWI fly ash", Chemosphere 42, pp. 803-809.

McKay G., 2002, "Dioxin characterisation, formation and minimisation during municipal solid waste (MSW) incineration: review", Chem. Eng. J., 86, pp. 343–368.

Meij R, Winkel H, (2007), "The emissions of heavy metals and persistent organic pollutants from modern coal-fired power stations", Atmospheric Environment 41, pp. 9262–9272.

Miller, S.J., 1999, "Advanced hybrid particulate collector and method of operation", U.S. Patent 5,938,818.

Miller, S.J., 2003, "Advanced hybrid particulate collector and method of operation", U.S. Patent 6,544,317.

Milligan M. S., Altwicker E. R., 1996, "Chlorophenol reactions on fly ash. 1. Adsorption/desorption equilibria and conversion to polychlorinated dibenzo-p-dioxins", Environmental Science & Technology (30), pp. 225-229.

N

Narukawa, K.; Mori, Y.; Sato, E.; Kobayashi, N.; Nishiyama, A.; Oide, M.; 2001, "The study on the effect of RDF chlorine in the 1.3 MW_{th} CFB pilot plant", Proceedings of the 16th International Conference on Fluidized Bed Combustion, (FBC01-0202).

NATO/CCMS, 1988, "International toxicity equivalency factor (I-TEF) method of risk assessment for complex mixtures of dioxins and related compounds". North Atlantic Treaty Organization, Committee on the Challenges of Modern Society. Report No. 176.

O

Ogawa H, Orita N, Horaguchi M, Suzuki T, Okada M, Yasuda S., 1996, "Dioxin reduction by sulfur component addition", Chemosphere, 32, pp. 151–157.

Olie K., Addink R., Schoonenboom M., 1997, "Metals as Catalysts during the Formation and Decomposition of Chlorinated Dioxins and Furans in Incineration Processes", Volume 48, J. Air Waste Manage., Vol. 48, pp. 101-105.

P

Pandelova, M, Lenoir, D, Kettrup A, Schramm, K-W., 2005, "Primary Measures for Reduction of PCDD/F in Co-Combustion of Lignite Coal and Waste: Effect of Various Inhibitors", Enviro. Sci. Tech., 39, pp. 3345-3350.

Pandelova M, Stanev I, Henkelmann B, Lenoir D, Schramm K-W, 2009, "Correlation of PCDD/F and PCB at combustion experiments using wood and hospital waste. Influence of $(NH_4)_2SO_4$ as additive on PCDD/F and PCB emissions", Chemosphere, 75, pp. 685-691

Perkins R., 2005, "Electricity sector restructuring in India: an environmentally beneficial policy?", Energy Policy, 33, pp. 439–449.

Pinto F., André R.N., Abelha P., Crujeira A.T., Gulyurtlu I., 2009, Chapter "Control of Flue Gases Produced by New Coal Utilization Technologies: Combustion and Gasification" from the Book "Flue Gases: Research, Technology and Economics", NOVA Publishers, ISBN: 978-1-60692-449-5.

POPs (2007) "Handbook for POPs Laboratory Databank", UNEP Chemicals Branch, DTIE, October 2007

[http://www.chem.unep.ch/pops/laboratory/POPs_Labs_Databank_Handbook_2007_en.pdf]

POPs (2001) "Stockholm Convention on Persistent Organic Pollutants"

[http://chm.pops.int/Portals/0/Repository/conf/UNEP-POPS-CONF-4-AppendixII.5206ab9e-ca67-42a7-afee-9d90720553c8.pdf]

R

Raask E., 1985, "The mode of occurrence and concentration of elements in coal", Progress in Energy and Combustion Science, 11, pp. 97-118.

Raghunathan K., B.K. Gullett, 1996, Role of sulfur in reducing PCDD and PCDF formation, Environ. Sci. Technol. 30, pp. 1827–1834.

Rühl, C., 2007, "Energy Security and 'Reciprocity'", BP, Lisbon Energy Forum, October 2th.

Ruokojärvi P, Aatamila M., Tuppurainen K., Ruuskanen J., 2001, "Effect of urea on fly ash PCDD/F concentrations in different particle sizes", Chemosphere, Volume 43, Issues 4-7, pp. 757-762.

Ruokojärvi P.H., Asikainen A.H., Tuppurainen K.A., Ruuskanen J., 2004, "Chemical inhibition of PCDDyF formation in incineration Processes", Science of the Total Environment, 325, pp. 83–94.

Ryan P., Altwicker E.R., 2000, "The formation of polychlorinated dibenzo-p-dioxins/dibenzofurans from carbon model mixtures containing ferrous chloride", Chemosphere 40, pp. 1009–1014.

S

Salcedo R., Chibante V., Fonseca A.M., Cândido G., 2007, "Fine particle capture in biomass boilers with recirculating gas cyclones: Theory and practice", Powder Technology 172, pp. 89–98.

Salema D., 2008, "Co-Combustão of Biomass and Coal in Fluidized Bed: Impact in atmospheric emissions of NO_X, SO_2, CO, Dioxins and Furans, and Particulate Matter" (in Portuguese), M.Sc. Dissertation, FCT/UNL, Lisbon, Portugal.

Samaras P, Blumenstock M, Lenoir D, Schramm K-W, Kettrup A., 2000, "PCDDyF prevention by novel inhibitors: addition of inorganic S- and N- compounds in the fuel before combustion", Enviro. Sci Technol, 34, pp. 5092 –5096.

Sánchez-Hervás JM, Armesto L., Ruiz-Matínez, Otero-Ruiz J, Pandelova M, Schramm KW, 2005, "PCDD/PCDF emissions from co-combustion of coal and PVC in a bubbling fluidised bed boiler", Fuel, 84, pp. 2149-2157.

SEPA 2003, "GB 13223-2003: Emission standard of air pollutants for thermal power plants" [http://www.sepa.gov.cn/image20010518/5297.pdf]

Shaub, W.M., Tsang,W., 1983, "Dioxin formation in incinerators", Environmental Science & Technology (17), pp. 721-730.

Sloss L., Henderson C., Topper J.; 2003, "Environmental standards and controls and their influence on development of clean coal technologies", India-IEA Joint Conference on Coal and Electricity in India, September, IEA Clean Coal Centre, London, UK.

Stieglitz L, Vogg H., 1987, "On formation condition of PCDDyF in fly ash from municipal waste incinerators", Chemosphere 16, pp. 1917 –1922.

Stieglitz L., Zwick G., Beck J., Roth W., Vogg H., 1989, "On the *de novo* synthesis of PCDD/PCDF on fly ash of municipal waste incinerators" Chemosphere, 18 (1-6), pp. 1219-1226.

Stieglitz L., Bautz H., Roth W., Zwick G., 1997, "Investigation of Precursor Reactions in the De-Novo-Synthesis of PCDD/PCDF on Fly Ash", Chemosphere 34, pp. 1083–1090.

Stieglitz L., 1998, "Selected topics on the de novo synthesis of PCDD/PCDF on fly ash", Environmental Engineering Science (15), pp. 5-18.

Streibel T., Nordsieck H., Neuer-Etscheidt K., Schnelle-Kreis J., Zimmermann R., 2007, "Experimental and statistical determination of indicator parameters for the evaluation of fly ash and boiler ash PCDD/PCDF concentration from municipal solid waste incinerators", Chemosphere 67, pp. S155-S163.

T

Tarelho, L.A.C., 2001, "Controlo de emissões gasosas poluentes resultantes da combustão de carvão em leito fluidizado" (in Portuguese), PhD. Thesis, Aveiro University, Portugal.

Thipse S.S., Dreizin E.L., 2002, "Metal partitioning in products of incineration of municipal solid waste", Chemosphere, Vol. 46(6), pp. 837-849.

Thomas V.M., McCreight C.M., 2008, "Relation of chlorine, copper and sulphur to dioxin emission factors", Journal of Hazardous Materials, 151, pp. 164-170.

Topper, J., 2003, "Environmental Standards and Controls and their Influence on Development of Clean Coal, IEA Clean Coal Centre "Coal and Electricity in India", September.

Tropsha A., Gramatica P., Gombar V., 2003, "The importance of Being Earnest: Validation is the Absolute Essential for Sucessfuel Application and Interpretation of QSPR Models", QSAR Comb. Sci., 22, pp. 69-77.

Tuppurainen, K., Halonen I. And Ruokojarve P., 1998, "Formation of PCDDs and PCDFs in municipal waste combustion and its inhibition mechanisms: a review", Chemosphere, 36(7), pp. 1493-1511.

U

UNEP, 1999, "Dioxin and Furan Inventories - National and Regional Emissions of PCDD/PCDF", UNEP, Geneva, Switzerland

UNEP, 2013 - United Nations Environment Programme, Division of Technology, Industry and Economics, Chemicals Branch.

(available at http://www.chem.unep.ch/default.htm)

V

Van den Berg M., Birnbaum L. S., Denison M, De Vito M., Farland W., Feeley M., Fiedler H., Hakansson H., Hanberg A., Haws L., Rose M., Safe S., Schrenk D., Tohyama C, Tritscher A., Tuomisto J., Tysklind M., Walker N., Peterson R., ,2006, "The 2005 World Health Organization Reevaluation of Human and Mammalian Toxic Equivalency Factors for Dioxins and Dioxin-Like Compounds. Review.", Toxicological Sciences 93(2), pp. 223–241.

Van Caneghem J., Vermeulen I., Block C., Van Brecht A., Van Royen P., Jaspers M., Wauters G., Vandecasteele C., 2012, "Destruction and formation of PCDD/Fs in a fluidised bed combustor co-incinerating automotive shredder residue with refuse derived fuel and wastewater treatment sludge", Journal of Hazardous Materials 207–208, pp. 152–158.

Van Doorn J., Bruyn P., Vermeij, P., 1996, "Combined combustion of biomass, municipal sludge and coal in an atmospheric fluidised bed installation", Proc. 9th European Bioenergy Conference, Vol. 2, pp. 1007-1012.

Vehlow,J.; Rittmeyer, C.; Pfang-Stotz, G.; Vogg, H.; Mark, F.; Kayen, H.; Freiesleben, W.; Lescuyer, J.; 1995, "Co-combustion of waste plastics and municipal solid waste in the Karlsruhe test incinerator Tamara", Proceedings of the International Conference on Solid Waste Management: Thermal Treatment and Waste-to-Energy Technologies, Air & Waste Management Association, Washington DC, USA, pp. 405-413.

Verhults, D., Buekens, A., Spencer, P.J., Eriksson, G.; 1996, "Thermodynamic behaviour of chlorides and sulfates under the conditions of incineration furnaces", Environ. Sci. Technol., 30, pp. 50-56.

Vogg H, Metzger M, Stieglitz L., 1987, "Recent findings on the formation and decomposition of PCDDyF in municipal solid waste incineration", W aste Manage Res,5, pp. 285 –294.

W

Wang J, Yamada O, Nakazato T, Zhang Z-G, Suzuki Y, Sakanishi K, 2008, Statistical analysis of the concentrations of trace elements in a wide diversity of coals and its implications for understanding elemental modes of occurrence, Fuel 87, pp. 2211–2222.

Wehrmeier A., Lenoir D., Schramm K.-W., Zimmermann R., Hahn K., Henkelmann B., Kettrup A., 1998, "Patterns of isomers of chlorinated dibenzo-p-dioxins as tool for elucidation of thermal formation mechanisms", Chemosphere (36), pp. 2775-2801.

Wilde H. de, Kroon P., Bleeker A., 2007, "Impact of future biomass use on the atmospheric PM10 concentration in the Netherlands", Proc. of DustConf. 2007, Maastricht.

Wikström E., Ryan S., Touati A., Gullett B. K., 2003, "Key parameters for de novo formation of polychlorinated dibenzo-p-dioxins and dibenzofurans", Environmental Science & Technology, 37, pp. 1962-1970.

WEO, 2011, "World Energy Outlook 2011", International Energy Agency, OECD/IEA, Paris. ISBN: 978-92-64-12413-4.

Wobst, M., Wichmann, H., Bahadir, M., 2001, "Distribution behavior of heavy metals investigated in a laboratory-scale incinerator", Chemosphere, Vol. 44(5), pp. 981-987.

X

Xie, W.; Liu, K.; Pan, W.-P.; Riley, J., 1999, "Interaction between emissions of SO_2 and HCl in fluidized bed combustors", Fuel, Vol. 78 (12), 1425-1436.

Xie Y, Xie W, Liu K, Dicken L, Pan W-P, Riley JT., 2000, "The Effect of Sulfur Dioxide on the Formation of Molecular Chlorine during Co-Combustion of Fuels", Energy and Fuels, 14 (3), pp. 597-602.

Y

Yan, R., Gauthier, D., Flamant, G., Gautrin, M., 1999, "An equilibrium analysis to determine the speciation of trace elements in the flue gas from a coal-fired fluidised-bed boiler", Proceedings of the 15th International Conference on Fluidized Bed Combustion, Ed. Reuther, R.B.-ASME, (FBC99-0073).

Yan R., Gauthier D., Flamant G., 2001, "Partitioning of trace elements in the flue gas from coal combustion", Combustion and Flame, 120, pp. 49-60.

Z

Zhao Y, Zhang J., Huang W, Wang Z, Li Y, Song D, Zhao F, Zheng C, 2008, "Arsenic emission during combustion of high arsenic coals from Southwestern Guizhou, China", Energy Conversion and Management 49, 2008, pp. 615–624.

Papers